



5-2009

Proposed mechanism of action of saxitoxin in aquatic systems based on expression profiling in lower eukaryotes

Kathleen Daumer Cusick
University of Tennessee

Follow this and additional works at: https://trace.tennessee.edu/utk_graddiss

Recommended Citation

Cusick, Kathleen Daumer, "Proposed mechanism of action of saxitoxin in aquatic systems based on expression profiling in lower eukaryotes. " PhD diss., University of Tennessee, 2009.
https://trace.tennessee.edu/utk_graddiss/6030

This Dissertation is brought to you for free and open access by the Graduate School at TRACE: Tennessee Research and Creative Exchange. It has been accepted for inclusion in Doctoral Dissertations by an authorized administrator of TRACE: Tennessee Research and Creative Exchange. For more information, please contact trace@utk.edu.

To the Graduate Council:

I am submitting herewith a dissertation written by Kathleen Daumer Cusick entitled "Proposed mechanism of action of saxitoxin in aquatic systems based on expression profiling in lower eukaryotes." I have examined the final electronic copy of this dissertation for form and content and recommend that it be accepted in partial fulfillment of the requirements for the degree of Doctor of Philosophy, with a major in Microbiology.

Gary S. Sayler, Major Professor

We have read this dissertation and recommend its acceptance:

Accepted for the Council:

Carolyn R. Hodges

Vice Provost and Dean of the Graduate School

(Original signatures are on file with official student records.)

To the Graduate Council:

I am submitting herewith a dissertation written by Kathleen Daumer Cusick entitled "Proposed Mechanism of Action of Saxitoxin in Aquatic Systems Based on Expression Profiling in Lower Eukaryotes." I have examined the final electronic copy of this dissertation for form and content and recommend that it be accepted in partial fulfillment of the requirement for the degree of Doctor of Philosophy, with a major in Microbiology.

We have read this dissertation
and recommend its acceptance:

Gary S. Saylor, Major Professor

Jeffrey M. Becker

Barry D. Bruce

Steven. W. Wilhelm

Jay L. Garland

Accepted for the Council:

Carolyn R. Hodges
Vice Provost and Dean of the Graduate School

(Original signatures are on file with official student records.)

**Proposed Mechanism of Action of Saxitoxin in Aquatic Systems
Based on Expression Profiling in Lower Eukaryotes**

A Dissertation
Presented for the
Doctor of Philosophy Degree
The University of Tennessee, Knoxville

Kathleen D. Cusick
May 2009

Dedication

This dissertation is absolutely and unequivocally dedicated to my husband, Greg Cusick. I will never forget standing outside my newly-rented little house in 4th and Gill on a particular day in August 2004, waving as his blue truck disappeared down the street, back towards Florida, tears streaming down my face. I had told him – and myself as well – that I would only be gone one and a half years, and would return to Florida and Kennedy Space Center to conduct most of my research. Four and a half years later, I sit in a bigger house (still in 4th and Gill, sometimes I wonder whether people ever leave this neighborhood) finishing this dissertation. I spent most of my time here in Knoxville conducting my experiments, never making it back to KSC as I had thought. However, throughout the years, my husband has supported me unwaveringly (both emotionally and financially!), all the while maintaining his amazing job and our house in Florida. And so, thank-you, thank-you, thank-you, Greg, for all YOUR hard work and sacrifice these past few years helping me achieve this degree.

Acknowledgements

This research, much like the trails leading to “Rocky Top,” in the Smokies, has followed a winded and twisting path. I have to thank my committee members for their guidance and input during this journey: my advisor, Dr. Gary Sayler, for his knowledge and patience; Dr. Steve Wilhelm, to whom I owe an office chair as I wore out the one in his office discussing copper homeostasis; Dr. Jeff Becker, who provided me with essential yeast background; Dr. Jay Garland, for asking me when I was going to get my PhD; and Dr. Barry Bruce, who made at least one groundbreaking, brilliant comment at each committee meeting – especially that CYC6 suggestion. They are a very well-traveled bunch and it was sometimes very tough to get them all in one place at one time for a committee meeting (and then Barry would still walk in late), but this research ended up encompassing many different topics, and all of them were able to make specific contributions at different points throughout its duration.

Thank-you to CEB lab personnel both past and present for your support and advice. Special thanks to Jack McPherson, Jenn DeBruyn, Shawn Hawkins, and Kim Cook.

I would also like to thank Dr. Rebecca Morgan, Theresa Johnston and Amy; meeting them was a serendipitous event, and the lessons I learned from them I will carry with me not only on to the “playing field,” but through life.

Thank my parents, Ed and Helen Daumer, for their love and support not only during my time here at UT but throughout my life.

One final thank-you: to my neighbors, the Parkers, for their kindness and friendship. They really are the best neighbors in the world. And we will catch that raccoon, Tim!

Abstract

Saxitoxin is a secondary metabolite produced by several species of dinoflagellates and cyanobacteria. The molecular target in mammals and higher eukaryotes is the sodium channel protein in nerve and muscle cells, where it binds with high affinity and effectively blocks the inward flow of sodium ions. The molecular target of saxitoxin in lower eukaryotes, such as those inhabiting the same ecosystems as the toxin-producing algae, is not known. The role of the toxin in the ecology of the algae is also a mystery.

This dissertation sought to determine the molecular effects and possible target of saxitoxin on lower eukaryotes as a means to gain insights on the function of the toxin within the ecosystem. Global expression profiling with the yeast *Saccharomyces cerevisiae* using the Affymetrix GeneChip identified a set of genes commonly associated with copper homeostasis as being significantly differentially expressed upon short-term exposure to saxitoxin. The pattern of regulation of these genes was then compared to the patterns generated upon exposure to excess copper and excess iron using quantitative reverse-transcriptase PCR. The repression of two genes, *FET3* and *CTR1*, suggested intracellular copper levels may be compromised when cells were in the presence of saxitoxin.

To further explore the hypothesis of saxitoxin altering internal copper levels, a comparative transcriptomics study was performed with the green alga *Chlamydomonas reinhardtii*. Expression profiles of a pre-defined set of genes were compared following exposure to saxitoxin and excess copper, with results indicating that saxitoxin was also altering copper homeostasis in *C. reinhardtii*. The established model of copper transport in *S. cerevisiae* coupled with the known structural design of the Ctr1 protein suggests that saxitoxin is binding to plasma membrane copper transporters, in a manner analogous to that of sodium channel binding.

The final section of this dissertation examined the phylogenetic relationship between two varieties of the dinoflagellate *Pyrodinium bahamense*. While var. *compressum* is an established saxitoxin producer, it has been determined that var. *bahamense* was the source of recent saxitoxin outbreaks in the western Atlantic.

Based on small subunit ribosomal RNA gene sequences, the two are 99% identical, suggesting a reclassification based on genetic rather than morphological features.

Table of Contents

PART I.....	1
LITERATURE REVIEW	1
BACKGROUND OF SAXITOXIN	2
<i>Molecular Description</i>	2
<i>Phylogenetic Distribution and Biosynthesis</i>	2
<i>Molecular Pharmacology</i>	4
<i>Environmental Impacts and Threats to Human Health</i>	8
<i>Ecological Functions</i>	8
DNA MICROARRAYS	12
<i>Microarrays for Global Expression Profiling</i>	12
<i>Platform Overview</i>	13
REAL-TIME REVERSE-TRANSCRIPTASE PCR	17
<i>Background</i>	17
<i>Reverse Transcription Reaction</i>	18
<i>Enzyme Format</i>	19
<i>Detection Chemistries</i>	20
DNA-Binding Dyes	20
Hydrolysis Probes	20
Hairpin Probes	21
Hybridization Probes	24
<i>Methods of Quantification</i>	24
Absolute Quantification	24
The Importance of PCR Amplification Efficiency in Relative Quantification	25
Relative Quantification Models	28
<i>Comparison of Methods</i>	31
<i>Normalization</i>	32
RIBOSOMAL RNA GENES FOR SPECIES IDENTIFICATION.....	33
GENERAL OBJECTIVES AND HYPOTHESES	36
REFERENCES	38
PART II.....	46
TRANSCRIPTIONAL PROFILING OF SACCHAROMYCES CEREVISIAE	
UPON EXPOSURE TO SAXITOXIN	46
ABSTRACT	47
INTRODUCTION	48
METHODS	50
<i>Yeast Strains</i>	50
<i>Chemicals</i>	51
<i>Growth Curves</i>	51
<i>Physiological Screening: Bioluminescent Microtiter Plate Assay</i>	51
<i>Saxitoxin Exposures</i>	52

<i>Cell Harvesting</i>	52
<i>Total RNA Extraction</i>	52
<i>Microarray Analyses</i>	53
<i>Microarray Statistical Analysis</i>	54
<i>Quantitative Reverse-Transcriptase PCR</i>	54
Primer and Probe Design	54
Determination of Primer Specificity	55
Assay Optimization.....	57
Preparation of RNA Standards.....	58
Preparation of Standard Curve.....	61
Validation of ACT1 as an Appropriate Housekeeping Gene.....	61
<i>qRT-PCR Data Normalization and Statistical Analyses</i>	62
RESULTS	64
<i>Growth Curves</i>	64
<i>Bioluminescent Yeast Screen</i>	64
<i>Microarray Analyses</i>	64
<i>Verification of Microarray Results</i>	67
DISCUSSION	67
APPENDIX	78
REFERENCES	84
PART III	90
COMPARISON OF SACCHAROMYCES CEREVISIAE EXPRESSION PROFILES FOLLOWING EXPOSURE TO SAXITOXIN, COPPER, AND IRON	90
ABSTRACT	91
INTRODUCTION	92
METHODS AND MATERIALS	95
<i>Yeast Strains</i>	95
<i>Chemicals</i>	95
<i>Growth Curves</i>	96
<i>Saxitoxin and Metal Exposures</i>	96
<i>Cell Harvesting and Total RNA Extraction</i>	97
<i>Quantitative Reverse-Transcriptase PCR</i>	97
Development of ENB1 and SLF1 Assays.....	97
<i>Data Normalization</i>	98
<i>Statistical Analysis: Single Treatment</i>	98
<i>Statistical Analysis: Comparison of Normalized Values among Treatments</i>	98
RESULTS	99
<i>Media Selection</i>	99
<i>Growth Curves</i>	99
<i>Expression Profiling</i>	102
DISCUSSION	110
APPENDIX I	116
REFERENCES	119

PART IV	123
ROLE OF THE TRANSCRIPTIONAL REGULATOR MAC1P IN MEDIATING GENE EXPRESSION UPON EXPOSURE TO SAXITOXIN IN SACCHAROMYCES CEREVISIAE	123
ABSTRACT	124
INTRODUCTION	125
INTRODUCTION	125
METHODS AND MATERIALS	127
<i>Yeast Strains</i>	127
<i>Growth Curves</i>	127
<i>Halo Assays</i>	128
<i>Chemicals</i>	128
<i>Saxitoxin Exposures</i>	128
<i>Cell Harvesting and Total RNA Extraction</i>	129
<i>Quantitative Reverse-Transcriptase PCR</i>	129
<i>Data Normalization</i>	129
<i>Statistical Analysis: Exposed versus Control</i>	129
<i>Statistical Analysis: Between Strains</i>	130
RESULTS	130
<i>Growth Curves</i>	130
<i>Halo Assays</i>	131
<i>Expression Profiling</i>	131
DISCUSSION	137
REFERENCES	139
PART V.....	145
EXPRESSION PROFILE COMPARISONS IN <i>CHLAMYDOMONAS REINHARDTII</i> FOLLOWING EXPOSURE TO SAXITOXIN AND COPPER	145
ABSTRACT	146
INTRODUCTION	147
METHODS AND MATERIALS	149
<i>Chemicals</i>	149
<i>Strains and Culture Conditions</i>	150
<i>Growth Curves</i>	150
<i>Saxitoxin and Copper Exposures</i>	150
<i>Cell Harvesting</i>	151
<i>RNA Extraction</i>	151
<i>DNase Treatment</i>	153
<i>Real-Time Reverse-Transcriptase PCR</i>	153
Real-Time RT-PCR Assays	153
PCR Efficiencies.....	154
<i>Data Normalization and Analysis</i>	156
<i>Statistics</i>	156

RESULTS	157
<i>Growth Curve</i>	157
<i>Gene Expression Profiling</i>	157
DISCUSSION	161
APPENDIX I	166
REFERENCES	170
PART VI	176
PHYLOGENETIC ANALYSIS OF <i>PYRODINIUM BAHAMENSE</i> VAR. <i>BAHAMENSE</i> FROM THE INDIAN RIVER LAGOON, FL BASED ON SMALL SUBUNIT RIBOSOMAL DNA SEQUENCES.....	176
ABSTRACT	177
INTRODUCTION	178
METHODS AND MATERIALS	180
<i>Sample Collection</i>	180
<i>Cell Isolation</i>	180
<i>DNA Extraction from Multiple Cells</i>	183
Freeze-thaw.....	183
<i>DNA Extraction from Single Cells</i>	183
Freeze-thaw	183
<i>Primer Sets</i>	183
<i>PCR Reagents</i>	184
<i>Thermocycling Programs</i>	187
<i>Cloning and Phylogenetic Analysis of <i>P. bahamense</i> SSU rDNA</i>	187
<i>Verification of DNA Extraction and Dinoflagellate-Specific Primer Sets using <i>Alexandrium fundyense</i></i>	188
Genomic DNA Extraction from Pure Culture and Isolated Cells (<i>A. fundyense</i>).....	188
18S Community Primers to Examine DNA Extraction Efficiency from Freeze-Thaw Lysis.....	189
Optimization of Dinoflagellate-Specific Primers	189
RESULTS	190
<i>DNA Extraction of <i>P. bahamense</i> environmental samples</i>	190
<i>Primer Sets and PCR Conditions</i>	192
<i>Successful Amplification with Primer Set <i>Pcomp400F/PcompR</i></i>	192
<i>Successful Amplification with Primer Set <i>Pcomp400F/PcompR2b</i></i>	193
DISCUSSION	193
APPENDIX I	200
REFERENCES	205
PART VII.....	208
CONCLUSIONS	208
EXPRESSION PROFILING TO ELUCIDATE THE MECHANISM OF ACTION OF SAXITOXIN ON LOWER EUKARYOTES	209

PHYLOGENETIC ANALYSIS OF P. BAHAMENSE.....	212
REFERENCES	213
VITA.....	214

List of Tables

TABLE II-1. LIST OF GENES EXAMINED WITH QUANTITATIVE REVERSE-TRANSCRIPTASE PCR FOLLOWING EXPOSURE TO SAXITOXIN ... ERROR! BOOKMARK NOT DEFINED.	
TABLE II-2. PRIMER SEQUENCES, ANNEALING TEMPERATURES, AND EXPECTED PRODUCT SIZE OF GENOMIC DNA TARGETS USED IN THE CREATION OF <i>IN-VITRO</i> TRANSCRIBED RNA STANDARDS..... ERROR! BOOKMARK NOT DEFINED.	
TABLE II-3. PCR EFFICIENCY OF EACH QRT-PCR ASSAY AS DERIVED FROM THE SLOPE OF INDIVIDUAL STANDARD CURVES..... ERROR! BOOKMARK NOT DEFINED.	
TABLE II-4. GENES INVOLVED IN COPPER AND IRON HOMEOSTASIS AND SULFUR METABOLISM IDENTIFIED AS SIGNIFICANTLY DIFFERENTIALLY EXPRESSED (p<0.01) IN MICROARRAY ANALYSIS FOLLOWING EXPOSURE TO 16 mM SAXITOXIN.....	68
TABLE II-6. AVERAGE FOLD-CHANGE OF GENES AMONG DIFFERENT SAXITOXIN TREATMENTS.....	69
TABLE II-5. COMPLETE LIST OF GENES IDENTIFIED AS SIGNIFICANTLY DIFFERENTIALLY EXPRESSED IN MICROARRAY EXPERIMENTS.... ERROR! BOOKMARK NOT DEFINED.	
TABLE III-1. PRIMER AND PROBE SEQUENCES, GENE FUNCTION, AND AMPLICON SIZE OF THE QUANTITATIVE REVERSE-TRANSCRIPTASE ASSAYS DEVELOPED FOR <i>ENB1</i> AND <i>SLF1</i>	117
TABLE III-2. PRIMER SEQUENCES, ANNEALING TEMPERATURES, AND EXPECTED PRODUCT SIZE USED FOR CONSTRUCTION OF <i>IN-VITRO</i> TRANSCRIBED STANDARDS OF <i>ENB1</i> AND <i>SLF1</i>	118
TABLE III-3. PCR EFFICIENCY OF <i>SLF1</i> AND <i>ENB1</i> QRT-PCR ASSAYS.....	118
TABLE IV-1. AVERAGE LINEAR FOLD-CHANGE OF COPPER AND IRON HOMEOSTASIS GENES IN WILD-TYPE BY4742 AND <i>MAC1</i> Δ FOLLOWING EXPOSURE TO 16 mM SAXITOXIN	136
TABLE V-1. PRIMER AND PROBE SEQUENCES AND FUNCTION OF GENE EXAMINED WITH REAL-TIME RT-PCR	ERROR! BOOKMARK NOT DEFINED.
TABLE V-2. AVERAGE PCR EFFICIENCIES FOR EACH ASSAY AS CALCULATED WITH LINREGPCR	169
TABLE VI-1. LIST OF PRIMERS USED IN ATTEMPTS TO AMPLIFY VARIOUS REGIONS OF THE SSU rRNA GENE FROM <i>PYRODINIUM BAHAMENSE</i>	185

TABLE VI-2. LIST OF PRIMER COMBINATIONS USED IN ATTEMPTING TO AMPLIFY 18S
RDNA REGIONS FROM ENVIRONMENTAL SAMPLES OF *P. BAHAMENSE* 186

List of Figures

- FIGURE I-1. MOLECULAR STRUCTURE OF SAXITOXIN AND ITS DERIVATIVES **ERROR! BOOKMARK NOT DEFINED.**
- FIGURE I-2. REVISED PATHWAY FOR SAXITOXIN BIOSYNTHESIS..... **ERROR! BOOKMARK NOT DEFINED.**
- FIGURE I-3. STRUCTURAL ORGANIZATION OF THE *SXT* GENE CLUSTER IN THE CYANOBACTERIUM *CYLINDROSPERMOPSIS RACIBORSKII* T3 **ERROR! BOOKMARK NOT DEFINED.**
- FIGURE I-4. MAP OF GLOBAL PST DISTRIBUTION AS OF 2006 **ERROR! BOOKMARK NOT DEFINED.**
- FIGURE I-5. OVERVIEW OF RNA SAMPLE PREPARATION, HYBRIDIZATION, AND SCANNING USING THE AFFYMETRIX GENECHIP **ERROR! BOOKMARK NOT DEFINED.**
- FIGURE I-6. REAL-TIME RT-PCR USING THE TAQMAN ASSAY **ERROR! BOOKMARK NOT DEFINED.**
- FIGURE I-7. EXAMPLE OF EXTERNAL STANDARD CURVE USED IN ABSOLUTE QUANTIFICATION..... **ERROR! BOOKMARK NOT DEFINED.**
- FIGURE I-8. rDNA ORGANIZATION IN EUKARYOTIC CELLS.... **ERROR! BOOKMARK NOT DEFINED.**
- FIGURE II-2. EFFECTS OF SAXITOXIN ON CONSTITUTATIVE BIOLUMINESCENCE OF *S. CEREVISIAE* CEB585..... **ERROR! BOOKMARK NOT DEFINED.**
- FIGURE II-3. GENES DIFFERENTIALLY EXPRESSED IN MICROARRAY WERE CLASSIFIED INTO FUNCTIONAL GROUPS BASED ON MOLECULAR AND BIOLOGICAL FUNCTIONS **ERROR! BOOKMARK NOT DEFINED.**
- FIGURE II-4. NORMALIZED EXPRESSION PROFILES OBTAINED FROM qRT-PCR ASSAYS FOR A SUBSET OF GENES IDENTIFIED AS SIGNIFICANTLY DIFFERENTIALLY EXPRESSED IN MICROARRAY EXPERIMENTS.... **ERROR! BOOKMARK NOT DEFINED.**
- FIGURE II-1. GROWTH CURVES OF *S. CEREVISIAE* S288C GROWN IN YPD BROTH AND EXPOSED TO A RANGE OF SAXITOXIN CONCENTRATIONS RANGING FROM 0-32 mM **ERROR! BOOKMARK NOT DEFINED.**
- FIGURE III-1. COPPER AND IRON UPTAKE IN *S. CEREVISIAE* **ERROR! BOOKMARK NOT DEFINED.**

FIGURE III-2. GROWTH CURVES OF <i>S. CEREVISIAE</i> S288C CONDUCTED WITH A RANGE OF COPPER CONCENTRATIONS	100
FIGURE III-3. GROWTH CURVES OF <i>S. CEREVISIAE</i> S288C CONDUCTED WITH A RANGE OF IRON CONCENTRATIONS	101
FIGURE III-4. AVERAGE NORMALIZED TRANSCRIPT COPY NUMBERS FOR EACH FUNCTIONAL GENE FOLLOWING EXPOSURE TO SAXITOXIN ERROR! BOOKMARK NOT DEFINED.	
FIGURE III-5. AVERAGE NORMALIZED TRANSCRIPT COPY NUMBERS FOR EACH FUNCTIONAL GENE FOLLOWING EXPOSURE TO COPPER SULFATE..... ERROR! BOOKMARK NOT DEFINED.	
FIGURE III-6. AVERAGE NORMALIZED TRANSCRIPT COPY NUMBERS FOR EACH FUNCTIONAL GENE FOLLOWING EXPOSURE TO FERRIC SULFATE..... ERROR! BOOKMARK NOT DEFINED.	
FIGURE III-7. COMPARISON IN GENE REGULATION LEVELS AMONG SAXITOXIN, COPPER, AND IRON TREATMENTS	106
FIGURE III-8. RIBBON STRUCTURE OF FET3P (REDRAWN FROM (TAYLOR ET AL. 2005)) ILLUSTRATING THE LOCATIONS OF THE FOUR COPPER IONS REQUIRED FOR ENZYME FUNCTION.....	111
FIGURE III-9. DOMAIN ORGANIZATION AND TOPOLOGY OF CTR1 PROTEIN.	113
FIGURE IV-1. GROWTH CURVES OF WILD-TYPE BY4742 AND <i>MAC1</i> Δ IN SYNTHETIC COMPLETE BROTH SUPPLEMENTED WITH 0.2% CASAMINO ACIDS.....	132
FIGURE IV-2. HALO ASSAYS PERFORMED WITH WILD-TYPE BY4742 AND <i>MAC1</i> Δ	133
FIGURE IV-3. NORMALIZED TRANSCRIPT COPIES IN WILD-TYPE BY4742 AS MEASURED FOLLOWING EXPOSURE TO 16 mM SAXITOXIN IN SCCA	134
FIGURE IV-4. NORMALIZED TRANSCRIPT COPIES IN BY4742 <i>MAC1</i> Δ AS MEASURED FOLLOWING EXPOSURE TO 16 mM SAXITOXIN IN SCCA	135
FIGURE V-3. COMPARISON IN AVERAGE GENE EXPRESSION LEVELS IN <i>C. REINHARDTII</i> FOLLOWING EXPOSURE TO 16 mM SAXITOXIN AND 8 mM COPPER SULFATE	158
FIGURE V-4. COPPER SULFATE AND COPPER GLUTAMATE TARGET THE PLASMA MEMBRANES IN <i>ALEXANDRIUM</i> SPP.	164

FIGURE V-1. COMPARISON OF PCR EFFICIENCIES BETWEEN <i>RBC L</i> AND <i>TRX M</i> ASSAYS	167
FIGURE V-2. STANDARD CURVE USED IN RELATIVE QUANTIFICATION OF GENE EXPRESSION IN <i>C. REINHARDTII</i>	168
FIGURE VI-1. SAMPLING SITES IN THE INDIAN RIVER LAGOON.....	181
FIGURE VI-2. LIGHT MICROSCOPY IMAGE REPRESENTATIVE OF <i>P. BAHAMENSE</i> CELLS ISOLATED FROM SITES WITHIN THE INDIAN RIVER LAGOON.....	182
FIGURE VI-7. GEL IMAGE OF GENOMIC DNA FROM <i>P. BAHAMENSE</i> ENVIRONMENTAL SAMPLES	191
FIGURE VI-8. NEIGHBOR-JOINING TREE OF SSU rDNA SEQUENCES FROM INDIAN RIVER LAGOON, FL (SITE VR13).....	194
FIGURE VI-9. NEIGHBOR-JOINING TREE OF SSU rDNA SEQUENCES FROM INDIAN RIVER LAGOON, FL (SITE ML02)	196
FIGURE VI-3. GEL IMAGE OF PCR-AMPLIFIED SSU rDNA FROM <i>A. FUNDEYENSE</i> USING UNIVERSAL PRIMERS FOR EUKARYOTE SSU rDNA	201
FIGURE VI-4. DINOFLAGELLATE-SPECIFIC PRIMER SETS TESTED ON <i>A. FUNDYENSE</i> GENOMIC DNA	202
FIGURE VI-5. OPTIMIZATION OF PRIMER SET 18SCOMF1/DINO18SR1	203
FIGURE VI-6. SPECIFICITY OF PRIMER SET 18SCOMF1/DINO18SR1 FOR DINOFLAGELLATE SSU rDNA.....	204

Part I
Literature Review

Background of Saxitoxin

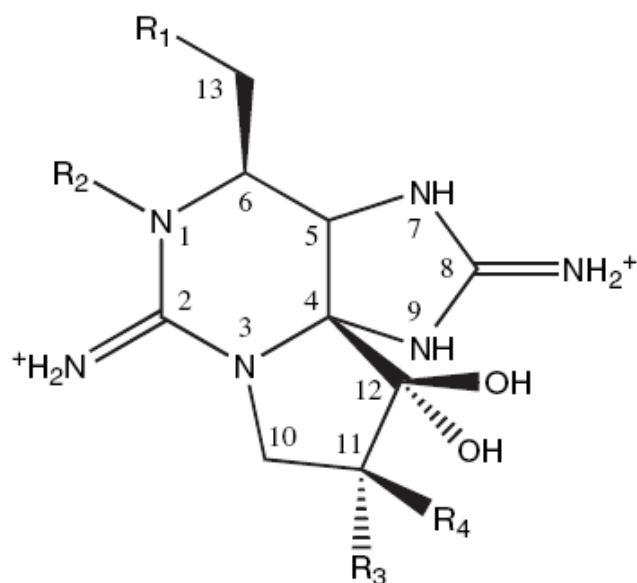
Molecular Description

Saxitoxin is a naturally-occurring secondary metabolite produced by microorganisms from several phyla inhabiting a range of aquatic environments. Due to its molecular target and resulting detrimental effects on human health, it is often described as a potent neurotoxin. It is typically referred to as the parent molecule in the class of compounds also known as Paralytic Shellfish Toxins (PSTs), of which there are over 20 derivatives. The toxicity of the derivatives varies by approximately 2 orders of magnitude (Hall 1990), with saxitoxin (STX) being the most toxic.

Saxitoxin and its congeners are based on a perhydropurine skeleton with two permanent guanidinium moieties. The 1,2,3- and 7,8,9-guanidino groups of saxitoxin possess pKa's of 11.3 and 8.2, respectively, so that at physiological pH, the 1,2,3-guanidino carries a positive charge, whereas the 7,8,9-guanidino group is partially deprotonated. Due to its polar nature, saxitoxin is able to dissolve in water and lower alcohols but remains insoluble in organic solvents (<http://www3.aims.gov.au/arnat/arnat-0008.htm>). Variations in functional groups at four defined positions around the ring define the different congeners (Figure I-1). The divisions consist of the carbamate toxins, all of which have a carbamoyl at the R1 position; the N-sulfocarbamoyl toxins; the decarbamoyl toxins; and the deoxydecarbamoyl toxins. Of the different classes, the carbamate toxins are considered the most toxic.

Phylogenetic Distribution and Biosynthesis

Organisms responsible for the production of saxitoxin occur throughout a range of aquatic habitats. Dinoflagellates from the genera *Alexandrium*, *Gymnodinium*, and *Pyrodinium* (Harada et al. 1982b, Oshima et al. 1987, Anderson et al. 1990) are established toxin producers in marine and estuarine (Hallegraeff et al. 1988) systems, while filamentous cyanobacteria from the genera *Planktothrix* (Pomati et al. 2000), *Lyngbya* (Carmichael et al. 1997), *Anabaena* (Negri & Jones 1995), *Aphanizomenon* (Ferreira et al. 2001) and *Cylindrospermopsis* (Lagos et al. 1999) are the predominate producers in freshwater systems. Molecular phylogeny and



R-1	R-2	R-3	R-4	Compound name
Carbamates	-H	-H	-H	STX
	-OH	-H	-H	neoSTX
$\begin{array}{c} \text{O} \\ \parallel \\ -\text{C}-\text{O}-\text{NH}_2 \end{array}$	-OH	$-\text{OSO}_3^-$	-H	GTX-1
	-H	$-\text{OSO}_3^-$	-H	GTX-2
	-H	-H	$-\text{OSO}_3^-$	GTX-3
	-OH	-H	$-\text{OSO}_3^-$	GTX-4
N-sulfocarbamates	-H	-H	-H	GTX-5
	-OH	-H	-H	GTX-6
$\begin{array}{c} \text{O} \quad \text{H} \\ \parallel \quad \\ -\text{C}-\text{O}-\text{N}-\text{SO}_3^- \end{array}$	-OH	$-\text{OSO}_3^-$	-H	C-3
	-H	$-\text{OSO}_3^-$	-H	C-1
	-H	-H	$-\text{OSO}_3^-$	C-2
	-OH	-H	$-\text{OSO}_3^-$	C-4
Decarbamoyl toxins	-H	-H	-H	dcSTX
	-OH	-H	-H	dcneoSTX
-OH	-OH	$-\text{OSO}_3^-$	-H	dcGTX-1
	-H	$-\text{OSO}_3^-$	-H	dcGTX-2
	-H	-H	$-\text{OSO}_3^-$	dcGTX-3
	-OH	-H	$-\text{OSO}_3^-$	dcGTX-4
Deoxy toxins	-H	-H	-H	doSTX
	-OH	$-\text{OSO}_3^-$	-H	doGTX-2
-H	-OH	-H	$-\text{OSO}_3^-$	doGTX-3

Figure I-1. Molecular structure of saxitoxin and its derivatives (figure modified from (Kellmann & Neilan 2007). Abbreviations: C, C-toxin; dc, decarbamoyl; do, deoxy; GTX, gonyautoxin; STX, saxitoxin.

phylogenetic inferences based on thecal plate homology and ultrastructure in dinoflagellates show a random distribution among dinoflagellate genera for the ability of toxin production.

Though the capacity for toxin production is scattered across both pro- and eukaryotic groups, the pathway for saxitoxin biosynthesis is believed to be similar between cyanobacteria and dinoflagellates (Shimizu 1993), and was initially proposed based on extensive studies using labeled precursors with the dinoflagellate *Alexandrium tamarense* and the cyanobacterium *Aphanizomenon flos-aquae* (Shimizu 1993, Shimizu 1996). However, recent genetic information (Kellmann et al. 2008), coupled with screening of the biosynthetic intermediates and the recent *in-vitro* biosynthesis of saxitoxin (Kellmann & Neilan 2007), has resulted in modifications of the original pathway (Figure I-2).

The gene cluster coding for saxitoxin biosynthesis (Figure I-3), recently discovered in a toxic strain of cyanobacterium, is approximately 35 kb and contains 26 proteins (Kellmann et al. 2008). Bioinformatic analysis suggests that saxitoxin biosynthesis evolved in an ancient cyanobacterium, with some of the genes acquired through horizontal gene transfer with other bacteria. Characteristics of the gene cluster, such as its structural organization and presence of transposases, suggest that several of its cassettes are mobile. Similar genetic information has not yet been obtained for dinoflagellates, though it is reportedly underway (Kellmann et al. 2008).

Molecular Pharmacology

The molecular target of saxitoxin is the sodium channel protein of nerve and muscle cells in mammals. It binds with high affinity to site 1 of the alpha subunit, preventing the passage of sodium ions through the cell membrane and thus blocking the passage of nerve impulses (Catterall 1985). In most organisms, the sodium channel protein consists solely of the alpha subunit, a single polypeptide comprised of 1,820 amino acid residues that form four homologous domains which are connected by shorter stretches of non-homologous residues.

Each domain of the alpha subunit folds into six transmembrane alpha-helices. Through the analysis of interactions with mutated forms of μ -conotoxin (GIIIA), it

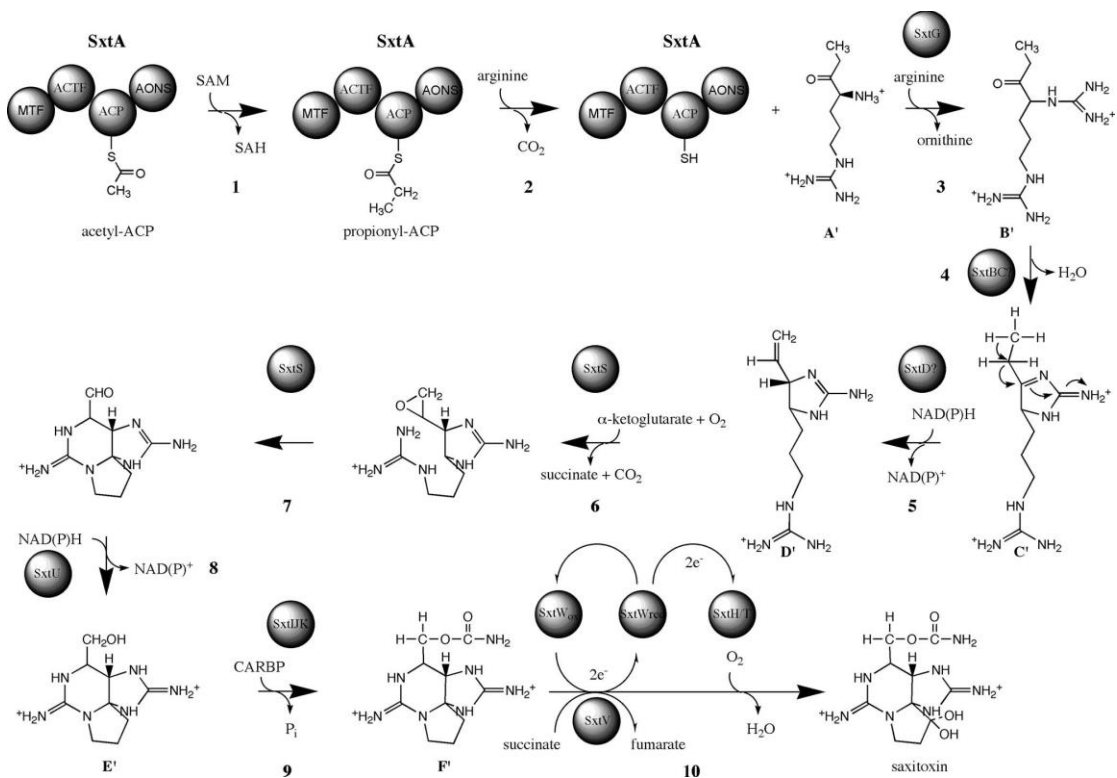


Figure I-2. Revised pathway for saxitoxin biosynthesis, including putative gene functions (redrawn from (Kellmann et al. 2008)). The reaction steps are proposed as follows: 1-2, Saxitoxin biosynthesis is believed to initiate with SxtA. The original model proposed condensation of arginine to acetate as the initial step, with the methyl side chain introduced later. However, in the revised reaction scheme, the acyl carrier protein (ACP) is loaded with acetate from acetyl Co-A, followed by methylation of acetyl-ACP by SxtA3. SxtA4 then performs the Claisen condensation. The presence of the putative intermediate, designated A', was confirmed via LC-MS-MA, while the originally-proposed intermediate was not detected; 3, Amidino transfer from arginine to α -amino A' group (B') via SxtG; 4, First cyclization via retroaldol cleavage of ammonia from cytidine (SxtB); 5-8, Hydroxylation and bicyclicization via SxtD, SxtS, and SxtU; 9-10, Final reactions involve carbamoyl transfer and dihydroxylation, though the exact order remains unknown.

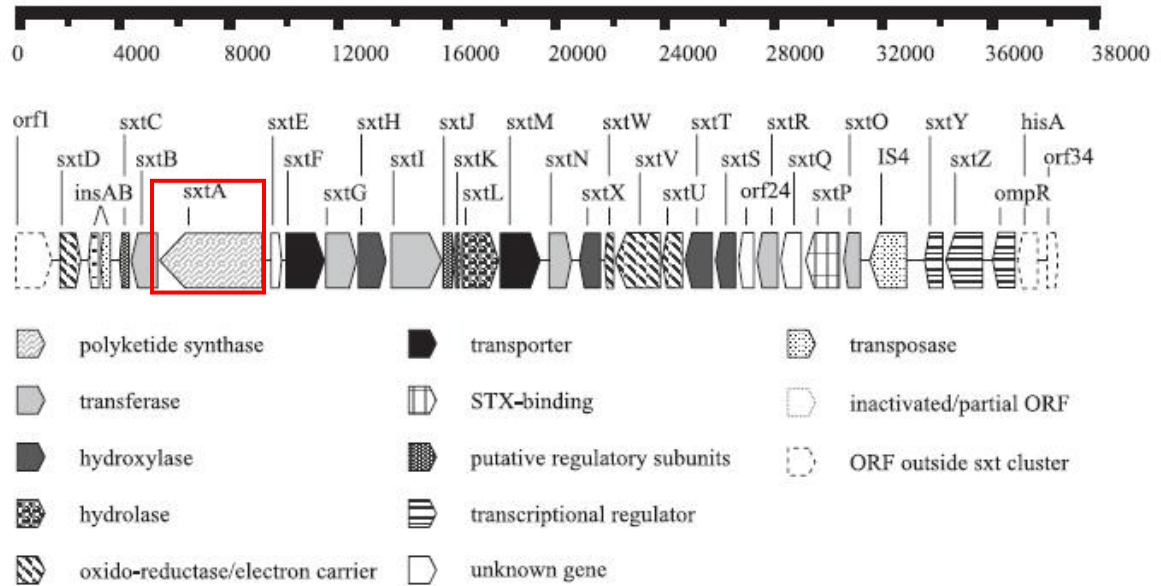


Figure I-3. Structural organization of the *sxt* gene cluster in the cyanobacterium *Cylandrospormopsis raciborskii* T3 (redrawn from (Kellmann et al. 2008)). The *sxtA* (red box) gene codes for a protein that is homologous to a polyketide-synthase and is comprised of four catalytic domains: SxtA1 contains three conserved sequence motifs for SAM-dependent methyltransferases; SxtA2 is related to N-acetyl transferases; SxtA3 is related to an acyl carrier protein; while SxtA4 is homologous to class II aminotransferases, the only enzymes known to perform Claisen condensation of amino acids. Abbreviations: IS4, insertion sequence 4; ompR, transcriptional regulator of *ompR* family; hisA, two-component histidine kinase.

was determined that the four sodium channel domains are arranged in clockwise configuration (Li et al. 2001). A central pore is formed through the arrangement of the transmembrane helices of the four domains, with a voltage gate situated at the interior of the pore and a selectivity filter at the outer vestibule. Extracellular loops between the fifth and sixth transmembrane helices of each domain are known as pore-forming (P) loops. These loops fold back into the membrane to form the outer lining of the pore and the selectivity filter.

Two clusters of predominantly negatively charged residues contribute to toxin sensitivity (Terlau et al. 1991). Cluster one is comprised of the residues aspartic acid(D)384 in domain I, glutamic acid(E)942 in domain II, lysine(K)1423 in domain III, and alanine(A)1714 in domain IV, while cluster two contains E387, E945, methionine(M)1425, and D1717 (located in domains I-IV, respectively). It has been suggested that these clusters may form ring structures that line the outer lip of the pore. An inactivation gate that is controlled by a voltage sensor is situated between the third and fourth domains; a binding site in the sodium channel causes conformational changes when bound with the inactivation gate, thus closing the channel to sodium ions.

The 7,8,9 guanidinium moiety is necessary for the blocking action of saxitoxin (Baden & Trainer 1993). Saxitoxin is able to effectively block the inward flow of sodium ions into the cell in a dose-dependent manner, with no effect on the resting membrane potential or potassium channels. Guanidinium is able to act as a cationic substitute for the sodium ion in action potential generation; thus, it has been proposed that it is the guanidinium moiety that enters the channel, while the remainder of the toxin blocks further ion passage into the channel. Studies of sodium channel inhibition at different pH values have shown that saxitoxin has a greater effect at neutral pH, due to protonation of its hydroxyl groups (Baden & Trainer 1993). Both the guanidinium and hydroxyl groups are needed for sodium channel recognition by the toxin, as modifications near either of these moieties have resulted in loss of biological function of the toxin.

Environmental Impacts and Threats to Human Health

The environmental impacts of saxitoxin are being felt increasingly on a global scale, as essentially all coastal regions have been exposed to PSTs (Figure I-4). These PST outbreaks are also felt on a socioeconomic scale, due to their effects on both human health and the financial health of industries such as fisheries and tourism. Saxitoxin and its congeners are the causative agents of paralytic shellfish poisoning (PSP), and, more recently, Pufferfish Poisoning (PFP) (Landsberg et al. 2006). In the case of PSP, filter-feeding mollusks and crustaceans ingest the toxic cells, concentrating the toxins within the organs and tissues. The shellfish themselves are typically not affected by the toxins, as their nerve and muscle cells are operated mainly by voltage-gated calcium channels rather than sodium channels (Kao 1993). Human consumption of the toxic shellfish results in respiratory paralysis, and, in some cases, death, as the PSTs are highly lethal. PFP is a similar illness, except that bioaccumulation occurs in pufferfish rather than shellfish. Comparing the LD₅₀ value of saxitoxin to that of cyanide illustrates the lethality of saxitoxin: while the LD₅₀ for saxitoxin in mice is 8-10 µg kg⁻¹, that of cyanide is 10 mg kg⁻¹ (Deeds et al. 2008); thus, a single dose of approximately 200 µg is fatal for the average weight human being. It is also worth noting that saxitoxin and ricin are the only two natural toxins classified as Schedule I Chemical Warfare Agents per the Chemical Weapons Convention in 1993 (www.fas.org 2008).

Ecological Functions

Due to their detrimental affects on human health, saxitoxin and its derivatives are often described as potent neurotoxins. However, these molecules are actually secondary metabolites, compounds produced by the cell when all the requirements for the primary metabolites have been met (Lucker 1984). Thus, “toxin” is an anthropogenic term; it is the descriptor assigned to these molecules due to their effects on humans.

In the evolutionary sense, dinoflagellates are an ancient group: the first evidence of their existence dates back to the early Triassic period (245-208 million years ago). Thus, toxin production did not emerge for the purpose of the blocking of

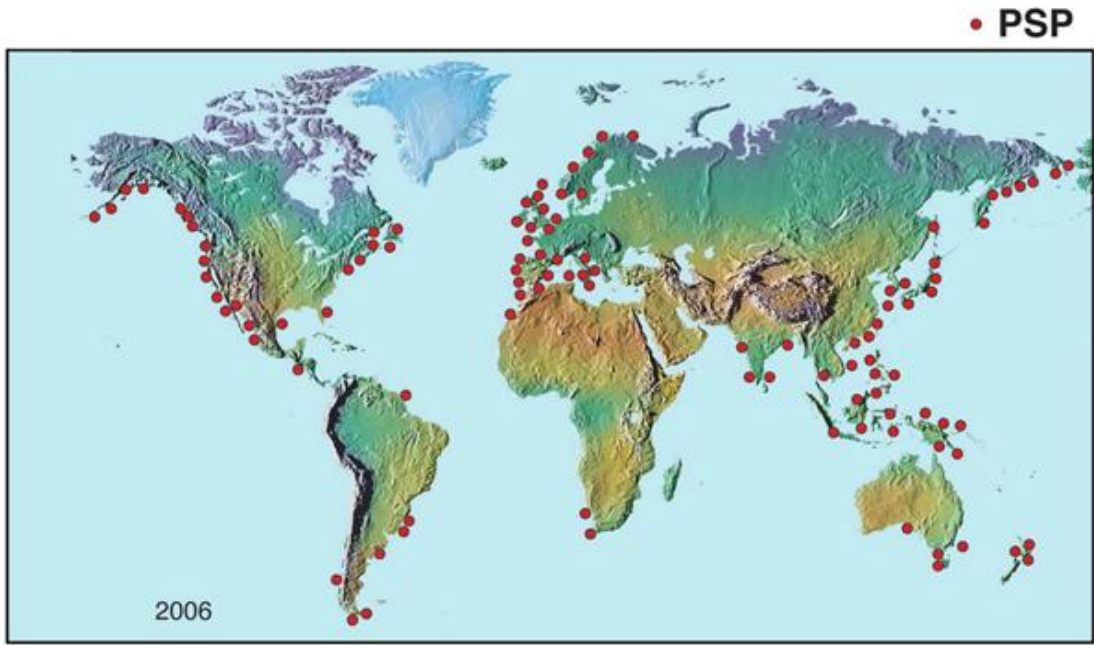


Figure I-4. Map of global PST distribution as of 2006 (<http://www.whoi.edu>).

the sodium channel in humans and other mammals. It is likely that these molecules are not intended to serve a toxic role, or, as is the case with tetrodotoxin, that the toxin even has the same function among different species (Wyatt & Jenkinson 1997).

Tetrodotoxin is similar to saxitoxin in both structure and function, and is able to bind to both the voltage-gated sodium and potassium channels. Tetrodotoxin is widely distributed among the animal kingdom, with varied functions: in the blue ringed octopus (*Hapalochlaena maculosa*) and tropical flatworms, it is used to paralyze the prey, while in pufferfish (*Fugu niphobles*) it functions as a pheromone (Wyatt & Jenkinson 1997, Ritson-Williams et al. 2006).

A multitude of hypotheses have been proposed as to the role these toxins serve. PSTs have been suggested to function as pheromones, as they possess some of the same characteristics of established pheromone molecules; these include low levels of secretion (10^{-9} - 10^{-10} M) and profiles similar to that of terrestrial animal species, in which a mixture of compounds, rather than a single species, is produced (Wyatt & Jenkinson 1997). Immunolocalization of saxitoxin in the nucleus of toxic dinoflagellates in close proximity to the chromosomes (Anderson & Cheng 1988) suggests that it may play a role in chromosome structural organization; the two positively-charged guanidinium groups may bind in a manner analogous to that of polyamines or other divalent cations. However, the question then becomes: what molecule functions as the substitute for saxitoxin in non-toxic cells? Due to the large number of nitrogen atoms within saxitoxin, it has also been speculated that the molecule may play a role in nitrogen storage, though this suggestion has been countered with the fact that nitrogen storage would be accomplished in a more bioenergetically efficient fashion through the use of lower molecular weight compounds such as amino acids or urea (Cembella 1998).

The most popular and well-studied hypothesis as to the role of saxitoxin is that it functions as a grazing deterrent. Many different organisms, including multiple zooplankton species, larval and adult fish, and larval and adult macroinvertebrates have all been shown to feed on PST-producing dinoflagellates; however, its effects have shown a range of results (Zimmer & Ferrer 2007). Numerous studies on the

bioaccumulation of saxitoxin have shown the ability of bivalves and crustaceans to accumulate high levels of the toxin (Robineau et al. 1991, Negri & Jones 1995, Oikawa et al. 2005), in effect refuting its role as a grazing deterrent in mollusks. A multitude of effects have been observed in zooplankton exposed to PSTs, ranging from a decrease in prey consumption and swimming rates, to no effects, to a stimulation in feeding (White 1981, Camacho & Thacker 2006).

Contradicting results exist in the literature as to whether zooplankton species actively reject toxic cells. Some results seem to suggest that dinoflagellate cells containing PSTs could be discerned by copepods prior to ingestion (Teegarden 1999). While multiple species of copepods have exhibited little to no change in feeding behavior when presented with toxic cells, subsequent effects then included an increase in mortality and a decrease in reproductive success (Frangoulos et al. 2000, da Costa et al. 2005, Barreiro et al. 2006). A suggested scenario has been that grazing pressure is alleviated in toxin-producing species allowing for bloom formation; however, recent lab-based studies refute this scenario (Barreiro et al. 2006). Ecosystem modeling that included multiple species of phyto- and zooplankton along with bacteria in an enclosed system indicated that the overall impact of toxin production was small and would not cause appreciable modifications in the long-term evolution of the system (Solé et al. 2006).

Most studies presume that it is the production of saxitoxin that alters the feeding behaviors or reproductive mechanisms of zooplankton. However, both toxic and non-toxic strains of *Alexandrium* spp. are able to produce an extracellular compound with allelopathic effects on other species of dinoflagellates, the ultimate outcomes of which were loss of motility and cell lysis (Tillmann & John 2002). Similar results have recently been obtained with gastropod larvae: exposure to toxic or non-toxic *Alexandrium* spp. resulted in feeding inhibition and ultimate death by an as-yet unidentified compound (Juhl et al. 2008).

In some situations where saxitoxin appears to act as a grazing deterrent, the grazers (both zooplankton and fish) typically discard the cells after contact, suggesting that the toxin targets the gustatory and/or olfactory senses (Zimmer &

Ferrer 2007). Electrophysiological experiments with different species of fish have shown sensitive and specific gustatory receptor responses to saxitoxin and tetrodotoxin (Yamamori et al. 1987); additionally, both larval and adult newts exhibit different responses to similar concentrations of the two toxins (Zimmer & Ferrer 2007). Collectively, these data indicate that while the two toxins share the same molecular target in higher vertebrates and mammals, different targets exist within lower vertebrates.

DNA Microarrays

Microarrays for Global Expression Profiling

While the molecular target of saxitoxin has been clearly defined in mammals, its mechanism of action on the lower eukaryotic community members (i.e. protists and zooplankton) that are found within the same aquatic systems as the toxic cells remains unknown. First used in the fields of molecular medicine and pharmacology (Celis et al. 2000, Cooper 2001, Luo & Geschwind 2001, DeFilippis et al. 2003), global expression profiling through the use of DNA microarrays is fast becoming a common tool in the field of ecotoxicology as a means of evaluating the effects of a toxicant on an organism or cell.

“Ecotoxicogenomics” examines the gene or protein expression in non-target organisms in response to toxicant exposures (Snape et al. 2004). Previous methods used to assess the impacts of contaminants within aquatic systems were based on the measurement of whole-organism end-point responses such as growth, reproduction, and mortality. However, these methods provided little information on the mechanism of action of the contaminant. DNA microarrays are now being used in ecotoxicology, with the goal of obtaining the genetic signature of an organism in response to a contaminant. This genetic signature, as defined by its gene expression profile, can provide insights into the mechanism of action of the contaminant (Lettieri 2006). Understanding the mechanism of action may aid in predicting responses across a range of phylogenetic groups that are present in aquatic ecosystems, estimating the effects at the population level, and assessing the impacts of the contaminant in

chronic versus short-term exposures (Snape et al. 2004). Additionally, the resulting genetic signature can be used in the development of biomarkers for the contaminant.

Two different types of biomarkers exist: biomarkers of effect are derived from the mechanism of action, while biomarkers of exposure are based on the genetic signature (Robbens et al. 2007). While expression profiling aids in the development of biomarkers for a contaminant within a system, it is also necessary to understand the effects of the contaminant within the system in which it is naturally occurring. Cognizance of these effects allows for better predictive capabilities of water quality and overall ecosystem health. Linking expression data to environmental parameters may allow for an understanding of the factors driving toxin production from an ecosystem rather than a culture-based standpoint.

Platform Overview

DNA microarrays (also known as DNA hybridization arrays, cDNA microarrays, or high-density oligonucleotide arrays) allow the examination of expression levels in thousands of genes simultaneously. In general, gene-specific sequences (probes) are immobilized onto a solid state matrix. Labeled nucleic acids from biological samples (targets) are then hybridized to the probes, with the premise that the greater the amount of labeled target, the greater the output signal. Two of the most common platforms consist of oligonucleotide or DNA-based arrays fabricated onto glass slides or nylon membranes (Freeman et al. 2000). cDNA microarrays consist of large fragments (typically 400-2,000 bp) of genes generated via PCR (Brown & Botstein 1999), while oligonucleotide arrays, pioneered by Affymetrix and also known as GeneChips®, consist of multiple sets of short (25 bp) synthetic DNA. These GeneChips have become the industry standard in microarray-based research (Ragoussis & Elvidge 2006).

Two main procedures are used to produce DNA microarrays: mechanical gridding, and a combined photolithographic/combinatorial chemistry technique developed and marketed primarily by Affymetrix (Deyholos & Galbraith 2001). In the mechanical gridding technique, pins are used to robotically deposit the probes in a regular pattern onto the solid surface. In the photolithography/combinatorial

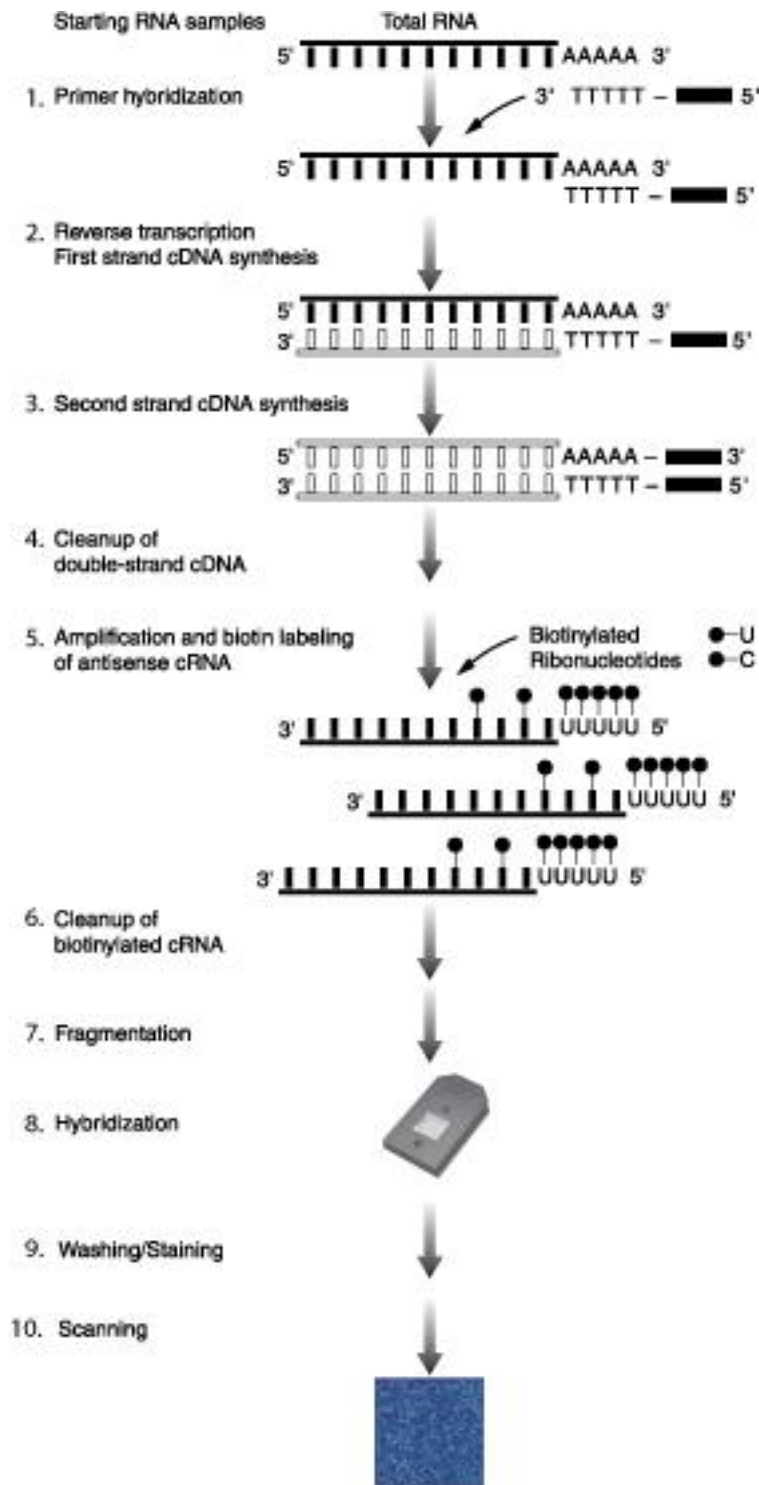
chemistry technique employed by Affymetrix, a UV light source passes through a mask that directs where oligonucleotide synthesis takes place on the array surface, with the resulting probes reaching a density of over several hundred thousand per square centimeter.

All formats use the same basic scheme of sample preparation in that mRNA is reverse-transcribed into cDNA and labeled with a fluorescent dye. One of the most-recognized labeling schemes utilizes the Cy3 (excitation 550 nm/emission 570 nm) and Cy5 (excitation 650 nm/emission 670 nm) dyes. During reverse transcription, one of the samples (either treated or control) is labeled with the Cy3 dye (green), the other with the Cy5 (red). The two labeled cDNA samples are mixed and hybridized to the array. The fluorescence ratio is then determined as the log of Cy5 to Cy3 intensity. Thus, induced genes are typically visualized as red, repressed as green.

With the Affymetrix GeneChips, labeled targets are prepared as cRNA, which is transcribed from the first-strand cDNA. Biotinylated nucleotides are incorporated during cRNA transcription, and the targets are visualized after hybridization by staining with streptavidin-phycoerythrin conjugates. The amount of light emitted at 570 nm is proportional to the amount of bound target, with signal output visualized by differing shades of blue (Figure I-5).

Affymetrix GeneChips interrogate transcript presence and abundance with a probe set comprised of 11-20 probe pairs. Each probe is 25-mer long. Each probe pair consists of a perfect match (PM) probe, with an exact complementary sequence to that of the target gene, and a mismatch probe (MM), in which the thirteenth basepair is altered in order to measure non-specific binding. The intensity data generated through probe binding are initially collected as .cel files, and must be normalized to provide a single expression value for each probe set. Different algorithms for probe-level analysis exist, including RMA (Robust Multichip Analysis) and GC-RMA (GeneChip-Robust Multichip Analysis), both developed by Irizarry et al. (Irizarry et al. 2003b), PLIER (Probe Logarithmic Intensity Error), and Affymetrix' own MAS5 (Microarray Suite) (Affymetrix 2003). All algorithms normalize across the entire set

Figure I-5. Overview of RNA sample preparation, hybridization, and scanning using the Affymetrix GeneChip: (1,2) Total RNA is reverse transcribed using a primer containing a T7-oligo(dT) promoter; (3, 4) Following second strand synthesis, double-stranded cDNA is spin-column purified and serves as template for the in-vitro transcribed reaction; (5, 6, 7) Biotinylated nucleotide analogs are included in the in-vitro transcription reaction. cRNA is then cleaved into 35-200bp fragments for subsequent hybridization; (8, 9) Following an overnight hybridization, arrays are washed and stained with a streptavidin-phycoerythrin conjugate; (10) Scanning at 570 nm produces an image of differing intensities of blue representative of transcript abundance. Intensity values are then normalized using one of several different algorithms.



of GeneChip data, with the exception of the MAS5 algorithm, which occurs on a per chip basis.

In this dissertation, probe-level data were initially normalized using both the GC-RMA and MAS5 algorithms, and ultimately, the expression values generated via GC-RMA normalization were used for statistical analysis. Though the GC-RMA method uses only the PM probe signal, in contrast to the MAS5 method which includes both PM and MM, this method has been shown to offer higher sensitivity and better accuracy than the MAS5 (Irizarry et al. 2003a). The GC-RMA algorithm consists of three steps. The first step is a background correction that utilizes a robust linear model to neutralize background noise and processing artifacts. The model takes into account each probe's sequence information so that the measured intensity can be adjusted for the effects of non-specific binding due to differences in bond strength between the base pairs. In the second stage, a quantile normalization aligns expression values on a common scale. The third stage uses an iterative polishing procedure to summarize the data and generate a single expression value for each probe set.

Expression profiling performed in this dissertation utilized the Affymetrix GeneChip Yeast Genome 2.0 Array, which contains probe sets for both the budding yeast *Saccharomyces cerevisiae* and the fission yeast *Schizosaccharomyces pombe*. Probes were designed based on the sequence data in GenBank (as of May 2004); the array contains 5,744 probe sets for 5,841 of the 5,845 genes of *S. cerevisiae*.

Real-Time Reverse-Transcriptase PCR

Background

Whereas DNA microarrays capture the overall expression profile of a cell or organism, real-time reverse transcription PCR allows for the precise measurement of individual genes. In real-time PCR, target amplification and detection are combined into a single step, and the fluorescence accumulated over the course of the PCR is directly proportional to the initial template amount (Higuchi et al. 1993). All methods of real-time PCR utilize the parameter referred to as the threshold cycle number, or

C_T ; this is the cycle of the PCR when fluorescence rises above that of background levels, and is indicative of the amount of target present in the sample. This method has been further developed to include quantification of messenger RNA transcripts, and has now become a common tool for the measurement of gene expression.

Many different parameters must be taken into account when initiating the real-time RT-PCR assay (also commonly referred to as quantitative RT-PCR and quantitative real-time RT-PCR), including reaction format (“two enzyme/one tube” versus “two enzyme/two tube”); primer and enzyme (RT and DNA polymerase) selection; the type of detection chemistry; method of quantification; and data normalization. While consideration must be given to the entire process of the real-time RT-PCR assay, from primer design to data processing, some of the prominent factors used in deciding the assay formats used in this dissertation are discussed briefly below.

Reverse Transcription Reaction

The first step of the real-time RT-PCR assay is the reverse transcription of the RNA into DNA, as the RNA cannot serve as the template for the PCR. The RT-PCR assay can be initiated with three different primer types: random hexamers, oligo-dTs, or target-specific primers. Random hexamers prime at multiple points along the transcript, resulting in more than one cDNA per original target. Approximately 30% of real-time RT-PCR assays utilize random hexamers (Bustin et al. 2005). Though non-specific, priming with random hexamers yields the greatest amount of cDNA. However, most cDNA will be derived from ribosomal RNA, which can present a problem if the target mRNA is present at low copy number (Bustin & Nolan 2004). Additionally, random hexamers can overestimate mRNA copy numbers up to 19-fold compared to sequence-specific primers (Bustin 2000, Bustin & Nolan 2004).

Oligo-dTs offer more specificity in the priming of the RT reaction than random hexamers, as they will not transcribe ribosomal RNA. Oligo-dTs are used in approximately 40% of real-time RT-PCR assays (Bustin et al. 2005). This method is believed to be the most appropriate choice if the goal is to amplify several mRNA targets from a limited quantity of RNA (Bustin et al. 2005). However, it must also be

realized that the reverse transcriptase may fail to reach the region targeted by the primers in the PCR reaction if the mRNA contains significant secondary structures, or if the target sequence is at the 5' end of a long mRNA (Bustin & Nolan 2004). Also, RNA lacking a poly-A tail will not be transcribed.

Sequence-specific primers transcribe the most specific cDNA and offer the greatest level of sensitivity. This is of particular use if the transcript is present at low copy number. Reactions primed by gene-specific primers have been found to be linear over a wider range than the same reactions primed with random hexamers (Bustin & Nolan 2004). However, if limited quantities of RNA are available, it may not be possible to return to the original sample and amplify a second target. This is the method of choice for approximately 20% of real-time RT-PCR assays (Bustin et al. 2005).

Regardless of which method of priming is used in the RT reaction, the real-time PCR assay requires gene-specific primers.

Enzyme Format

Reverse transcription and the real-time PCR assay may be performed in a two enzyme/one tube or two enzyme/two tube format. There are advantages and disadvantages associated with each format. In the two enzyme/one tube (also referred to as one-step) format, cDNA synthesis to target amplification and detection are performed in a single tube. With the two enzyme/two tube (two-step) format, the RT reaction is performed separately from the real-time PCR assay. Data acquired with the two-step real-time RT-PCR is reported to be quite reproducible (Wong & Medrano 2005); however, this is dependent on the type of detection chemistry used, as research performed throughout the course of this study found the one-step format to provide greater reproducibility and less variation. The one-tube format has been reported to be less sensitive than the two-tube format, as illustrated by a shift in threshold cycle number (C_T) corresponding to a one order of magnitude difference in initial template copy number (Bustin 2002).

Concomitant with the type of format is the choice of which reverse transcriptase system to use. In general, the quantity of RNA in a reverse transcription

assay determines the choice of reverse transcriptase system based on the manufacturer's specifications. A detailed study was recently published that compared several of the leading commercial reverse transcriptase systems and the results obtained under a variety of conditions, including transcript abundance (low, medium, and high) in samples containing low or high levels of background RNA (Levesque-Sergerie et al. 2007); while most enzymes performed accordingly based on manufacturer's specifications, others were shown to contain substantial amounts of PCR inhibitors, which can greatly affect the resulting expression profile. Therefore, when deciding on the type of enzyme format to use, the reverse transcriptase system used in that format must also be evaluated.

Detection Chemistries

DNA-Binding Dyes

In the simplest method of detection, a fluorescent dye (typically SYBR Green) binds to double-stranded DNA. The amount of amplified DNA is monitored by measuring the fluorescence immediately following the extension step of each cycle (Morrison et al. 1998). During the reaction, specificity is determined only through the primers, as the presence of any double-stranded DNA will generate fluorescence. Additional specificity is achieved by performing a melting curve analysis, in which fluorescence is plotted as a function of temperature as the temperature is increased above the melting temperature of the amplicon (Ririe et al. 1997). A melting peak at the T_M of the amplicon distinguishes it from non-target DNA products (such as primer-dimers) which melt at lower temperatures and display broader peaks.

Hydrolysis Probes

Several probe-based detection formats exist, all of which rely on the annealing of a sequence-specific probe to an internal region within the target amplicon. These probe-based formats include hydrolysis probes, hairpin probes, and hybridization probes.

Hydrolysis probes are best exemplified by the Taqman® assay. In this assay, the 5'-nuclease activity of the DNA polymerase hydrolyzes the probe while it is annealed to its target amplicon. Sequence-specific primers are designed to produce an

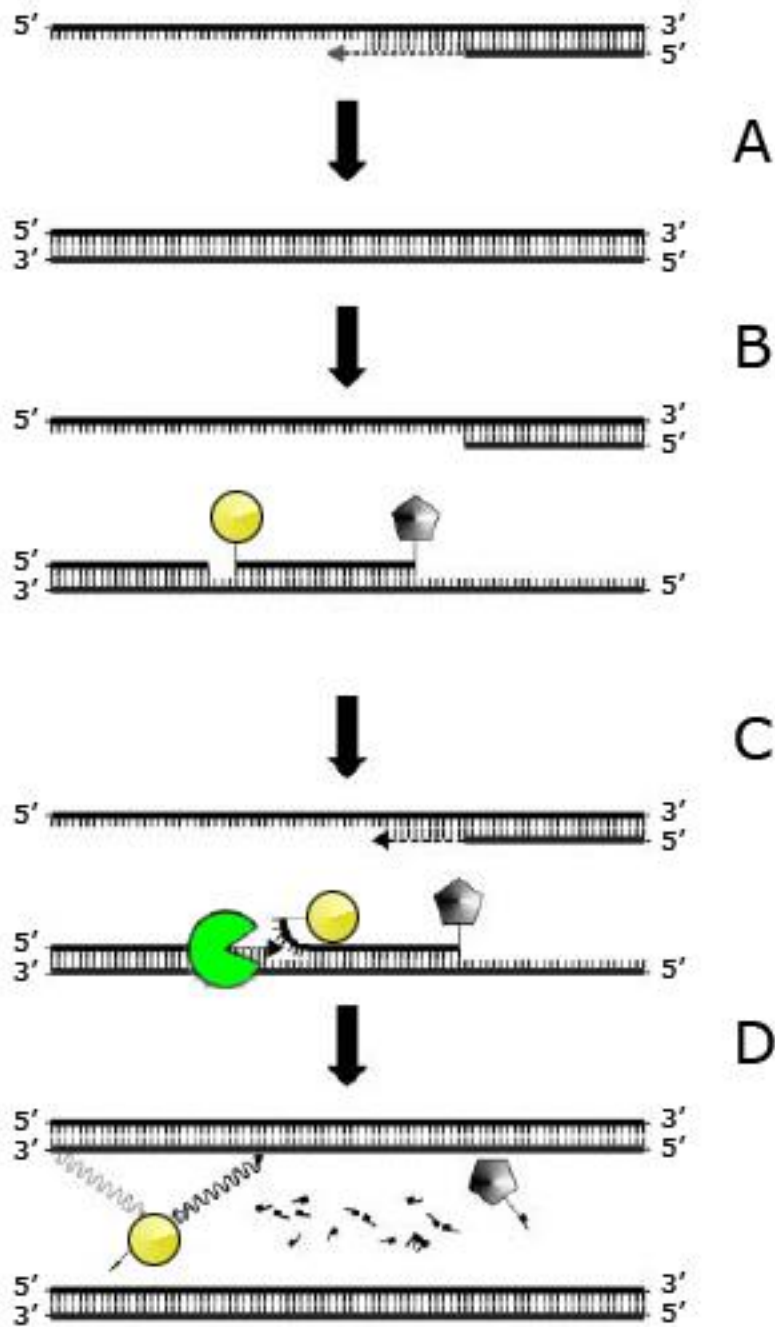
amplicon with a length of 100–150 bp. The sequence-specific probe is labeled with a reporter dye on the 5'-end, the emission spectrum of which is quenched by a second fluorescent dye on the 3'-end (Heid et al. 1996) as a result of fluorescence resonance energy transfer (FRET). As the exonuclease activity of the polymerase is specific for double-stranded DNA, the probe must be bound to its complementary strand in order for degradation, and thus fluorescence, to occur. The probe is designed to have a T_M 10°C above that of the primers. This allows the probe to anneal to its complementary sequence prior to primer extension by the polymerase, as annealing and extension are combined in a single step (typically between 60-62°C). Degradation of the probe by the polymerase separates the reporter and quencher dyes, resulting in fluorescence emission by the reporter dye (Figure I-6).

Hairpin Probes

The appropriately-named hairpin probes are distinguished by their stem-and-loop structure. The Scorpion assay combines the primer and probe into a single molecule. The Scorpion primer contains a 5' extension consisting of a fluorophore on the 5' end, a stem-loop structure containing the probe sequence, a quencher dye, and a DNA polymerase blocker to prevent extension of the probe region. One round of PCR incorporates the target sequence into the same strand as the Scorpion primer; in the following round, primer annealing leads to hybridization of probe and target sequence; separation of fluorophore and quencher results in increased fluorescence (Whitcombe et al. 1999).

Molecular beacons also utilize a stem-and-loop structure. The loop region is complementary to the target amplicon sequence, while the stem is formed by complementary arm sequences located on either side of the probe sequence (Tyagi & Kramer 1996). A fluorophore is attached to the end of one arm, a quencher to the second. In the absence of target molecules, the stem-and-loop structure is maintained, resulting in efficient quenching of the fluorophore. When molecular beacons encounter the complementary target sequence, they undergo a conformational change in which the stems dissociate and a probe/hybrid forms that is longer and more stable than the stem structure (Bonnet et al. 1999). This conformational change results in

Figure I-6. Real-time RT-PCR using the Taqman assay. (A.) The reverse transcription reaction can be performed with random hexamers, oligodTs, or gene-specific primers, in a separate tube from that of real-time PCR or as sequential reactions within the same tube. (B) Following denaturation of the PCR product, gene-specific primers and a dual-labeled probe internal to the region targeted by the primers anneal to the DNA. Fluorescence is quenched due to the close proximity of the fluorophores to each other. (C, D) The exonuclease activity of the *Taq* polymerase hydrolyzes the probe during extension, eliminating the FRET between the two fluorophores and resulting in a fluorescent signal. The level of fluorescence is proportional to the amount of target.



separation of fluorophore and quencher and restores fluorescence, allowing detection of target molecules.

Hybridization Probes

Hybridization probes also utilize FRET in the detection of target nucleic acids; however, the energy transfer functions in the opposite manner as for hydrolysis probes. While FRET reduces fluorescence emission in hydrolysis probes, it increases it in hybridization probes. Hybridization probes employ a set of PCR primers and either one or two sequence-specific probes (for a brief review, see Wong & Medrano 2005). In the two-probe format, an acceptor dye is situated at the 3'-end of the first probe, whose emission spectrum overlaps with the excitation spectrum of the donor dye located on the 5'-end of the second probe. During the annealing step, the two probes hybridize to the target sequence in a head-to-tail arrangement. This brings the two dyes in close proximity to each other, resulting in an increase in FRET between the two dyes and the emission of a detectable signal. The generation of a fluorescent signal is dependent on both probes binding to their target sequences, thus increasing the sensitivity and specificity of the reaction. In the one-probe format, the reverse primer is labeled with the acceptor dye, replacing the need for one of the probes.

Methods of Quantification

Absolute Quantification

Two types of quantification can be used to measure changes in gene expression: absolute and relative. Absolute quantification determines the precise amount of target, typically expressed as copy number or concentration, while relative quantification measures the ratio between the target and reference transcripts. In absolute quantification, the amount of target is determined using an external standard of known concentration that contains primer and probe (depending on the type of detection chemistry used) binding sites identical to that of the target. A standard curve is generated by plotting the C_T values against the log of amount of standard. All methods of quantification, whether absolute or relative, then require adjustment of the threshold level to above that of background fluorescence values yet still within the exponential phase of the PCR, before reagents become limiting and fluorescence

plateaus. Thus, the standard curve created with the external standards provides a linear relationship between the C_T and initial amount of template, and so the concentration of the target within samples is determined based on the resulting C_T (Figure I-7).

While the application of external standard curves for absolute quantification is often referred to as the “gold standard” (Scheffe et al. 2006), one of its criticisms is that it assumes all standards and samples have equal amplification efficiencies (Wong & Medrano 2005). However, this can easily be resolved by preparing a dilution series of one or several samples and calculating the amplification efficiency based on the resulting slope. Additionally, with the inception of LinRegPCR (discussed below), the amplification efficiency of each dilution of the standard along with the efficiency of each sample can quickly and easily be obtained.

Several different types of molecules can be used as standards: RNA, double-stranded DNA (typically plasmid-based), or cDNA. The enzyme format used is one of the deciding factors as to the type of standard used; for example, RNA standards would not be applicable in the two enzyme/two tube format, nor would DNA standards be appropriate with the two enzyme/one tube format. One of the advantages of including a standard curve with each assay is that the highest dilution levels provide the sensitivity level of the assay: the greatest dilution that provides consistent C_T s indicates the lowest copy number that can be quantified with confidence (Bustin & Nolan 2004).

The Importance of PCR Amplification Efficiency in Relative Quantification

Determination of the PCR amplification efficiency of both target and reference genes is a necessity in methods of relative quantification. PCR efficiency directly influences the C_T value and resulting gene expression ratios, which, in most cases, are derived from the C_T (Scheffe et al. 2006). There are two common ways to determine PCR efficiency, based on the standard curve or the PCR kinetic curve. Some models of relative quantification calculate the individual PCR efficiencies (E) of target and reference gene through the use of standard curves. The C_T versus log dilution RNA or cDNA is plotted and the resulting slope (generated via linear

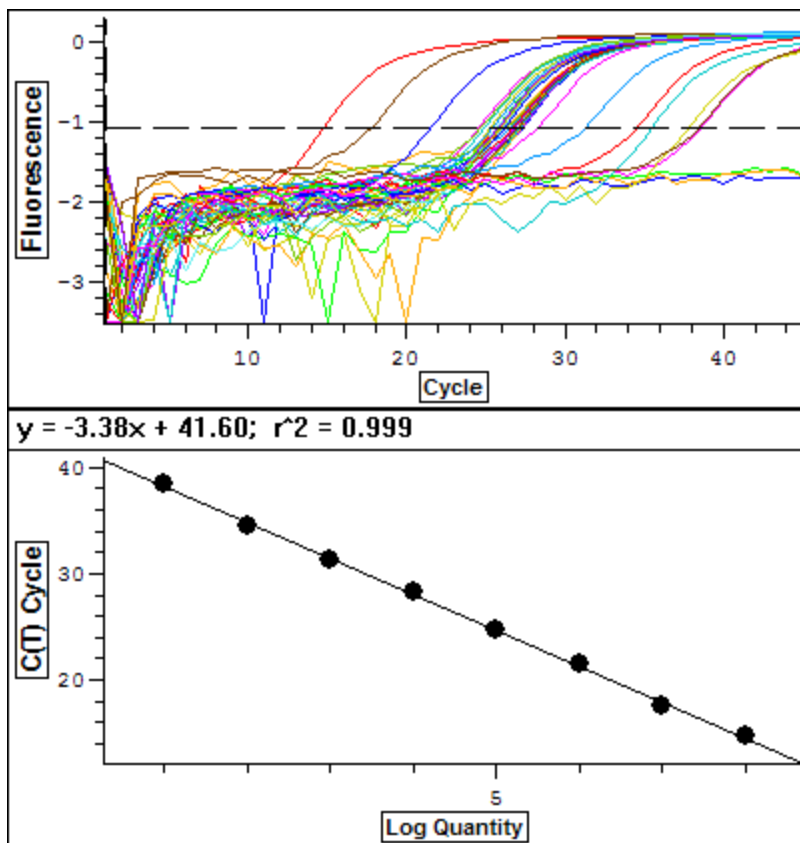


Figure I-7. Example of external standard curve used in absolute quantification.

regression) is applied to the efficiency calculation. While this recognizes the difference in E between reference and target, it still assumes that in all samples, the E of each amplicon is constant. PCR efficiencies calculated from standard curves based on known RNA inputs can result in efficiencies that vary over a 0.2 range; likewise, the efficiencies calculated from a dilution series of a cDNA sample may differ by 0.26 (Ramakers et al. 2003). The impact of the PCR efficiency on the resulting gene expression profile cannot be denied: a difference in amplification efficiency of 0.05 between two samples that were initially equal can result in a 2-fold difference in product amount after 26 cycles of PCR (Freeman et al. 1999), while a difference of 0.15 results in a 16-fold difference (Schefe et al. 2006).

Many methods are available for determining PCR efficiency via the PCR kinetic curve, including several methods of relative quantification that integrate calculation of PCR efficiency into their models (<http://www.assayefficiency.com/>, Liu & Saint 2002, Peirson et al. 2003, Tichopad et al. 2004). A method has also been developed for calculating the PCR efficiency of individual samples based on the level of fluorescence at each cycle of the PCR (Ramakers et al. 2003). Linear regression analysis calculates the intercept and slope from a series (typically 4–6) of data points (fluorescence) from the log-linear phase of the PCR. A computer program entitled LinRegPCR is freely available upon request (e-mail: bioinfo@amc.uva.nl; subject: LinRegPCR) that implements the algorithm and linear regression analysis on data exported from a variety of real-time detection systems (Ramakers et al. 2003). Thus, methods developed previously which relied on the construction of standard curves for determination of PCR efficiency can now easily incorporate PCR efficiency with this program.

In calculating PCR efficiency, it should be noted that two variations of the equation can be found throughout the literature: $E = 10^{(-1/\text{slope})}$ and $E = 10^{(-1/\text{slope})} - 1$. The nomenclature associated with PCR efficiency is such that these calculations correlate to values of “2” and “1,” which are used interchangeably when referring to ideal exponential amplification. For example, the amplification plot (Peirson et al. 2003) and Liu and Saint (Liu & Saint 2002) models for relative quantification use “1”

when referring to ideal amplification efficiency, while several others use “2” (Pfaffl 2001, Ramakers et al. 2003). These equations have also been described as: exponential amplification = $10^{(-1/\text{slope})}$, while PCR amplification efficiency = $10^{(-1/\text{slope})} - 1$ (Wong & Medrano 2005).

Relative Quantification Models

Standard Curve Method (Livak 1997). This method requires the generation of a standard curve that is then used to determine the quantity of the target within unknown samples. The target quantity is derived from the standard curve, which can be any stock RNA or cDNA as long as it contains the appropriate target, and then divided by the target quantity of the calibrator. The calibrator (i.e. control) is treated as the 1x sample, and so target quantity is expressed as an *n*-fold difference relative to the calibrator quantity. As the sample quantity is divided by the calibrator quantity, the units of the standard curve drop out; the only required values are the relative dilutions used in the standard curve. In order to normalize to a housekeeping gene, standard curves are prepared for both the target and the reference genes; to calculate normalized target amount, the target quantity is divided by the reference quantity. Relative expression values are then generated by dividing the normalized target values by the normalized calibrator values.

It can be difficult to perform statistical analysis on the values generated with the standard curve method. If target and reference genes are amplified in separate tubes, values of both genes are averaged separately, with mean target quantity then normalized to mean reference quantity, in effect reducing each gene to a single value. Also, it is not appropriate to perform statistical analysis on the unnormalized values, as they have not been corrected for different starting template amounts (one of the functions of the reference gene).

Comparative C_T method. This method utilizes arithmetic formulas to determine relative fold-change. The final calculation, derived from a series of equations that assume exponential amplification in the PCR, determine fold-change based on $2^{-\Delta\Delta C_T}$, in which the $\Delta\Delta C_T = (C_{T\text{sample}} - C_{T\text{ref}}) - (C_{T\text{control}} - C_{T\text{ref control}})$ (Livak 1997, Livak & Schmittgen 2001). Thus, the data are presented as the fold-

change in gene expression normalized to a reference gene and relative to an untreated control.

Before the comparative C_T equation can be applied, it is necessary to verify that the PCR efficiencies of the target and reference genes are approximately equal (Livak & Schmittgen 2001). This is done by comparing how the ΔC_T between the two varies with dilution: a dilution series is performed with both the target and reference, and the ΔC_T resulting from the difference in $C_{T\text{target}} - C_{T\text{reference}}$ versus log template dilution is plotted. If the absolute value of the slope is <0.1 , the amplification efficiencies are considered similar, and the comparative C_T method is applicable for use.

This method assumes that the amplification efficiencies are at or near 2 (i.e. doubling every cycle), as it is derived from an initial calculation based on exponential amplification of the PCR. This can result in an overestimation of starting template amounts. Also, this method has been shown to be sensitive to variations in PCR efficiency: with a 0.04 range between target and reference genes (i.e. from 1.78-1.82), a 4-fold error in fold difference will occur (Ramakers et al. 2003). As is the case with the standard curve method, it is difficult to perform statistical analysis on the values obtained with the comparative C_T , as the values of target and reference gene are averaged separately before performing the final calculation.

This method does not require the starting amounts of RNA or cDNA to be equal in all reactions, relying on the reference gene for this standardization. A derivation of the comparative C_T method also exists for cases where equal starting template amounts are used (Livak 1997).

Pfaffl Model. In the model presented by Pfaffl (Pfaffl 2001), the relative expression ratio of a target gene is calculated based on the PCR efficiencies and the difference in $C_{T\text{S}}$ between unknown and control samples and expressed in comparison to a reference gene with the equation: $(E_{\text{target}})^{\Delta C_{T\text{target}}^{\text{(control-sample)}}} \div (E_{\text{ref}})^{\Delta C_{T\text{ref}}^{\text{(control-sample)}}$. In the original model, the PCR efficiencies of both target and reference gene were calculated based on the slopes derived from the plot of C_T versus dilution series with the equation $E = 10^{(-1/\text{slope})}$. However, with the inception of the LinRegPCR

program (Ramakers et al. 2003), amplification efficiencies can now be obtained from the raw fluorescence data, eliminating the need for dilution series. The relative expression software tool (REST), which can be run in Microsoft Excel, automates data analysis using this model. It implements a statistical model (Pair Wise Fixed Reallocation Randomization Test) to determine the significance of the relative expression ratio, and also indicates if the reference gene is appropriate for use in normalization (Pfaffl et al. 2002).

Gene Expression's C_T Difference (GED). This model has recently been introduced (2006) and also incorporates the PCR efficiencies of target and reference genes when determining the expression ratio. If the average E s of target and reference are used (which is preferential to using the E s of individual samples, which increases the variation (Peirson et al. 2003)), the formula, derived from that of the exponential amplification equation, is as follows: relative expression ratio = $(1 + E(\text{Gene of Interest}))^{-\Delta C_T(\text{Gene of Interest})} / (1 + E(\text{Reference Gene}))^{-\Delta C_T(\text{Reference Gene})}$, where $\Delta C_T(\text{gene}) = C_T(\text{gene, sample of interest}) - C_T(\text{gene, control})$ (Scheffe et al. 2006). In this model, PCR efficiency is calculated with the LinRegPCR program (Ramakers et al. 2003).

Amplification Plot Method. The amplification plot method applies an algorithm, based on the change in fluorescence throughout the exponential phase, to the amplification profile to determine the amplification efficiency from each sample (Peirson et al. 2003). A linear regression is applied to defined cycles of exponential amplification as identified from the midpoint of the PCR. The signal range is calculated to allow for accurate determination of the amplification rate around the midpoint of the reaction (i.e. exponential phase) as defined by fluorescence maximum and standard deviation. Linear regression is then used to calculate the slope of log fluorescence around the midpoint, based on a minimum of three cycles, and amplification efficiency is calculated as $E = 10^{(1/\text{slope})} - 1$. Relative expression is determined using a PCR-amplification derived equation that incorporates E and C_T to determine starting fluorescence, which is proportional to the starting template quantity: $R_0 = R_{CT} * (1 + E)^{-C_T}$, where R_0 = starting fluorescence, C_T = threshold

cycle, and R_{CT} = fluorescence at that cycle. A Microsoft Excel workbook entitled Data Analysis for Real-Time PCR (DART-PCR) has been developed in conjunction with this model that calculates results from the raw data, including statistical analysis of PCR efficiencies (Peirson et al. 2003).

Liu and Saint. In this method, the amplification efficiency for each reaction is calculated from the kinetic curve and the initial amount of gene transcript derived and normalized (Liu & Saint 2002). (It should be noted that in this model, the PCR kinetics are based on the exponential phase; later models implied that this method utilized the reaction kinetics of the entire PCR (Peirson et al. 2003)). The starting fluorescence and PCR efficiency are derived from an equation fit to the early exponential phase of PCR kinetic data; the equation was derived from that describing the PCR amplification, with fluorescence values substituted for template amount ($R_n = R_0 * (1 + E)^n$, where R_n = fluorescence at cycle n , R_0 = initial fluorescence, E = amplification efficiency, n = cycle number). The fluorescence data and PCR efficiencies of both target and reference gene are integrated into the equations of the model, allowing for normalization and determination of relative expression. With this method, the needs for standard curves and validation experiments are eliminated. This method is similar to that of the Amplification Plot method in that both are derived from the equation describing PCR amplification.

Comparison of Methods

Numerous comparisons have been performed among the different methods of quantification, all with different results. For relative expression in general, the comparative C_T has been shown to overestimate fold-change (Peirson et al. 2003, Chini et al. 2007), yet in a recent study comparing six methods of relative quantification, the comparative C_T was shown to perform among the best (Cikos et al. 2007). Additionally, very similar results have been achieved, in both fold-change and statistical significance, using both absolute and relative quantification, specifically with the standard curve and amplification plot methods (Peirson et al. 2003). It should be noted that relative quantification only allows for the determination of the fold-change ratio, and while in most cases this is sufficient, being able to compare actual

transcript copy numbers, such as with absolute quantification, can provide additional insights into the state of the cell or organism. However, for most researchers, the absolute transcript number is not necessary, and one of the many methods of relative quantification can be employed to determine changes in gene expression.

Normalization

Both absolute and relative quantification require normalization of the target mRNA expression. Several different strategies exist for the normalization of target mRNA. These include: normalization to sample size (i.e. unit weight or mass), total RNA, the measurement of a reference or housekeeping gene, and the incorporation of an artificial molecule at the extraction step (Huggett et al. 2005). Of these different strategies, normalization to a reference gene is the most common and widely used. However, in many cases, expression of the reference gene is assumed to remain constant and is employed without proper validation. In general, the “reference” or “housekeeping” gene serves two purposes: (I) to discern the change in regulation of functional genes by standardizing them to a gene whose expression is unaffected by the treatment; and, especially in situations where expression values cannot be standardized to a unit of measure (such as total cells or weight) (II) to standardize the functional gene to compensate for bias that may have arisen during the cell harvesting and extraction processes.

Experimental results are highly dependent on the reference gene chosen; additionally, statistically significant differences in target gene expression have been shown to occur as a function of reference gene selection (Dheda et al. 2005). If the reference gene displays variability in expression due to experimental conditions, the results obtained with respect to the target gene will be incorrect (Tricarico et al. 2002). Significant variation in expression was shown to exist when target mRNA was normalized to 10 commonly-used housekeeping genes and the 18S rRNA gene (Tricarico et al. 2002). Also, if the reference gene has a large measurement of error, the noise of the assay will be increased and small changes will not be detected. Numerous reports cite the extensive variability and large measurement of error found in classic reference genes, such as glyceraldehyde-3-phosphate dehydrogenase

(GAPDH), β -actin, and the 18S rRNA (Bustin 2000, Huggett et al. 2005).

Additionally, in selecting an appropriate reference gene, the technical aspects of the assay must also be considered. For example, 18S rRNA can only be used as a reference if random hexamers are used in priming the RT reaction, as this molecule does not contain a poly-A tail.

The use of multiple reference genes has been advocated and different methods for identifying the most suitable combination of reference genes have been proposed (Bustin et al. 2005). However, this may not be a practical option if only limited amounts of RNA or funds are available. It must be realized that normalization strategies will differ; however, for whatever method is decided upon, it is imperative that the reference genes selected be properly verified by (I) determining their variability under experimental conditions and (II) determining their measurement of error.

Ribosomal RNA Genes for Species Identification

The use of ribosomal RNA gene sequences as molecular markers provides a culture-independent means for species identification and the establishment of phylogenetic relationships. Based on large subunit (LSU) rDNA sequences, dinoflagellates are true eukaryotes, sharing close relationships with ciliates and yeast (Lenaers et al. 1989). In general, eukaryotic rRNA is composed of four genes interspersed with non-coding regions. The genes coding for the 18S or small subunit (SSU), 5.8S, and 28S or LSU ribosomal RNA are found clustered together in an operon-like arrangement; internal transcribed spacer units (ITS) flank the 5.8S gene. In most eukaryotes, the 5S gene is not found on the same unit as the other three (however, in yeast, the 5S is located on the same unit but is transcribed in the opposite direction and with RNA polymerase III rather than RNA polymerase I). Eukaryotic rRNA consists of a tandem array of repeating rRNA units, with the units varying in size and number among organisms. Figure I-8 depicts the structural organization of one rRNA unit. The SSU rDNA sequence contains both regions of high conservation among all organisms and diagnostic variable regions specific for

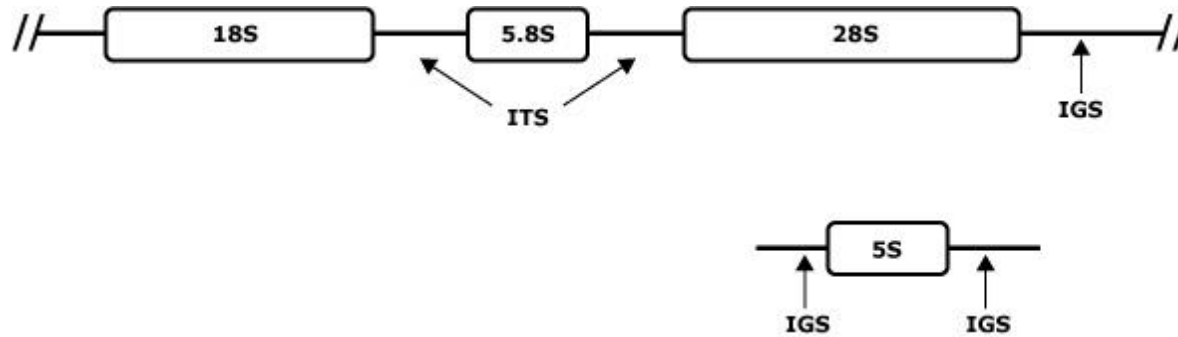


Figure I-8. rDNA organization in eukaryotic cells. The rDNA is composed of repeating units of the 18S, 5.8S, and 28S genes. In most eukaryotes, 5S is located on a separate cluster; in yeast it occurs with the other three types but is transcribed in from RNA polymerase III in the opposite direction. IGS= Intergenic Spacer Regions (also known as Non-Transcribed Spacers, or NTS); ITS = Internal Transcribed Spacers.

closely related groups (Moyer 2001). Specifically, the dinoflagellate SSU has been shown to contain three hypervariable regions (Sadler et al. 1992). The LSU rRNA gene is comprised of a conserved structural core interspersed with 12 divergent domains identified as D1-D12; of these, D2, D8, and D12 in particular display high rates of variation and length (Michot et al. 1984). In general, the SSU rDNA sequences have been widely used as biomarkers, as their essential role in protein synthesis ensures their ubiquitous distribution and functional conservation across organisms, while the variable regions dispersed throughout highly conserved regions allow for phylogenetic comparisons across a wide range of evolutionary distance (Moyer 2001).

A portion of this dissertation sought to identify whether genetic differences existed between two varieties of the dinoflagellate *Pyrodinium bahamense*. *P. bahamense* is the sole species within its genus and has been designated as one of two varietal forms, *bahamense* or *compressum*, based on morphology and biochemical characteristics (Steidinger et al. 1980). Historically, *P. bahamense* var. *compressum* has been found throughout the Indo-Pacific region and var. *bahamense* in the Atlantic. Until recently, one of the distinguishing differences between the two was the absence of toxin production in var. *bahamense*. However, saxitoxin outbreaks in the past few years in the Indian River Lagoon, FL, determined *P. bahamense* var. *bahamense* as the source (Landsberg et al. 2006). This marked the first occurrence of toxin production in the Atlantic variety, and raised the question of whether the use of varietal status was warranted. While SSU rDNA sequences have been published for the variety designated *compressum*, no such genetic information exists for var. *bahamense*. Part VI of this dissertation utilizes the SSU rRNA gene for the genetic identification of the dinoflagellate currently classified as *P. bahamense* var. *bahamense* in the Indian River Lagoon, FL, based on single-cell amplification from environmental samples.

General Objectives and Hypotheses

One of the driving influences of this dissertation was the initial outbreak of saxitoxin in the Indian River Lagoon, FL in 2002. While the source of the saxitoxin was not positively identified for some time, it led to bans on pufferfish harvesting and repeated closures of aquaculture farms in the lagoon. The source of the saxitoxin was recently determined to be the dinoflagellate *Pyrodinium bahamense* var. *bahamense* based on ELISA and mouse bioassay (MBA) analyses of both clonal cultures and natural bloom samples (Landsberg et al. 2006). *P. bahamense* has been classified as a single species with two distinct varietal forms, *compressum* and *bahamense*; one of the key distinguishing characteristics between the two was the lack of toxin production in var. *bahamense* (Steidinger et al. 1980). The outbreaks in the Indian River Lagoon are the first reported occurrences of saxitoxin in this variety. The factors which stimulated the toxin production remain unknown. Throughout the literature, the debate remains as to the evolutionary role these toxins, as illustrated by the many different hypotheses discussed above.

While the sodium channel has been identified as the target of saxitoxin in mammalian cells, its molecular target in lower eukaryotic organisms remains unknown. This dissertation sought to determine the molecular target in lower eukaryotes in order to elucidate the role of this toxin in the context of the algae that produce it. The overall objectives of this dissertation can be summarized as follows:

- to determine the mechanism of action of saxitoxin on lower eukaryotes through global expression profiling with the yeast *Saccharomyces cerevisiae*
- to perform a comparative transcriptomics analysis between *S. cerevisiae* and other lower eukaryotes
- to determine the genetic relationship of the dinoflagellate *P. bahamense* var. *bahamense* to that of the toxin-producing variety *compressum*

The first study (Part II) examined the general hypothesis that the transcriptional profile obtained through the differential expression of genes within *S.*

cerevisiae would aid in eliciting the mechanism of action of saxitoxin in lower eukaryotes.

The second study (Parts III and IV) tested the hypothesis that expression patterns in a subset of genes in *S. cerevisiae* following exposure to saxitoxin are similar to those involved in metal homeostasis, with the specific hypothesis that the patterns are similar to those of excess copper. Part IV explored whether gene expression in response to saxitoxin was mediated by the transcription factor Mac1p.

The third study (Part V) examined the general hypothesis that transcriptional data obtained with *S. cerevisiae* can be extrapolated to other eukaryotic organisms (in this study, the green alga *Chlamydomonas reinhardtii*) with the specific aim of using comparative transcriptomics as a means for providing information on the role of the toxin within aquatic ecosystems

The fourth study (Part VI) tested the hypothesis that the organism responsible for saxitoxin in the Indian River Lagoon, FL is genetically the same as the variety *compressum*, based on SSU rDNA sequences.

References

- Affymetrix (2003) GeneChip expression analysis.
- Anderson DM, Cheng TP-O (1988) Intracellular localization of saxitoxins in the dinoflagellate *Gonyaulax tamarensis*. *Journal of Phycology* 24:17-22
- Anderson DM, Kulis DM, Sullivan JJ, Hall S, Lee C (1990) Dynamics and physiology of saxitoxin production by the dinoflagellates *Alexandrium* spp. *Marine Biology* 104:511-524
- Baden DG, Trainer VL (1993) Mode of action of toxins of seafood poisoning. In: *Algal Toxins in Seafood and Drinking Water*. Academic Press
- Barreiro A, Guisande C, Frangopulos M, Gonzalez-Fernandez A, Munoz S, Perez D, Magadan S, Maneiro I, Riveiro I, Iglesias P (2006) Feeding strategies of the copepod *Acartia clausi* on single and mixed diets of toxic and non-toxic strains of the dinoflagellate *Alexandrium minutum*. *Marine Ecology-Progress Series* 316:115-125
- Bonnet G, Tyagi S, Libchaber A, Kramer FR (1999) Thermodynamic Basis of the Enhanced Specificity of Structured DNA Probes. *Proceedings of the National Academy of Sciences of the United States of America* 96:6171-6176
- Brown PO, Botstein D (1999) Exploring the new world of the genome with DNA microarrays. *Nat Genet* 21:33-37
- Bustin S (2000) Absolute quantification of mRNA using real-time reverse transcription polymerase chain reaction assays. *J. Mol. Endocrin.* 25:169-193
- Bustin SA (2002) Quantification of mRNA using real-time reverse transcription PCR(RT-PCR): trends and problems. *J Molecular Endocrinology* 29:23-39
- Bustin SA, Benes V, Nolan T, Pfaffl MW (2005) Quantitative real-time RT-PCR - a perspective. *J. Mol. Endocrin.* 34:597-601
- Bustin SA, Nolan T (2004) Pitfalls of Quantitative Real-Time Reverse-Transcription Polymerase Chain Reaction. *J Biomol Tech* 15:155-166
- Camacho FA, Thacker RW (2006) Amphipod herbivory on the freshwater cyanobacterium *Lyngbya wollei*: Chemical stimulants and morphological defenses. *Limnology and Oceanography* 51:1870-1875

- Carmichael WW, Evans WR, Yin QQ, Bell P, Moczydlowski E (1997) Evidence for paralytic shellfish poisons in the freshwater cyanobacterium *Lyngbya wollei* (Farlow ex Gomont) comb. nov. *Appl. Environ. Microbiol.* 63:3104-3110
- Catterall WA (1985) The voltage sensitive sodium channel: a receptor for multiple neurotoxins. In: Anderson W, and Baden (ed) *Toxic Dinoflagellates*. Elsevier Science Publishing Co, Inc., p 329-342
- Celis JE, Kruhøffer M, Gromova I, Frederiksen C, Østergaard M, Thykjaer T, Gromov P, Yu J, Pálsdóttir H, Magnusson N, Ørntoft TF (2000) Gene expression profiling: monitoring transcription and translation products using DNA microarrays and proteomics. *FEBS Letters* 480:2-16
- Cembella AD (1998) Ecophysiology and metabolism of paralytic shellfish toxins in marine microalgae. In: Anderson DM, Cembella AD, Hallegraeff G (eds) *Physiological Ecology of Harmful Algal Blooms, Vol G 41*. Springer-Verlag, Berlin, p 381-403
- Chini V, Foka A, Dimitracopoulos G, Spiliopoulou I (2007) Absolute and relative real-time PCR in the quantification of *tst* gene expression among methicillin-resistant *Staphylococcus aureus*: evaluation by two mathematical models. *Letters in Applied Microbiology* 45:479-484
- Cikos S, Bukovska A, Koppel J (2007) Relative quantification of mRNA: comparison of methods currently used for real-time PCR data analysis. *Bmc Molecular Biology* 8
- Cooper CS (2001) Applications of microarray technology in breast cancer research. *Breast Cancer Research* 3:158-175
- da Costa RM, Franco J, Cacho E, Fernandez F (2005) Toxin content and toxic effects of the dinoflagellate *Gyrodinium corsicum* (Paulmier) on the ingestion and survival rates of the copepods *Acartia grani* and *Euterpina acutifrons*. *Journal of Experimental Marine Biology and Ecology* 322:177-183
- Deeds JR, Landsberg JH, Etheridge SM, Pitcher GC, Longan SW (2008) Non-traditional vectors for paralytic shellfish poisoning. *Mar. Drugs* 6:308-348
- DeFilippis V, Raggio C, Moses A, Fruh K (2003) Functional genomics in virology and antiviral drug discovery. *Trends in Biotechnology* 21:452-457
- Deyholos MK, Galbraith DW (2001) High-density microarrays for gene expression analysis. *Cytometry* 43:229-238

- Dheda K, Huggett JF, Chang JS, Kim LU, Bustin SA, Johnson MA, Rook GAW, Zumla A (2005) The implications of using an inappropriate reference gene for real-time reverse transcription PCR data normalization. *Analytical Biochemistry* 344:141-143
- Ferreira FMB, Soler JMF, Fidalgo ML, Fernandez-Vila P (2001) PSP toxins from *Aphanizomenon flos-aquae* (cyanobacteria) collected in the Crestuma-Lever reservoir (Douro river, northern Portugal). *Toxicon* 39:757-761
- Frangoulos M, Guisande C, Maneiro I, Riveiro I, Franco J (2000) Short-term and long-term effects of the toxic dinoflagellate *Alexandrium minutum* on the copepod *Acartia clausi*. *Marine Ecology-Progress Series* 203:161-169
- Freeman WM, Robertson DJ, Vrana KE (2000) Fundamentals of DNA hybridization arrays for gene expression analysis. *Biotechniques* 29:1042-+
- Freeman WM, Walker SJ, Vrana KE (1999) Quantitative RT-PCR: Pitfalls and potential. *Biotechniques* 26:112-+
- Hall S, Strichartz, G., Moczydlowski, E., Ravindran, A., Reichardt, P.B. (1990) The saxitoxins: sources, chemistry, and pharmacology. In: Hall S, Strichartz, G. (ed) *Marine Toxins*, Vol 418. Am. Chem. Soc. Symp. Ser., p 29-65
- Hallegraeff GM, Steffensen DA, Wetherbee R (1988) 3 Estuarine Australian Dinoflagellates That Can Produce Paralytic Shellfish Toxins. *Journal of Plankton Research* 10:533-541
- Harada T, Oshima Y, Yasumoto T (1982) Studies on Paralytic Shellfish Poisoning in Tropical Waters .4. Structures of 2 Paralytic Shellfish Toxins, Gonyautoxin-V and Gonyautoxin-Vi Isolated from a Tropical Dinoflagellate, *Pyrodinium Bahamense* Var *Compressa*. *Agricultural and Biological Chemistry* 46:1861-1864
- Heid CA, Stevens J, Livak KJ, Williams PM (1996) Real time quantitative PCR. *Genome Research* 6:986-994
- Higuchi R, Fockler C, Dollinger G, Watson R (1993) Kinetic Pcr Analysis - Real-Time Monitoring of DNA Amplification Reactions. *Bio-Technology* 11:1026-1030
- <http://www3.aims.gov.au/arnat/arnat-0008.htm> (2005)
- <http://www.encyclopedia.gene-quantification.info/>
- <http://www.who.edu> (2008)

- Huggett J, Dheda K, Bustin S, Zumla A (2005) Real-time RT-PCR normalisation; strategies and considerations. *Genes and Immunity* 6:279-284
- Irizarry RA, Bolstad BM, Collin F, Cope LM, Hobbs B, Speed TP (2003a) Summaries of Affymetrix GeneChip probe level data. *Nucl. Acids Res.* 31:e15
- Irizarry RA, Hobbs B, Collin F, Beazer-Barclay YD, Antonellis KJ, Scherf U, Speed TP (2003b) Exploration, normalization, and summaries of high-density oligonucleotide array probe level data. *Biostatistics* 4:249-264
- Juhl AR, Martins CA, Anderson DM (2008) Toxicity of *Alexandrium lusitanicum* to gastropod larvae is not caused by paralytic-shellfish-poisoning toxins. *Harmful Algae* 7:567-573
- Kao CY (1993) Paralytic shellfish poisoning. In: *Algal toxins in seafood and drinking water*. Academic Press Ltd., p 75-86
- Kellmann R, Mihali TK, Jeon YJ, Pickford R, Pomati F, Neilan BA (2008) Biosynthetic intermediate analysis and functional homology reveal a saxitoxin gene cluster in cyanobacteria. *Applied and Environmental Microbiology* 74:4044-4053
- Kellmann R, Neilan BA (2007) Biochemical characterization of paralytic shellfish toxin biosynthesis *in vitro*. *Journal of Phycology* 43:497-508
- Lagos N, Onodera H, Zagatto PA, Andrinolo D, Azevedo SMFQ, Oshima Y (1999) The first evidence of paralytic shellfish toxins in the freshwater cyanobacterium *Cylindrospermopsis raciborskii*, isolated from Brazil. *Toxicon* 37:1359-1373
- Landsberg JH, Hall S, Johannessen JN, White KD, Conrad SM, Abbott JP, Flewelling LJ, Richardson RW, Dickey RW, Jester ELE, Etheridge SM, Deeds JR, Van Dolah FM, Leighfield TA, Zou YL, Beaudry CG, Benner RA, Rogers PL, Scott PS, Kawabata K, Wolny JL, Steidinger KA (2006) Saxitoxin puffer fish poisoning in the United States, with the first report of *Pyrodinium bahamense* as the putative toxin source. *Environmental Health Perspectives* 114:1502-1507
- Lenaers G, Maroteaux L, Michot B, Herzog M (1989) Dinoflagellates in evolution: A molecular phylogenetic analysis of large subunit RNA. *J Mol Evol.* 29:40-51
- Lettieri T (2006) Recent applications of DNA microarray technology to toxicology and ecotoxicology. *Environmental Health Perspectives* 114:4-9

- Levesque-Sergerie J-P, Duquette M, Thibault C, Delbecchi L, Bissonnette N (2007) Detection limits of several commercial reverse transcriptase enzymes: impact on the low- and high-abundance transcript levels assessed by quantitative RT-PCR. *BMC Molecular Biology* 8:93
- Li RA, Ennis IL, French RJ, Dudley Jr. SC, Tomaselli GF, Marban E (2001) Clockwise domain arrangement of the sodium channel revealed by microconotoxin (GIIIA) docking orientation. *J Biol Chem* 276:11072-11077
- Liu W, Saint DA (2002) A New Quantitative Method of Real Time Reverse Transcription Polymerase Chain Reaction Assay Based on Simulation of Polymerase Chain Reaction Kinetics. *Analytical Biochemistry* 302:52-59
- Livak KJ (1997) Relative quantitation of gene expression. User bulletin #2 for the ABI PRISM 7700 sequence detection system. Applied Biosystems, Foster City, CA, USA
- Livak KJ, Schmittgen TD (2001) Analysis of Relative Gene Expression Data Using Real-Time Quantitative PCR and the 2- $^{-\Delta\Delta CT}$ Method. *Methods* 25:402-408
- Lucker M (1984) Secondary metabolism in microorganisms, plants, and animals, Vol. Springer-Verlag, New York
- Luo Z, Geschwind DH (2001) Microarray applications in neuroscience. *Neurobiology of Disease* 8:183-193
- Michot B, Hassouna N, Bachellerie J-P (1984) Secondary structure of mouse 28S rRNA and general model for the folding of the large rRNA in eukaryotes. *Nucl. Acids Res.* 12:4259-4281
- Morrison TB, Weis JJ, Wittwer CT (1998) Quantification of low-copy number transcripts by continuous SYBR Green I monitoring during amplification. *Biotechniques* 24:954-962
- Moyer CL (2001) Molecular Phylogeny: Application and Implications for Marine Microbiology. In: Paul JH (ed) *Methods in Microbiology: Marine Microbiology*. Academic Press, San Diego, CA, p 375-394
- Negri AP, Jones GJ (1995) Bioaccumulation of paralytic shellfish poisoning (PSP) toxins from the cyanobacterium *Anabaena circinalis* by the freshwater mussel *Alathyria condola*. *Toxicon* 33:667-678

- Oikawa H, Satomi M, Watabe S, Yano Y (2005) Accumulation and depuration rates of paralytic shellfish poisoning toxins in the shore crab *Telmessus acutidens* by feeding toxic mussels under laboratory controlled conditions. *Toxicon* 45:163-169
- Oshima Y, Hasegawa M, Yasumoto T, Hallegraeff G, Blackburn S (1987) Dinoflagellate *Gymnodinium Catenatum* as the Source of Paralytic Shellfish Toxins in Tasmanian Shellfish. *Toxicon* 25:1105-1111
- Peirson SN, Butler JN, Foster RG (2003) Experimental validation of novel and conventional approaches to quantitative real-time PCR data analysis. *Nucleic Acids Research* 31
- Pfaffl MW (2001) A new mathematical model for relative quantification in real-time RT-PCR. *Nucl. Acids Res.* 29:No.9:00
- Pfaffl MW, Horgan GW, Dempfle L (2002) Relative expression software tool (REST(C)) for group-wise comparison and statistical analysis of relative expression results in real-time PCR. *Nucl. Acids Res.* 30:e36-
- Pomati F, Sacchi S, Rossetti C, Giovannardi S, Onodera H, Oshima Y, Neilan BA (2000) The freshwater cyanobacterium *Planktothrix* sp. FP1: Molecular identification and detection of paralytic shellfish poisoning toxins. *Journal of Phycology* 36:553-562
- Ragoussis J, Elvidge G (2006) Affymetrix GeneChip® system: moving from research to the clinic. *Expert Review of Molecular Diagnostics* 6:145-152
- Ramakers C, Ruijter JM, Deprez RHL, Moorman AFM (2003) Assumption-free analysis of quantitative real-time polymerase chain reaction (PCR) data. *Neuroscience Letters* 339:62-66
- Ririe KM, Rasmussen RP, Wittwer CT (1997) Product Differentiation by Analysis of DNA Melting Curves during the Polymerase Chain Reaction. *Analytical Biochemistry* 245:154-160
- Ritson-Williams R, Yotsu-Yamashita M, Paul VJ (2006) Ecological functions of tetrodotoxin in a deadly polyclad flatworm. *PNAS* 103:3176-3179
- Robbens J, van der Ven K, Maras M, Blust R, De Coen W (2007) Ecotoxicological risk assessment using DNA chips and cellular reporters. *Trends in Biotechnology* 25:460-466

- Robineau B, Gagné JA, Fortier L, Cembella AD (1991) Potential impact of a toxic dinoflagellate (*Alexandrium excavatum*) bloom on survival of fish and crustacean larvae. *Marine Biology* 108:293-301
- Sadler LA, McNally KL, Govind NS, Brunk CF, Trench RK (1992) The Nucleotide-Sequence of the Small Subunit Ribosomal-RNA Gene from *Symbiodinium Pilosum*, a Symbiotic Dinoflagellate. *Current Genetics* 21:409-416
- Scheffe JH, Lehmann KE, Buschmann IR, Unger T, Funke-Kaiser H (2006) Quantitative real-time RT-PCR data analysis: current concepts and the novel "gene expression's C_T difference" formula. *J. Mol. Med.* 84:901-910
- Shimizu Y (1993) Microalgal metabolites. *Chem. Rev.* 93:1685-1698
- Shimizu Y (1996) Microalgal metabolites: a new perspective. *Annu. Rev. Microbiol.* 50:431-465
- Snape JR, Maund SJ, Pickford DB, Hutchinson TH (2004) Ecotoxicogenomics: the challenge of integrating genomics into aquatic and terrestrial ecotoxicology. *Aquatic Toxicology* 67:143-154
- Solé J, Estrada M, Garcia-Ladona E (2006) Biological control of harmful algal blooms: A modelling study. *Journal of Marine Systems* 61:165-179
- Steidinger KA, Tester LS, Taylor FJR (1980) A redescription of *Pyrodinium bahamense* var. *compressa* (Bohm) stat. nov. from Pacific red tides. *Phycologia* 19:329-337
- Teegarden GJ (1999) Copepod grazing selection and particle discrimination on the basis of PSP toxin content. *Marine Ecology-Progress Series* 181:163-176
- Terlau H, Heinemann SH, Stuhmer W, Pusch M, Conti F, Imoto K, Numa S (1991) Mapping the site of block by tetrodotoxin and saxitoxin of sodium channel II. *FEBS Letters* 293:93-96
- Tichopad A, Didier A, Pfaffl MW (2004) Inhibition of real-time RT-PCR quantification due to tissue-specific contaminants. *Molecular and Cellular Probes* 18:45-50
- Tillmann U, John U (2002) Toxic effects of *Alexandrium* spp. on heterotrophic dinoflagellates: an allelochemical defence mechanism independent of PSP-toxin content. *Mar. Ecol. Prog. Series* 230:47-59

- Tricarico C, Pinzani P, Bianchi S, Paglierani M, Distante V, Pazzagli M, Bustin SA, Orlando C (2002) Quantitative real-time reverse transcription polymerase chain reaction: normalization to rRNA or single housekeeping genes is inappropriate for human tissue biopsies. *Analytical Biochemistry* 309:293-300
- Tyagi S, Kramer FR (1996) Molecular beacons: Probes that fluoresce upon hybridization. *Nature Biotechnology* 14:303-308
- Whitcombe D, Theaker J, Guy SP, Brown T, Little S (1999) Detection of PCR products using self-probing amplicons and fluorescence. *Nat Biotech* 17:804-807
- White AW (1981) Marine zooplankton can accumulate and retain dinoflagellate toxins and cause fish kills. *Limnol. Oceanogr.* 26:103-109
- Wong ML, Medrano JF (2005) Real-time PCR for mRNA quantitation. *Biotechniques* 39:75-85
- www.fas.org (2008) Federation of American Scientists.
- Wyatt T, Jenkinson IR (1997) Notes on *Alexandrium* population dynamics. *J. Plankton Res.* 19:551-575
- Yamamori K, Nakamura M, Hara TJ (1987) Gustatory Responses to Tetrodotoxin and Saxitoxin in Rainbow Trout (*Salmo gairdneri* and Arctic Char *Salvelinus alpinus*: A Possible Biological Defense Mechanism. *Annals of the New York Academy of Sciences* 510:727-729
- Zimmer RK, Ferrer RP (2007) Neuroecology, Chemical Defense, and the Keystone Species Concept. *Biol Bull* 213:208-225

Part II

Transcriptional Profiling of *Saccharomyces cerevisiae* upon exposure to saxitoxin

Abstract

Saxitoxin is a potent neurotoxin produced by several species of dinoflagellates and cyanobacteria. The molecular target of saxitoxin in higher eukaryotes is the voltage-gated sodium channel; however, its target in lower eukaryotic organisms which lack this target remains unknown. The goal of this study was to obtain the transcriptional fingerprint of the model lower eukaryote *Saccharomyces cerevisiae* upon exposure to saxitoxin to identify potential genes suitable for biomarker development. Microarray analyses identified multiple genes associated with copper and iron homeostasis and sulfur metabolism as significantly differentially expressed upon exposure to saxitoxin. Quantitative reverse-transcriptase (qRT-PCR) assays were developed to verify the results of the microarray and to generate expression profiles in a subset of the differentially regulated genes across multiple exposure times and concentrations. The qRT-PCR assays validated the results of the microarray, and demonstrated that overall, genes tended to respond in a consistent manner to saxitoxin across different treatments. In general, the genes encoding the metallothioneins *CUP1* and *CRS5* were induced following exposure to saxitoxin, while those encoding the ferric/cupric reductase *FRE1* and the copper uptake transporter *CTR1* were repressed. The gene encoding the multicopper ferroxidase *FET3*, part of the high-affinity iron uptake system, was also induced in all treatments, along with the *STR3* gene, which codes for the cystathionine beta-lyase found in the methionine biosynthetic pathway.

Introduction

Saxitoxin is a naturally-occurring secondary metabolite produced by microorganisms from several phyla inhabiting a range of aquatic environments. Due to its molecular target and resulting detrimental effects on human health, it is often described as a potent neurotoxin. Dinoflagellates from the genera *Alexandrium*, *Gymnodinium*, and *Pyrodinium* (Harada et al. 1982b, Oshima et al. 1987, Anderson et al. 1990) are established toxin producers in marine and estuarine (Hallegraeff et al. 1988) systems, while filamentous cyanobacteria from the genera *Planktothrix* (Pomati et al. 2000), *Lyngbya* (Carmichael et al. 1997), *Anabaena* (Negri & Jones 1995), *Aphanizomenon* (Ferreira et al. 2001) and *Cylindrospermopsis* (Lagos et al. 1999) are the predominate producers in freshwater systems. Saxitoxin is often referred to as the parent molecule in the class of compounds also known as Paralytic Shellfish Toxins (PSTs), of which there are over 20 derivatives. The toxicity of the derivatives varies by approximately 2 orders of magnitude (Hall 1990), with saxitoxin being the most toxic. Saxitoxin and its congeners are based on a perhydropurine skeleton with two permanent guanidinium moieties. Variations in functional groups at four defined positions around the ring define the different congeners. The detrimental effects of saxitoxin may be felt on multiple levels: (I) bioaccumulation in shellfish leads to paralytic shellfish poisoning (PSP) in humans, which can ultimately result in death via respiratory paralysis; (II) the potential for ecosystem-level effects upon cellular release of the toxin upon bloom termination; and (III) the potential for use as a weapon of chemical warfare, as saxitoxin and ricin are the only two natural toxins classified as Schedule 1 Chemical Warfare Agents.

The molecular target of saxitoxin in mammals is the sodium channel protein in nerve and muscle cells. It binds with high affinity to site 1 of the alpha subunit, preventing the passage of sodium ions through the cell membrane and thus blocking the passage of nerve impulses (Catterall 1985). Humans are typically exposed to saxitoxin through consumption of contaminated fish and shellfish, whose dietary habits include ingestion of the toxic microorganisms. However, saxitoxin's mode of

action on the lower eukaryotic community members within aquatic environments remains unknown.

One of the ways with which to measure a cell's or organism's adaption to environmental perturbations is through changes in gene expression. DNA microarrays provide a platform to perform genome-wide expression profiling, allowing the changes in thousands of genes to be measured simultaneously. Since its advent, DNA microarrays have been used to determine gene functions and regulatory motifs; in modeling pathways and cell circuitry; to classify disease specimens; and in the identification of molecular targets for drugs (Lockhart & Winzeler 2000). More recently, microarray expression profiling has been used in the field of ecotoxicogenomics to determine the mechanism of action of specific toxicants and to establish "genetic signatures" for identification of the toxicant (Lettieri 2006, Robbens et al. 2007). Both types of information allow for the identification of genes which can be used in the development of biomarkers of effect and biomarkers of exposure, respectively (Robbens et al. 2007).

Ecotoxicological risk assessment has typically been based on the effective concentration (EC_{50}) and/or lethal concentration (LC_{50}) endpoint in organisms from different trophic levels. However, the gains made in molecular techniques such as transcriptional profiling and DNA chips, which allow for the identification of biomarker genes, provide an alternative to animal testing (Robbens et al. 2007). Currently, the mouse bioassay is accepted by the AOAC as the current standard for detecting and measuring saxitoxin, and is the only method approved by the United States Food and Drug Administration for the detection and quantitation of PSTs in shellfish extracts. However, this method has come under criticism in recent years by animal rights and ethical groups, as this assay measures the time to death of live mice after intraperitoneal injection of the suspected toxic sample.

The yeast *Saccharomyces cerevisiae* provides a tractable model for examining the molecular targets of environmental perturbations such as algal toxins in the lower eukaryotic community. The genome has been sequenced and many of its approximately 6,000 genes studied and annotated in detail; this information is

available through numerous databases and resources, including an open-access scientific database on yeast molecular biology and genetics (www.yeastgenome.org). In addition, the yeast system is unicellular, fast-growing, and non-pathogenic, and can be genetically manipulated with relative ease. As such, it is a well-characterized system that is amenable to DNA microarray analysis.

Previous gene expression profiles obtained from DNA microarrays utilizing *S. cerevisiae* have been used to draw correlations among the structures of multiple agricultural fungicides to gene expression patterns (Kitagawa 2003); to identify potential biomarkers for the pesticide thiuram (Kitagawa 2002); and to examine the toxicity of textile wastewater discharged into the environment (Kim et al. 2006). Expression profiling with *S. cerevisiae* has also been used to elucidate the mechanism of action of antifungal agents (Agarwal et al. 2003) and anti-cancer agents (Watanabe et al. 2002) in the field of drug development. Additionally, yeast DNA microarrays have been used to characterize the “environmental stress response,” (Gasch et al. 2000, Causton et al. 2001) the results of which have been applied not only in yeast studies but with other organisms as well, such as the Pacific oyster *Crassostrea gigas* (Meistertzheim et al. 2007), the black tiger shrimp *Penaeus monodon* (de la Vega et al. 2007), and the protozoan parasite *Entamoeba histolytica* (MacFarlane et al. 2005).

The objective of this study was to obtain the transcriptional fingerprint of *S. cerevisiae* to saxitoxin using DNA microarrays, with the hypothesis that a set of genes would be differentially expressed upon exposure to saxitoxin. Expression patterns in a subset of the differentially regulated genes were also examined across various exposure times and concentrations using quantitative reverse-transcriptase PCR in order to determine if cells responded to saxitoxin in a consistent manner.

Methods

Yeast Strains

The constitutively bioluminescent strain CEB585 (W3031B/A, ATTC #201240, MATa, *ade2-1*, *can1-100*, *his3-11, 15*, *leu2-3, 112*, *trp1-1*, *ura3-1*) of *S. cerevisiae* was used for the bioluminescent screening assay (Gupta et al. 2003). The

luxA, *B*, *C*, *D*, and *E* genes from the bacterium *Photobacterium luminescens* have been cloned into yeast expression vectors and functionally expressed in this strain, resulting in autonomous light production. *S. cerevisiae* S288C (ATTC #204508, MAT α , *SUC2*, *mal*, *mel*, *gal2*, *CUP1*, *flo1*, *flo8-1*, *hap1*) was used for DNA microarray and qRT-PCR experiments.

Chemicals

Saxitoxin (catalog number S1417) used for growth curves and bioluminescent screening assays and cycloheximide were purchased from Sigma Aldrich (St. Louis, MO). Saxitoxin used in the majority of the gene expression experiments was purchased from National Research Council Canada (NRCC) (CRM-STX-e). The saxitoxin was lyophilized, concentrated and re-suspended in deionized water (pH 5.5) at a final concentration of 100 μ g ml⁻¹.

Growth Curves

S. cerevisiae S288C was grown overnight in YPD (1% yeast extract, 2% peptone, 2% dextrose) and re-inoculated into fresh YPD to a starting OD₆₀₀=0.28. Cultures were then aliquoted into sterile 2-ml tubes. Due to the small volume of saxitoxin available for both physiological and gene expression studies, growth curves were performed in 200 μ l volumes, with a single biological replicate at each concentration. Saxitoxin was added to the cultures at final concentrations of 0 (control), 0.32, 3.2, 16, and 32 μ M. The control consisted of 0.03N acetic acid. Cell counts were performed every 2-3 hours, and data recorded as cells ml⁻¹.

Physiological Screening: Bioluminescent Microtiter Plate Assay

S. cerevisiae CEB585 was grown overnight in modified minimal media (YMM) (Routledge 1996) lacking uracil and leucine at 28°C. Upon reaching an OD₆₀₀=1.0, an equal volume of saxitoxin or cycloheximide was added to final concentrations of 6.5 and 16 μ M saxitoxin or 7 and 17 μ M cycloheximide. Controls consisted of 0.03N acetic acid and water, as these served as the carriers for saxitoxin and cycloheximide, respectively. Cultures were distributed in 200 μ l volumes to a 96-well microtiter plate. Bioluminescence was measured every 15 minutes for eight

hours in a Microbeta Plus liquid scintillation counter (Perkin-Elmer, Wellesley, MA) with an integration time of 1 s well⁻¹.

Saxitoxin Exposures

Cultures of *S. cerevisiae* S288C were grown in YPD to OD₆₀₀=1.0. 400µl from individual 10-ml overnight cultures was transferred to sterile 2-ml tubes. Saxitoxin (NRCC) was added to the tubes at a final concentration of 16 µM (20 µl). Upon toxin addition, the sample was mixed gently and incubated with moderate agitation (30rpm) at 30°C for 45 minutes. Controls consisted of deionized water (pH 5.5). Three biological replicates were performed under these conditions for microarray analysis. Additional exposures were performed for analysis with qRT-PCR at a concentration of 8 µM for 45 and 90 minutes, and 16 µM for 90 minutes. Two additional exposures were also performed at 16 µM for 45 minutes for a total of five samples at this condition.

Cell Harvesting

Cells were harvested following the protocol of (Causton et al. 2001). Briefly, the total culture volume was transferred to pre-cooled 2-ml tubes and centrifuged for 3 minutes at 4°C (4,000g). The pellet was re-suspended in ice-cold diethylpyrocarbonate (DEPC)-treated water and centrifuged at room temperature for 2.5 minutes. The supernatant was decanted and the pellet placed immediately in liquid nitrogen.

Total RNA Extraction

A protocol was designed that combined the initial steps of the hot phenol method (Causton et al. 2001) with the spin-column technology of the RNEasy kit (Qiagen, Valencia, CA). Total RNA was extracted from frozen cell pellets by an initial incubation with equal volumes of pre-warmed phenol:chloroform:isoamylalcohol (125:24:1, Ambion, Foster City, CA) and TES (10 nM Tris pH 7.5, 10 mM EDTA, 0.5% SDS) for 1 hour at 65°C with frequent mixing. Samples were centrifuged at 4°C for 20 minutes. The aqueous layer was extracted and combined with the lysis buffer of the RNEasy kit and 70% ethanol in ratios of 350 µl per 100 µl sample, to create RNA-selective binding conditions. The remaining steps

followed the manufacturer's protocol. The optional on-column DNase treatment was extended to one hour. Samples were eluted using a sodium citrate buffer (The RNA Storage Solution, Ambion, Foster City, CA). The total RNA concentration and purity of each sample were measured with the Nanodrop-1000 (Nanodrop Technologies Inc., Wilmington, DE). An aliquot of each was reserved for subsequent analysis with quantitative reverse-transcriptase PCR assays.

Microarray Analyses

The microarray experiments were designed to comply with MIAME guidelines (Brazma et al. 2001, <http://www.mged.org/Workgroups/MIAME/miame.html> 2008). Total RNA was processed by the Affymetrix Core Facility at the University of Tennessee (Knoxville, TN) following the protocols of the Affymetrix GeneChip® Expression Analysis Technical Manual. The one-cycle eukaryotic target labeling assay was used for cDNA synthesis, *in vitro* transcription, and target labeling. Briefly, 1 µg from each sample was reverse-transcribed using a T7-Oligo(dT) promoter primer for first-strand synthesis. Following second-strand synthesis, the double-stranded cDNA was spin-column purified and served as template for the *in vitro* transcription reaction. *In vitro* transcription was performed with the T7 RNA polymerase. A biotinylated nucleotide analog was included in the reaction for biotin labeling. Labeling controls consisted of the *Bacillus subtilis* genes *lys*, *phe*, *thr*, and *dap*. The biotin-labeled cRNA was fragmented into segments 35-200 basepairs (bp) in length via metal-induced hydrolysis.

Prior to hybridization, the probe arrays were pre-incubated at 45°C for 10 minutes with the hybridization buffer (100 mM MES, 1M [Na⁺], 20 mM EDTA, 0.01% Tween-20), which was removed with a sterile pipet tip upon sample loading. Arrays were hybridized for 16 hours at 45°C. Hybridization controls included the *E. coli* *bioB*, *bioC*, *bioD*, and *cre* genes. Following hybridization, arrays were washed and stained with streptavidin-phycoerythrin for 10 minutes at 25°C, washed, and stained with an anti-streptavidin antibody solution (at final concentrations of 1x stain buffer, 2 mg ml⁻¹ BSA, 0.1 mg ml⁻¹ goat IgG stock, and 3 µg ml⁻¹ biotinylated

antibody). This was followed by a second stain with streptavidin-phycoerythrin. Arrays were immediately scanned with a GeneChip 7G high-resolution scanner. Each array scan was quality checked for the presence of control genes and background signal values. Intensity values for all transcripts were obtained from the scanned image (.cel) files of the chips. The intensity values of the six arrays were background-corrected and normalized with the GC-RMA algorithm (ArrayAssist, Stratagene, La Jolla, CA) and exported into excel files for statistical analysis with ArrayStat.

The Affymetrix GeneChip Yeast Genome 2.0 Array was used in the microarray analyses. This array consists of probes sets to detect transcripts from both *S. cerevisiae* and *Schizosaccharomyces pombe*. The array contains 5,744 probe sets for 5,841 of the 5,845 genes present in *S. cerevisiae*. The probe sets for *S. cerevisiae* have been designed based on the sequence information available in GenBank. Probe sets are comprised of 11 pairs of 25-mer oligonucleotides.

Microarray Statistical Analysis

Three intensity values were generated for each transcript from three biological replicate experiments at each condition; if there was only one valid observation for a gene within a condition, that datum was disregarded for analysis. Outliers were detected by examining standardized residuals automatically using ArrayStat software. A curve-fit random error estimate method was used for a proportional model with offset. The data were transformed logarithmically, and assessed with a Z-test for two independent conditions. Transcripts with a fold-change linear ratio greater than or equal to 1.3 or less than or equal to 0.7 with a p -value <0.01 were considered differentially expressed and used for further analyses. The molecular and biological processes of the genes were obtained from the *Saccharomyces* Genome Database (SGD) (www.yeastgenome.org). Upon publication of the manuscript prepared from this study, microarray data from this experiment will be deposited into GEO.

Quantitative Reverse-Transcriptase PCR

Primer and Probe Design

Quantitative reverse-transcriptase PCR (qRT-PCR) was used to verify the results obtained in the microarray analysis, and to examine whether the response of

the selected genes varied in response to different saxitoxin exposures. qRT-PCR reactions based on the Taqman® probe methodology were performed in triplicate in a DNA engine equipped with the Chromo4 detector (MJ Research Inc., Waltham, MA). Based on the results of the microarray analysis, the following genes were selected for further interrogation with qRT-PCR: *CRS5*, *CTR1*, *CUP1*, *FET3*, and *FRE1*, all of which are involved in copper and iron homeostasis; *STR3*, which is a part of the sulfur amino acid biosynthetic pathway; and the housekeeping gene *ACT1*. Primers and probe targeted an approximately 100 bp region of the coding sequence of each gene; coding sequences were obtained from the SGD. Primers and probe were designed using the Primer3 software, following the guidelines of Dorak (www.dorak.info/genetics/realtime.html), with an annealing temperature of 60°C. The primers, probe and gene function of each assay are listed in Table II-1.

Probes and forward primers were examined for potential secondary structures at 60°C, and the reverse primers at 50°C, using Mfold (Zuker 2003). The potential for self and cross dimer formation was examined for each of the primer sets using an online oligonucleotide analysis tool (<https://www.operon.com/oligos/toolkit.php>). Self-complementarity was determined using the oligonucleotide properties calculator (<http://www.basic.northwestern.edu/biotools/oligoalc.html>). Oligonucleotide primers and 5'(FAM)-3'BHQ probes were obtained from Biosearch Technologies (Novato, CA).

Determination of Primer Specificity

For each target, primer specificity was initially evaluated with temperature gradient PCR reactions. Template consisted of diluted total RNA from a sample in which the gene of interest was identified as differentially expressed in the microarray (in the case of down-regulated genes, the corresponding control sample was used as template). The Quantitect Probe RT-PCR kit (Qiagen, Valencia, CA) was used for all reactions. Each reaction contained: 12.5 µl 2x Quantitect Probe RT-PCR Master Mix, 600 nm forward and reverse primers, 0.25 µl QuantiTect RT Mix, 4.25 µl nuclease-free water, and 5 µl diluted template. Reactions were conducted on a DNA Engine Diad thermocycler (MJ Research, Waltham, MA) using the following protocol: 50°C

Table II-1. List of genes examined with quantitative reverse-transcriptase PCR following exposure to saxitoxin at different concentrations and lengths of time. Primer and probe sequences, along with target amplicon size, were designed for use with the Taqman assay. *ACT1* served as the reference gene and was used to normalize all functional gene expression data.

Assay Target	Gene Description	Primer/Probe Sequence	Amplicon Size (bp)
<i>ACT1</i>	B-Actin	F:5'-ACCGCTGCTCAATCTTCTTCAA R:5'-AGCTTCTGGGGCTCTGAATC 5'-(FAM)ATCCTACGAACCTCCAGATGGTCAAGTCAT(BHQ)	96
<i>CRS5</i>	Copper-binding metallothionein	F:5'-CTGTTCTGGCGGTGAAAAGT R:5'-TCACAAGTGCACGTGGTTTC 5'-(FAM)CCTCAATGTAAGAGTTGTGGTGAAAAATGC(BHQ)	102
<i>CTR1</i>	Copper uptake transmembrane transporter	F:5'-ATGTCCAGTGCAGCAAAC R:5'-GGTGTACTGCTCATCGACAT 5'-(FAM)CGATGGGAAGCAGTTCAATGTCAGGTATGT(BHQ)	107
<i>CUP1</i>	Metallothionein	F:5'-GTGCCAATGCCAATGTGGTA R:5'-GCATTTGTCGTCGCTGTTAC 5'-(FAM)AATGAACAATGCCAAAAATCATGTAGCTGC(BHQ)	91
<i>FET3</i>	Multicopper ferroxidase	F:5'-TTGACCAACGGAATGAACAA R:5'-TTGGACATTGCGTCAAGAAG 5'-(FAM)TACTTCTATGCATTTCCACGGTCTCTTCCA(BHQ)	106
<i>FRE1</i>	Ferric and cupric reductase	F:5'-TATTTCCCAAGCTGCGCTAT R:5'-ATTCTCATAGGCACATGCTG 5'-(FAM)ACTGTAAAAACATCAATTGGCTGGGTTTCAG(BHQ)	109
<i>STR3</i>	Cystathionine beta-lyase	F:5'-GTGGTATGACGGCGCTAGAC R:5'-GGGTGCCTCCATAAAGATCA 5'-(FAM)TCTTACTTAACGGCACTGACAACCATACGC(BHQ)	108

for 30 minutes, 95°C for 15 minutes, and 30 cycles of denaturing at 94°C for 15 seconds and annealing/extension at 60°C for 1 min. For each assay, the PCR product was visualized on a 1% agarose gel; a band at approximately 100 bp indicated primers were specific for the target of interest (data not shown).

Assay Optimization

The conditions of the qRT-PCR reaction were optimized for each assay; this included the forward and reverse primer concentrations, the probe concentration, and the annealing/extension time. Initially, primer concentrations of 400, 600, and 800 nM (final concentrations) were evaluated with probe concentrations of 50, 100, and 200 nM, at temperatures of 58, 60, and 62°C. Reactions were preformed in triplicate. The PCR efficiency of each reaction was determined using LinRegPCR (Ramakers et al. 2003). Primer concentrations of 600 and 800 nM, a probe concentration of 200 nM, and annealing/extension temperatures of 58 and 60°C typically yielded greater PCR efficiencies and lower C_{T_s} . The probe concentration of 200 nM was deemed optimal and used in all future assays, at primer concentrations of 600 or 800 nM. For most assays, 600 nM 60°C clearly yielded the optimal conditions. For assays in which multiple conditions yielded similar values, the Student's *t*-test was used to determine if a significant difference existed between both the PCR efficiencies and C_{T_s} of these reactions. The Quantitect Probe RT-PCR kit (Qiagen, Valencia, CA) was used for all assays.

Based on the results of the optimization, all assay reactions used for microarray verification and additional expression measurements consisted of 12.5 μ l 2x Quantitect Probe RT-PCR Master Mix, the optimized concentrations of primers (typically 600 nM or 800 nM), 200 nM probe, 0.25 μ l QuantiTect RT Mix, 5 μ l of template, and adjusted to a final volume of 25 μ l with nuclease-free water. Template consisted of a 1:100 dilution of the total RNA extract of each sample. The following protocol was used for all assays: 50°C for 30 minutes, 95°C for 15 minutes, and 45 cycles of denaturing at 94°C for 15 seconds and annealing/extension at 60°C for 1 min.

Preparation of RNA Standards

Full-length transcripts of the genes described above (summarized in Table II-1) were generated via *in vitro* transcription to create 8-point external standard curves for each assay. Genomic DNA was extracted from *S. cerevisiae* S288C with the DNeasy Tissue Kit (Qiagen, Valencia, CA). Briefly, cells were grown overnight to a final cell concentration of 1×10^8 . Three aliquots of 5×10^7 cells were harvested by centrifugation for 10 minutes at 5,000g. Spheroplasts were generated by incubation with 200 units lyticase dissolved in sorbitol buffer (1 M sorbitol; 100 mM sodium EDTA; 14 mM β -mercaptoethanol) for 45 minutes at 30°C. Spheroplasts were then lysed by incubation with proteinase K for 3 hours at 55°C. The remaining steps of the protocol followed the manufacturer's instructions. DNA was eluted in nuclease-free water and quantified using Hoechst dye with a DyNA Quant 200 fluorometer (Amersham Biosciences, Piscataway, NJ).

For the creation of each RNA standard, primers were designed to amplify the entire gene plus an additional 5-10 nucleotides up- and downstream of the gene. The genomic DNA sequence of each gene, along with 1 kb of sequence up-and downstream, was obtained from the SGD. The primers, annealing temperatures, and expected product sizes used to amplify each gene of interest are listed in Table II-2. All PCRs were carried out with Ready-to-Go PCR Beads (Amersham Biosciences, Piscataway, NJ) to which was added 400 nm forward and reverse primer, 30 ng genomic DNA, and nuclease-free water to a final volume of 25 μ l. General thermalcycling conditions consisted of: 95°C for 5 minutes, 30 cycles of denaturing at 94°C for 30 seconds, annealing at a temperature 5°C lower than the lowest T_M of the primer set, and extension at 72°C based on a rate of 1000 bp min^{-1} (Sambrook & Russell 2001), with a final elongation step of 72°C for 10 min to complete any partial polymerizations. PCR products were visualized by gel electrophoresis to confirm product amplification of the proper size.

Concomitant with gel electrophoresis, an aliquot of the PCR product was cloned into the pCR2.1 vector using a TOPO TA cloning kit (Invitrogen, Carlsbad, CA) following the manufacturer's instructions. Plasmid DNA was purified using the

Table II-2. Primer sequences, annealing temperatures, and expected product size of genomic DNA targets used in the creation of *in-vitro* transcribed RNA standards. Gene ID is consistent with that in Table II-1.

Gene ID	Primer Sequences	T _a	Product Size (bp)
<i>ACT1</i>	F: 5'-GAATAGGATCTTCTACTACATCAGC R: 5'-AATAGAAATAGAGAGAGAGGTACATAC	56°C	1,577
<i>CRS5</i>	F: 5'-CTATATAAGAAGGGCGCACA R: 5'-ACCTTATATTTAGTTCAT	51°C	391
<i>CTR1</i>	F: 5'-AGTGTATTATATTTGACATTCA R: 5'-AGAAGATATAGGTGGACGAA	47°C	1,278
<i>CUP1</i>	F: 5'-CTGTACAATCAATCAATCAATC R: 5'-TGAATATATTAAGACTATTCGTT	48°C	242
<i>FET3</i>	F: 5'-ATTAGAACTAGATGACTAACG R: 5'-GCAAAATACATGATCTTCCTT	50°C	1,945
<i>FRE1</i>	F: 5'-CTCTTCCATGCTTCAGTTCC R: 5'-TAGATTTAGAACCCGCATTTGA	52.5°C	2,302
<i>STR3</i>	F: 5'-GCATAGAAGCAAAAAGATGC R: 5'-TCCCTTACAATTTCGAACTC	51.5°C	1,418

Wizard Plus Minipreps kit (Promega, Madison, WI). An *EcoRI* restriction digest was used to screen for inserts of the proper size, with visualization on a 1% agarose gel. Clones containing inserts of the correct size were then sequenced using the M13 forward and reverse primers on an ABI 3100 genetic analyzer (Applied Biosystems, Foster City, CA) at the Molecular Biology Resource Facility, University of Tennessee (Knoxville, TN), and confirmed with the sequence information from the SGD using the BLAST alignment tool.

Clones that displayed the following characteristics were selected for *in vitro* transcription: (I) DNA sequences identical to that of the target sequence, including the primer and probe binding sites and regions immediately up- and downstream of the intended target (Qiagen 2003); and (II) proper DNA template orientation, resulting in generation of the sense transcript from the T7 RNA polymerase promoter. Clones chosen for subsequent *in vitro* transcription were grown overnight in 100 ml of Luria-Bertrani broth supplemented with 50 $\mu\text{g L}^{-1}$ kanamycin and the plasmids purified using the Wizard Plus Midipreps kit (Promega, Madison, WI) following the manufacturer's instructions.

To create a transcript of defined length, the plasmid was digested with *SpeI*. The only exception to this was the *FRE1* standard, which was digested with *BamHI*, due to the fact that *SpeI* cut within the genomic sequence. *BamHI* did not cut within the sequence and produced a 5' overhang. To ensure adequate template for the *in vitro* transcription reaction, two restriction digests were performed; in each, 5 μg plasmid DNA was combined with 25 U *SpeI*, 5 μl Buffer B, and nuclease-free water in a total reaction volume of 50 μl . Plasmids were digested for 4-6 hours at 37°C with mild agitation. An aliquot (10 μl) of the digested and control (no enzyme) reactions were electrophoresed on an agarose gel and viewed under UV illumination to confirm linearization. The remaining volumes of the two digests were combined and cleaned using the Qiaquick Clean-Up kit (Qiagen, Valencia, CA), with elution in 30 μl HPLC-purified water. DNA was quantified using Hoechst dye with a DyNA Quant 200 fluorometer.

The T7 Ribomax Express kit (Promega, Madison, WI) was used for *in vitro* transcription following manufacturer's instructions. The product was then cleaned using the RNEasy mini kit, starting with the spheroplast lysis step: Buffer RLT (lysis buffer) and 70% ethanol were added in ratios of 350 μl per 100 μl of sample. The optional on-column DNase digestion was included and extended to one hour. Products were eluted in 38 μl of sodium citrate buffer (The RNA storage solution, Ambion, Foster City, CA), and an aliquot of the cleaned reaction visualized on a 1x TAE gel to confirm successful *in vitro* transcription. RNA sample preparation, including buffers and reagents used in gel electrophoreses, followed the recommended guidelines of the *in vitro* transcription kit.

Preparation of Standard Curve

RNA concentration and purity were determined with the NanoDrop-1000. The copy number of standard RNA molecules was determined using the equation: $(X \text{ g } \mu\text{l}^{-1} \text{ RNA} / [\text{transcript length in nucleotides} \times 340]) \times 6.022 \times 10^{23} = Y \text{ molecules } \mu\text{l}^{-1}$ (Qiagen 2003). The RNA standard stock solution was diluted in nuclease-free water to a working concentration of $2 \times 10^8 \text{ copies } \mu\text{l}^{-1}$. A dilution series was prepared that ranged from 2×10^7 to $2 \times 10^{-1} \text{ copies } \mu\text{l}^{-1}$. Five μl of each dilution were used per reaction, yielding a standard curve that ranged from 10^8 to 10^1 copies. The standard curve for each assay was performed in triplicate prior to use in measurement of *S. cerevisiae* gene expression upon exposure to saxitoxin.

Validation of ACT1 as an Appropriate Housekeeping Gene

For each assay, the transcript copies of individual samples were normalized to their respective *ACT1* values in an attempt to neutralize sample bias that may have arisen from sample harvesting or RNA extraction. This was done by dividing the transcript copies of the functional gene by the transcript copies of *ACT1*. Prior to normalization with *ACT1*, its effective employment as a housekeeping gene was validated by comparing the transcripts ng total RNA^{-1} between control and exposed samples and by calculating the fold-change at each treatment. There was no statistical significant difference in the transcripts ng total RNA^{-1} between exposed and control samples of *ACT1* at any of the treatments, and the fold-change remained relatively

unchanged among the various treatments. These analyses verified the appropriate use of *ACT1* as a housekeeping gene, as its expression was not affected by saxitoxin exposure.

The PCR efficiency of each assay was also calculated and compared to that of *ACT1*. The plot of $C_{(T)}$ versus log template amount was used to determine the linearity and slope of each reaction; the PCR efficiency of each assay was then calculated based on the slope of the standard curve with the equation: $E = 10^{(-1/\text{slope})} - 1$ (Arezi et al. 2003). Table III-3 lists the slope, PCR efficiency, and r^2 value of each assay. The PCR efficiencies of all assays were found to be similar, allowing *ACT1* to be used as an accurate reference.

qRT-PCR Data Normalization and Statistical Analyses

Expression changes were determined via absolute quantification using the *in vitro* transcribed standards. Data for each functional gene were initially measured as transcript copies ng total RNA⁻¹; these values were normalized by dividing the transcript copies ng total RNA⁻¹ of each sample to its corresponding *ACT1* transcript copies ng total RNA⁻¹ value (these data are hereafter referred to as “normalized transcript copies”).

For each gene at each treatment, normalized values were analyzed for statistical significance (SPSS v.15, Chicago, IL) between exposed and control; if samples passed the tests for equal variance (Levene’s test) and normality (Shapiro-Wilkes), the independent samples *t*-test was applied to the normalized transcript copies of treatment and control. The Mann-Whitney U-test with Monte Carlo correction was applied if samples were not normally distributed. The average fold-change was calculated by dividing the average normalized transcript copy number of exposed by average normalized transcript copy number of control. Fold-change range was calculated with the equation:

$$\sqrt{(s_E \div \bar{x}_E)^2 + (s_C \div \bar{x}_C)^2},$$

where s = standard deviation, \bar{x} = average normalized transcript copy number, E = exposed, and C = control.

Table II-3. PCR efficiency of each qRT-PCR assay as derived from the slope of individual standard curves using the equation $E = 10^{(-1/\text{slope})} - 1$.

Target	Slope	PCR E (%)	r²
<i>ACT1</i>	-3.28	102	0.993
<i>CRS5</i>	-3.56	91	1.000
<i>CTR1</i>	-3.17	107	0.994
<i>CUP1</i>	-3.43	96	0.999
<i>FET3</i>	-3.37	98	0.999
<i>FRE1</i>	-3.41	97	0.999
<i>STR3</i>	-3.21	105	0.998

The regulation of each functional gene at each treatment was examined to determine if genes responded in a consistent manner by plotting the normalized fold-change in each of the four treatments.

Results

Growth Curves

Saxitoxin did not affect the growth of *S. cerevisiae* S288C at any of the concentrations tested (Figure II-1, Appendix I).

Bioluminescent Yeast Screen

The screening assay was used in conjunction with the growth curves to examine the physiological effects of saxitoxin on yeast cells. Saxitoxin affected the constitutive bioluminescence of *S. cerevisiae* CEB585 at both 6.5 μ M and 16 μ M. Initial bioluminescence output was decreased at both concentrations in comparison to the cycloheximide-exposed and control cultures (Figure II-2). While the exact mechanism by which saxitoxin affected the bioluminescence is not known, growth curves performed independently of the screening assay indicated that the decrease in light output was not a function of cell death, as growth was unaffected by the toxin (Figure II-1, Appendix I). As the intent was to examine the initial transcriptional response of yeast upon short-term exposure to saxitoxin, a 45 min exposure time was chosen at a concentration of 16 μ M based on the results of the bioluminescent screen.

Microarray Analyses

The microarray analysis identified 52 genes as significantly differentially expressed, approximately 1% of the yeast genome. Of the 52 genes, 22 were down-regulated (fold-change ratio ≤ 0.7) and 30 were upregulated (fold-change ratio ≥ 1.3). Functional groups with multiple genes affected included those involved in metal transport and homeostasis, sulfur amino acid biosynthesis, and ribosome biogenesis and assembly (Figure II-3).

Down-regulated genes included two involved in copper ion import (*CTR1* and *FRE1*) and 5 involved with ribosome biogenesis and assembly (*LTV1*, *DHR2*, *RRP12*, *HCA4*, and *AAH1*). Among the upregulated genes were those with molecular

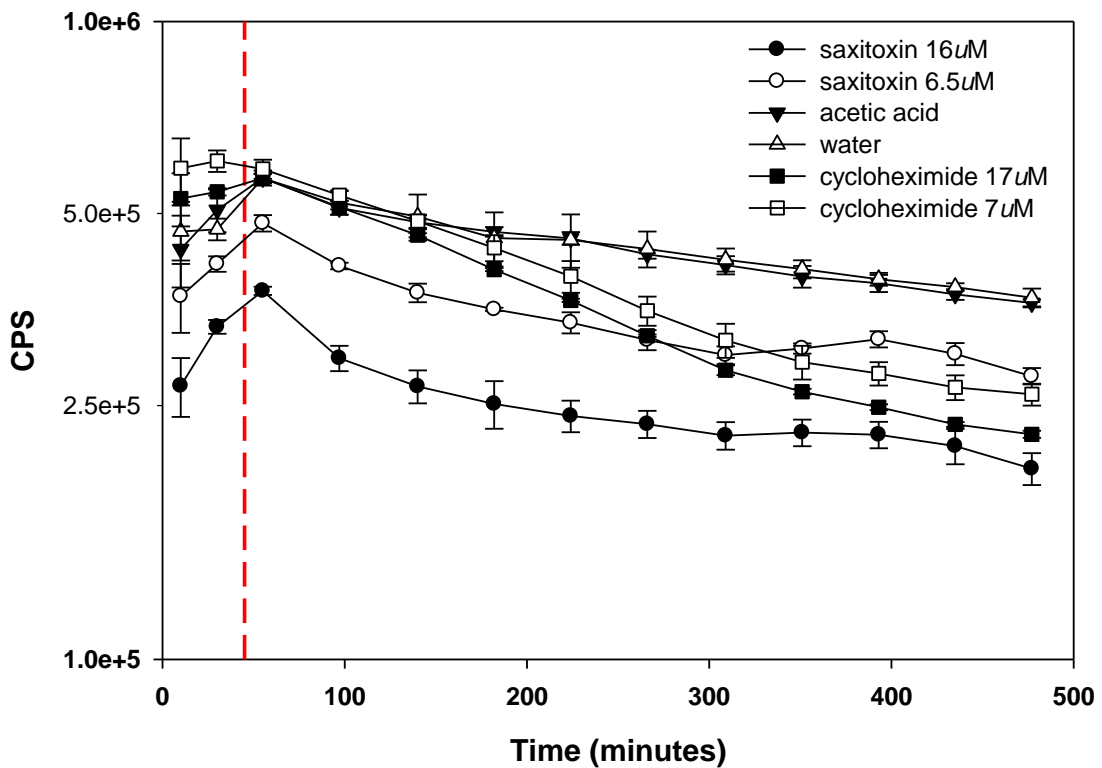


Figure II-2. Effects of saxitoxin on constitutive bioluminescence of *S. cerevisiae* CEB585. Exposures were performed in 96-well microtiter plates with 200 μ l mid-exponential ($OD_{600}=1.0$) yeast culture per well. Output was recorded as counts per second (CPS) on a Microbeta Plus liquid scintillation counter for eight hours. Positive controls consisted of cycloheximide at approximately the same concentrations as saxitoxin. Negative controls consisted of acetic acid for saxitoxin and water for cycloheximide. Vertical dashed line represents exposure time chosen for microarray experiments.

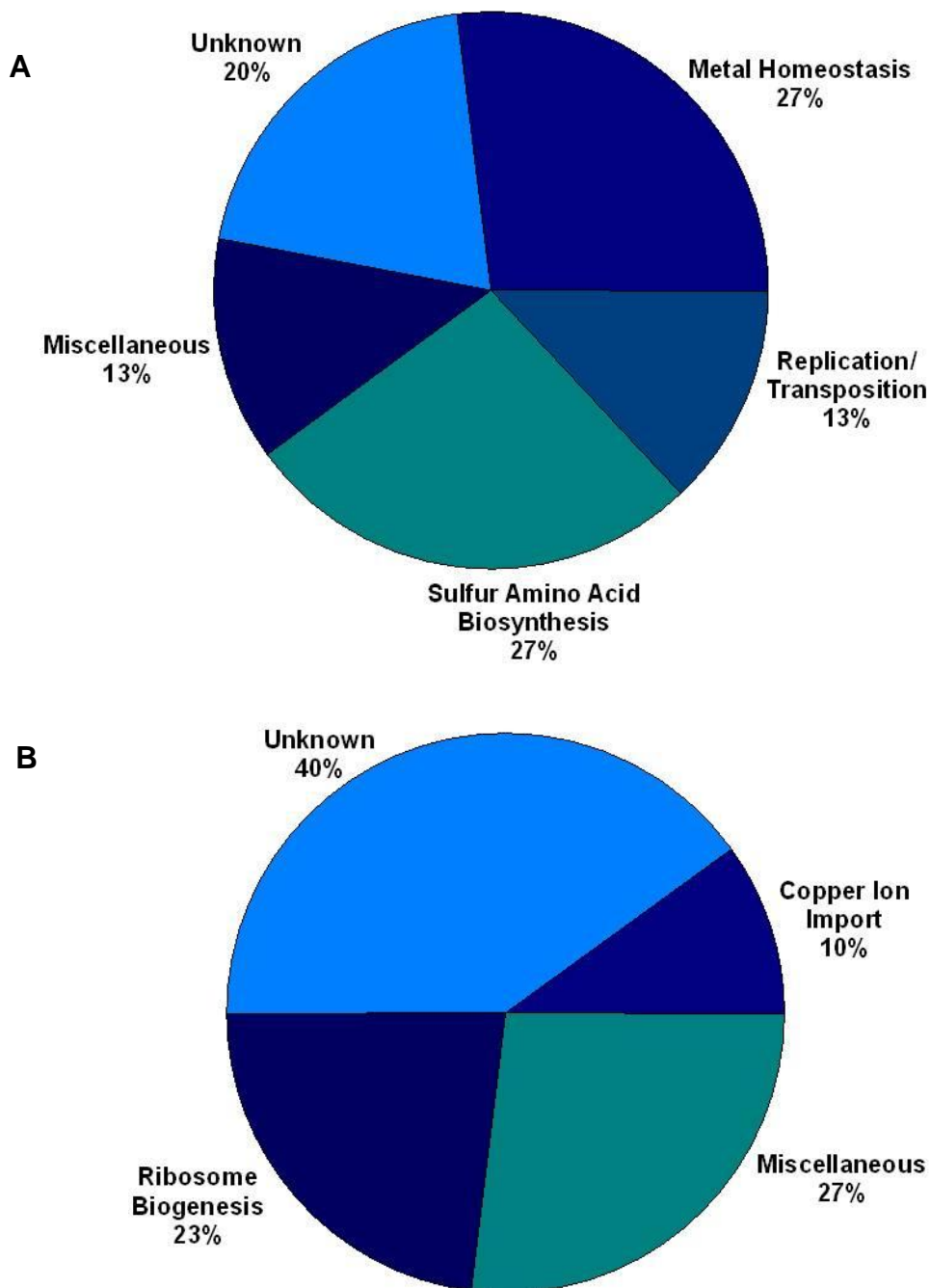


Figure II-3. Genes were classified into functional groups based on their molecular and/or biological functions listed in the Saccharomyces Genome Database. A number of related genes were significantly induced (A.) or repressed (B.) following exposure to 16 μ M saxitoxin for 45 min. Functional groups comprising less than 5% of the total were classified as miscellaneous.

functions related to metal ion binding and/or homeostasis, primarily copper and iron, and 8 whose functions included sulfur amino acid biosynthesis and/or metabolism (Table II-4). A complete list of the genes significantly differentially expressed in the microarray can be found in Appendix I (Table II-5).

Verification of Microarray Results

Quantitative RT-PCR results verified those obtained with the DNA microarray at the exposure condition of 16 μ M saxitoxin for 45 minutes (Table II-6). While the results obtained with qRT-PCR are in agreement with the microarray data, the levels of expression are enhanced, and this may be due to two factors: (I) the algorithm used in the microarray analysis (GC-RMA) compresses fold-change by 10-20% (Irazarri 2003); and (II) the assays utilized gene-specific primers, which synthesize the most specific cDNA and are considered the most sensitive of the priming options for qRT-PCR reactions (Bustin & Nolan 2004).

These assays were also used to examine the expression profile of the selected functional genes at additional concentrations and lengths of exposure to determine if *S. cerevisiae* responds to saxitoxin in a consistent manner over time and concentration. A summary of the differential expression changes (expressed as linear ratios) of each target gene at the various exposures is listed in Table II-6. The regulation of the selected genes behaved in a similar manner among all exposure conditions (Figure II-4, a-f), with the exception of *CTR1*. This gene was down-regulated at the shorter exposure times, but was not differentially expressed at the extended exposure times (Figure II-4a). *CUP1* was the most highly expressed gene among those examined with qRT-PCR, with statistically significant up-regulation in three of the four treatments (Figure II-4c and Table II-6). These data indicate that overall, *S. cerevisiae* gene expression responded to saxitoxin in a relatively consistent manner, an essential trait for genes with the potential for biomarker development.

Discussion

The genetic signature obtained upon exposure to saxitoxin included differential expression of genes typically associated with copper and iron

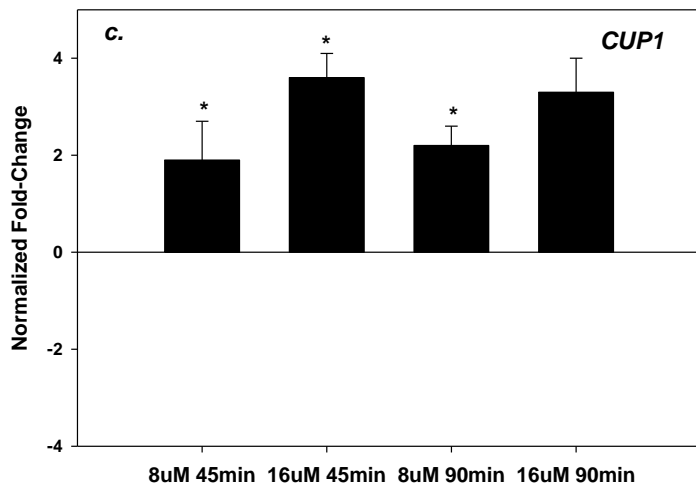
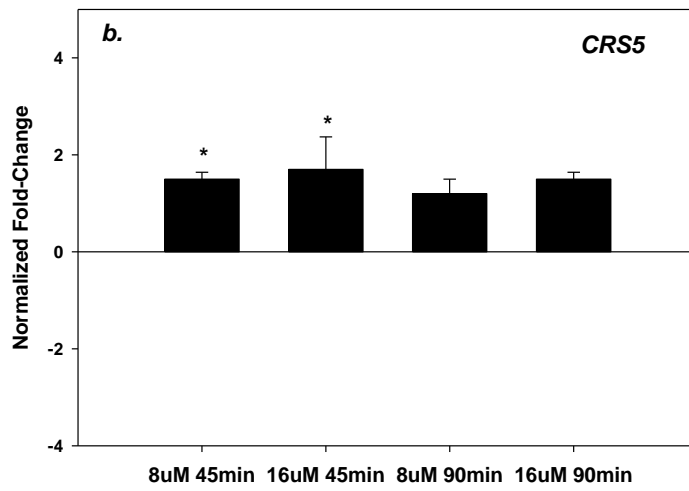
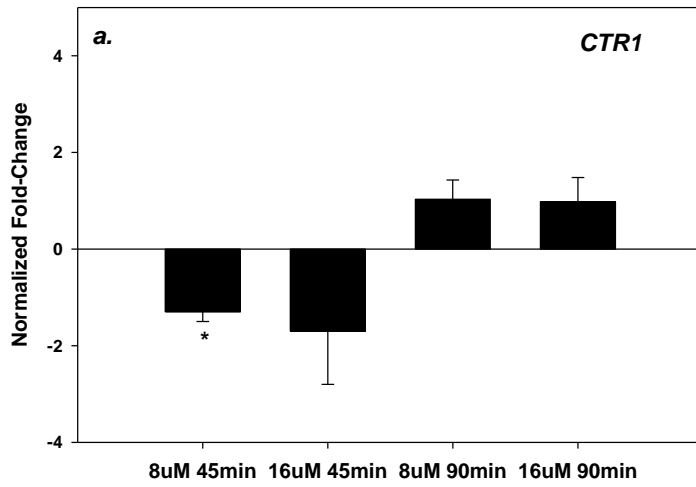
Table II-4. Genes involved in copper and iron homeostasis and sulfur metabolism identified as significantly differentially expressed ($p < 0.01$) in microarray analysis following exposure to 16 μ M saxitoxin.

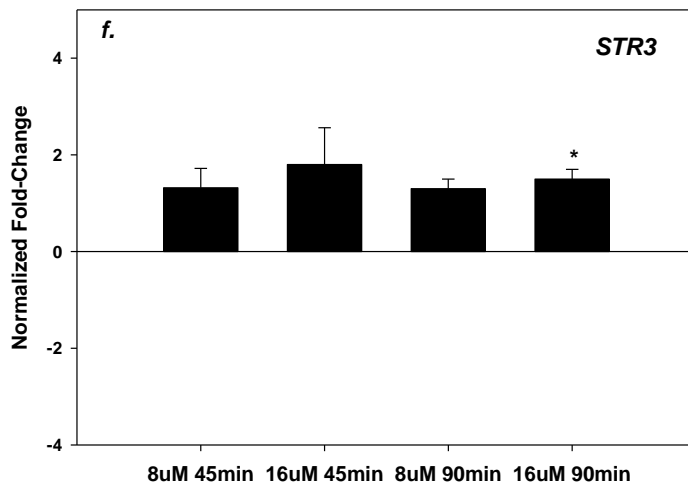
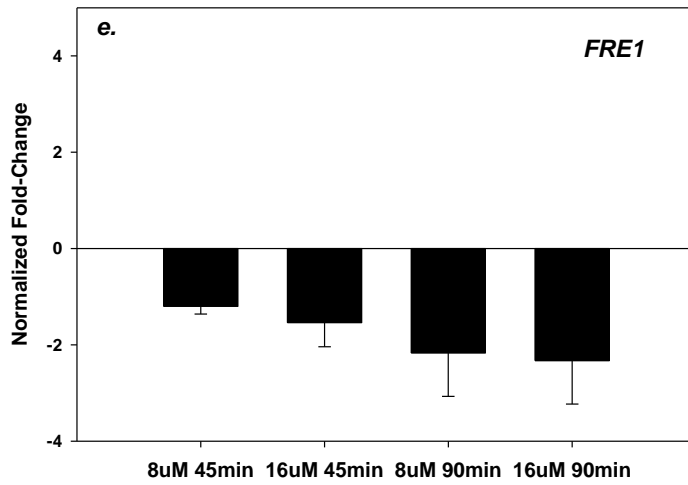
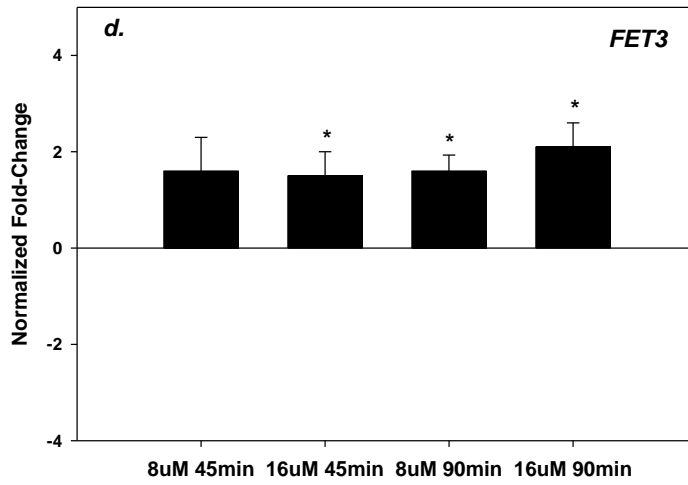
Gene Name	Description	Linear Ratio
Copper and Iron Homeostasis		
CTR1	Copper uptake transmembrane transporter	0.34
FRE1	Ferric and cupric reductase; reduces siderophore-bound iron and oxidized copper prior to uptake by transporters	0.64
FET3	Multicopper oxidase required for high-affinity iron uptake; mediates resistance to copper ion toxicity	1.31
SLF1	Copper-dependent mineralization of copper sulfide complexes on cell surface	1.34
CUP1	Metallothionein; binds copper and mediates resistance to high concentrations of copper and cadmium	1.41
CRS5	Copper-binding metallothionein	1.46
ENB1	Ferric enterobactin transporter	1.32
Sulfur Metabolism		
SAM3	S-adenosylmethionine permease, required for utilization of S-adenosylmethionine as a sulfur source	1.44
MET10	Assimilatory sulfite reductase (alpha subunit); converts sulfite into sulfide	1.4
MET14	Adenylylsulfate kinase; sulfate assimilation and methionine metabolism	1.4
MET28	Transcriptional activator involved in sulfur metabolism regulation	1.52
MET1	S-adenosyl-L-methionine uroporphyrinogen III transmethylase; sulfate assimilation and methionine biosynthesis	1.57
MET32	Transcriptional regulator involved in sulfur amino acid metabolism and methionine biosynthesis	1.66
MET2	L-homoserine-O-acetyltransferase; catalyzes first step of methionine biosynthetic pathway	1.68
STR3	Cystathionine beta-lyase; sulfur amino acid biosynthesis and methionine biosynthesis	2.14

Table II-6. Average fold-change of genes among saxitoxin treatments and in comparison to microarray values. * indicates significance at $p < 0.05$ level for qRT-PCR values. (All microarray values significant at $p < 0.01$ level.)

Gene ID	8 μ M 45min	16 μ M 45min	8 μ M 90min	16 μ M 90min	Array
<i>CTRI</i>	0.78 (± 0.2)*	0.58 (± 1.1)	1.03 (± 0.4)	0.98 (± 0.5)	0.34
<i>CRS5</i>	1.47 (± 0.14)*	1.7 (± 0.67)*	1.23 (± 0.3)	1.47 (± 0.14)	1.46
<i>CUPI</i>	1.85 (± 0.8)*	3.63 (± 0.5)*	2.16 (± 0.4)*	3.3 (± 0.7)	1.41
<i>FET3</i>	1.6 (± 0.7)	1.5 (± 0.5)*	1.6 (± 0.33)*	2.1 (± 0.5)*	1.31
<i>FRE1</i>	0.86 (± 0.16)	0.65 (± 0.5)	0.46 (± 0.9)	0.43 (± 0.9)	0.64
<i>STR3</i>	1.32 (± 0.4)	1.75 (± 0.76)	1.27 (± 0.2)	1.46 (± 0.2)*	2.14

Figure II-4. Normalized expression profiles obtained from qRT-PCR assays for a subset of genes identified as significantly differentially expressed in microarray experiments across various exposure times and saxitoxin concentrations. * indicates significant difference from control ($p < 0.05$). (a.) *CTR1* was repressed at the shorter exposure times but remained unchanged during 90 min exposures. (b.-d.) *CRS5*, *CUP1*, and *FET3* were upregulated at all exposure times and saxitoxin concentrations. (e.) *FRE1* was repressed at all exposure times and concentrations. (f.) *STR3*, which codes for an enzyme involved in sulfur amino acid biosynthesis, was also induced in all treatments.





homeostasis. In this study, exposure to saxitoxin induced the expression of *CUP1*, *CRS5*, and *FET3*, which previously have been shown to be upregulated under conditions of excess copper (Gross et al. 2000). *CUP1* and *CRS5* code for small, cysteine-rich metallothioneins that sequester excess copper ions (Karin et al. 1984, Culotta et al. 1994) via thiol-mediated interactions, one of the predominant mechanisms used to alleviate metal ion toxicity (Perego & Howell 1997). There are no reports in the literature of these genes being induced by molecules similar in structure to saxitoxin. While excess copper has been shown to induce expression of *FET3*, it is not involved in copper detoxification, but instead encodes a multicopper oxidase required for the high-affinity uptake of Fe(II). In *S. cerevisiae*, the correlation between copper and iron is a function of the requirement for copper in the high affinity iron transport system (Dancis et al. 1994b), as the yeast Fet3 protein specifically requires four copper ions for its activity (Taylor et al. 2005). Fet3p has also been shown to aid in copper resistance via a cuprous oxidase activity that occurs in the extracellular space of the cell (Shi et al. 2003). In addition to genes associated with the primary system of copper detoxification (Cup1p), the microarray analysis also identified *SLF1* as upregulated upon exposure to saxitoxin. *SLF1* is believed to be a part of a copper detoxification system, separate from that of Cup1p, that results in sulfide generation and copper sulfide biomineralization at the cell surface (Yu et al. 1996).

Exposure to saxitoxin also resulted in the repression of *CTR1* and *FRE1*, whose proteins are involved in copper ion import. *CTR1* encodes a membrane protein required for both high affinity copper and iron uptake, (Dancis et al. 1994b), while *FRE1* encodes a plasma membrane ferric and cupric reductase that participates in both high-affinity iron and copper transport into the cell (Dancis et al. 1992, Hassett & Kosman 1995). A mechanistic link exists between Ctr1p and Fet3p, as copper uptake regulated through Ctr1p provides the copper ions needed for the proper functioning of Fet3p (Klausner & Dancis 1994).

Expression of *ENBI*, an enterobactin transporter (Heymann 2000) that is part of the non-reductive iron uptake system, was also upregulated in the array. Genes

belonging to the nonreductive siderophore-iron transport system have previously been shown to be induced under conditions of copper deprivation (van Bakel et al. 2005). This suggests saxitoxin may be hindering activity of the high-affinity, reductive system, possibly through copper ion displacement, thereby restricting Fet3p function. Given that copper and iron homeostasis genes are differentially regulated upon exposure of *S. cerevisiae* to saxitoxin, it appears that the toxin competes with the uptake of copper or displaces copper ions in an as-yet unidentified manner. Experiments performed to identify the copper regulon in *S. cerevisiae* suggested that the copper-induced expression of *FET3* is due to a transient decrease in the cellular iron levels (Gross et al. 2000); in the case of saxitoxin, displacement of copper ions by saxitoxin at Ctr1p may prevent proper rationing of intracellular copper levels.

Another means of alleviating heavy metal toxicity in a wide range of organisms including yeast, algae, photosynthetic protists, higher plants, and even humans is the chelation of the metal by either glutathione (GSH) or, in the case of species capable of photosynthesis, phytochelatins (PCs), low-molecular weight sulfur-containing peptides derived from GSH (Mendoza-Cozatl 2005). While budding yeast have evolved a highly specific response to excess copper, the transcriptional profile of the fission yeast *Schizosaccharomyces pombe* to excess copper suggests a more general stress response, as genes coding for glutathione S-transferase, thioredoxin, zinc metallothionein, and superoxide dismutase were shown to be induced upon exposure to elevated copper levels (van Bakel 2007).

GSH synthesis requires the sulfur assimilation and cysteine biosynthetic pathways. The microarray analyses performed here identified multiple genes whose products are involved in sulfur amino acid metabolism (Table II-4). Yeast metabolize extracellular sulfate via the sulfate assimilation pathway, in which activated sulfate is reduced in two successive reactions to generate sulfide for use in cysteine, methionine, and S-adenosylmethionine (SAM) biosynthesis (Thomas & Surdin-Kerjan 1997). The first gene of the sulfur assimilation pathway differentially expressed was *MET14*, an APS kinase whose activity results in the formation of PAPS (3'-phospho-5'-adenylylsulfate), believed to be toxic and thus requiring a

delicate balance in concentrations. *MET10*, *MET1*, and *MET2*, which encode for proteins involved in the sequential reduction of sulfate to sulfide for eventual incorporation into homocysteine (Hansen 1994, 1996, 1997, Thomas & Surdin-Kerjan 1997), were also upregulated in response to saxitoxin, along with the transcriptional activator *MET28*. Homocysteine is then typically channeled into the cysteine and methionine biosynthetic pathways. However, most of the genes associated with these pathways were not identified as differentially expressed upon exposure to saxitoxin; one exception was *STR3*, whose protein converts cystathionine to homocysteine (Hansen 2000). *MET32*, which encodes for a protein involved in the transcriptional regulation of methionine metabolism, was also upregulated; interestingly, Met32p may also play a role in co-regulating genes involved in copper and iron homeostasis (Moler et al. 2000). *SAM3*, which encodes for a permease specific for the transport of SAM across the plasma membrane, was also upregulated in response to saxitoxin.

In *S. cerevisiae*, genes involved in sulfate assimilation have been shown to be induced in response to arsenite; however, a large portion of the sulfur was channeled into glutathione (GSH) biosynthesis, presumably to provide adequate GSH for metal conjugation and cellular redox buffering (Thorsen et al. 2007). Genes in the GSH biosynthetic pathway have also been shown to be induced by cadmium and mercury (Dormer 2000, Westwater 2002); however, none of these genes were identified as differentially expressed in response to saxitoxin. Though more testing is required, the combination of copper detoxification genes and sulfur amino acid biosynthetic genes suggest a unique genetic signature for saxitoxin. While it is not known if saxitoxin enters the yeast cell, it may be postulated that if uptake of the toxin does occur, Cup1p and Crs5p sequester the molecules, effectively performing a role similar to GSH. It can further be postulated that multiple genes involved in sulfur amino acid metabolism were also differentially expressed due to the role of sulfur in thioether ligation of Cu(I) in enzymes that either sequester free copper ions (Cup1p and Crs5p) or utilize copper as a cofactor (Fet3p).

This is the first study to examine the transcriptional response of a lower eukaryote to the algal toxin saxitoxin and as such to provide baseline information on molecular targets with the potential for development as environmental biomarkers of saxitoxin. While the toxin is present in aquatic ecosystems, one of the main disadvantages in performing expression profiling with sentinel species from these systems is their lack of extensive genetic information. Thus, the model lower eukaryote *S. cerevisiae* was used for these profiling experiments, as the biological and molecular functions of many of its genes have already been determined. The genetic signature obtained in this study can then be extrapolated to experiments with eukaryotic species found within the same ecosystem as the toxin-producing organisms. Understanding how toxins influence biological systems is essential to developing better predictive capabilities of water quality, allowing for the intelligent development of water quality indicators such as biomarkers or reporter gene assays. In this study, an overall expression profile of *S. cerevisiae* to saxitoxin was obtained. The regulation of a subset of these genes at different time points and concentrations was then examined, and determined to respond in a stable and consistent manner to the toxin. These expression data may be of value in the development of biomarker genes for algal toxins, while the overall transcriptional profile may provide preliminary insights on the eco-evolutionary role of the toxin within the context of algal ecology.

Acknowledgements

Julia Stair Gouffon at the Affymetrix Core Facility, UT Knoxville, performed the sample preparation, hybridization, and scanning in the microarray experiments. Jim Fleming provided the ArrayStat program. Ann Reed at the Statistical Consulting Center, UT Knoxville, provided guidance on the statistical analysis

Appendix

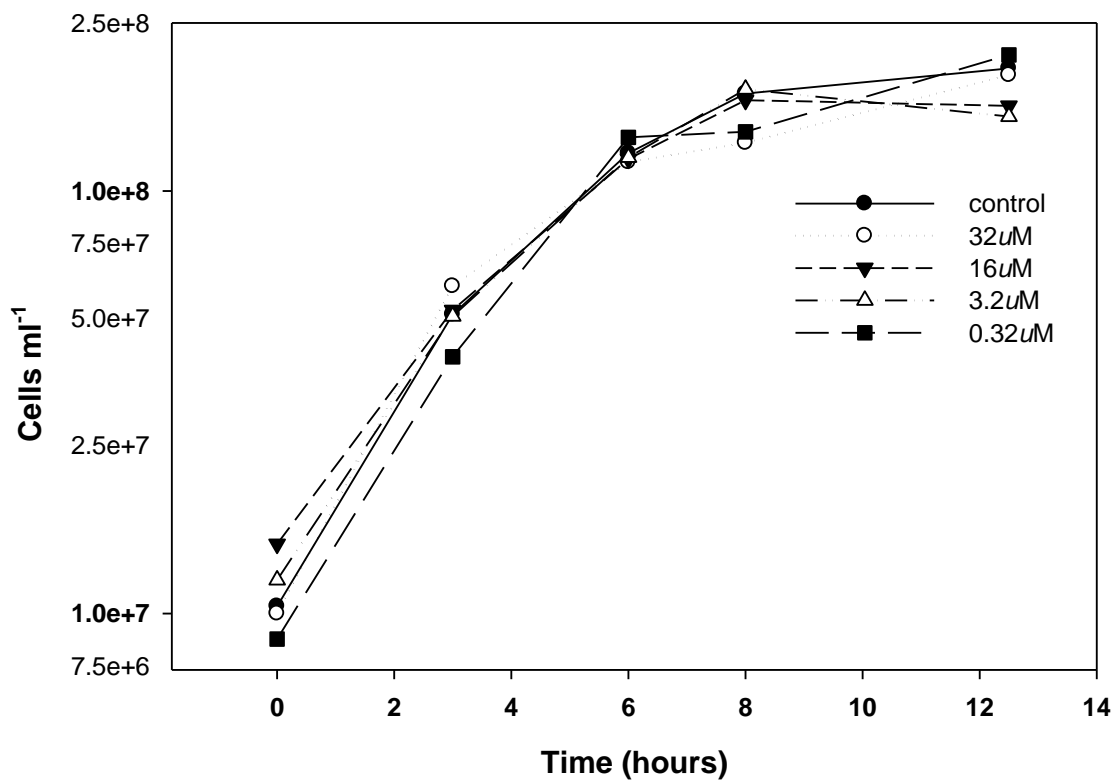


Figure II-1. Growth curves of *S. cerevisiae* S288C grown in YPD broth and exposed to a range of saxitoxin concentrations ranging from 0-32 μM . Cell counts were performed every 2-3 hours until cultures reached stationary phase. Growth was not affected at any of the concentrations tested.

Table II-5. Complete list of genes identified as significantly differentially expressed in microarray experiments.

Gene ID	Description	Functional Category	FC	z	p-value
<i>Induced</i>					
STR3	Cystathionine beta-lyase; methionine biosynthetic process	Sulfur Amino Acid Biosynthesis	2.14	9.40	0.0
MET2	L-homoserine-O-acetyltransferase, catalyzes first step of methionine biosynthesis	Sulfur Amino Acid Biosynthesis	1.68	6.43	0.000
MET32	Transcriptional regulator of sulfur amino acid metabolism and methionine biosynthesis	Sulfur Amino Acid Biosynthesis	1.66	6.25	0.000
TPO3	Spermine-specific polyamine transport protein	Transport	1.60	5.79	0.000
MET1	S-adenosyl-L-methionine uroporphyrinogen III transmethylase; biosynthesis of siroheme	Sulfur Amino Acid Biosynthesis	1.57	5.60	0.000
YOL014W	Unknown	Unknown	1.55	5.38	0.000
YGL258W-A	Unknown	Unknown	1.54	5.37	0.000
MET28	Transcriptional activator in sulfur metabolism	Sulfur Amino Acid Biosynthesis	1.52	5.14	0.000
VHS1	Cytoplasmic serine/threonine protein kinase	Protein Phosphorylation	1.50	4.97	0.000
YGR109W-A	Retrotransposon	Replication/Transposition	1.49	4.93	0.000
YPK2	Serine/threonine protein kinase	Protein Phosphorylation	1.48	4.84	0.000
RGS2	GTPase activating protein	Miscellaneous	1.48	5.11	0.000
CRS5	Copper-binding metallothionein	Copper Homeostasis	1.46	5.75	0.000
HEM3	Phorphobilinogen deaminase; catalyzes third step in	Metal Homeostasis	1.44	5.10	0.000

	the heme biosynthetic pathway				
SAM3	S-adenosylmethionine permease, required for utilization of S-adenosylmethionine as a sulfur source	Sulfur Amino Acid Biosynthesis	1.44	4.48	0.000
CUP1	Metallothionein; binds copper and mediates resistance to excess copper and cadmium	Copper Homeostasis	1.41	5.21	0.000
MET14	Adenylylsulfate kinase;involved in sulfate assimilation and methionine metabolism	Sulfur Amino Acid Biosynthesis	1.40	4.71	0.000
MET10	Alpha subunit of assimilatory sulfite reductase; converts sulfite into sulfide	Sulfur Amino Acid Biosynthesis	1.40	4.67	0.000
YRF1-1-7	DNA helicase	Replication and Transcription	1.36	3.80	0.000
YHR022C	Nucleotide binding	Replication/Transposition	1.34	3.65	0.000
SLF1	Polysome-associated RNA binding protein; copper-dependent mineralization of copper sulfide complexes on cell surface	Metal Homeostasis	1.34	3.70	0.000
YNL295W	Unknown	Unknown	1.33	3.55	0.000
TKL2	Transketolase activity; metal ion binding	Metal Homeostasis	1.32	3.49	0.000
SPO16	Spore formation	Unknown	1.32	3.46	0.001
ENB1	Endosomal ferric enterobactin transporter	Metal Homeostasis	1.32	3.46	0.001
FET3	Ferro-O ₂ -oxidoreductase required for high-affinity iron uptake	Metal Homeostasis	1.31	3.32	0.001
YNR068C	Unknown	Unknown	1.31	4.04	0.000
RTT107	Regulator of Ty1 transposition	Replication/Transposition	1.30	3.28	0.001
YMR084W	Unknown	Unknown	1.30	3.27	0.001

YDR261C-D	Transposable element; metal ion binding	Metal Homeostasis	1.30	3.25	0.001
<i>Repressed</i>					
CTR1	Copper uptake transmembrane transporter	Copper Ion Import	-2.91	-13	0.000
YOR186W	Unknown	Unknown	-1.68	-6.4	0.000
ORF	Unknown	Unknown	-1.61	-6.2	0.000
FRE1	Ferric reductase and cupric reductase	Copper Ion Import	-1.55	-6.7	0.000
CRC1	Mitochondrial inner membrane carnitine transporter	Fatty acid metabolism	-1.46	-4.7	0.000
YMR003W	Proposed S/mar DNA-binding protein Tho1 (hypothetical)	Unknown	-1.44	-5.1	0.000
YLR264C-A	Unknown	Unknown	-1.44	-4.5	0.000
GPX1	Glutathione peroxidase activity	Stress	1.42	-4.3	0.000
YLR157W-C	Unknown	Unknown	-1.39	-4	0.000
YER053C-A	Unknown	Unknown	-1.38	-4	0.000
LTV1	Involved in ribosomal small subunit export from nucleus	Ribosome Biogenesis	-1.37	-4.4	0.000
YMR182W-A	Unknown	Unknown	-1.37	-3.9	0.000
DHR2	RNA helicase activity	Ribosome Biogenesis	-1.37	-4.4	0.000
PCL7	Cyclin-dependent protein kinase regulator activity	Glycogen Metabolism	-1.36	-3.8	0.000
YLR164W	Unknown	Unknown	-1.35	-3.7	0.000
AGX1	Aminotransferase; catalyzes the synthesis of glycine from glyoxylate	Amino Acid Biosynthesis	-1.33	-3.6	0.000
RRP12	Protein required for export of the ribosomal subunits	Ribosome Biogenesis	-1.33	-4	0.000

YDR018C	Acyltransferase activity	Phospholipid Biosynthesis	-1.32	-3.4	0.001
RTN2	Unknown	Unknown	-1.30	-3.3	0.001
CBP4	Mitochondrial protein required for assembly of ubiquinol cytochrome-c reductase complex	Electron Transport	-1.30	-3.2	0.001
HCA4	Helicase; involved in 18S synthesis	Ribosome Biogenesis	-1.27	-3.3	0.001
AAH1	Adenine deaminase; adenine catabolism and ribosome biogenesis and assembly	Ribosome Biogenesis	-1.26	-3.3	0.001

References

- Agarwal AK, Rogers PD, Baerson SR, Jacob MR, Barker KS, Cleary JD, Walker LA, Nagle DG, Clark AM (2003) Genome-wide expression profiling of the response to polyene, pyrimidine, azole, and echinocandin antifungal agents in *Saccharomyces cerevisiae*. *Journal of Biological Chemistry* 278:34998-35015
- Anderson DM, Kulis DM, Sullivan JJ, Hall S, Lee C (1990) Dynamics and physiology of saxitoxin production by the dinoflagellates *Alexandrium* spp. *Marine Biology* 104:511-524
- Arezi B, Xing W, Sorge JA, Hogrefe HH (2003) Amplification efficiency of thermostable DNA polymerases. *Analytical Biochemistry* 321:226-235
- Brazma A, Hingamp P, Quackenbush J, Sherlock G, Spellman P, Stoeckert C, Aach J, Ansorge W, Ball CA, Causton HC, Gaasterland T, Glenisson P, Holstege FCP, Kim IF, Markowitz V, Matese JC, Parkinson H, Robinson A, Sarkans U, Schulze-Kremer S, Stewart J, Taylor R, Vilo J, Vingron M (2001) Minimum information about a microarray experiment (MIAME) - toward standards for microarray data. *Nat Genet* 29:365-371
- Bustin SA, Nolan T (2004) Pitfalls of Quantitative Real-Time Reverse-Transcription Polymerase Chain Reaction. *J Biomol Tech* 15:155-166
- Carmichael WW, Evans WR, Yin QQ, Bell P, Moczydlowski E (1997) Evidence for paralytic shellfish poisons in the freshwater cyanobacterium *Lyngbya wollei* (Farlow ex Gomont) comb. nov. *Appl. Environ. Microbiol.* 63:3104-3110
- Catterall WA (1985) The voltage sensitive sodium channel: a receptor for multiple neurotoxins. In: Anderson W, and Baden (ed) *Toxic Dinoflagellates*. Elsevier Science Publishing Co, Inc., p 329-342
- Causton HC, Ren B, Koh SS, Harbison CT, Kanin E, Jennings EG, Lee TI, True HL, Lander ES, Young RA (2001) Remodeling of Yeast Genome Expression in Response to Environmental Changes. *Mol. Biol. Cell* 12:323-337
- Culotta VC, Howard WR, Liu XF (1994) CRS5 encodes a metallothionein-like protein in *Saccharomyces cerevisiae*. *J. Biol. Chem.* 269:25295-25302
- Dancis A, Roman DG, Anderson GJ, Hinnebusch AG, Klausner RD (1992) Ferric Reductase of *Saccharomyces cerevisiae*: Molecular Characterization, Role in Iron Uptake, and Transcriptional Control by Iron. *Proceedings of the National Academy of Sciences* 89:3869-3873

- Dancis A, Yuan DS, Haile D, Askwith C, Eide D, Moehle C, Kaplan J, Klausner RD (1994) Molecular characterization of a copper transport protein in *S. cerevisiae*: An unexpected role for copper in iron transport. *Cell* 76:393-402
- de la Vega E, Hall MR, Wilson KJ, Reverter A, Woods RG, Degnan BM (2007) Stress-induced gene expression profiling in the black tiger shrimp *Penaeus monodon*. *Physiol. Genomics* 31:126-138
- Dormer UH, Westwater, J, McLaren, N.F., Kent, N.A., Mellor, J., Jamieson, D.J. (2000) Cadmium-inducible expression of the yeast *GSH1* gene requires a functional sulfur-amino acid regulatory network. *J Biol Chem* 275:32611-32616
- Ferreira FMB, Soler JMF, Fidalgo ML, Fernandez-Vila P (2001) PSP toxins from *Aphanizomenon flos-aquae* (cyanobacteria) collected in the Crestuma-Lever reservoir (Douro river, northern Portugal). *Toxicon* 39:757-761
- Gasch AP, Spellman PT, Kao CM, Carmel-Harel O, Eisen MB, Storz G, Botstein D, Brown PO (2000) Genomic Expression Programs in the Response of Yeast Cells to Environmental Changes. *Mol. Biol. Cell* 11:4241-4257
- Gross C, Kelleher M, Iyer VR, Brown PO, Winge DR (2000) Identification of the Copper Regulon in *Saccharomyces cerevisiae* by DNA Microarrays. *J. Biol. Chem.* 275:32310-32316
- Gupta RK, Patterson SS, Ripp S, Simpson ML, Sayler GS (2003) Expression of the *Photobacterium luminescens lux* genes (*luxA*, *B*, *C*, *D*, and *E*) in *Saccharomyces cerevisiae*. *Fems Yeast Research* 4:305-313
- Hall S, Strichartz, G., Moczydlowski, E., Ravindran, A., Reichardt, P.B. (1990) The saxitoxins: sources, chemistry, and pharmacology. In: Hall S, Strichartz, G. (ed) *Marine Toxins*, Vol 418. Am. Chem. Soc. Symp. Ser., p 29-65
- Hallegraef GM, Steffensen DA, Wetherbee R (1988) 3 Estuarine Australian Dinoflagellates That Can Produce Paralytic Shellfish Toxins. *Journal of Plankton Research* 10:533-541
- Hansen J, Cherest, H., Kielland-Brandt, M.C. (1994) Two divergent *MET10* genes, one from *Saccharomyces cerevisiae* and one from *Saccharomyces carlsbergensis*, encode the alpha subunit of sulfite reductase and specify potential binding sites for FAD and NADPH. *Journal of Bacteriology* 176:6050-6058

- Hansen J, Johannesen, P.F. (2000) Cysteine is essential for transcriptional regulation of the sulfur assimilation genes in *Saccharomyces cerevisiae*. *Mol Gen Genet* 263:535-542
- Hansen J, Kielland-Brandt, M.C. (1996) Inactivation of *MET2* in brewer's yeast increases the level of sulfite in beer. *J Biotechnology* 50:75-87
- Hansen J, Muldbjerg, M., Cherest, H., Surdin-Kerjan, Y. (1997) Siroheme biosynthesis in *Saccharomyces cerevisiae* requires the products of both the *MET1* and *MET8* genes. *FEBS Letters* 401:20-24
- Harada T, Oshima Y, Yasumoto T (1982) Studies on Paralytic Shellfish Poisoning in Tropical Waters .4. Structures of 2 Paralytic Shellfish Toxins, Gonyautoxin-V and Gonyautoxin-Vi Isolated from a Tropical Dinoflagellate, *Pyrodinium Bahamense* Var *Compressa*. *Agricultural and Biological Chemistry* 46:1861-1864
- Hassett R, Kosman DJ (1995) Evidence for Cu(II) Reduction as a Component of Copper Uptake by *Saccharomyces cerevisiae*. *J. Biol. Chem.* 270:128-134
- Heymann P, Ernst, J.F., Winkelmann, G. (2000) A gene of the major facilitator superfamily encodes a transporter for enterobactin (Enb1p) in *Saccharomyces cerevisiae*. *Biometals* 13:65-72
- <http://www.mged.org/Workgroups/MIAME/miame.html> (2008) MGED Society: Minimum Information About a Microarray Experiment - MIAME.
- <https://www.operon.com/oligos/toolkit.php>
- Irazarry RA, Bolstad, B.M., Collin, F., Cope, L.M., Hobbs, B., Speed, T.P. (2003) Summaries of Affymetrix GeneChip probe level data. *Nucl. Acids Res.* 31:e15
- Karin M, Najarian R, Haslinger A, Valenzuela P, Welch J, Fogel S (1984) Primary Structure and Transcription of an Amplified Genetic Locus: The *CUP1* Locus of Yeast. *Proceedings of the National Academy of Sciences* 81:337-341
- Kim HJ, Rakwal R, Shibato J, Iwahashi H, Choi JS, Kim DH (2006) Effect of textile wastewaters on *Saccharomyces cerevisiae* using DNA microarray as a tool for genome-wide transcriptomics analysis. *Water Research* 40:1773-1782
- Kitagawa E, Momose, Y., and Iwahashi, H. (2003) Correlation of the structures of agricultural fungicides to gene expression in *Saccharomyces cerevisiae* upon exposure to toxic doses. *Environ. Sci. Technol.* 37:2788-2793

- Kitagawa E, Takahashi, J., Momose, Y., and Iwahashi, H. (2002) Effects of the pesticide thiuram: genome-wide screening of indicator genes by yeast DNA microarray. *Environ. Sci. Technol.* 36:3908-3915
- Klausner RD, Dancis A (1994) A genetic approach to elucidating eukaryotic iron metabolism. *FEBS Letters* 355:109-113
- Lagos N, Onodera H, Zagatto PA, Andrinolo D, Azevedo SMFQ, Oshima Y (1999) The first evidence of paralytic shellfish toxins in the freshwater cyanobacterium *Cylindrospermopsis raciborskii*, isolated from Brazil. *Toxicon* 37:1359-1373
- Lettieri T (2006) Recent applications of DNA microarray technology to toxicology and ecotoxicology. *Environmental Health Perspectives* 114:4-9
- Lockhart DJ, Winzeler EA (2000) Genomics, gene expression and DNA arrays. *Nature* 405:827-836
- MacFarlane RC, Shah PH, Singh U (2005) Transcriptional profiling of *Entamoeba histolytica* trophozoites. *International Journal for Parasitology* 35:533-542
- Meistertzheim AL, Tanguy A, Moraga D, Thebault MT (2007) Identification of differentially expressed genes of the Pacific oyster *Crassostrea gigas* exposed to prolonged thermal stress. *Febs Journal* 274:6392-6402
- Mendoza-Cozatl D, Loza-Tavera, H., Hernandez-Navarro, A., Moreno-Sanchez, R. (2005) Sulfur assimilation and glutathione metabolism under cadmium stress in yeasts, protists, and plants. *FEMS Microbiology Reviews* 29:653-671
- Moler EJ, Radisky DC, Mian IS (2000) Integrating naive Bayes models and external knowledge to examine copper and iron homeostasis in *S. cerevisiae*. *Physiol. Genomics* 4:127-135
- Negri AP, Jones GJ (1995) Bioaccumulation of paralytic shellfish poisoning (PSP) toxins from the cyanobacterium *Anabaena circinalis* by the freshwater mussel *Alathyria condola*. *Toxicon* 33:667-678
- Oshima Y, Hasegawa M, Yasumoto T, Hallegraeff G, Blackburn S (1987) Dinoflagellate *Gymnodinium Catenatum* as the Source of Paralytic Shellfish Toxins in Tasmanian Shellfish. *Toxicon* 25:1105-1111
- Perego P, Howell SB (1997) Molecular mechanisms controlling sensitivity to toxic metal ions in yeast. *Toxicology and Applied Pharmacology* 147:312-318

- Pomati F, Sacchi S, Rossetti C, Giovannardi S, Onodera H, Oshima Y, Neilan BA (2000) The Freshwater Cyanobacterium *Planktothrix* sp. FP1: Molecular Identification and Detection of Paralytic Shellfish Poisoning Toxins. *Journal of Phycology* 36:553-562
- Qiagen (2003) QuantiTect Probe RT-PCT Handbook
- Ramakers C, Ruijter JM, Deprez RHL, Moorman AFM (2003) Assumption-free analysis of quantitative real-time polymerase chain reaction (PCR) data. *Neuroscience Letters* 339:62-66
- Robbens J, van der Ven K, Maras M, Blust R, De Coen W (2007) Ecotoxicological risk assessment using DNA chips and cellular reporters. *Trends in Biotechnology* 25:460-466
- Routledge EJ, and J.P. Sumpter (1996) Estrogenic activity of surfactants and some of their degradation products assessed using a recombinant yeast screen. *Environmental Toxicology and Chemistry* 15:241-248.
- Sambrook J, Russell DW (2001) *Molecular cloning: a laboratory manual*, Vol. Cold Spring Harbor Laboratory Press, Cold Spring Harbor, NY.
- Shi X, Stoj C, Romeo A, Kosman DJ, Zhu Z (2003) Fre1p Cu²⁺ Reduction and Fet3p Cu¹⁺ Oxidation Modulate Copper Toxicity in *Saccharomyces cerevisiae*. *J. Biol. Chem.* 278:50309-50315
- Taylor AB, Stoj CS, Ziegler L, Kosman DJ, Hart PJ (2005) The copper-iron connection in biology: Structure of the metallo-oxidase Fet3p. *Proceedings of the National Academy of Sciences* 102:15459-15464
- Thomas D, Surdin-Kerjan Y (1997) Metabolism of sulfur amino acids in *Saccharomyces cerevisiae*. *Microbiol. Mol. Biol. Rev.* 61:503-532
- Thorsen M, Lagniel G, Kristiansson E, Junot C, Nerman O, Labarre J, Tamas MJ (2007) Quantitative transcriptome, proteome, and sulfur metabolite profiling of the *Saccharomyces cerevisiae* response to arsenite. *Physiol. Genomics* 30:35-43
- van Bakel H, Strengman, Wijmenga C, Holstege CP (2005) Gene expression profiling and phenotype analysis of *S. cerevisiae* in response to changing copper reveals six genes with new roles in copper and iron metabolism. *Physiol. Genomics* 22:356-367

Watanabe CMH, Supekova L, Schultz PG (2002) Transcriptional Effects of the Potent Eneidyne Anti-Cancer Agent Calicheamicin [γ]11. *Chemistry & Biology* 9:245-251

Westwater J, McLaren, N.F., Dormer, U.H., Jamieson, D.J. (2002) The adaptive response of *Saccharomyces cerevisiae* to mercury exposure. *Yeast* 19:233-239

www.dorak.info/genetics/realtime.html Real-Time PCR. May 2008

Yu W, Farrell RA, Stillman DJ, Winge DR (1996) Identification of *SLF1* as a new copper homeostasis gene involved in copper sulfide mineralization in *Saccharomyces cerevisiae*. *Mol. Cell. Biol.* 16:2464-2472

Zuker M (2003) Mfold web server for nucleic acid folding and hybridization prediction. *Nucleic Acids Research* 31:3406-3415

Part III

Comparison of *Saccharomyces cerevisiae* Expression Profiles Following Exposure to Saxitoxin, Copper, and Iron

Abstract

Recent microarray expression profiling with *Saccharomyces cerevisiae* identified multiple genes involved in copper and iron homeostasis as being significantly differentially regulated following exposure to saxitoxin. Copper and iron homeostasis are tightly linked in *S. cerevisiae* due to the requirement of copper ions for the proper functioning of the Fet3 protein within the high-affinity iron uptake system. This study sought to compare expression profiles within a defined set of genes associated with copper and iron homeostasis in *S. cerevisiae* following short-term exposure to excess copper, excess iron, or saxitoxin. In the previous array experiments, *S. cerevisiae* cells were cultured in a rich medium; here, a minimal medium was used, in which the copper and iron concentrations were decreased relative to levels in which the original profile was generated. Quantitative reverse-transcriptase PCR with absolute quantification was used to measure changes in gene expression. While the degree of expression varied among treatments, the pattern of regulation following exposure to saxitoxin was identical to that of iron and highly similar to that of copper. The key difference between copper and saxitoxin was the regulation of *FET3*; a proposed mechanism for the action of saxitoxin on the yeast cell is discussed in the context of the expression patterns of *FET3* and the gene encoding the copper transporter *CTR1*.

Introduction

Saxitoxin, a secondary metabolite produced by several species of dinoflagellates and cyanobacteria, is often described as a potent neurotoxin due to its detrimental effects on human health. The compound and its many derivatives are able to bind to the voltage-gated sodium channel in nerve and muscle cells, leading to death via respiratory paralysis. However, investigations into the factors which influence toxin production, and its effects on the lower community members that exist within the same ecosystem as the toxin-producers, have produced more questions than answers. Most data on saxitoxin levels are derived from culture-based studies, with the predominant concept that saxitoxin is retained within the cells that produce it. Available data on extracellular saxitoxin levels within the environment are scant. However, both intracellular and extracellular toxin levels were measured during recent bloom events on the west coast of the United States: extracellular toxin levels were found to be greater than intracellular levels just after the peak of a bloom, indicating their release into the water column (Lefebvre et al. 2008).

Many theories have been put forth as to the proposed role of saxitoxin and its analogues. These include, with varying degrees of scientific support: involvement in an endosymbiotic relationship with bacteria; as a nitrogen storage reserve due to the high number of nitrogen atoms found within its structure (Cembella 1998); to assist in chromosome structural organization in a manner similar to polyamines and cations (Anderson & Cheng 1988); as a chemical defense against zooplankton predators (Zimmer & Ferrer 2007); and as pheromones (Wyatt & Jenkinson 1997). To date, there exists scant transcriptomic data that would aid in identifying (I) the molecular target of the toxin on the phyto- and zooplankton species occurring in the same community as the toxin-producing organisms and (II) the proposed ecological role of the toxin.

The yeast *Saccharomyces cerevisiae* provides a tractable model for elucidating possible molecular targets within lower eukaryotes, as its genome has been sequenced and the molecular and biological functions of many of the genes determined. The “environmental stress response” was defined through global

expression profiling with the yeast system (Gasch et al. 2000, Causton et al. 2001), and has since been applied to profiling studies with varied other organisms, such as the aquatic fungus *Blastocladiella emersonii* (Georg & Gomes 2007), the intertidal crustacean *Petrolisthes cinctipes* (Teranishi & Stillman 2007), and the coral reef fish *Pomacentrus moluccensis* (Kassahn et al. 2007), indicating the ability to extrapolate expression data obtained with yeast to other less-accessible eukaryotes. Additionally, the yeast system contains genes with homologs in many other organisms (Mustacchi et al. 2006).

Recent microarray analysis with *S. cerevisiae* identified genes involved in copper and iron homeostasis as being significantly differentially expressed upon short-term exposure to saxitoxin. Copper and iron homeostasis are tightly linked in *S. cerevisiae*, and the mechanisms of both systems have been well-characterized (Eide 1998, Puig & Thiele 2002). A brief overview is provided here (Figure III-1), primarily in the context of the genes examined in this study.

Both Cu(II) and Fe(III) are reduced prior to transport across the cell membrane by the cupric/ferric reductase Fre1p (Dancis et al. 1992, Hassett & Kosman 1995). Cu(I) then crosses into the cell via the high affinity copper transporter Ctr1p (Dancis et al. 1994b). The copper chaperone Atx1p trafficks the copper to the P-type ATPase Ccc2p, localized in the post-Golgi network, where it is then translocated into the lumen of the Golgi and loaded onto the multicopper oxidase Fet3p (Huffman & O'Halloran 2000). Posttranslational insertion of four copper ions is essential for the activity of Fet3p (Taylor et al. 2005). Upon coordination of the copper ions, Fet3p forms a complex with the iron permease Ftr1p (Stearman et al. 1996). Together, these enzymes cotranslocate to the plasma membrane, where they function in the cell-surface high-affinity iron uptake system. Thus, the link between copper and high-affinity iron uptake is the requirement of the copper ions to form the Fet3p holoenzyme (Dancis et al. 1994b). In addition to this high-affinity iron uptake system, *S. cerevisiae* also possesses a non-reductive, low-affinity iron uptake system comprised of a set of structure-specific transporters (Arn1p, Arn2p/Taf1p, Arn3p/Sit1p, Arn4p/Enb1p) (Philpott 2002) that are copper-independent.

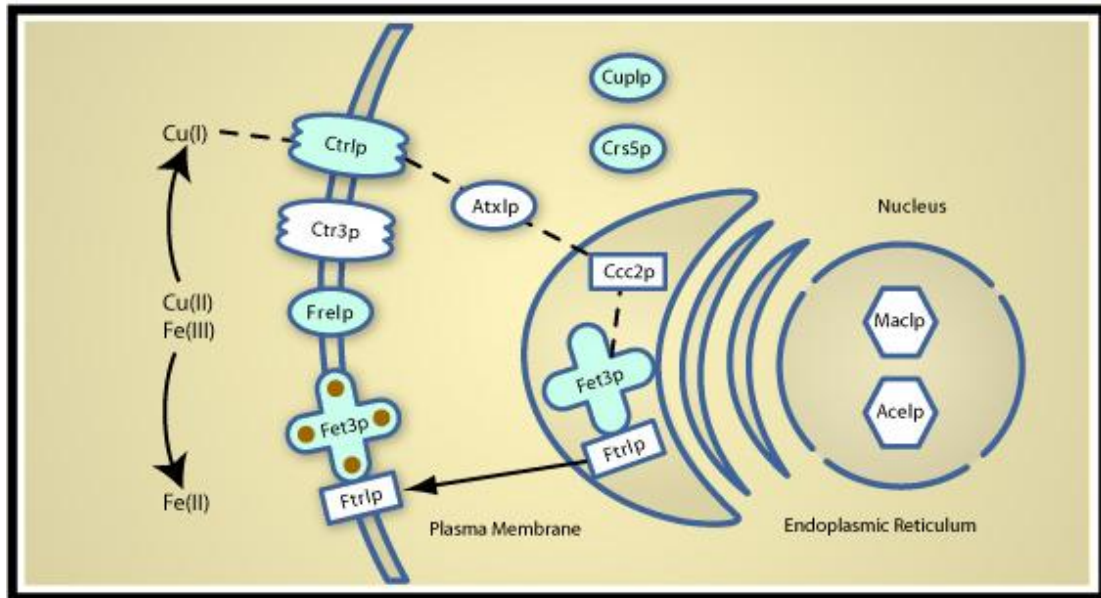


Figure III-1. Copper and iron uptake in *S. cerevisiae*. Cu(II) and Fe(III) are reduced by Fre1p prior to uptake into the cell. Cu(I) is transported across the plasma membrane by Ctr1p. Once inside the cell, it is trafficked to varied destinations by multiple copper chaperone proteins. One of the destinations for Cu(I) is the multicopper oxidase Fet3p. Cu(I) ions are shuttled from Ctr1p via Atx1p and Ccc2p to the apoenzyme form of Fet3p, located in the endoplasmic reticulum. Upon posttranslational insertion of four copper ions, Fet3p forms a complex with Ftr1p; this complex translocates to the plasma membrane, where it functions in high-affinity iron (Fe(II)) uptake.

Conditions of copper excess induce the expression of Cup1p and Crs5p, small, cysteine-rich metallothioneins that sequester excess copper ions in the cytoplasm (Karin et al. 1984, Culotta et al. 1994) via thiol-mediated interactions. A secondary copper detoxification has also been proposed, separate from that of Cup1p, that results in sulfide generation and copper sulfide biomineralization at the cell surface via Slf1p (Yu et al. 1996).

The objective of this study was to determine if the transcriptional profile of *S. cerevisiae* upon exposure to saxitoxin was similar to that of either excess copper or excess iron, as defined by the expression of a subset of genes primarily associated with copper and iron homeostasis. The hypothesis being tested in this set of experiments was that the profile obtained following exposure to saxitoxin would be similar to that obtained in response to excess copper. However, as several plasma membrane enzymes are utilized in the permeation of both metals, it was deemed prudent to also determine the profile in response to excess iron.

Methods and Materials

Yeast Strains

Saccharomyces cerevisiae S288C (ATTC #204508, MAT α , *SUC2*, *mal*, *mel*, *gal2*, *CUP1*, *flo1*, *flo8-1*, *hap1*) was used for all growth curves and gene expression experiments.

Chemicals

Four vials of saxitoxin were purchased from National Research Council Canada (NRCC) (CRM-STX-e) at a concentration of approximately 65 μ M each. The contents of the vials were combined and the saxitoxin lyophilized, concentrated and re-suspended in deionized water (pH 5.5) at a final concentration of 100 μ g ml⁻¹. Copper sulfate (as cupric sulfate, CuSO₄) and iron sulfate (as ferric sulfate, Fe₂SO₄³) were purchased from Sigma Aldrich (St. Louis, MO). A 2 mM stock solution of copper sulfate was prepared in sterile deionized water, filter-sterilized with a 0.2 μ M nitrocellulose filter, and stored in a sterile polycarbonate bottle. On the days of exposure, a 200 μ M working solution was freshly prepared in sterile deionized water.

A 1 mM stock solution of iron sulfate was prepared in the same manner as for copper sulfate and stored in a light-tight container. The working solutions of both copper sulfate and iron sulfate were prepared at concentrations that allowed for volumes similar to that of saxitoxin to be added to the yeast cultures.

Growth Curves

S. cerevisiae was grown overnight in synthetic complete media (SC) (2% dextrose, 0.67% yeast nitrogen base without amino acids, and supplemented with amino acid mixture plus adenine (20 $\mu\text{g ml}^{-1}$) and uracil (20 $\mu\text{g ml}^{-1}$)) (Sherman 2002) and re-inoculated into fresh SC media in 10 mL volumes at a starting $\text{OD}_{600}=0.06\text{--}0.08$. The 200 μM copper sulfate solution was added to final concentrations of 0, 4 μM , and 8 μM . Additionally, growth curves with excess copper were conducted in the same culture volumes as for gene expression experiments (400 μL), to ensure that growth was not affected by culture size. The OD_{600} was measured every 2–3 hours with the Biophotometer. Iron sulfate was added to final concentrations of 0, 20, and 40 μM . The OD_{600} was measured every 2–3 hours over a 24-hour period with a Beckman DU-600 Spectrophotometer. Growth curves were conducted in duplicate for iron exposures. As the results of a previous study (van Bakel et al. 2005) indicated that 8 μM copper sulfate did not inhibit cell growth, only single growth curves were performed for each of the copper concentrations.

Saxitoxin and Metal Exposures

Cultures of *S. cerevisiae* S288C were grown in SC to $\text{OD}_{600}=1.0$. Four hundred microliters from individual 10 mL overnight cultures were transferred to sterile 2 mL tubes. Saxitoxin, copper sulfate, or iron sulfate was added to individual cultures at final concentrations of 16 μM , 8 μM , or 32 μM , respectively. Upon addition of saxitoxin or metal, the sample was mixed gently and incubated with moderate agitation (30rpm) at 30°C for 45 minutes. Controls consisted of deionized water (pH 5.5). Five biological replicates were performed under these conditions for gene expression analysis.

Cell Harvesting and Total RNA Extraction

Cells were harvested following the protocol of (Causton et al. 2001) and stored immediately in liquid nitrogen. Total RNA was extracted following the protocol described in Part II. Total RNA was quantified using the Nano-drop 1000 (Wilmington, DE).

Quantitative Reverse-Transcriptase PCR

Quantitative reverse-transcriptase PCR (qRT-PCR) was used to examine the response of a suite of metal-homeostasis genes previously identified by microarray analysis and described in Chapter II: *CUP1*, *CRS5*, *CTR1*, *FRE1*, and *FET3*. Expression of *STR3*, which codes for a protein involved in sulfur amino acid metabolism, was also measured, along with *ACT1*, which served as the reference gene for data normalization. Two additional assays were also developed which targeted the *SLF1* and *ENB1* genes, as the microarray analyses had identified these genes as significantly differentially expressed upon exposure to saxitoxin.

qRT-PCR reactions using Taqman® probes and gene-specific primers were performed in triplicate in a DNA engine equipped with the Chromo4 detector (MJ Research Inc., Waltham, MA). The Quantitect Probe RT-PCR kit (Qiagen, Valencia, CA) was used for all assays. Assay reactions consisted of 12.5 µl 2x Quantitect Probe RT-PCR Master Mix, the optimized concentrations of primers (600 nm or 800 nm), 200 nm probe, 0.25 µl QuantiTect RT Mix, 5 µl of template, and adjusted to a final volume of 25 µl with nuclease-free water. Template consisted of a 1:100 dilution of the total RNA extract of each sample. The following protocol was used for all assays: 50°C for 30 minutes, 95°C for 15 minutes, and 45 cycles of denaturing at 94°C for 15 seconds and annealing/extension at 60°C for 1 min.

Development of ENB1 and SLF1 Assays

Gene-specific primers and Taqman probes were designed for the *ENB1* and *SLF1* targets and the assays optimized following the methods described previously (Part II). The primer and probe sequences and gene function of these additional assays are listed in Table III-1 (Appendix I). For each assay, primer specificity was evaluated by visualization of the PCR product on a 1% agarose gel; a band at the

expected size (approximately 100 basepairs [bp]) indicated primers were specific for the target of interest (data not shown).

Full-length *in-vitro* transcribed standards were constructed for *ENBI* and *SLF1* using the protocols described previously (Part II). The primers, annealing temperatures, and expected product sizes used in the construction of the *ENBI* and *SLF1* standards are listed in Table III-2 (Appendix I). Standard curves were performed in triplicate to assess the PCR efficiency and reproducibility of the assays. The PCR efficiency of each assay was calculated based on the slope of the standard curve with the equation: $E = 10^{(-1/\text{slope})} - 1$ (Arezi et al. 2003) The PCR efficiencies (Table III-3, Appendix I) were similar to existing assays and also that of the reference gene *ACT1*.

Data Normalization

Expression data for all genes were collected and normalized using absolute quantification as described in Chapter II. Briefly, functional gene data were initially measured as transcript copies ng total RNA⁻¹ using the RNA standard curves; these values were then normalized to the corresponding *ACT1* transcript copies ng total RNA⁻¹ of each sample.

Statistical Analysis: Single Treatment

For each gene at each treatment, normalized values were analyzed for statistical significance (SPSS v.15, Chicago, IL) between exposed and control samples with the independent samples *t*-test if data passed the tests for equal variance (Levene's test) and normality (Shapiro-Wilkes). The Mann-Whitney U-test with Monte Carlo correction was applied if samples were not normally distributed. The average fold-change and fold-change range were calculated as described in Part II. The average fold-change of each functional gene in each treatment was plotted to visualize the degree of similarity in regulation.

Statistical Analysis: Comparison of Normalized Values among Treatments

Normalized functional gene data were also compared across treatment types to determine if the levels of regulation differed significantly from each other as a result of compound exposure. The normalized transcript value of each exposed sample was

divided by the sample's normalized control value; this transformation yielded the differential expression of individual samples. These data were then analyzed for statistical significance. If samples displayed equal variance and were normally distributed, a one-way ANOVA with post-hoc Tukey was applied. Data in which the error of variance were not equal were analyzed with a one-way ANOVA with post-hoc Tahmane's *t*.

Results

Media Selection

Previously, *S. cerevisiae* S288C was grown in YPD when exposed to saxitoxin. As the goal of this current work was to determine if the transcriptional profile of select genes was similar to that of excess copper or iron, synthetic complete media was utilized for growth curves and expression studies in order to minimize the levels of metals found in the media. The concentration of copper (as copper sulfate) in YPD has been measured at 0.3 μM (Hassett et al. 2000); the concentration of copper (as copper sulfate) contained in the yeast nitrogen base, a component of the SC media, was calculated to be 0.1 μM based on elemental levels provided by the supplier. However, this value was not measured analytically, and the ratios of the various elements as listed by the manufacturer versus the true levels have been found to vary by up to 3-fold (Abelovska 2007). While cellular functions and phenotypic viability may be altered when grown in synthetic versus complete media due to differences in element levels (Abelovska 2007), yeast growth was not drastically altered when cultured in SC. Additionally, transcriptional profile comparisons among saxitoxin and excess copper and iron were conducted at concentrations that did not inhibit growth in SC liquid media.

Growth Curves

Yeast growth was not affected at any of the copper (Figure III-2) or iron concentrations (Figure III-3) tested. It had previously been shown that saxitoxin did not affect yeast growth up to concentrations of 32 μM (Part II). Thus, it was desirable to select concentrations of copper and iron that were considered excessive yet not

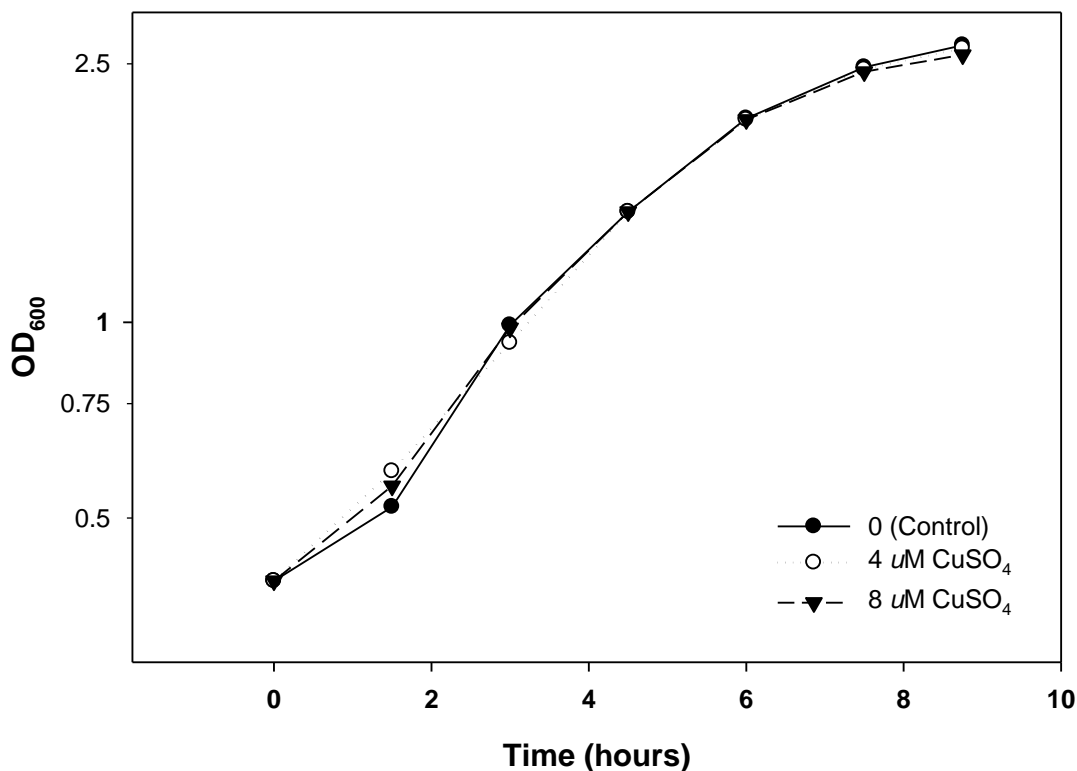


Figure III-2. Growth curves of *S. cerevisiae* S288C were conducted with a range of copper concentrations to determine the final concentration at which to perform expression profiling. Overnight cultures were re-inoculated into 10 mL of SC broth and aliquoted into 2 mL sterile tubes in 400 μ L volumes to simulate conditions used in gene expression experiments. Cupric sulfate dissolved in deionized water was added to final concentrations of 4 and 8 μ M; controls consisted of deionized water. Cultures were grown at 30°C with rapid agitation (200 rpm). Growth was monitored by measuring the OD₆₀₀ every 2-3 hours with the Biophotometer. A single biological replicate was performed at each concentration to confirm previous reports that growth was not affected at the 8 μ M concentration.

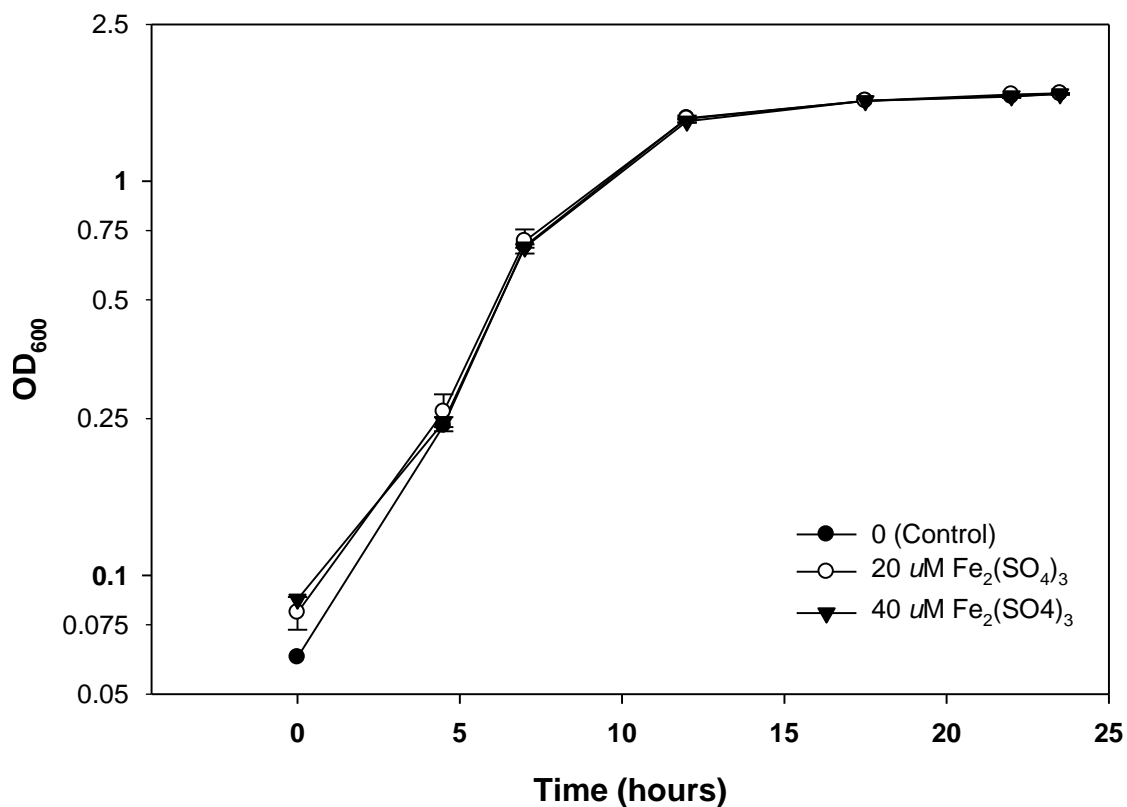


Figure III-3. Growth curves of *S. cerevisiae* S288C were conducted with a range of iron concentrations to determine the final concentration at which to perform expression profiling. Overnight cultures were re-inoculated into 10 mL of SC broth to an OD₆₀₀=0.06-0.08. Ferric sulfate dissolved in deionized water was added to final concentrations of 20 and 40 μM. Controls consisted of deionized water (0 μM). Cultures were grown at 30°C with rapid agitation (200 rpm). Growth was monitored by measuring the OD₆₀₀ every 2-3 hours over a 24-hr period. Two biological replicates were performed at each concentration.

toxic, and which did not affect the growth of the cells. An exposure concentration of 8 μM copper sulfate was selected based on previous microarray studies performed at this concentration (van Bakel et al. 2005), which also desired a level that avoided a large stress response that could confound the results. An exposure concentration of 32 μM ferric sulfate was chosen based on concentrations employed in prior studies that examined yeast physiology and gene regulation upon exposure to excess iron (Dancis et al. 1992, Ruotolo et al. 2008).

Expression Profiling

The transcriptional profile of *S. cerevisiae* resulting from short-term exposure to saxitoxin is similar to that of excess copper and identical to excess iron. *CRS5*, *CTR1*, *CUP1*, and *FRE1* were all significantly differentially expressed (relative to controls) across the three treatments (Figures III-4, III-5, and III-6). The primary difference among expression profiles was due to the regulation of *FET3*: while expression of this gene remained unchanged following exposure to 8 μM copper sulfate, it was repressed approximately two-fold in response to 32 μM iron sulfate and greater than 3.5-fold following exposure to 16 μM saxitoxin (Figure III-7a).

While overall this suite of metal-homeostasis genes displayed similar trends in expression (i.e. repressed or induced), the level of regulation varied (Figure III-7, a-h). This was most notable in the metallothionein *CUP1*, which was significantly induced greater than 6-fold under conditions of copper excess, in comparison to the 2-fold level of induction seen in response to saxitoxin (Figure III-7b). Excess iron exposure also resulted in an approximately three-fold level of induction in this gene (Figure III-7b), which is primarily used in the sequestering of excess copper and cadmium ions. The metallothionein *CRS5* was induced at similar levels among all treatments, with the greatest induction occurring following exposure to copper (Figure III-7c). The ferric/cupric reductase *FRE1* was also down-regulated at similar levels among all treatments (Figure III-7d). The copper transporter *CTR1* was significantly down-regulated in all treatments, but was repressed at greater levels following exposure to copper and saxitoxin (greater than 2-fold in both) than to iron (less than 2-fold) (Figure III-7e).

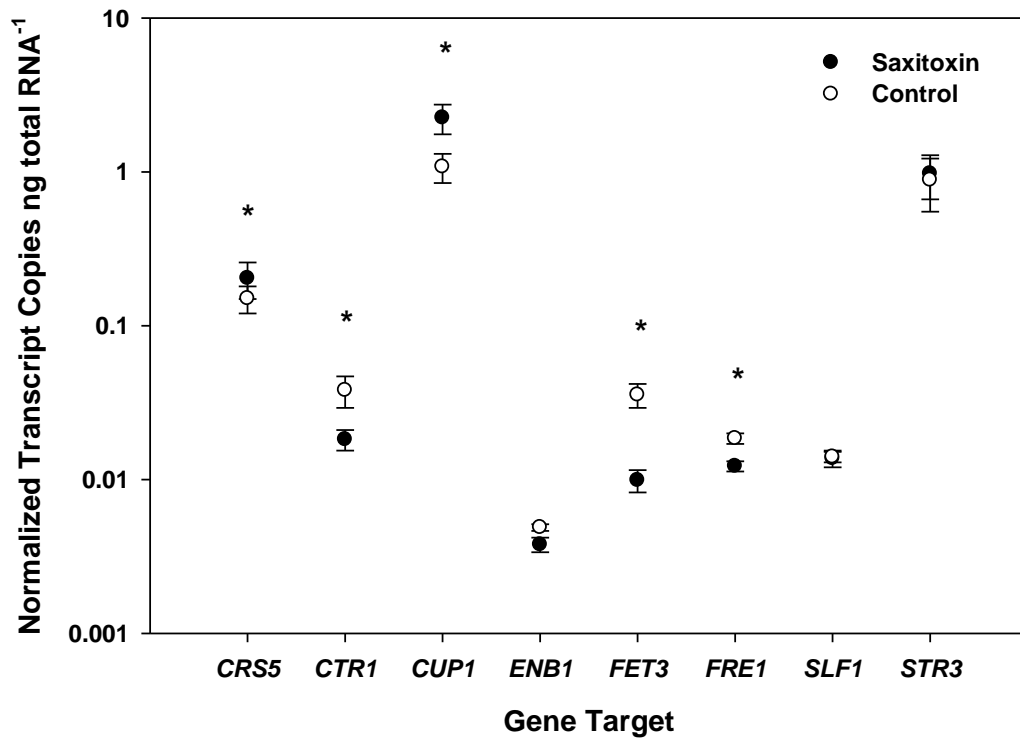


Figure III-4. Average normalized transcript copy numbers for each functional gene following exposure to saxitoxin or control (water). Functional gene transcript copies were initially measured per ng total RNA⁻¹ followed by normalization of each sample to its respective *ACT1* transcript copy value. * indicates significant difference (one-tailed $p < 0.05$).

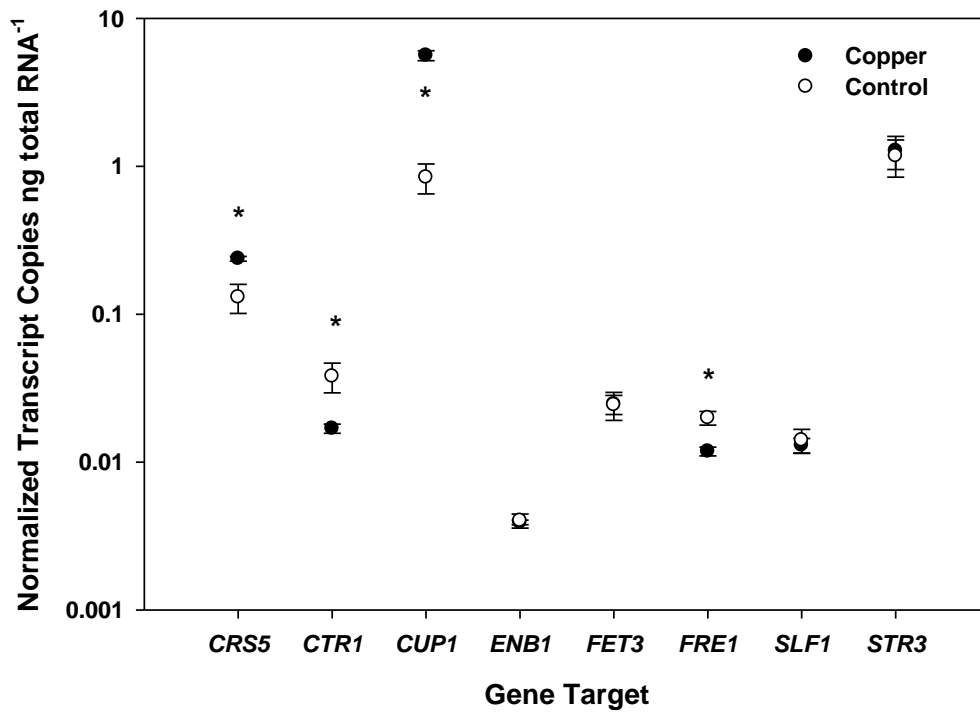


Figure III-5. Average normalized transcript copy numbers for each functional gene following exposure to copper sulfate or control (water). Functional gene transcript copies were initially measured per ng total RNA⁻¹ followed by normalization of each sample to its respective *ACT1* transcript copy value. * indicates significant difference (one-tailed $p < 0.05$).

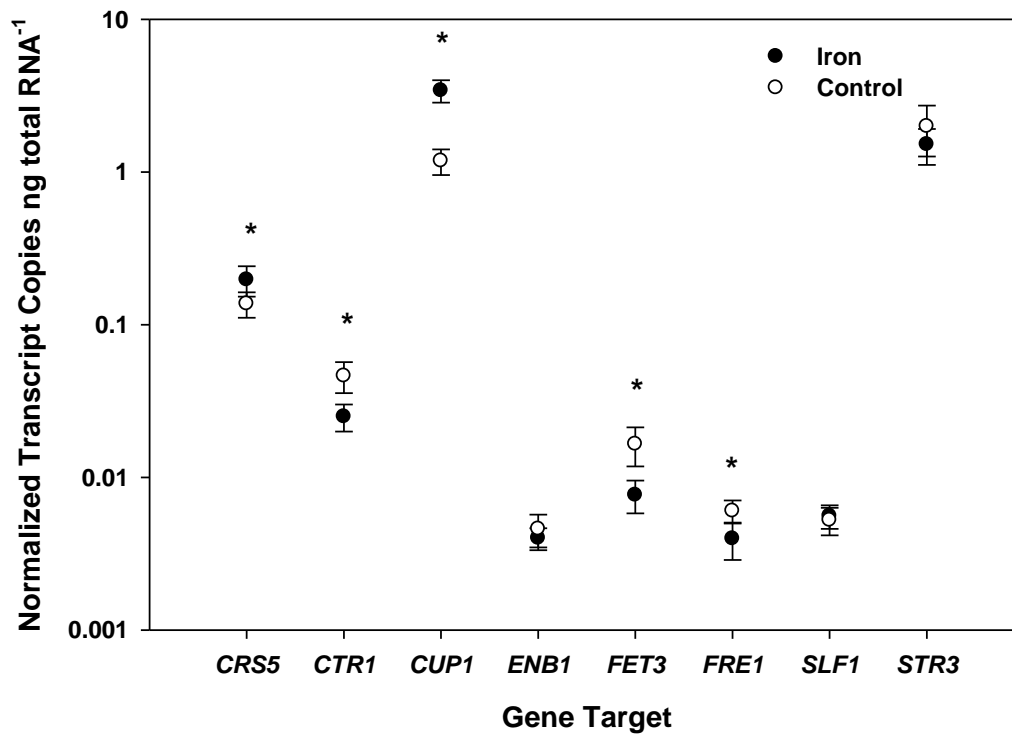
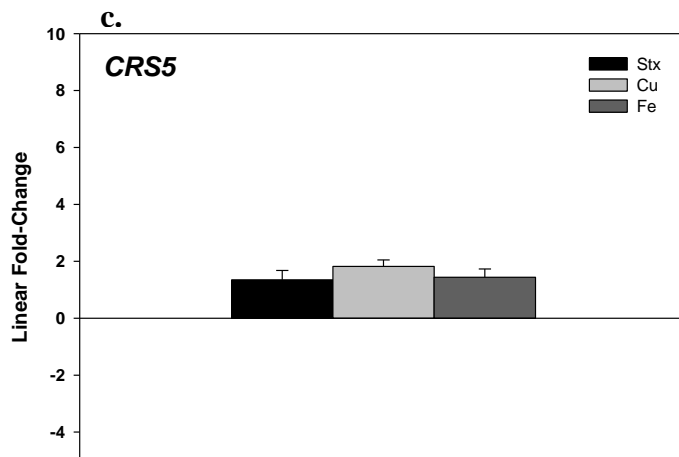
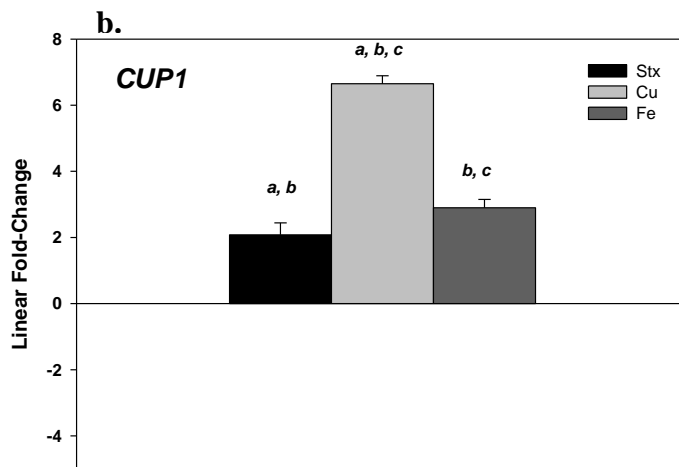
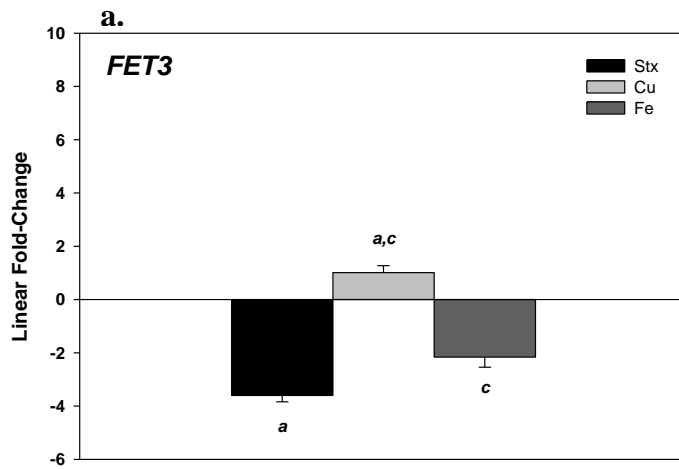
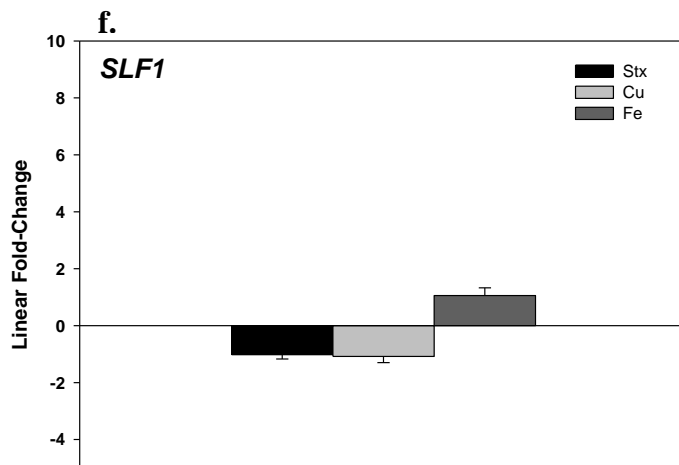
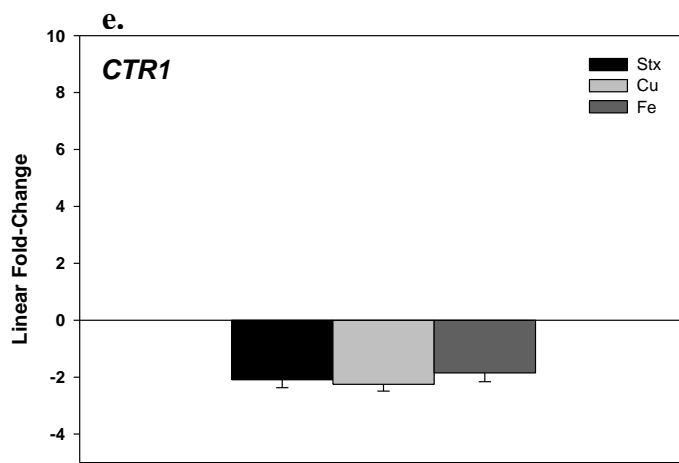
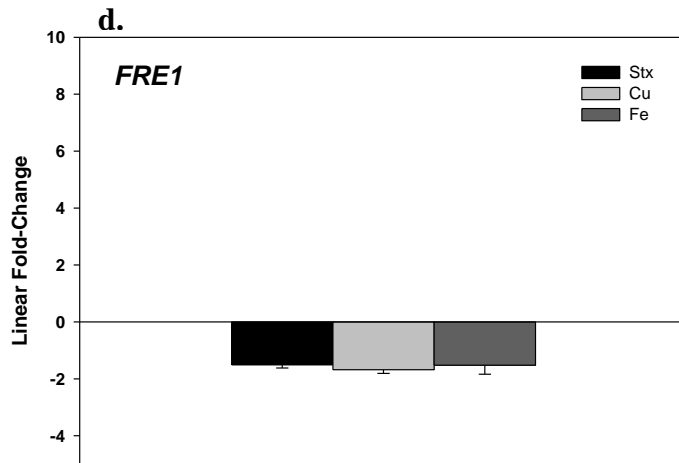
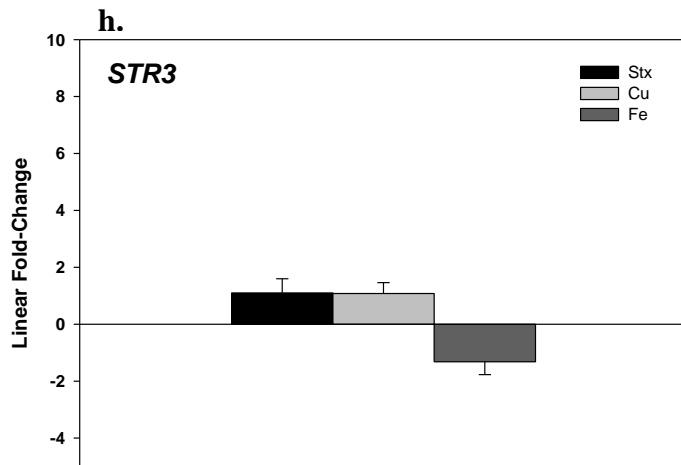
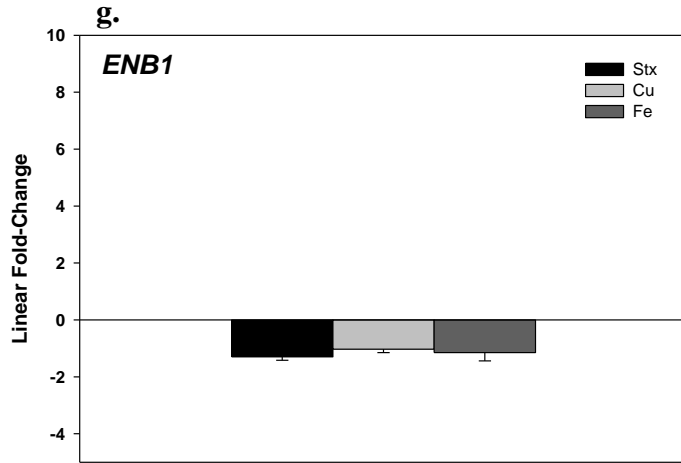


Figure III-6. Average normalized transcript copy numbers for each functional gene following exposure to ferric sulfate or control (water). Functional gene transcript copies were initially measured per ng total RNA⁻¹ followed by normalization of each sample to its respective *ACT1* transcript copy value. * indicates significant difference (one-tailed $p < 0.05$).

Figure III-7. Comparison in gene regulation levels among saxitoxin, copper, and iron treatments. (a) saxitoxin and iron *FET3* expression levels were significantly repressed in comparison to copper, which remained unchanged; (b) *CUPI* was induced in copper treatments at levels significantly greater than those for saxitoxin and iron; (c) *CRS5* was induced at approximately equal levels among all three treatments; (d.) *FRE1* and (e.) *CTR1* were repressed at comparable levels among all treatments; (f.) *SLF1*, (g.) *ENB1*, and (h.) *STR3* expression remained relatively unchanged among all treatments.







The regulation of the *SLF1* and *ENB1* genes were examined in this study because of their roles in metal homeostasis. *STR3* was profiled as previous microarray analysis (Part II) identified this gene as having the highest level of induction following exposure to saxitoxin. All three genes showed minimal expression changes, none of which were statistically significant at the $p < 0.05$ level (Figure III-7, f-h).

Discussion

The repression of *FET3* in this work is in direct contrast to the previous microarray study in which it was induced following exposure to saxitoxin at the same concentration and length of time; this variation in expression may provide a valuable link in understanding the mechanism of action of saxitoxin on yeast cells. The only variable between the two exposures was the media: cells were grown in YPD for the microarray study, and SC in this study. YPD is a rich media, and the amount of metals included in the media is also greater than that of the minimal media; thus, SC was specifically used in this study in order to decrease the ambient metal concentrations. Calculating the difference in the amount of copper between the two media based solely on manufacturer's information (without performing independent analytical measurements), the amount of copper as copper sulfate in YPD was 3 times greater than in the SC.

The Fet3 protein is a multicopper oxidase involved in the high-affinity iron uptake system in *S. cerevisiae* (Askwith et al. 1994) and requires the posttranslational insertion of four copper ions for its activity (Figure III-8) (Taylor et al. 2005). The source of the copper ions needed for proper FET3p functioning comes from the high-affinity copper transporter Ctr1p (Askwith et al. 1994, Dancis et al. 1994a, Dancis et al. 1994b). In this study, *CTR1* was repressed at approximately the same levels following exposure to either copper or saxitoxin. The 3.5-fold level of repression observed in *FET3* following exposure to saxitoxin as compared to unchanging expression levels after copper exposure suggests that the enzyme may not be receiving an adequate supply of copper ions in the saxitoxin treatments. This suggests

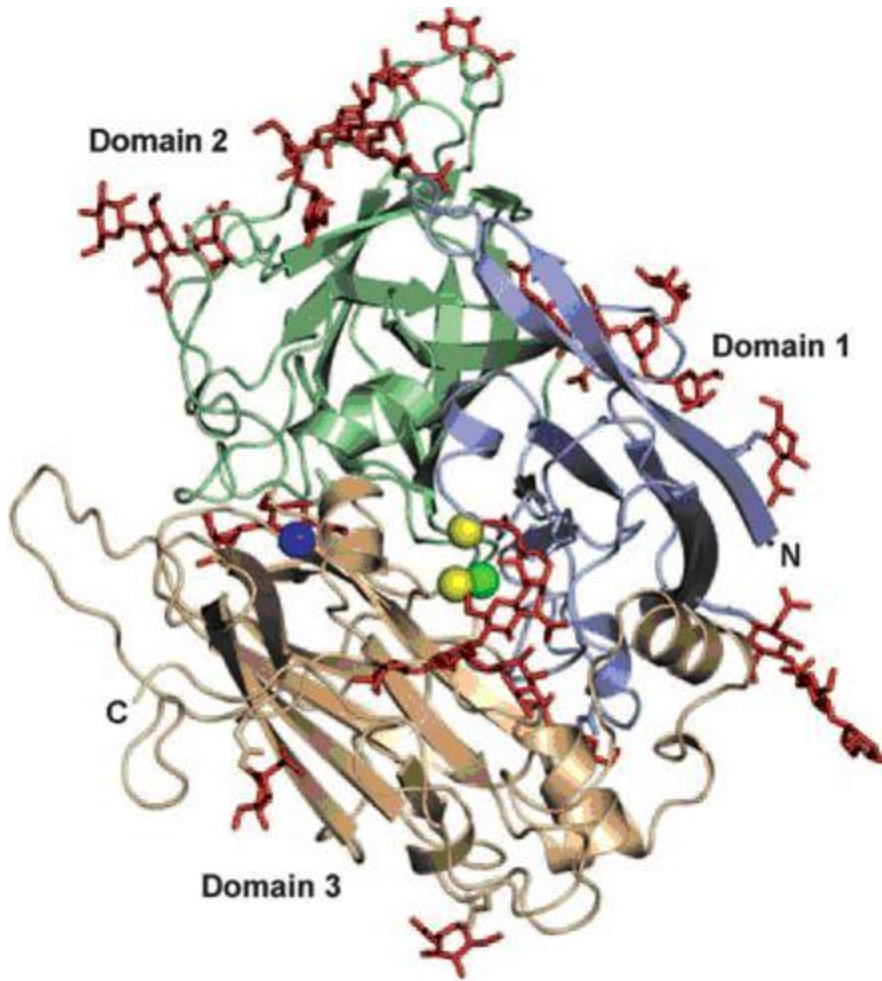


Figure III-8. Ribbon structure of Fet3p (redrawn from Taylor et al. 2005) illustrating the locations (via posttranslational insertion) of the four copper ions required for enzyme function. Color scheme of copper ions corresponds to domain location (T1 copper = blue, T2 coppers = yellow, T3 copper = green). Crystal structure of Fet3p determined to 2.8 Å resolution.

that saxitoxin is either displacing copper ions at Ctr1p, or that the molecule is chelating the copper ions in the cell's external environment.

Examining the structure of the Ctr1p and the transport of copper ions across the membrane may provide a working hypothesis as to how saxitoxin is functioning with respect to Ctr1p. A recent projection structure of the human copper transporter (hCTR1) at 6 Å resolution revealed that the hCTR1 is trimeric, with a radial symmetry typical of certain ion channels such as potassium or gap junction channels; in addition, there appears to be a copper permeable pore at the interface between the subunits along the center 3-fold axis of the trimer (Aller & Unger 2006). It has yet to be determined whether Ctr proteins function as transporters, channels, or hybrids. The three transmembrane domain (TM) segments contain large aromatic residues; the partial negative charges of these residues may be able to "solvate" the copper ions through the pore (De Feo et al. 2007). The N-terminal region of CTR1 has a large number of methionine residues which form M-X-X-M or M-X-M motifs (Figure III-9); it has been proposed that these met motifs play a role in copper binding (Puig & Thiele 2002). Additionally, a single conserved methionine residue approximately 20 residues upstream of the first transmembrane domain in the N-terminal extracellular domain has been shown to be essential for Cu(I) transport (Nose et al. 2006). It has been shown that the methionine motifs are able to selectively bind Cu(I) via met-only coordination (Nose et al. 2006).

The presence of a particular glycine motif (GXXXG [GG4]) on TM3 of Ctr1p suggests a functional model similar to that of the potassium channel GYG motif: the GG4 motif may contribute to selectivity and gating, with the state of the gate regulated by the occupancy of both the intra- and extracellular metal binding sites (Aller & Unger 2006). The molecular target of saxitoxin in mammalian nerve and muscle cells is the voltage-gated sodium channel, where it binds with high affinity to the selectivity filter via its positively-charged 7,8,9-guanidinium moiety, effectively blocking the passage of sodium ions into the cell. It is possible that Ctr1p is the molecular target in lower eukaryotes, and that saxitoxin binds to the selectivity filter of Ctr1p, thus preventing the passage of Cu(I) ions into the cell. The down-regulation

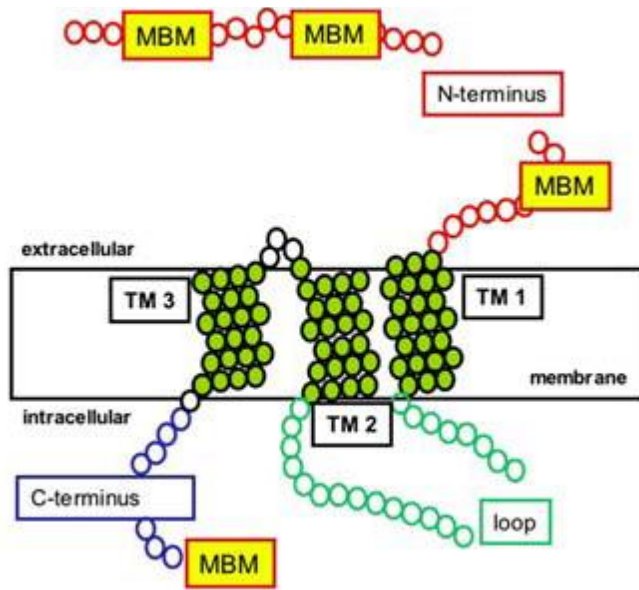


Figure III-9. Domain organization and topology of Ctr1 protein.
 (Redrawn from De Feo et al. 2007).

of *FET3*, whose holoenzyme requires four copper ions transported specifically from Ctr1p, appears to suggest this.

The core of this study utilized qRT-PCR with absolute quantification in order to compare the expression profiles of a specific set of genes across different treatments. While the normalized transcript values reflected the changes in gene expression, they also illustrated the abundance of each functional gene. This information can be useful in assessing the overall physiology of the yeast cells following exposures to specific compounds. In saxitoxin treatments, *CTR1*, *FRE1*, and *FET3* were all produced at approximately equal transcript levels (~0.01, Figure III-4). Copper exposure produced transcript levels of *CTR1* and *FRE1* comparable to those of saxitoxin treatments (Figure III-5). However, *FET3* was produced at higher transcript levels. Additionally, iron exposures resulted in transcript levels of *CTR1*, *FRE1*, and *FET3* comparable to those of saxitoxin (Figure III-6).

The response of the *CTR1*, *FRE1*, and *FET3* genes following excess iron exposure was as expected, given their roles in metal reduction and permeation. *CTR1* is regulated at the level of transcription by copper, and *FRE1* by iron and copper (Dancis et al. 1992, Dancis et al. 1994a, Hassett & Kosman 1995). While *CTR1* repression is not iron-dependent, it relies on the reductase activity of Fre1p to provide a suitable substrate; thus, repression of *CTR1* under excess iron levels is not unexpected.

The metallothioneins CUP1p and CRS5p have also been shown to be regulated at the level of transcription by elevated copper levels (Karin et al. 1984, Culotta et al. 1994). *CUP1* displayed a marked increase in transcript levels following exposure to copper in comparison to saxitoxin and iron, in keeping with its well-defined role in copper detoxification. However, the transcript levels produced in response to excess iron were surprising. Cup1p is well-recognized for its ability to sequester excess copper and cadmium ions. Elevated expression levels following exposure to iron indicate this gene either plays an as-yet unidentified role in iron homeostasis or was induced due to extraneous conditions under which the

experiments were conducted, such as a lower rate of agitation during culture exposures.

LacZ fusion assays indicate that *CUP1* regulation may also occur via the interaction of other metals with Ace1p, the transcriptional regulator of *CUP1* (Okuyama et al. 1999). This contradicts previous reports that Ace1p-mediated expression of CUP1p/lacZ fusions was specific for Cu(II) (Thorvaldson et al 1993). Additionally, *in-vitro* studies have shown rapid metal exchange between Zn- or Cd-Ace1p and Cu(I) (Dameron et al 1993). Therefore, it is possible that under the conditions employed here, *CUP1* was induced as a more general response to excess metal levels.

This study provides insights as to the possible mechanism of action of saxitoxin in aquatic ecosystems, both via the effects on other community members through extracellular release of the toxin, and also the role of the toxin within the ecology of the algae. Yeast serve as the prototype for all eukaryotic cells, as most fundamental cellular processes are conserved from yeast to humans (Mustacchi et al. 2006) and are typically discovered in yeast first. The expression data collected here, especially that of *CTR1* and *FET3*, warrants further study at the protein level.

Appendix I

Table III-1. Primer and probe sequences, gene function, and amplicon size of the quantitative reverse-transcriptase assays developed for *ENB1* and *SLF1*.

Assay Target	Gene Description	Primer/Probe Sequence	Amplicon Size (bp)
<i>ENB1</i>	non-reductive iron uptake	F: 5'-TCACTCAAGACCGCCCTACT R: 5'-CAAACTGTTAGCGGCATAGG 5'(FAM)-CTGTTTTTGCAGGGTTACTGTACTGGACTC(BHQ)	106
<i>SLF1</i>	secondary copper detoxification system	F:5'-CACCAATACCAACCACATCG R:5'-CTTGGCTTTGCAGTCTTTGA 5'(FAM)-CATGGAAATCATCTTCGCCAGATAGCAATA(BHQ)	103

Table III-2. Primer sequences, annealing temperatures, and expected product size used for construction of *in-vitro* transcribed standards of *ENB1* and *SLF1*.

Gene ID	Primer Sequence	T _a	Product Size (bp)
<i>ENB1</i>	5'-GAATGTCTCTCTGAAAATGCT	51.7°C	1,852
	5'-CTAGTACTCTCCAGCTCAAT		
<i>SLF1</i>	5'-ATCAATCATAAAGTGAATTCA	43.5°C	1,382
	5'-AATATTGTCTAAAATTAATCA		

Table III-3. PCR efficiency of *SLF1* and *ENB1* qRT-PCR assays as calculated by the slope with the equation $E = 10^{(-1/\text{slope})} - 1$.

Target	Slope	PCR E (%)	r ²
<i>SLF1</i>	-3.36	98	0.999
<i>ENB1</i>	-3.35	99	0.999

References

- Abelovska L, Bujdos, M., Kubova, J., Petrezselyova, S., Nosek, J., Tomaska, L. (2007) Comparison of element levels in minimal and complex media. *Can. J. Microbiol.* 53:533-535
- Aller SG, Unger VM (2006) Projection structure of the human copper transporter CTR1 at 6-Å resolution reveals a compact trimer with a novel channel-like architecture. *Proceedings of the National Academy of Sciences of the United States of America* 103:3627-3632
- Anderson DM, Cheng TP-O (1988) Intracellular localization of saxitoxins in the dinoflagellate *Gonyaulax tamarensis*. *Journal of Phycology* 24:17-22
- Arezi B, Xing W, Sorge JA, Hogrefe HH (2003) Amplification efficiency of thermostable DNA polymerases. *Analytical Biochemistry* 321:226-235
- Askwith C, Eide D, Van Ho A, Bernard PS, Li L, Davis-Kaplan S, Sipe DM, Kaplan J (1994) The *FET3* gene of *S. cerevisiae* encodes a multicopper oxidase required for ferrous iron uptake. *Cell* 76:403-410
- Causton HC, Ren B, Koh SS, Harbison CT, Kanin E, Jennings EG, Lee TI, True HL, Lander ES, Young RA (2001) Remodeling of Yeast Genome Expression in Response to Environmental Changes. *Mol. Biol. Cell* 12:323-337
- Cembella AD (1998) Ecophysiology and metabolism of paralytic shellfish toxins in marine microalgae. In: Anderson DM, Cembella AD, Hallegraeff G (eds) *Physiological Ecology of Harmful Algal Blooms, Vol G 41*. Springer-Verlag, Berlin, p 381-403
- Culotta VC, Howard WR, Liu XF (1994) *CRS5* encodes a metallothionein-like protein in *Saccharomyces cerevisiae*. *J. Biol. Chem.* 269:25295-25302
- Dancis A, Haile D, Yuan DS, Klausner RD (1994a) The *Saccharomyces cerevisiae* copper transport protein (Ctr1p). Biochemical characterization, regulation by copper, and physiologic role in copper uptake. *J. Biol. Chem.* 269:25660-25667
- Dancis A, Roman DG, Anderson GJ, Hinnebusch AG, Klausner RD (1992) Ferric Reductase of *Saccharomyces cerevisiae*: Molecular Characterization, Role in Iron Uptake, and Transcriptional Control by Iron. *Proceedings of the National Academy of Sciences* 89:3869-3873

- Dancis A, Yuan DS, Haile D, Askwith C, Eide D, Moehle C, Kaplan J, Klausner RD (1994b) Molecular characterization of a copper transport protein in *S. cerevisiae*: An unexpected role for copper in iron transport. *Cell* 76:393-402
- De Feo CJ, Aller SG, Unger VM (2007) A structural perspective on copper uptake in eukaryotes. *Biometals* 20:705-716
- Eide D (1998) The molecular biology of metal ion transport in *Saccharomyces cerevisiae*. *Annu. Rev. Nutr.* 18:441-469
- Gasch AP, Spellman PT, Kao CM, Carmel-Harel O, Eisen MB, Storz G, Botstein D, Brown PO (2000) Genomic Expression Programs in the Response of Yeast Cells to Environmental Changes. *Mol. Biol. Cell* 11:4241-4257
- Georg RC, Gomes SL (2007) Transcriptome Analysis in Response to Heat Shock and Cadmium in the Aquatic Fungus *Blastocladiella emersonii*. *Eukaryotic Cell* 6:1053-1062
- Hassett R, Dix DR, Eide DJ, Kosman DJ (2000) The Fe(II) permease Fet4p functions as a low affinity copper transporter and supports normal copper trafficking in *Saccharomyces cerevisiae*. *Biochemical Journal* 351:477-484
- Hassett R, Kosman DJ (1995) Evidence for Cu(II) Reduction as a Component of Copper Uptake by *Saccharomyces cerevisiae*. *J. Biol. Chem.* 270:128-134
- Huffman DL, O'Halloran TV (2000) Energetics of Copper Trafficking between the Atx1 Metallochaperone and the Intracellular Copper Transporter, Ccc2. *J. Biol. Chem.* 275:18611-18614
- Karin M, Najarian R, Haslinger A, Valenzuela P, Welch J, Fogel S (1984) Primary Structure and Transcription of an Amplified Genetic Locus: The *CUP1* Locus of Yeast. *Proceedings of the National Academy of Sciences* 81:337-341
- Kassahn KS, Caley MJ, Ward AC, Connolly AR, Stone G, Crozier RH (2007) Heterologous microarray experiments used to identify the early gene response to heat stress in a coral reef fish. *Molecular Ecology* 16:1749-1763
- Lefebvre KA, Bill BD, Erickson A, Baugh KA, O'Rourke L, Costa PR, Nance S, Trainer VL (2008) Characterization of intracellular and extracellular saxitoxin levels in both field and cultured *Alexandrium* spp. samples from Sequim Bay, Washington. *Marine Drugs* 6:103-116
- Mustacchi R, Hohmann S, Nielsen J (2006) Yeast systems biology to unravel the network of life. *Yeast* 23:227-238

- Nose Y, Rees EM, Thiele DJ (2006) Structure of the Ctr1 copper transPORER reveals novel architecture. *Trends in Biochemical Sciences* 31:604-607
- Okuyama M, Kobayashi Y, Inouhe M, Tohyama H, Joho M (1999) Effects of some heavy metal ions on copper-induced metallothionein synthesis in the yeast *Saccharomyces cerevisiae*. *Biometals* 12:307-314
- Philpott CC, Protchenko, O., Kim, Y.W., Boresky, Y., Shakoury-Elizeh, M. (2002) The response of iron deprivation in *Saccharomyces cerevisiae*: expression of siderophore-based systems of iron uptake. *Biochemical Society Transactions* 30:698-702
- Puig S, Thiele DJ (2002) Molecular mechanisms of copper uptake and distribution. *Current Opinion in Chemical Biology* 6:171-180
- Ruotolo R, Marchini G, Ottonello S (2008) Membrane transporters and protein traffic networks differentially affecting metal tolerance: a genomic phenotyping study in yeast. *Genome Biology* 9:R67
- Sherman F (2002) Getting started with yeast. *Methods Enzymol.* 350:3-41
- Stearman R, Yuan DS, Yamaguchi-Iwai Y, Klausner RD, Dancis A (1996) A Permease-Oxidase Complex Involved in High-Affinity Iron Uptake in Yeast. *Science* 271:1552-1557
- Taylor AB, Stoj CS, Ziegler L, Kosman DJ, Hart PJ (2005) The copper-iron connection in biology: Structure of the metallo-oxidase Fet3p. *Proceedings of the National Academy of Sciences* 102:15459-15464
- Teranishi KS, Stillman JH (2007) A cDNA microarray analysis of the response to heat stress in hepatopancreas tissue of the porcelain crab *Petrolisthes cinctipes*. *Comparative Biochemistry and Physiology Part D: Genomics and Proteomics* 2:53-62
- van Bakel H, Strengman, Wijmenga C, Holstege CP (2005) Gene expression profiling and phenotype analysis of *S. cerevisiae* in response to changing copper reveals six genes with new roles in copper and iron metabolism. *Physiol. Genomics* 22:356-367
- Wyatt T, Jenkinson IR (1997) Notes on *Alexandrium* population dynamics. *J. Plankton Res.* 19:551-575
- Yu W, Farrell RA, Stillman DJ, Winge DR (1996) Identification of *SLF1* as a new copper homeostasis gene involved in copper sulfide mineralization in *Saccharomyces cerevisiae*. *Mol. Cell. Biol.* 16:2464-2472

Zimmer RK, Ferrer RP (2007) Neuroecology, Chemical Defense, and the Keystone Species Concept. *Biol Bull* 213:208-225

Part IV

Role of the Transcriptional Regulator Mac1p in Mediating Gene Expression Upon Exposure to Saxitoxin in *Saccharomyces cerevisiae*

Abstract

Copper homeostasis in *Saccharomyces cerevisiae* is tightly regulated. The transcription factor Mac1p serves as the nutritional copper sensor, regulating the levels of genes typically involved in copper uptake, while the Ace1p transcription factor induces the expression of a set of genes associated with detoxification under conditions of copper stress. Mac1p induces the expression of the copper transporter Ctr1p and the ferric/cupric reductase Fre1p for the transport of copper into the cell. Previously, *CTR1* and *FRE1* were shown to be significantly repressed following exposure to saxitoxin. This study employed a *mac1Δ* mutant to test the hypothesis that saxitoxin repression of *CTR1* and *FRE1* is dependent on Mac1p. Quantitative reverse-transcriptase PCR was used to measure changes in gene expression in wild-type BY4742 and *mac1Δ* mutant cells following exposure to saxitoxin. *CTR1* and *FRE1* were both repressed in wild-type cells but remained unchanged (*FRE1*) or were slightly induced (*CTR1*) in *mac1Δ* mutants. These results suggest that Mac1p mediates the response of *CTR1* and *FRE1* to saxitoxin. The results are discussed in the context of external copper levels and the transport capabilities of Ctr1p. Additionally, expression data are compared with those collected with strain S288C.

Introduction

Copper homeostasis in *S. cerevisiae* is tightly regulated, with mechanisms of both transcriptional induction and repression mediated by copper ions. Exposure to elevated copper levels ($\geq 1 \mu\text{M}$) triggers the regulatory protein Ace1p (Labbe et al. 1997, Brown et al. 2002), which induces the expression of the metallothioneins Cup1p and Crs5p and the superoxide dismutase Sod1p (Karin et al. 1984, Thiele 1988, Buchman et al. 1989, Greco et al. 1990, Culotta et al. 1994). The binding of copper ions induces a conformational change in the cysteine-rich N-terminal domain of Ace1p, resulting in a polynuclear Cu(I)-cysteinyll thiolate cluster that allows Ace1p to bind to the promoter regions of the above-mentioned genes in a sequence-specific manner, thus initiating transcription (Fürst et al. 1988, Buchman et al. 1989, Dameron et al. 1991).

A different set of genes is induced only under conditions of copper starvation, including *FRE1*, *CTR1*, and *CTR3*, all of which are involved in copper reduction and transport across the plasma membrane. In contrast to *CUP1*, *CRS5*, and *SOD1*, these genes have been shown to be strongly repressed when exposed to micromolar ($\geq 1 \mu\text{M}$) concentrations of copper (Labbe et al. 1997). *FRE1* codes for a cupric/ferric reductase and is down-regulated in response to both iron and copper (Dancis et al. 1992, Hassett & Kosman 1995), while *CTR1* and *CTR3* code for high-affinity copper transporters whose repression is specific to copper ions (Dancis et al. 1994a, Dancis et al. 1994b, Labbe et al. 1997). Additionally, toxic copper levels ($\geq 10 \mu\text{M}$) have been shown to result in degradation of the Ctr1p (Ooi et al. 1996).

CTR1, *CTR3*, and *FRE1* are regulated in a copper-sensitive and specific manner by Mac1p (Jungmann et al. 1993, Labbe et al. 1997). Gene induction occurs through Mac1p binding to specific sequences within the promoter regions defined as CuREs (copper-responsive elements); two CuREs are required in order for Mac1p to bind (Labbe et al. 1997). Mac1p binding to the CuREs is copper-ion dependent: while coordination of Cu(I) ions within Mac1p is required for CuRE binding, excess levels of Cu(I) disrupt binding, indicating that Mac1p is able to sense different copper ion levels through an as-yet unidentified mechanism, possibly a phosphorylation

modification (Heredia et al. 2001). In this respect, Mac1 serves as the “nutritional” copper sensor, while Ace1p functions as a “toxic” copper sensor.

Mac1p contains both a DNA-binding domain and a transactivation domain, the activities of both of which were shown to be inhibited in copper-replete cells (Graden & Winge 1997, Labbe et al. 1997), indicating that copper regulation of Mac1p activity is the result of a direct interaction between copper ions and the protein (Jensen & Winge 1998). The C-terminal region contains two cysteine-rich motifs, similar to those found within Ace1p (Graden & Winge 1997), to which a total of eight copper ions bind (Graden & Winge 1997, Jensen & Winge 1998). The first cysteine-rich motif in the C-terminal domain binds four copper ions in a configuration similar to that of Ace1p (Brown et al. 2002), while the second functions as a copper-dependent transactivation domain (Voutsina et al. 2001). The N-terminal region of Mac1p contains the DNA-binding domain, along with two bound zinc ions (Jensen et al. 1998). Thus, in addition to similarities between the C-terminal cysteine-rich motifs, the N-terminal 40 residues of Mac1p (the DNA-binding domain) are homologous to the N-terminal DNA-binding zinc module of Ace1p. Overall, inhibition of Mac1p involves the copper-dependent loss of DNA binding activity (Labbe et al. 1997) and copper-dependent inhibition of the transactivation domain function (Georgatsou et al. 1997, Graden & Winge 1997). Therefore, it is likely that Mac1p is repressed by copper ions due to a copper-induced intramolecular interaction between the N-terminal DNA-binding domain and the C-terminal transactivation domain (Jensen & Winge 1998). In summary, copper binds to both transcription factors (Ace1p and Mac1p) through the formation of similar polycopper clusters (Brown et al. 2002) with contrasting results: while Cu(I) binding to Ace1p results in a conformational change that allows Ace1p to bind to promoter sequences and induce gene expression, Cu(I) binding to Mac1p inhibits its function as a transcriptional activator.

The objective of this study was to compare the expression profile in a wild-type *S. cerevisiae* strain to a *mac1* deletion mutant following exposure to saxitoxin. Of specific interest was the regulation of the *CTR1* and *FRE1* genes, for which

Mac1p is the transcriptional regulator. The experiments described here were designed to test the hypothesis that saxitoxin repression of *CTR1* and/or *FRE1* is dependent on Mac1p. Repression of *CTR1* or *FRE1* within the *mac1* deletion mutant would indicate that saxitoxin is acting directly on the genes, or that a regulatory protein other than Mac1p also influences expression of these genes. No change in expression of these genes in the *mac1*Δ mutant indicates that saxitoxin is acting on the transcriptional regulator Mac1p.

Methods and Materials

Yeast Strains

S. cerevisiae wild-type BY4742 (*MATα his3Δ1 leu2Δ0 lys2Δ0 ura3Δ0*) and the deletion mutant BY4742*mac1*Δ from the *Saccharomyces* Genome Deletion project were obtained from Open Biosystems. Yeast strains were grown at 30°C in synthetic complete (SC) broth (Sherman 2002) (media composition as described in Part III).

Growth Curves

Growth curves were performed in order to determine the rate of growth and approximate time of entry into mid-exponential phase of each strain. An initial comparison was done using SC and SC supplemented with 0.2% casamino acids (SCCA) (Difco) to determine optimal conditions for growth. Individual colonies were inoculated into 2 mL of SC or SCCA and cultured at 30°C with rapid agitation (200rpm) for 24 hours. While the SCCA cultures had reached saturation by this time, none to minimal growth was observed in the SC cultures. Therefore, larger-scale growth curves were conducted with SCCA. Yeast cells were re-inoculated into 10ml SCCA to a starting $OD_{600}=0.03-0.05$ using 120 μl from the 2 mL cultures. Growth was monitored by measuring the OD_{600} every 3–4 hours with a Beckman DU-600 Spectrophotometer.

Halo Assays

Halo assays were performed to determine the sensitivity of the deletion strain and wild-type BY4742 to saxitoxin. Strains were grown overnight in YPD and then harvested and washed three times with sterile deionized water. Yeast cells were counted and adjusted to 5×10^6 cells ml^{-1} using sterile deionized water. The one milliliter cell suspension was added to 3 ml 0.8% noble agar, vortexed briefly, and spread onto YPD plates. Plates were cooled at room temperature and 5 μl of saxitoxin was spotted onto the top agar at final concentrations of 16 and 32 μM . A control of 5 μl deionized water was also spotted onto the top agar. Plates were incubated at 30°C for two days. Halo assays were also performed in which *mac1* Δ and wild-type BY4742 were grown overnight in SC broth and plated onto SC plates, as this was the media in which gene expression experiments were to be performed. As an additional control, halo assays were also performed with *S. cerevisiae* S288C, to ensure that any zones of clearing that occurred with the BY4742 strains were due solely to saxitoxin exposure.

Chemicals

Saxitoxin was purchased from National Research Council Canada (NRCC) (CRM-STX-e). The saxitoxin was lyophilized, concentrated and re-suspended in deionized water (pH 5.5) at a final concentration of 100 $\mu\text{g ml}^{-1}$.

Saxitoxin Exposures

Cultures of *S. cerevisiae* BY4742 and BY4742*mac1* Δ were grown in SCCA to $\text{OD}_{600}=1.0$. Due to limited quantities of saxitoxin, the volume of yeast culture used for saxitoxin exposures was decreased from 400 μl to 200 μl . Thus, 200 μl from individual 10 mL overnight cultures was transferred to sterile 2 mL tubes and saxitoxin added to individual cultures at a final concentration of 16 μM . Upon addition of saxitoxin, samples were mixed gently and incubated with moderate agitation (30rpm) at 30°C for 45 min. Controls consisted of deionized water (pH 5.5). Three biological replicates for each strain were performed under these conditions for gene expression analysis.

Cell Harvesting and Total RNA Extraction

Cells were harvested following the protocol of Causton (Causton et al. 2001) and stored immediately in liquid nitrogen. Total RNA was extracted following the protocol described previously (Part II).

Quantitative Reverse-Transcriptase PCR

Quantitative reverse-transcriptase PCR (qRT-PCR) was used to examine the response of a set of genes for which assays had previously been developed: *ACT1*, *CUP1*, *CRS5*, *CTR1*, *FRE1*, *FET3*, and *STR3* (Part II), and *SLF1* and *ENB1* (Part III). qRT-PCR reactions utilized Taqman® probes and gene-specific primers. The Quantitect Probe RT-PCR kit (Qiagen, Valencia, CA) was used for all assays. Assay reactions consisted of 12.5 µl 2x Quantitect Probe RT-PCR Master Mix, the optimized concentrations of primers (600 nm or 800 nm), 200 nm probe, 0.25 µl QuantiTect RT Mix, 5 µl of template, and adjusted to a final volume of 25 µl with nuclease-free water. Template consisted of a 1:50 dilution of the total RNA extract of each sample. The following protocol was used for all assays: 50°C for 30 minutes, 95°C for 15 minutes, and 45 cycles of denaturing at 94°C for 15 seconds and annealing/extension at 60°C for 1 min. All reactions were performed in triplicate on a DNA engine with the Chromo4 detector (MJ Research, Waltham, MA).

Data Normalization

Expression data were recorded and normalized using absolute quantification as described in Part II. Briefly, functional gene data were initially collected as copies ng⁻¹ based on *in-vitro* transcribed RNA standard curves; these values were further normalized to the corresponding *ACT1* copies ng⁻¹ of each sample.

Statistical Analysis: Exposed versus Control

For each gene at each treatment, normalized values were analyzed for statistical significance (SPSS v.15, Chicago, IL) between exposed and control samples with the independent samples *t*-test if data passed the tests for equal variance (Levene's test) and normality (Shapiro-Wilkes). The Mann-Whitney U-test with Monte Carlo correction was applied if samples were not normally distributed. The average fold-change and fold-change range of each gene were calculated as described

in Part II. Of specific interest was the difference in regulation of the *CTR1* and *FRE1* genes between the wild-type BY4742 and the *mac1* deletion mutant, as expression of these genes is dependent upon the transcriptional regulator Mac1p.

Statistical Analysis: Between Strains

The transcriptional response of functional genes was also compared between the wild-type BY4742 and the *mac1* Δ mutant following exposure to saxitoxin. The normalized transcript value of each exposed sample was divided by the sample's respective normalized control value; this transformation yielded the differential expression of individual samples. If data passed the tests for normality and equal variance, the independent samples *t*-test was applied to determine if there was a significant difference in expression values between the two strains. The Mann-Whitney U-test with Monte Carlo correction was applied if samples were not normally distributed.

Results

Growth Curves

Gene expression experiments necessitated the use of media with reduced levels of trace metals, particularly copper and iron, in order to more accurately compare the regulation of genes lacking the Mac1p transcriptional regulator for comparison with previous results obtained with *S. cerevisiae* S288C. However, it was imperative to assess the growth of the *mac1* Δ mutant in minimal media, as mutant strains have been known to exhibit reduced fitness in both rich and minimal media. Both strains exhibited little to minimal growth in SC media and robust growth in SCCA (data not shown). Therefore, growth curves were performed for both strains using SCCA in 10 mL volumes to gauge the approximate time needed for cultures of this volume to enter the exponential growth phase. This information was used to assess the health of individual cultures utilized in the gene expression experiments. Differences in gene expression may have been related to growth (i.e. robustness) of the culture, as mutant strains may lose their robustness over time (Dan Kostman, personal communication). Though *mac1* Δ exhibited a more rapid entry into

exponential phase than did the wild-type, this is attributed to the starting inoculums: the 2 mL overnight culture of *mac1* Δ was more turbid than the 2 mL overnight culture of the wild-type BY4742. Overall, both cultures were able to reach the exponential phase of growth in less than 24 hours, and thus SCCA was deemed a suitable culture for future gene expression experiments (Figure IV-1).

Halo Assays

No zones of clearing were observed on the YPD plates containing either wild-type BY4742 or the *mac1* Δ mutant, indicating that saxitoxin did not affect the growth of either of these strains at concentrations of 16 and 32 μ M (Figure IV-2). Halo assays were also performed in which both strains were overlaid onto SC plates, to ensure growth was not affected by culture conditions, as gene expression experiments were performed using a minimal media. The results of the halo assays performed with SC were identical to those obtained with the YPD plates, as no zones of clearing were observed on the minimal media plates (data not shown). Additionally, no zones of clearing were observed on either the YPD or SC plates containing *S. cerevisiae* S288C (data not shown). *S. cerevisiae* S288C served as an additional control, as it had already been established that saxitoxin did not affect the growth of this strain and any zones of clearing that appeared on the plates containing the BY4742 strains would have been attributable to saxitoxin.

Expression Profiling

In general, both strains exhibited minimal expression changes following exposure to 16 μ M saxitoxin. The metallothionein Cup1p was significantly yet minimally induced in both strains, at levels of 1.2-fold (wild-type) and 1.3-fold (*mac1* Δ mutant) (Figures IV-3 and IV-4, and summarized in Table IV-1). *CTR1* and *FRE1* were down-regulated in the wild-type 1.5- and 1.23-fold, respectively (Table IV-1), with *CTR1* significantly repressed in comparison to controls (Figure IV-3). *FRE1* remained unchanged in the *mac1* Δ mutant (Table IV-1), while *CTR1* was slightly induced, though this change was not significantly different from controls (Figure IV-4). Additionally, *FET3* was significantly upregulated approximately 1.5-fold in the wild-type yet repressed 1.3-fold in *mac1* Δ (Table IV-1). However, due to a

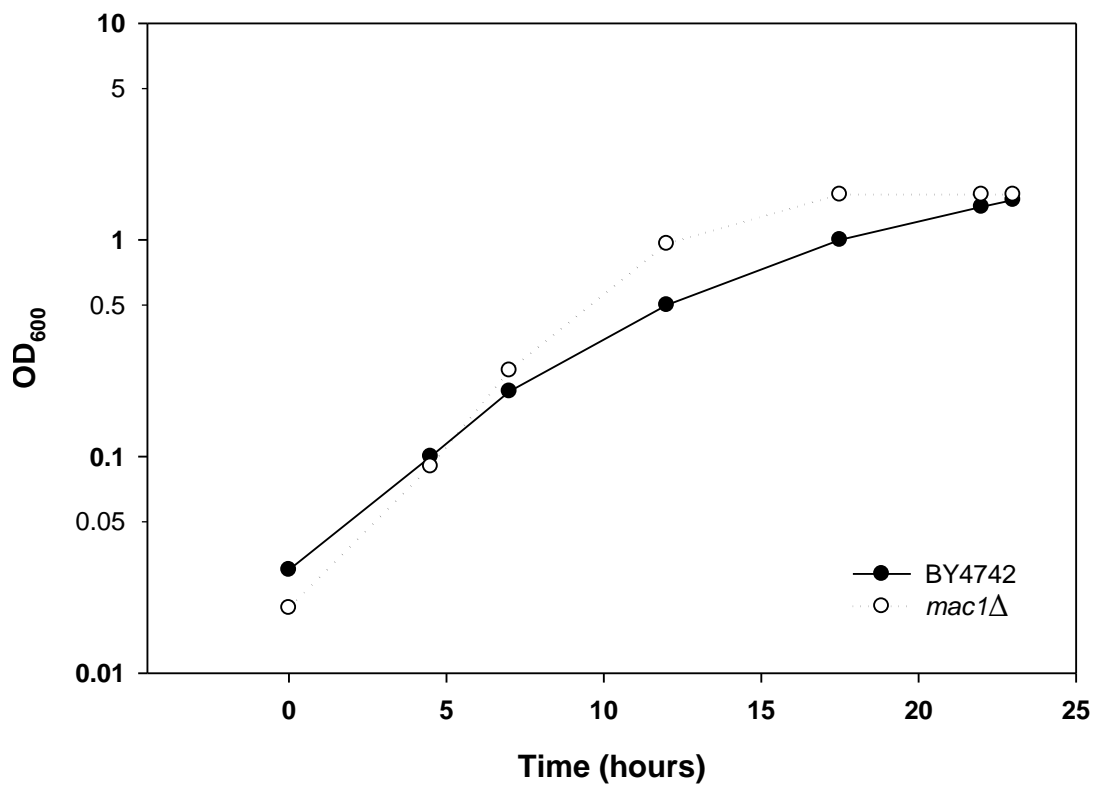


Figure IV-2. Growth curves of wild-type BY4742 and *mac1*Δ in synthetic complete broth supplemented with 0.2% casamino acids. Cultures were re-inoculated from an overnight culture to a starting OD₆₀₀=0.02–0.03 and incubated in 10 mL volumes at 30°C with rapid agitation. Growth was monitored by measuring the OD₆₀₀ every several hours. These growth curves were performed primarily to assess the robustness of the *mac1*Δ strain prior to gene expression experiments.

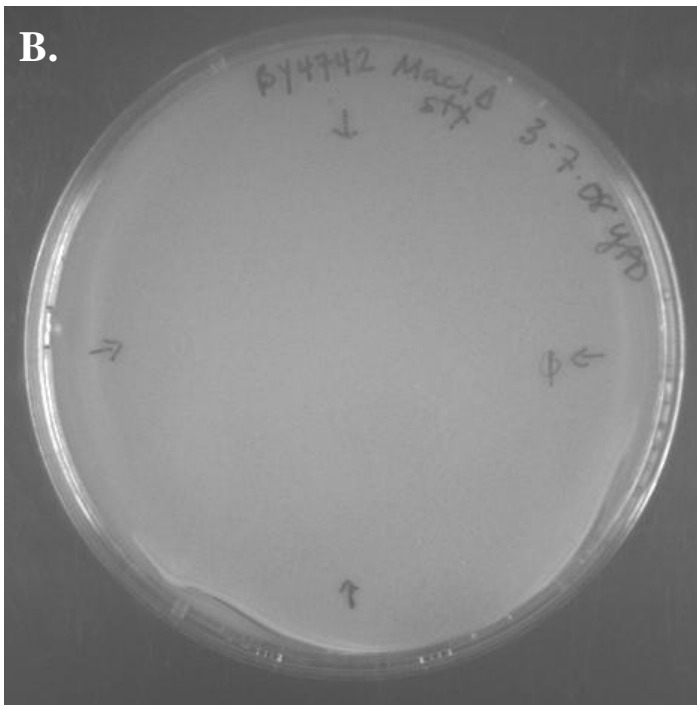
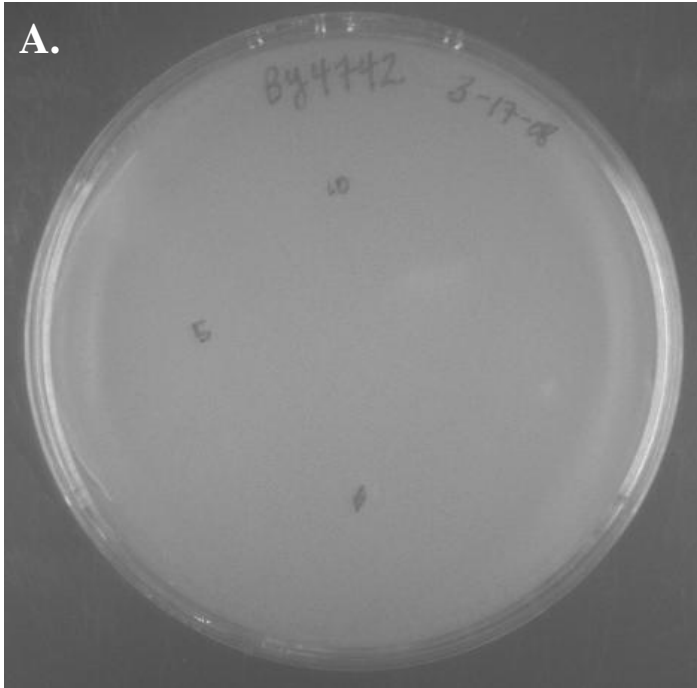


Figure IV-2. Halo assays performed with (A.) wild-type BY4742 and (B.) *mac1*Δ on YPD agar plates. No zones of clearing were observed at concentrations of 16 μ M and 32 μ M saxitoxin, indicating that saxitoxin did not affect the growth of either strain.

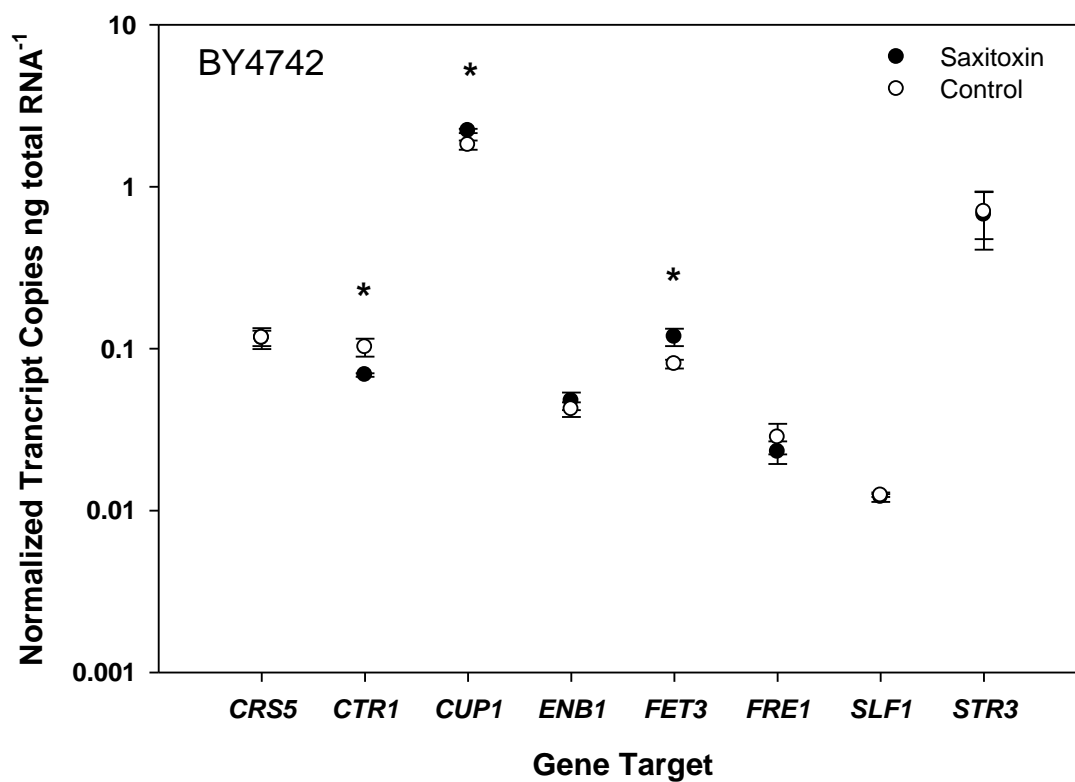


Figure IV-3. Normalized transcript copies in wild-type BY4742 as measured following exposure to 16 μ M saxitoxin in SCCA. * indicates significant difference between exposed and control at $p < 0.05$ level.

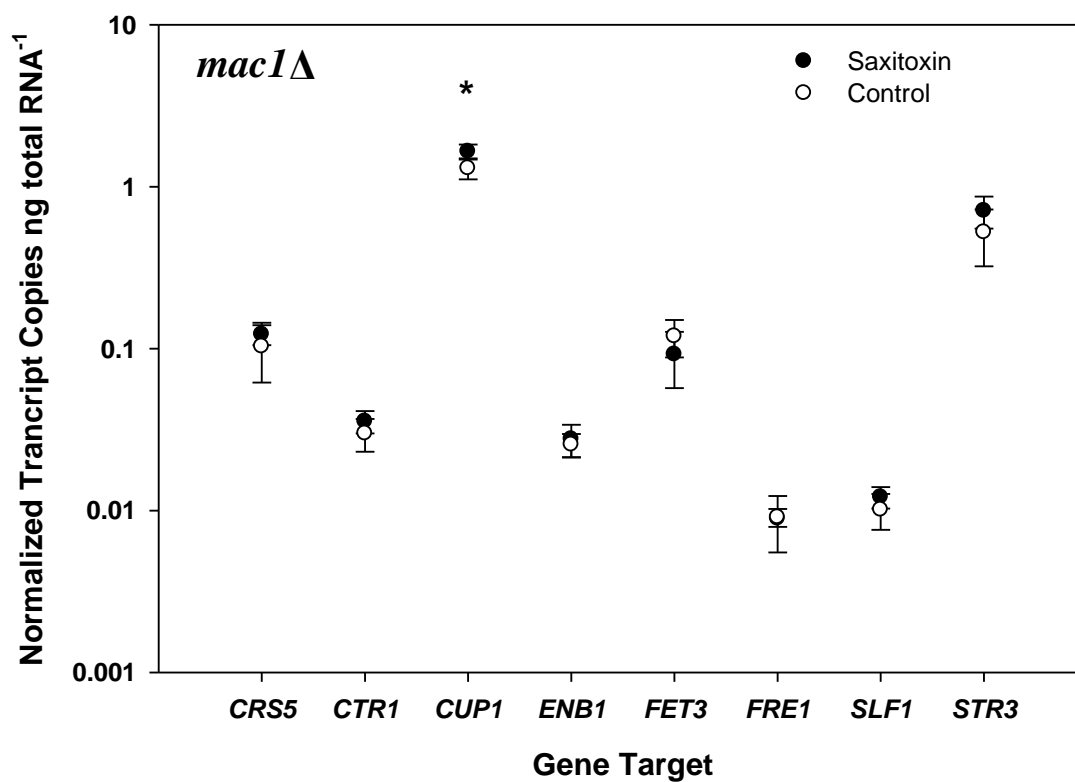


Figure IV-4. Normalized transcript copies in BY4742*mac1*Δ as measured following exposure to 16 μM saxitoxin in SCCA. * indicates significant difference between exposed and control at $p < 0.05$ level.

Table IV-1. Average linear fold-change of copper and iron homeostasis genes in wild-type BY4742 and *mac1*Δ following exposure to 16 μM saxitoxin. Absolute quantification was used to measure the transcripts ng total RNA⁻¹ of functional genes; these values were then normalized to the *ACT1* values of each sample.

*** indicates significant difference ($p < 0.05$) between sample and control,
^a indicates significant difference between strains.**

Gene ID	BY4742	<i>mac1</i> Δ
<i>CRS5</i>	1 (±0.18)	1.19 (±0.42)
<i>CTR1</i>	-1.5 (±0.13)*, ^a	1.19 (±0.28) ^a
<i>CUP1</i>	1.22 (±0.07)*	1.3 (±0.18)*
<i>ENB1</i>	1.13 (±0.16)	1.08 (±0.28)
<i>FET3</i>	1.47 (±0.14)*	-1.3 (±0.46)
<i>FRE1</i>	-1.23 (±0.27)	1 (±0.4)
<i>STR3</i>	1 (±0.51) ^a	1.36 (±0.45) ^a
<i>SLF1</i>	-1.02 (±0.07)	1.2 (±0.29)

greater level of variation among individual samples of the *mac1* Δ strain (data not shown), there was no significant difference in the levels of *FET3* expression between the wild-type and *mac1* Δ .

Discussion

Previous expression measurements with *S. cerevisiae* S288C indicated the response to saxitoxin was similar to that of excess levels of copper and iron. The experiments described here sought to further explore the mechanism of repression of the genes encoding the copper transporter *CTR1* and the cupric/ferric reductase *FRE1* upon exposure to saxitoxin. As Mac1p is the transcriptional regulator of both *CTR1* and *FRE1*, these genes were examined in a *mac1* deletion mutant. As *mac1* Δ was of the BY4742 background (Brachmann et al. 1998), the transcriptional regulation of these genes was also examined in the wild-type strain.

The expression data generated in this study with the wild-type and *mac1* Δ mutant do not provide a clear answer as to whether the transcriptional responses of *CTR1* and *FRE1* upon exposure to saxitoxin are mediated by Mac1p, or occur via an independent mechanism. Though levels of expression were reduced in comparison to those of S288C, *CTR1* was also significantly repressed in BY4742, indicating a consistent trend as a possible target for saxitoxin. Expression of *CTR1* in the *mac1* Δ mutant was slightly elevated, with no statistical significant difference between exposed and control samples (Figure IV-4). *FRE1* displayed a trend similar to that of *CTR1*: expression was repressed in the wild-type but remained unchanged in *mac1* Δ . Taken collectively, this limited set of expression data suggests that Mac1p mediates the response of *CTR1* and *FRE1* to saxitoxin in some undisclosed manner.

Overall, the expression levels among all genes in both the mutant and the wild-type were reduced in comparison to the values previously obtained with *S. cerevisiae* S288C (Part III). Two factors may have contributed to the differences seen in the expression levels among strains: (I) BY4742 was unable to grow in SC media at the same rate as S288C (e.g. BY4742 exhibited minimal growth after 3 days in SC, while S288C grown in SC reached the exponential growth phase in less than 24

hours), indicating differences in metabolic capabilities which may have been reflected in the expression levels; and (II) the media used here was supplemented with casamino acids, for the purpose of supporting a more robust growth. Copper levels in casamino acids have been analytically measured at $40 \mu\text{g g}^{-1}$ (Nolan & Nolan 1972); assuming a molecular weight of 250 as copper sulfate, this is a concentration of approximately $160 \mu\text{M}$ concentration. Supplementing the SC media with 0.2% casamino acids increases overall copper concentrations approximately 3-fold (from 160 nM to 480 nM), resulting in concentrations equal to or greater than that of the rich media YPD. As free copper is restricted to less than one atom per cell in *S. cerevisiae* (Rae et al. 1999), this increase in copper, coupled with the increase in amino acids, may have impacted the cell physiology and contributed to the differences in regulation between BY4742 and S288C. Different strains of *S. cerevisiae* in the wine industry have been shown to differ in copper resistance and the resulting ability for copper reduction and internal accumulation (Brandolini et al. 2002). Thus, it is possible that BY472 and S288C, though genetically almost identical, differ in their sensitivities to copper or saxitoxin, as manifested by different levels of gene regulation recorded here (BY4742) and in Part III (S288C).

Previous transcriptional profiling with strain S288C also revealed a highly specific detoxification mechanism in response to excess copper (van Bakel et al. 2005). However, expression profiling with a BY4742 *ace1* Δ mutant resulted in substantial differences in the overall profile, as the majority of genes grouped into the functional categories of proteosome function and stress response rather than metal detoxification. Though the BY4742 strain is based on that of S288C, differing only in the deletion of multiple commonly used selectable markers (Brachmann et al. 1998), expression profiles obtained with S288C may represent a strain-specific response, in regards to both excess copper (van Bakel et al. 2005) and saxitoxin (Part III).

Recognizing the differences in copper levels between SC and SCCA may also explain the induction of *FET3* in the wild-type in this study: while *FET3* has been shown to be upregulated in response to elevated copper levels (Gross et al. 2000), it was also induced following exposure to saxitoxin in YPD (Part II). In addition to

serving as part of the high-affinity iron uptake system, Fet3p aids in alleviating copper toxicity through the oxidation of Cu(I) to Cu(II) (Shi et al. 2003). Though *CTR1* was repressed in the wild-type, *FET3* may have received an adequate supply of copper ions as a result of the increased levels in the media, which may have been transported into the cell via Ctr3p. It is intriguing that *FET3*, whose expression is regulated by Aft1p (activator of ferrous transport) (Yamaguchi-Iwai et al. 1995) and not Mac1p, displayed contrasting levels of regulation between the wild-type and *mac1*Δ. However, it must also be recognized that *FET3* regulation in either strain may not have been a consequence of saxitoxin or copper, but instead served as an indicator of differences in iron homeostasis between the two strains as a result of the *MAC1* deletion.

While the data collected in this study suggest that Mac1p regulates the response of *CTR1* and *FRE1* to saxitoxin, the expression changes were too minimal to draw conclusive results. A more comprehensive set of experiments that includes both mRNA and protein data is required to realize the true effects of saxitoxin exposure on Mac1p, and, consequently, Ctr1p. Mac1p localizes to the nucleus (Jungmann et al. 1993, Jensen & Winge 1998), while Ctr1p and Fre1p are found within the plasma membrane. If Ctr1p is the target for the saxitoxin molecule, a subsequent step would be to determine whether the molecule permeates the Ctr1p pore. Recent studies have identified the ability of the anticancer agent cisplatin to be transported into the cell via Ctr1p. The uptake of this compound, structurally much larger than copper, has been demonstrated in both the yeast and human Ctr1p (De Feo et al. 2007). Additionally, copper and cisplatin have been shown to reduce each other's uptake in wild-type yeast cells but not *ctr1*Δ mutants, indicating that reduction is dependent on Ctr1p (Ishida et al. 2002). Mammalian homologs for Ctr1p exist (hCTR1 in humans, mCTR1 in mice), and it has been shown that *CTR1* is the route of entry for cisplatin not only in yeast (Lin et al. 2002), but in these cells as well (Ishida et al. 2002, Holzer et al. 2004). While the Ctr1p structural design most closely resembles that of channel proteins, (Aller & Unger 2006), molecular dynamics experiments modeling the assembly and transport activities of Ctr1p suggest that it

functions as a transporter rather than a channel protein (Sinani et al. 2007). It has also been suggested that Ctr1p uses a different mechanism of transport for copper and cisplatin, as the conformational changes observed during copper translocation did not occur during cisplatin uptake (Sinani et al. 2007). If Ctr1p is able to transport cisplatin via a structural change, it remains to be seen whether this protein is ubiquitous in nature with regards to substrate uptake into the cell.

References

- Aller SG, Unger VM (2006) Projection structure of the human copper transporter CTR1 at 6-Å resolution reveals a compact trimer with a novel channel-like architecture. *Proceedings of the National Academy of Sciences of the United States of America* 103:3627-3632
- Brachmann CB, Davies A, Cost GJ, Caputo E, Li J, Hieter P, Boeke JD (1998) Designer deletion strains derived from *Saccharomyces cerevisiae* S288C: A useful set of strains and plasmids for PCR-mediated gene disruption and other applications. *Yeast* 14:115-132
- Brandolini V, Tedeschi P, Capece A, Maietti A, Mazzotta D, Salzano G, Paparella A, Romano P (2002) *Saccharomyces cerevisiae* wine strains differing in copper resistance exhibit different capability to reduce copper content in wine. *World Journal of Microbiology & Biotechnology* 18:499-503
- Brown KR, Keller GL, Pickering IJ, Harris HH, George GN, Winge DR (2002) Structures of the Cuprous-Thiolate Clusters of the Mac1 and Ace1 Transcriptional Activators. *Biochemistry* 41:6469-6476
- Buchman C, Skroch P, Welch J, Fogel S, Karin M (1989) The *CUP2* gene product, regulator of yeast metallothionein expression, is a copper-activated DNA-binding protein. *Mol. Cell. Biol.* 9:4091-4095
- Causton HC, Ren B, Koh SS, Harbison CT, Kanin E, Jennings EG, Lee TI, True HL, Lander ES, Young RA (2001) Remodeling of Yeast Genome Expression in Response to Environmental Changes. *Mol. Biol. Cell* 12:323-337
- Culotta VC, Howard WR, Liu XF (1994) *CRS5* encodes a metallothionein-like protein in *Saccharomyces cerevisiae*. *J. Biol. Chem.* 269:25295-25302
- Dameron CT, Winge DR, George GN, Sansone M, Hu S, Hamer D (1991) A copper-thiolate polynuclear cluster in the ACE1 transcription factor. *Proceedings of the National Academy of Sciences of the United States of America* 88:6127-6131
- Dancis A, Haile D, Yuan DS, Klausner RD (1994a) The *Saccharomyces cerevisiae* copper transport protein (Ctr1p). Biochemical characterization, regulation by copper, and physiologic role in copper uptake. *J. Biol. Chem.* 269:25660-25667

- Dancis A, Roman DG, Anderson GJ, Hinnebusch AG, Klausner RD (1992) Ferric Reductase of *Saccharomyces cerevisiae*: Molecular Characterization, Role in Iron Uptake, and Transcriptional Control by Iron. *Proceedings of the National Academy of Sciences* 89:3869-3873
- Dancis A, Yuan DS, Haile D, Askwith C, Eide D, Moehle C, Kaplan J, Klausner RD (1994b) Molecular characterization of a copper transport protein in *S. cerevisiae*: An unexpected role for copper in iron transport. *Cell* 76:393-402
- De Feo CJ, Aller SG, Unger VM (2007) A structural perspective on copper uptake in eukaryotes. *Biometals* 20:705-716
- Fürst P, Hu S, Hackett R, Hamer D (1988) Copper activates metallothionein gene transcription by altering the conformation of a specific DNA binding protein. *Cell* 55:705-717
- Georgatsou E, Mavrogiannis LA, Fragiadakis GS, Alexandraki D (1997) The Yeast Fre1p/Fre2p Cupric Reductases Facilitate Copper Uptake and Are Regulated by the Copper-modulated Mac1p Activator. *J. Biol. Chem.* 272:13786-13792
- Graden JA, Winge DR (1997) Copper-mediated repression of the activation domain in the yeast Mac1p transcription factor. *PNAS* 94:5550-5555
- Greco MA, Hrab DI, Magner W, Kosman DJ (1990) Cu,Zn superoxide dismutase and copper deprivation and toxicity in *Saccharomyces cerevisiae*. *J. Bacteriol.* 172:317-325
- Gross C, Kelleher M, Iyer VR, Brown PO, Winge DR (2000) Identification of the Copper Regulon in *Saccharomyces cerevisiae* by DNA Microarrays. *J. Biol. Chem.* 275:32310-32316
- Hassett R, Kosman DJ (1995) Evidence for Cu(II) Reduction as a Component of Copper Uptake by *Saccharomyces cerevisiae*. *J. Biol. Chem.* 270:128-134
- Heredia J, Crooks M, Zhu Z (2001) Phosphorylation and Cu⁺ Coordination-dependent DNA Binding of the Transcription Factor Mac1p in the Regulation of Copper Transport. *J. Biol. Chem.* 276:8793-8797
- Holzer AK, Samimi G, Katano K, Naerdemann W, Lin X, Safaei R, Howell SB (2004) The Copper Influx Transporter Human Copper Transport Protein 1 Regulates the Uptake of Cisplatin in Human Ovarian Carcinoma Cells. *Mol Pharmacol* 66:817-823

- Ishida S, Lee J, Thiele DJ, Herskowitz I (2002) From the Cover: Uptake of the anticancer drug cisplatin mediated by the copper transporter Ctr1 in yeast and mammals. *Proceedings of the National Academy of Sciences* 99:14298-14302
- Jensen LT, Posewitz MC, Srinivasan C, Winge DR (1998) Mapping of the DNA Binding Domain of the Copper-responsive Transcription Factor Mac1 from *Saccharomyces cerevisiae*. *J. Biol. Chem.* 273:23805-23811
- Jensen LT, Winge DR (1998) Identification of a copper-induced intramolecular interaction in the transcription factor Mac1 from *Saccharomyces cerevisiae*. *EMBO J.* 17:5400-5408
- Jungmann J, Reins H-A, Lee J, Romeo A, Hassett R, Kosman D, Jentsch S (1993) MAC1, a nuclear regulatory protein related to Cu-dependent transcription factors is involved in Cu/Fe utilization and stress resistance in yeast. *EMBO J.* 12:5051-5056
- Karin M, Najarian R, Haslinger A, Valenzuela P, Welch J, Fogel S (1984) Primary Structure and Transcription of an Amplified Genetic Locus: The *CUP1* Locus of Yeast. *Proceedings of the National Academy of Sciences* 81:337-341
- Labbe S, Zhu Z, Thiele DJ (1997) Copper-specific Transcriptional Repression of Yeast Genes Encoding Critical Components in the Copper Transport Pathway. *J. Biol. Chem.* 272:15951-15958
- Lin X, Okuda T, Holzer A, Howell SB (2002) The Copper Transporter CTR1 Regulates Cisplatin Uptake in *Saccharomyces cerevisiae*. *Mol Pharmacol* 62:1154-1159
- Nolan RA, Nolan WG (1972) Elemental analysis of vitamin-free casamino acids. *Appl. Microbiol.* 24:290-291
- Ooi CE, Rabinovich E, Dancis A, Bonifacino JS, Klausner RD (1996) Copper-dependent degradation of the *Saccharomyces cerevisiae* plasma membrane copper transporter Ctr1p in the apparent absence of endocytosis. *EMBO J.* 15:3515-3523
- Rae TD, Schmidt PJ, Pufahl RA, Culotta VC, O'Halloran TV (1999) Undetectable intracellular free copper: The requirement of a copper chaperone for superoxide dismutase. *Science* 284:805-808
- Sherman F (2002) Getting started with yeast. *Methods Enzymol.* 350:3-41

- Shi X, Stoj C, Romeo A, Kosman DJ, Zhu Z (2003) Fre1p Cu²⁺ Reduction and Fet3p Cu¹⁺ Oxidation Modulate Copper Toxicity in *Saccharomyces cerevisiae*. J. Biol. Chem. 278:50309-50315
- Sinani D, Adle DJ, Kim H, Lee J (2007) Distinct Mechanisms for Ctr1-mediated Copper and Cisplatin Transport. J. Biol. Chem. 282:26775-26785
- Thiele DJ (1988) ACE1 regulates expression of the *Saccharomyces cerevisiae* metallothionein gene. Mol. Cell. Biol. 8:2745-2752
- van Bakel H, Strengman, Wijmenga C, Holstege CP (2005) Gene expression profiling and phenotype analysis of *S. cerevisiae* in response to changing copper reveals six genes with new roles in copper and iron metabolism. Physiol. Genomics 22:356-367
- Voutsina A, Fragiadakis GS, Boutla A, Alexandraki D (2001) The second cysteine-rich domain of Mac1p is a potent transactivator that modulates DNA binding efficiency and functionality of the protein. FEBS Letters 494:38-43
- Yamaguchi-Iwai Y, Dancis A, Klausner RD (1995) AFT1: a mediator of iron regulated transcriptional control in *Saccharomyces cerevisiae*. EMBO J. 14:1231-1239

Part V

Expression Profile Comparisons in *Chlamydomonas reinhardtii* Following Exposure to Saxitoxin and Copper

Abstract

Chlamydomonas reinhardtii is a unicellular green alga whose genome has recently been sequenced, making it a model photosynthetic organism on which to perform transcriptional profiling. This study utilized a comparative transcriptomics approach in order to more fully define the mechanism of action of the algal toxin saxitoxin on lower eukaryotes. A specific set of genes was selected for expression profiling in *C. reinhardtii* based on functional similarities with those identified as differentially expressed in the yeast *Saccharomyces cerevisiae* and coupled with previous reports in the literature of *C. reinhardtii* genes whose transcriptional regulation was influenced copper levels. Real-time reverse transcriptase PCR was used to compare the expression of the genes coding for cytochrome c6 (*CYC6*), coproporphyrinogen III oxidase (*CPX1*), glutathione synthetase (*GSH2*), and thioredoxins m (*TRX m*) and h (*TRX h*) upon exposure to saxitoxin or excess copper over a 24 h period. *CYC6*, *CPX1*, *TRX m* and *TRX h* all displayed contrasting patterns of regulation between the two treatments, while *GSH2* was repressed in both. The induction of *CYC6* and *CPX1* following saxitoxin exposure suggest that the toxin is altering copper homeostasis through an as-yet unidentified mechanism. A proposed mechanism of action based on the collective expression profiles of *S. cerevisiae* and *C. reinhardtii* is discussed in the context of the eco-evolutionary role this toxin may serve for the algae that produce it.

Introduction

Saxitoxin is a secondary metabolite produced by multiple species of dinoflagellates and cyanobacteria. Numerous studies on the factors stimulating toxin production, including environmental parameters such as nutrient amendments (Siu et al. 1997, Yin et al. 1997, Velzeboer et al. 2001, Leong et al. 2004, Hu et al. 2006), temperature (Castro et al. 2004, Navarro et al. 2006, Gedaria et al. 2007), and salinity (Gedaria et al. 2007); growth phase (Castro et al. 2004); cell cycle (Taroncher-Oldenburg et al. 1997); and bacterial associations (Vasquez et al. 2001, Uribe & Espejo 2003, Azanza et al. 2006, Maas et al. 2007), have been performed, yet the question still remains as to why the organisms produce this compound. The organisms capable of saxitoxin production span two kingdoms and a range of aquatic habitats yet are reputedly able to produce this unique molecule via the same biosynthetic route (Shimizu 1993). Recent work on the saxitoxin-producing cyanobacterium *Cylindrospermopsis raciborskii* T3 identified a gene cluster responsible for saxitoxin synthesis; the corresponding bioinformatics data suggest that a portion of these genes have been acquired via horizontal gene transfer from phylogenetically diverse bacterial species (Kellmann et al. 2008). The same information currently is unavailable at the present time (December 2008) for dinoflagellates.

Elucidating the mode of action of the toxin on lower eukaryotes through expression profiling may provide additional insights into the ecology of the algae that produce it. Recent transcriptional profiling with the yeast *Saccharomyces cerevisiae* revealed genes commonly associated with metal homeostasis and sulfur metabolism as being significantly differentially expressed upon exposure to saxitoxin (as presented in Part II). This study sought to determine whether expression profiles obtained with *S. cerevisiae* upon exposure to saxitoxin could be extrapolated to the unicellular green alga *Chlamydomonas reinhardtii*. The genome of *C. reinhardtii* has recently been sequenced and annotated (Merchant et al. 2007), facilitating the undertaking of comparative transcriptomic studies with both lower eukaryotes and photosynthetic plankton such as the dinoflagellates and cyanobacteria capable of

toxin production. The following genes were selected for expression profiling in *C. reinhardtii* based upon their association with either copper homeostasis or heavy metal sequestration: thioredoxins m (*TRX m*) and h (*TRX h*), coproporphyrinogen III oxidase (*CPXI*), glutathione synthetase (*GSH2*), and cytochrome c6 (*CYC6*).

Microarray analysis identified multiple genes as being differentially expressed in *C. reinhardtii* following exposure to excess levels of copper, including several genes in the thioredoxin system and *CPXI* (Jamers et al. 2006). Thioredoxins (TRXs) are small ubiquitous proteins that contain conserved cysteine residues within their active site; one of their primary functions is the redox regulation of chloroplast enzymes (Eklund et al. 1991, Jacquot et al. 1997). While the recently-completed annotation of the *C. reinhardtii* genome identified novel thioredoxins (Merchant et al. 2007), *TRX m* and *TRX h* were examined in this study because the expression of both had previously been shown to be regulated by heavy metals (Lemaire et al. 1999). *CPXI*, which codes for an enzyme in the heme biosynthetic pathway, was shown to be repressed upon exposure to excess levels of copper (Jamers et al. 2006), in accordance with earlier reports in which its expression was shown to be regulated by copper at the level of transcription (Hill & Merchant 1995).

Lower eukaryotic organisms such as protists, algae, and even some yeasts, have different mechanisms of alleviating heavy metal toxicity. One of the best-described mechanisms involves intracellular chelation by glutathione (GSH) (Mendoza-Cozatl 2005). In this respect, GSH functions in ways similar to metallothioneins in *S. cerevisiae*, and both the *CUP1* and *CRS5* metallothioneins were shown to be significantly induced following exposure to saxitoxin (Part II and Part III). GSH synthesis requires the sulfur assimilation and cysteine biosynthetic pathways, and multiple genes involved in sulfur assimilation were also identified as significantly upregulated in *S. cerevisiae* upon exposure to saxitoxin. GSH is synthesized from cysteine via two consecutive reactions; as glutathione synthetase (*GSH2*) catalyzes the second step of GSH biosynthesis (Mendoza-Cozatl 2005), this gene was selected for expression profiling in this study.

Cytochrome c6 (*CYC6*) catalyzes photosynthetic electron transfer between cytochrome *b_{6-f}* and the photosystem I (PSI) reaction center (Ho et al. 1979) and can be used interchangeably with plastocyanin in this capacity. Expression of *CYC6* and plastocyanin are regulated by copper ion availability (Wood 1978, Hill & Merchant 1992, Li & Merchant 1992). While plastocyanin is the enzyme of choice in copper-replete cells, *CYC6* is induced only when copper levels are low. In this respect, it is similar to the FET3p of *S. cerevisiae* in that, while it is not directly involved in copper homeostasis, its activity serves as a reflection of intracellular copper ion availability. *CYC6* was chosen for analysis in this study to further explore the hypothesis that saxitoxin molecules disrupt copper ion uptake by either chelating copper ions at the surface of the cell wall or binding to plasma membrane enzymes involved in copper ion transport.

The objective of this study was to perform a comparative transcriptomic analysis between *S. cerevisiae* and *C. reinhardtii* in an effort to more clearly define the mechanism of action of the saxitoxin molecule. A specific set of genes was selected in *C. reinhardtii* based on (I) biological and/or molecular functional similarities with genes identified as differentially expressed in *S. cerevisiae* following exposure to saxitoxin and (II) previous reports in the literature of genes whose transcriptional regulation was influenced by copper levels. The hypothesis of this study was that the expression profiles generated with this pre-defined set of genes (*TRX m*, *TRX h*, *GSH2*, *CPX1*, and *CYC6*) in *C. reinhardtii* would be similar following exposure to copper or saxitoxin.

Methods and Materials

Chemicals

Saxitoxin was purchased from National Research Council Canada (NRCC) (CRM-STX-e). Four vials of approximately 65 µM concentration each were lyophilized, combined and re-suspended in deionized water (pH 5.5) at a final concentration of 100 µg ml⁻¹. Saxitoxin was stored at -20°C in between exposures, as they were not conducted in a single day. Copper sulfate was purchased from Sigma

Aldrich (St. Louis, MO). A 2 mM stock solution was prepared in sterile deionized water, filter-sterilized with a 0.2 μ M nitrocellulose filter, and stored in a sterile polycarbonate bottle. On the days of exposures, a 200 μ M working solution was freshly prepared in sterile deionized water.

Strains and Culture Conditions

Wild-type *Chlamydomonas reinhardtii* (CC 1690, provided by Dr. John Burges, University of Wisconsin-Milwaukee) was grown in TAP media (Harris 1989), with slight modifications: BG11 served as the trace metals solution, supplemented with FeCl₃ and EDTA. Cultures were maintained in 50 mL volumes in 125 mL flasks at 24°C under continuous light (approximately 75 μ E) (hereafter referred to as stock cultures).

Growth Curves

For cultures used in gene expression experiments, 30 mL cultures were inoculated with 1 mL stock culture. Growth of the 30 mL cultures was monitored by measuring the OD₇₅₀ every 6-8 hours using a TD-700 fluorometer (Turner Designs, Sunnyvale, CA). Upon reaching mid-exponential phase, 400 μ l of culture was placed in a 4 mL glass scintillation vial for exposure to saxitoxin or copper.

Saxitoxin and Copper Exposures

C. reinhardtii was exposed to 8 μ M copper sulfate or 16 μ M saxitoxin for 24 hours. The length of exposure was selected based on previous studies of *C. reinhardtii* copper exposures at these time points (Jamers et al. 2006). Saxitoxin and copper concentrations were chosen as these were the concentrations from which the yeast expression profiles were derived. Additionally, prior *C. reinhardtii* expression data was available in the literature at the 8 μ M copper concentration (Jamers et al. 2006), providing a platform with which to initiate these comparative transcriptomic studies. Controls consisted of sterile deionized water (pH 5.5). To alleviate variation in expression data across treatments due to culture differences, one biological replicate each for saxitoxin, copper, and the control was derived from a single 30 mL culture. Three biological replicates were performed for each exposure condition.

As saxitoxin was only available in very limited quantities due to its sensitive nature and Schedule I classification, conditions had to be optimized for performing gene expression experiments with minimal culture volumes. It was desired to employ a larger number of replicates with smaller culture volumes, from which meaningful biological data could be derived. Therefore, additional control exposures were performed in order to provide samples with which to optimize the protocols for total RNA extraction, DNase treatment, and real-time RT-PCR reactions.

Cell Harvesting

The 400 μ l cultures were transferred to sterile 1.5 mL low-binding microfuge tubes and centrifuged at 16,000g for 10 min at 4°C. Cells were washed in 300 μ l nuclease-free water and centrifuged a second time at the same settings. The supernatant was decanted and the pellet placed immediately in liquid nitrogen. Samples were stored at -80°C until RNA extraction.

RNA Extraction

Two protocols were initially compared to determine the optimal method for total RNA extraction: the commercially-available RNeasy Plant Kit following the manufacturer's instructions (Qiagen, Valencia, CA) and the hot acid phenol method (Causton et al. 2001). Extraction yields were considerably higher with the hot acid phenol method than with the RNeasy Plant kit (average total RNA concentration 34.3 ± 12.3 ng μ l⁻¹ versus 5.85 ± 0.43 ng μ l⁻¹, respectively), and so this method was selected for subsequent RNA extractions. Multiple steps in the hot acid phenol protocol were then subject to modifications with the goal of optimizing total RNA concentration and purity levels. These modifications included: (I) initial SDS concentrations ranging from 0.5%-3%; (II) the inclusion of phase-loc during the phenol extraction steps; and (III) the use of sodium chloride rather than sodium acetate during the ethanol precipitation step.

Published methods have utilized SDS concentrations ranging from 1.25-3% for *C. reinhardtii* cell lysis (Dobberstein et al. 1977, Howell et al. 1977, Schloss et al. 1984); however, it has been noted that sodium chloride should be substituted for sodium acetate in RNA extractions utilizing SDS, as the SDS will then remain in

solution during the ethanol wash step

(<http://arbl.cvmbs.colostate.edu/hbooks/genetics/biotech/manip/conc.html>). For these reasons, a range of SDS concentrations were tested in the cell lysis step, with accompanying ethanol precipitations utilizing both sodium chloride and sodium acetate. Phase-lok was included in several of the extractions, as this compound creates a more distinct partition between aqueous and organic phases, aiding in the extraction of small volumes (the aqueous phase in these extractions was typically 200 μ l). Thus, an optimized RNA extraction protocol was developed for the purposes of this study and is reported here.

Total RNA was extracted from frozen cell pellets following the hot acid phenol protocol (Causton et al. 2001), with modifications. To the frozen cell pellet was added equal volumes of pre-warmed phenol:chloroform:isoamylalcohol (125:24:1 Ambion) and TES (10mM Tris pH 7.5, 10mM EDTA), with the final concentration of SDS increased from 0.5% to 2%. Cells were incubated at 65°C for 40 min, with vortexing every 10 min. RNA was extracted twice with acid phenol; at each extraction step, phase-lok was added to the tubes to facilitate physical separation of the aqueous and organic phases. Following extraction with 24:1 chloroform:isoamyl alcohol (Sigma Aldrich, St. Louis, MO), 22 μ l 3 M sodium acetate (equal to 1/10 the overall sample volume) was added and samples vortexed thoroughly. Six hundred fifty microliters (3x that of the total sample volume) of ice-cold ethanol was then added and samples vortexed for 2 min. Total RNA was then precipitated in a dry ice/ethanol slurry for 30 minutes. Following centrifugation (14,000g, 15 min, 4°C), total RNA was washed in 440 μ l 70% ethanol (a volume 2x that of the original sample). Samples were placed in a dry ice/ethanol slurry for 10 min prior to the final centrifugation (14,000g, 5 min, room temperature). Total RNA was re-suspended in 30 μ l nuclease-free water. The total RNA concentration and purity of each sample were measured with the Nanodrop-1000 (Nanodrop Technologies Inc., Wilmington, DE). Samples were then stored at -80°C.

DNase Treatment

Though in theory DNA should partition into the organic phase during the hot acid phenol extraction, it was determined that samples were still contaminated with small amounts of DNA. As the real-time RT-PCR reaction is sensitive enough to detect a single copy of a specific transcript (Wong & Medrano 2005) even trace amounts of DNA can produce erroneous results. Therefore, samples were then subject to a DNase treatment.

The additional control exposures described above served as the templates with which the DNase treatment conditions were optimized. Several different DNase treatment protocols were examined, including the use of an MnSO₄-based buffer (final concentration 450 µM) (Wang et al. 2002) or the commercially-available Buffer RDD (Qiagen, Valencia, CA) Samples were incubated for 30 min or 1 h at room temperature or 37°C. The success of the various treatments was determined by measurement with the Nanodrop-1000 and by performing “no RT” reactions.

The optimal treatment consisted of 1 µl (~1.25 Kunitz units) DNase (Qiagen, Valencia, CA) with Buffer RDD with an incubation time of 1 h at room temperature, followed by heat-inactivation of the enzyme at 70°C for 10 min. Based on the results of the DNase treatment optimization, aliquots of samples used in subsequent real-time RT-PCR were subject to DNase digestion in reactions consisting of 14 µl RNA extract, 1 µl DNase, 10x Buffer RDD, and nuclease-free water added to a final volume of 17 µl. Prior to real-time RT-PCR, samples were diluted to a concentration of 6 ng ul⁻¹.

Real-Time Reverse-Transcriptase PCR

Real-Time RT-PCR Assays

Real-time RT-PCR reactions based on the Taqman® probe methodology were used to examine changes in *C. reinhardtii* gene expression following exposure to saxitoxin or copper. Gene-specific primers and probe targeted an approximately 100 bp region of the coding sequence of each gene. Genomic and coding sequences were obtained from GenBank (www.ncbi.nlm.gov), and primers and/or probe were designed to span exon-exon boundaries when possible. Primers and probe were

designed using the Primer3 software, following the guidelines of Dorak (www.dorak.info/genetics/realtime.html), with an annealing temperature of 60°C. Table V-1 lists the primer/probe sequences, GenBank accession number, and brief description of each gene. Probes and forward primers were examined for potential secondary structures at 60°C, and the reverse primers at 50°C, using Mfold (Zuker 2003). The potential for self and cross dimer formation was examined for each of the primer sets using an online oligonucleotide analysis tool (<https://www.operon.com/oligos/toolkit.php>). Self-complementarity was determined using the oligonucleotide properties calculator (<http://www.basic.northwestern.edu/biotools/oligocalc.html>). Oligonucleotide primers and 5'(FAM)-3'BHQ probes were obtained from Biosearch Technologies (Novato, CA).

The Quantitect Probe RT-PCR kit (Qiagen, Valencia, CA) was used for all assays. Reactions consisted of 12.5 µl 2x Quantitect Probe RT-PCR Master Mix, 600 nm each forward and reverse primer, 200 nm probe, 0.25 µl QuantiTect RT Mix, 5 µl of template, and adjusted to a final volume of 25 µl with nuclease-free water. Template consisted of DNase-treated total RNA extracts diluted to a final concentration of 6ng µl⁻¹, so that 30 ng total RNA was used in each reaction. The following protocol was used for all assays: 50°C for 30 minutes, 95°C for 15 minutes, and 45 cycles of denaturing at 94°C for 15 seconds and annealing/extension at 60°C for 1 min. Reactions were performed in triplicate in a DNA engine equipped with the Chromo4 detector (MJ Research Inc., Waltham, MA).

PCR Efficiencies

The PCR efficiency of each assay was calculated using the program LinRegPCR (Ramakers et al. 2003). Additionally, the PCR efficiencies of the reference gene (*RBC L*) and a target gene (*TRX m*) were compared by determining how the ΔC_T of the two assays varied over a dilution series by plotting the ΔC_T versus log input RNA as described in the literature (Livak & Schmittgen 2001). With this method, if the absolute value of the slope is close to zero (<0.1), the efficiencies of the target and reference genes are considered similar. The absolute slope was

Table V-1. Primer and probe sequences and function of gene examined with real-time RT-PCR. Accession number refers to the GenBank number from which the sequences were obtained.

Gene ID	Description	Accession Number	Primer/Probe Sequence
<i>RBC L</i>	ribulose 1,5-bisphosphate carboxylase	J01399	F: 5'-CCTTCGTATTCCACCTGCTT R: 5'-CAACCTAAAAGACCACGACCA 5'-(FAM)ACATTCGTAGGTCCTCCACACGGTATTCA(BHQ)
<i>TRX m</i>	thioredoxin (chloroplast)	X80888	F: 5'-CCCGTCCTTGTGGATTTCT R: 5'-TTCAGCTTCACGCACTTGAG 5'-(FAM)CGAGATTGCGGGCGAGTACAAGGATAA(BHQ)
<i>TRX h</i>	thioredoxin (cytosol)	X80887	F: 5'-TTGTCGACTTCACTGCTACGT R: 5'-ATCGACCTTCAGGAAGATGAC 5'-(FAM)CTGTTTGAGACGCTGAGCAACGACTATG(BHQ)
<i>CPX1</i>	coproporphyrinogen III oxidase	XM_001701677	F: 5'-CCCACCATGCACTTCAACTA R: 5'-ACATAGCTGGGGGTGATGTC 5'-(FAM)CTTCGAGACTGAGGAGTGGAACGGCATC(BHQ)
<i>GSH2</i>	glutathione synthetase	XM_001691491	F: 5'-GTGCTTCTCACGTCCGCAAT R: 5'-GCATGAGCCAGAGAACACAA 5'-(FAM)CCGCATTGCTGTTCTTTGCAAACCTCTTAAA(BHQ)
<i>CYC6</i>	cytochrome c6	M67448	F: 5'-CGAGAAGACGCTGGACAAG R: 5'-CTTGCCATTCTCCACCTGAT 5'-(FAM)AGTACCTGGATGGCGGCTTCAAGGT(BHQ)

determined to be 0.02, indicating that the PCR efficiencies of *RBC L* and *TRX m* were similar (Figure V-1, Appendix I). The PCR efficiencies of *RBC L* and *TRX m* were also similar as calculated by the LinRegPCR program (Table V-2, Appendix I), indicating that the two methods yielded comparable results with regards to determination of PCR efficiency. Therefore, for the purposes of this study, the PCR efficiencies of each assay were determined via the LinRegPCR program; these values were then used to decide on an appropriate method of relative quantification.

Data Normalization and Analysis

Relative quantification using the standard curve method (Livak 1997) was used to examine gene expression changes in *C. reinhardtii* following exposure to excess copper or saxitoxin. This method typically requires the preparation of a standard curve for each assay. However, similar PCR efficiencies among reference and target gene assays allows for the creation of a single standard curve (Livak 1997). As PCR efficiencies were shown to be comparable among all genes (Table V-2, Appendix I), one standard curve was employed to determine the differential expression of the target genes (Figure V-2, Appendix I). With this method, the amount of target is determined from the standard curve and divided by the target quantity of the “calibrator” (i.e. control). The calibrator becomes the 1x sample, and all other target quantities are expressed relative to this amount as *n*-fold changes. Data are further normalized to a reference gene through the use of the standard curve, with each of the normalized target values then divided by the calibrator normalized target value to determine relative expression levels.

Statistics

The independent samples *t*-test was performed on the *RBC L* quantities of treated and control samples as derived from the standard curve using SPSS v.15 (Chicago, IL). There was no significant difference in quantity, indicating that *RBC L* expression was not affected by saxitoxin or copper exposures, and thus an appropriate reference gene.

With the standard curve method, when target and reference gene reactions are performed in separate tubes, the original protocol instructs that the normalized target

gene value be determined by dividing the mean target gene quantities by the mean reference gene quantities obtained via the standard curve (Livak 1997). This ultimately results in the target gene quantity being reduced to a single value and eliminates the opportunity for statistical analysis. However, recent studies (Sehringer et al. 2005, Cikos et al. 2007) have performed statistical analyses on values obtained using the standard curve method. Thus, in order to assess the significance of the levels of gene expression recorded in this study, a statistical analysis was performed on the data of each of the target genes. The target gene quantity of each treated sample was first normalized to its respective reference gene quantity; this same normalization step was also applied to the control samples. The independent samples *t*-test was then applied to the normalized quantities of the treated and control samples; the Mann-Whitney U-test was used in cases where the data were not normally distributed. The average linear fold-change was then determined by dividing the mean normalized target gene quantity of the treated samples by the mean normalized target gene quantity of the controls. The fold-change range for each target gene was then calculated using the equation described previously for *S. cerevisiae* expression profiling (Part II).

Results

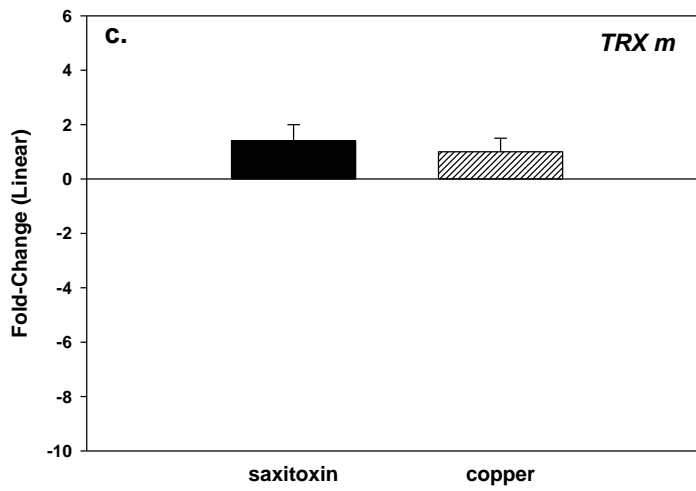
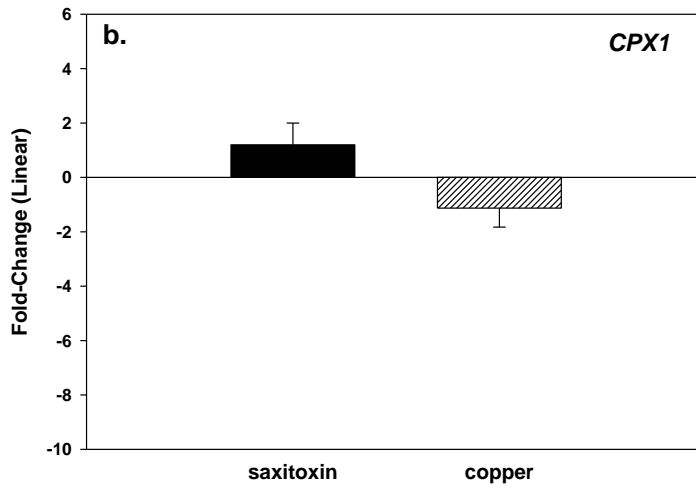
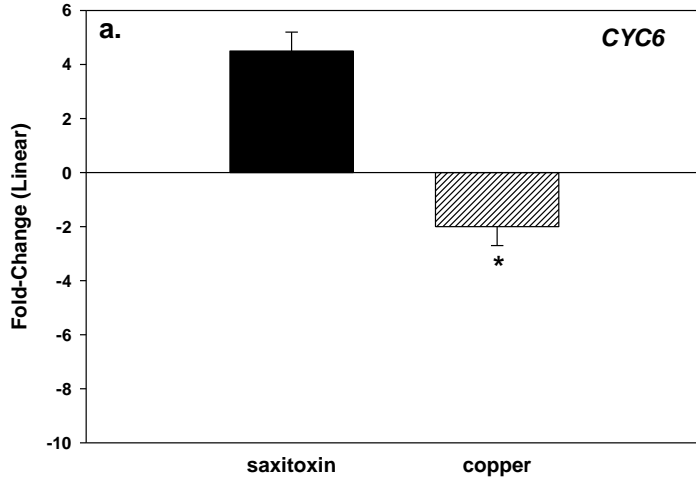
Growth Curve

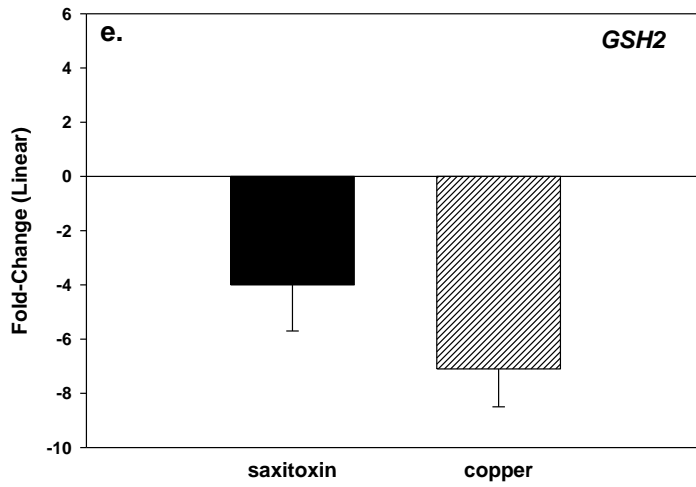
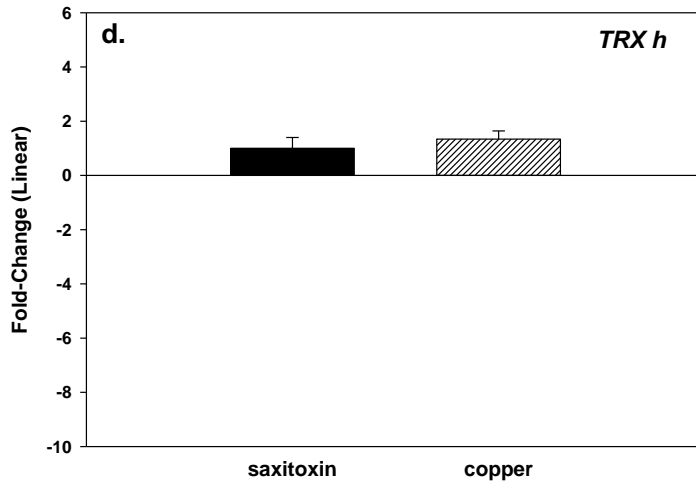
All cultures used for gene expression experiments displayed similar growth, reaching mid-exponential phase in 2-3 days (data not shown).

Gene Expression Profiling

Overall, different expression profiles were obtained for *C. reinhardtii* following 24 hour exposure to either 8 μ M copper or 16 μ M saxitoxin. Of the five genes profiled, *CYC6*, *CPX1*, *TRX m*, and *TRX h* displayed contrasting patterns in regulation between the saxitoxin and copper treatments, while *GSH2* regulation was similar between the two treatments (Figure V-3, a-e). *CYC6* was significantly repressed approximately 2-fold following copper exposure but showed a 4.5-fold level of induction in saxitoxin treatments (Figure V-3a). It is prudent to note that

Figure V-3. Comparison in average gene expression levels in *C. reinhardtii* following exposure to 16 μ M saxitoxin and 8 μ M copper sulfate: (a.) *CYC6* and (b.) *CPX1* displayed coordinated levels of expression, as both were upregulated following exposure to saxitoxin and repressed following exposure to copper; (c.) *TRX m* was upregulated in saxitoxin treatments but remained unchanged in copper treatments; (d.) *TRX h* remained unchanged in saxitoxin treatments but was mildly induced following exposure to copper; (e.) *GSH2* was repressed in both types of treatments. * indicates significance difference (one-tailed $p < 0.05$).





while the level of induction of *CYC6* in response to saxitoxin was not statistically significant ($p=0.06$), it is anticipated that re-analysis with additional samples will result in a statistically significant value. *CPXI* was down-regulated in copper exposures, similar to that observed in previous copper expression profiling experiments (Jamers et al. 2006). This gene was slightly upregulated following saxitoxin exposures (Figure V-3b), exhibiting a trend previously reported in the literature of coordinate expression of *CPXI* with that of *CYC6* (Hill & Merchant 1995). *TRX m*, which codes for the chloroplast isoform of thioredoxin, remained unchanged following exposure to copper but was upregulated approximately 1.4-fold in saxitoxin treatments (Figure V-3c). *TRX h*, the cytosol isoform of thioredoxin, exhibited a small level of induction (1.34-fold) in copper treatments but remained unchanged following exposure to saxitoxin (Figure V-3d).

The expression of *GSH2* displayed a similar trend following both saxitoxin and copper exposures, as it was repressed approximately 4-fold and 7-fold, respectively (Figure V-3e). However, this transcript was present in very low copies, as evidenced by high average C_T values (data not shown). Additionally, the values obtained for *GSH2* displayed greater variation in comparison to genes present at greater transcript levels, indicative of the Monte Carlo effect on template concentration: the lower the abundance of any template, the less likely its true abundance will be displayed in the amplified product (Bustin & Nolan 2004). This follows the trend noted in the literature of better precision at higher copy numbers (Morrison et al. 1998); thus, the levels of repression obtained here for *GSH2* should be interpreted with caution.

Discussion

Though the expression profiles obtained with *C. reinhardtii* following exposure to saxitoxin and excess copper are not similar, integrating the comparison of these profiles with those obtained for *S. cerevisiae* may provide insights into the proposed mechanism of the saxitoxin molecule on lower eukaryotic cells. In particular, the expression profiles of *CYC6* and *CPXI* in *C. reinhardtii* and that of the

multicopper oxidase Fet3 in *S. cerevisiae* suggest that saxitoxin is complexing with copper ions at the cell surface or blocking their transport into the cell in some manner. In some photosynthetic organisms, electron transfer from cytochrome *b_{6-f}* to photosystem I can be catalyzed effectively by either plastocyanin (a copper protein) under adequate copper levels or cytochrome *c6* (a heme protein) during copper-deficient conditions (Wood 1978), with enzyme selection based solely on copper availability (Hill et al. 1991, Li & Merchant 1992). At the level of transcription, an inverse relationship has been shown to exist between the abundance of *CYC6* mRNA and the availability of copper ions to the cell (Hill & Merchant 1992). In this study, expression of the *CYC6* gene of *C. reinhardtii* was elevated approximately 4.5-fold following exposure to saxitoxin. While plastocyanin expression was not examined, the induction of *CYC6* suggests low internal copper levels.

The slight induction of *CPX1* upon saxitoxin exposure provides further support for the concept of saxitoxin altering copper homeostasis through copper chelation or the blocking of copper ions at the cell surface, and thus creating low levels of copper within the cell's internal environment. *CPX1* has been shown to be upregulated in copper deficient cells, with expression regulated by copper at the level of transcription (Hill & Merchant 1995). *CPX1* and *CYC6* expression profiles following saxitoxin exposure exhibited a previously-defined pattern, as *CPX1* expression been shown to parallel that of *CYC6* in response to copper availability (Hill & Merchant 1995).

Previous experiments (Part III) determined that the expression of the *FET3* gene in *S. cerevisiae* remained unchanged following exposure to excess copper, yet was significantly repressed in saxitoxin treatments. The Fet3 protein specifically requires four copper ions for its activity (Taylor et al. 2005); thus, under conditions of copper excess, the requirement of copper ions is satisfied. Following saxitoxin exposures in minimal media, *FET3* was repressed 3.5-fold. One of the possibilities for repression may be a lack of copper ions for holoenzyme formation, as the copper transporter *CTR1* - from which Fet3p receives its copper ions - was also down-regulated following saxitoxin exposure. The Ctr1p structural design suggests a

functional model similar to that of the potassium channel, with the presence of a particular glycine motif contributing to the selectivity and gating of Ctr1p (Aller & Unger 2006). The molecular target of saxitoxin in mammalian cells is the sodium channel; it binds with high affinity to the alpha subunit, yet does not penetrate across the channel into the cell. As suggested in Part III, saxitoxin may be binding to the selectivity filter of the copper transporter, preventing the permeation of copper ions across the membrane.

Phytoplankton classes exhibit a range of sensitivities to copper in their environment; of these groups, cyanobacteria are the most sensitive (Le Jeune et al. 2006). Several species of cyanobacteria are documented toxin-producers, in addition to dinoflagellates from the genera *Alexandrium*, *Gymnodinium*, and *Pyrodinium*. Copper sulfate, and, more recently, copper glutamate, have commonly been used as algicides to treat water bodies such as lakes and dams that serve as water supply reservoirs (Haughey et al. 2000, Baptista & Vasconcelos 2006, Li et al. 2008). It has recently been demonstrated that the targets of copper sulfate and copper glutamate in *Alexandrium* spp. are the plasma membranes (cell, chloroplast, and mitochondria) (Li et al. 2008) (Figure V-4). It is an intriguing coincidence that one of the primary targets of saxitoxin in *S. cerevisiae* is the copper transporter, located in the plasma membrane, and the target of copper sulfate in dinoflagellates is the plasma membrane. Perhaps these toxins function in preventing the uptake of excess copper into the cell, such as that introduced by an algicidal agent. Toxin production would function as a resistance mechanism, leading to the repopulation of the cyanobacterial or dinoflagellate species, albeit now with an increased amount of toxin in the water body. Cyanobacterial species targeted by this treatment are able to acquire resistance to it, as copper-resistant mutants have been shown to arise in the toxic cyanobacterium *Microcystis aeruginosa* (García-Villada et al. 2004).

Assimilating the profiles of the *FET3* gene in *S. cerevisiae* and *CYC6* and *CPXI* in *C. reinhardtii* allows for a second alternative as to the function of saxitoxin. The possibility exists that the eco-evolutionary role of some algal toxins may be to function as metal chelators. Complexation between microcystins - peptide toxins

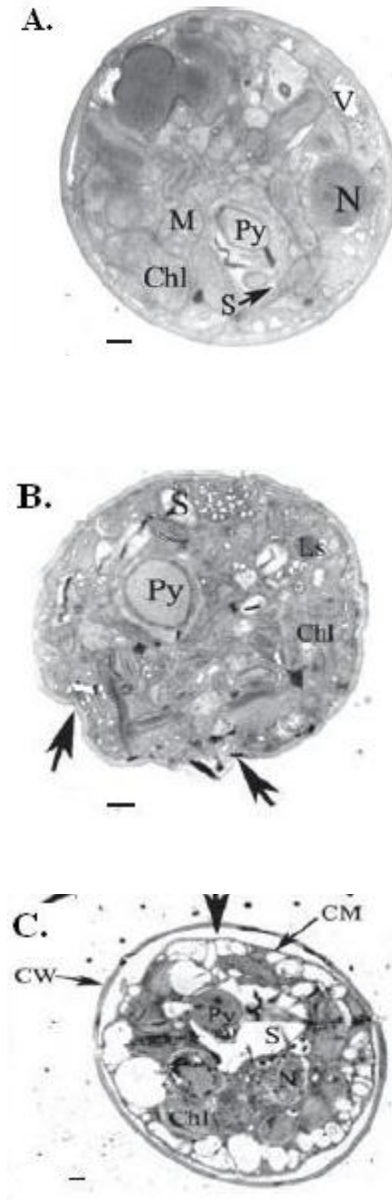


Figure V-4. Copper sulfate and copper glutamate target the plasma membranes in *Alexandrium* spp. TEM images illustrating (A.) control exposures, in which cell membranes are smooth and intact; (B.) in the presence of copper glutamate, the cell wall and plasma membrane became invaginated and started to break apart (indicated by arrows); and (C.) in the presence of copper sulfate, the ultrastructural changes were not as great as with copper glutamate, but still resulted in a shrunken plasma membrane, with space in between the membrane and cell wall (arrows). Scale bar is 1 μm in each. Images taken from Li et al. 2008.

produced by several species of cyanobacteria - and copper and zinc has been verified using analytical techniques (Humble et al. 1997, Saito et al. 2008). The ability of cyanobacteria to produce strong copper-binding ligands has also been demonstrated, though the structure of these ligands has yet to be determined (Wiramanaden et al. 2008). The potential exists for metal complexation to occur within the amino, carboxyl, nitrogen, and oxygen groups of the microcystin molecule (Crist et al. 1981). Though a non-protein and much smaller than microcystins, saxitoxin has similar groups that could also serve to function in the coordination binding of copper ions. In the experiments conducted with *S. cerevisiae* and *C. reinhardtii*, both of which possessed cell walls during the time of saxitoxin exposure, it can be hypothesized that proton-active functional groups on the cell surface (i.e. carboxyls, hydroxyls, amines) bound the saxitoxin, in effect forming a saxitoxin-ligand surface. This process would be similar to the deprotonation of metal ions and subsequent formation of metal-ligand surface complexes shown to occur in algae and cyanobacteria (Crist et al. 1981, Baptista & Vasconcelos 2006).

Microcystins are not the only toxins that appear to be associated with metal ions in some capacity. Studies examining the effects of copper and iron on domoic acid production in *Pseudo-nitzschia* species found that domoic acid production was induced by iron-deficient or excessive copper conditions (Maldonado et al. 2002). Additionally, copper supplementation has been shown to result in an increase in domoic acid production in *P. australis* (Rhodes et al. 2006). Taken collectively, these studies suggest a correlation between metal –particularly copper – levels in the environment and toxin production.

Appendix I

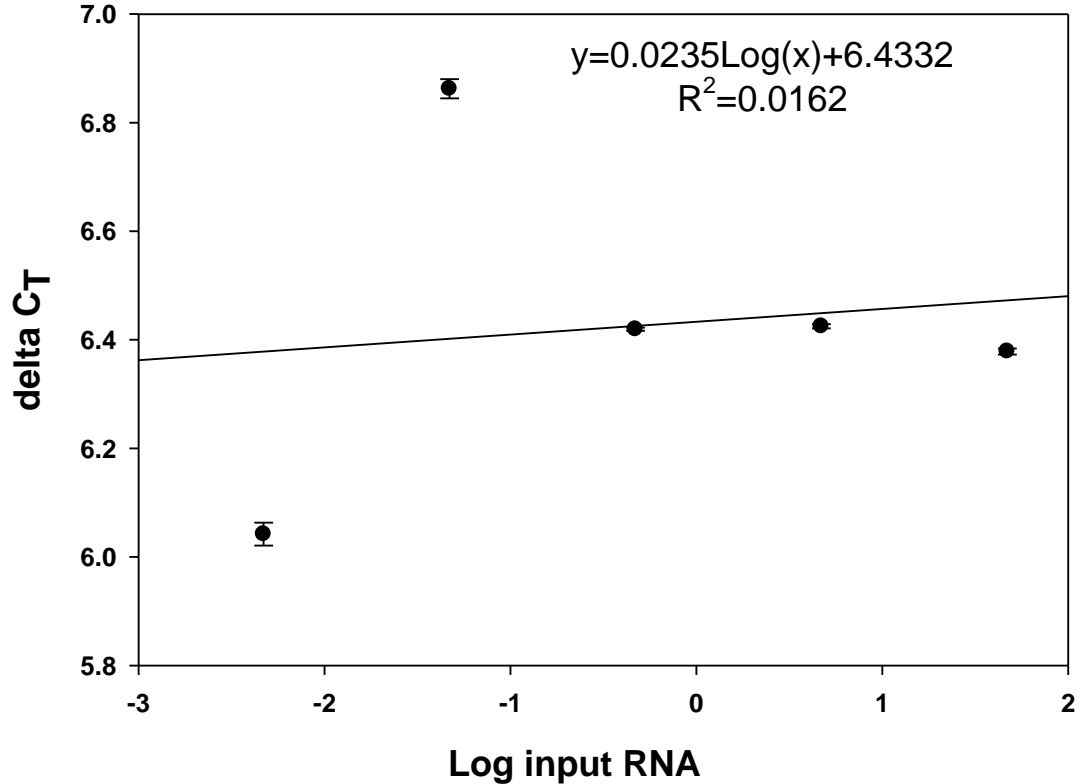


Figure V-1. Comparison of PCR efficiencies between *RBC L* and *TRX m* assays. The amplification efficiencies of a target gene (*TRX m*) and the reference gene (*RBC L*) were compared using real-time RT-CPR with Taqman detection. Template RNA was serially diluted over a range spanning five orders of magnitude. The slope resulting from the plot of the ΔC_T (C_T ref – C_T target) versus log input RNA was approximately 0.02, indicating comparable amplification efficiencies between reference and target gene assays.

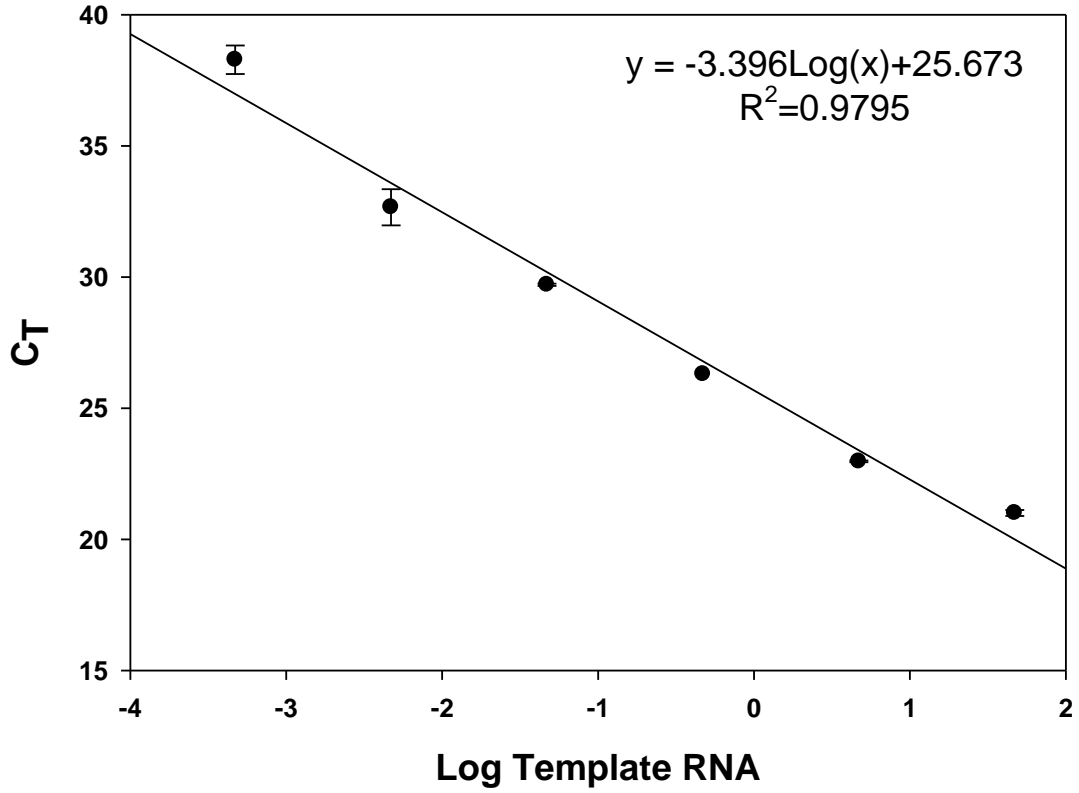


Figure V-2. Standard curve used in relative quantification of gene expression in *C. reinhardtii*. The standard curve was generated using the *RBC L* primers and probe. Dilutions spanned a 6 order of magnitude range. Error bars represent standard deviation of duplicate reactions.

Table V-2. Average PCR efficiencies for each assay as calculated with LinRegPCR (Ramakers et al. 2003).

Target ID	Saxitoxin PCR <i>E</i>	Control PCR <i>E</i>	Copper PCR <i>E</i>
<i>RBC L</i>	1.7	1.7	1.7
<i>CPX1</i>	1.56	1.5	1.5
<i>TRX m</i>	1.63	1.6	1.6
<i>GSH2</i>	1.64	1.63	1.69
<i>TRX h</i>	1.74	1.76	1.73
<i>CYC6</i>	1.63	1.6	1.5

References

- Aller SG, Unger VM (2006) Projection structure of the human copper transporter CTR1 at 6-Å resolution reveals a compact trimer with a novel channel-like architecture. *Proceedings of the National Academy of Sciences of the United States of America* 103:3627-3632
- Azanza MPV, Azanza RV, Vargas VMD, Hedreyda CT (2006) Bacterial endosymbionts of *Pyrodictum bahamense* var. *compressum*. *Microbial Ecology* 52:756-764
- Baptista MS, Vasconcelos MT (2006) Cyanobacteria metal interactions: requirements, toxicity, and ecological implications. *Crit. Rev. Microbiol.* 32:127-137
- Bustin SA, Nolan T (2004) Pitfalls of Quantitative Real-Time Reverse-Transcription Polymerase Chain Reaction. *J Biomol Tech* 15:155-166
- Castro D, Vera D, Lagos N, Garcia C, Vasquez M (2004) The effect of temperature on growth and production of paralytic shellfish poisoning toxins by the cyanobacterium *Cylindrospermopsis raciborskii* C10. *Toxicon* 44:483-489
- Causton HC, Ren B, Koh SS, Harbison CT, Kanin E, Jennings EG, Lee TI, True HL, Lander ES, Young RA (2001) Remodeling of Yeast Genome Expression in Response to Environmental Changes. *Mol. Biol. Cell* 12:323-337
- Cikos S, Bukovska A, Koppel J (2007) Relative quantification of mRNA: comparison of methods currently used for real-time PCR data analysis. *Bmc Molecular Biology* 8
- Crist RH, Oberholser K, Shank N, Ming N (1981) Nature of bonding between metallic ions and algal cell walls. *Environ. Sci. Technol.* 15:1212-1217
- Dobberstein B, Blobel G, Chua NH (1977) In vitro synthesis and processing of a putative precursor for the small subunit of ribulose-1,5-bisphosphate carboxylase of *Chlamydomonas reinhardtii*. *Proceedings of the National Academy of Sciences of the United States of America* 74:1082-1085
- Eklund H, Gleason FK, Holmgren A (1991) Structural and functional relations among thioredoxins of different species. *Proteins: Structure, Function, and Genetics* 11:13-28

- García-Villada L, Rico M, Altamirano M, Sánchez-Martín L, López-Rodas V, Costas E (2004) Occurrence of copper resistant mutants in the toxic cyanobacteria *Microcystis aeruginosa*: characterisation and future implications in the use of copper sulphate as algaecide. *Water Research* 38:2207-2213
- Gedaria AI, Luckas B, Reinhardt K, Azanza RV (2007) Growth response and toxin concentration of cultured *Pyrodictum bahamense* var. *compressum* to varying salinity and temperature conditions. *Toxicon* 50:518-529
- Harris E (1989) The *Chlamydomonas* Sourcebook: A Comprehensive Guide to Biology and Laboratory Use, Vol. Academic Press, San Diego, CA
- Haughey MA, Anderson MA, Whitney RD, Taylor WD, Losee RF (2000) Forms and fate of Cu in a source drinking water reservoir following CuSO₄ treatment. *Water Research* 34:3440-3452
- Hill KL, Li HH, Singer J, Merchant S (1991) Isolation and structural characterization of the *Chlamydomonas reinhardtii* gene for cytochrome c6. Analysis of the kinetics and metal specificity of its copper-responsive expression. *J. Biol. Chem.* 266:15060-15067
- Hill KL, Merchant S (1992) In vivo competition between plastocyanin and a copper-dependent regulator of the *Chlamydomonas reinhardtii* cytochrome c6 gene. *Plant. Physiol.* 100:319-326
- Hill KL, Merchant S (1995) Coordinate expression of coproporphyrinogen oxidase and cytochrome c6 in the green alga *Chlamydomonas reinhardtii* in response to changes in copper availability. *EMBO J.* 14:857-865
- Ho KK, Ulrich E, Krogmann DW, Gomez-Lojero C (1979) Isolation of photosynthetic catalysts from cyanobacteria. *Biochim. Biophys. Acta* 545:236-248
- Howell SH, Heizmann P, Gelvin S, Walker LL (1977) Identification and Properties of the Messenger RNA Activity in *Chlamydomonas reinhardtii* Coding for the Large Subunit of D-ribulose-1,5-bisphosphate Carboxylase. *Plant Physiol.* 59:464-470
- <http://arbl.cvmbs.colostate.edu/hbooks/genetics/biotech/manip/conc.html> (as of December 2008)
- <http://www.basic.northwestern.edu/biotools/oligocalc.html> (as of December 2008)
- <https://www.operon.com/oligos/toolkit.php> (as of December 2008)

- Hu HH, Chen WD, Shi YJ, Cong W (2006) Nitrate and phosphate supplementation to increase toxin production by the marine dinoflagellate *Alexandrium tamarense*. *Marine Pollution Bulletin* 52:756-760
- Humble AV, Gadd GM, Codd GA (1997) Binding of copper and zinc to three cyanobacterial microcystins quantified by differential pulse polarography. *Water Research* 31:1679-1686
- Jacquot J-P, Lancelin J-M, Meyer Y (1997) Tansley Review No.94. Thioredoxins: Structure and Function in Plant Cells. *New Phytologist* 136:543-570
- Jamers A, Van der Ven K, Moens L, Robbens J, Potters G, Guisez Y, Blust R, De Coen W (2006) Effect of copper exposure on gene expression profiles in *Chlamydomonas reinhardtii* based on microarray analysis. *Aquatic Toxicology* 80:249-260
- Kellmann R, Mihali TK, Jeon YJ, Pickford R, Pomati F, Neilan BA (2008) Biosynthetic intermediate analysis and functional homology reveal a saxitoxin gene cluster in cyanobacteria. *Applied and Environmental Microbiology* 74:4044-4053
- Le Jeune A-H, Charpin M, Deluchat V, Briand J-F, Lenain J-F, Baudu M, Amblard C (2006) Effect of copper sulphate treatment on natural phytoplanktonic communities. *Aquatic Toxicology* 80:267-280
- Lemaire S, Keryer E, Stein M, Schepens I, Issakidis-Bourguet E, Gerard-Hirne C, Miginiac-Maslow M, Jacquot J-P (1999) Heavy Metal Regulation of Thioredoxin Gene Expression in *Chlamydomonas reinhardtii*. *Plant Physiol.* 120:773-778
- Leong SCY, Murata A, Nagashima Y, Taguchi S (2004) Variability in toxicity of the dinoflagellate *Alexandrium tamarense* in response to different nitrogen sources and concentrations. *Toxicon* 43:407-415
- Li H, Miao J, Cui F, Li G (2008) Surfactant promotion of the inhibitory effects of cupric glutamate on the dinoflagellate *Alexandrium*. *J. Phycol.* 44:1364-1371
- Li HH, Merchant S (1992) Two metal-dependent steps in the biosynthesis of *Scenedesmus obliquus* plastocyanin. Differential mRNA accumulation and holoprotein formation. *J. Biol. Chem.* 267:9368-9375
- Livak KJ (1997) Relative quantitation of gene expression. User bulletin #2 for the ABI PRISM 7700 sequence detection system. Applied Biosystems, Foster City, CA, USA

- Livak KJ, Schmittgen TD (2001) Analysis of Relative Gene Expression Data Using Real-Time Quantitative PCR and the 2- $\Delta\Delta$ CT Method. *Methods* 25:402-408
- Maas EW, Latter RM, Thiele J, Waite AM, Brooks HJL (2007) Effect of multiple antibiotic treatments on a paralytic shellfish toxin-producing culture of the dinoflagellate *Alexandrium minutum*. *Aquatic Microbial Ecology* 48:255-260
- Maldonado M, T., Hughes MP, Rue EL, Wells ML (2002) The effect of Fe and Cu on growth and domoic acid production by *Pseudo-nitzschia multiseries* and *Pseudo-nitzschia australis*. *Limnol. Oceanogr.* 47:515-526
- Mendoza-Cozatl D, Loza-Tavera, H., Hernandez-Navarro, A., Moreno-Sanchez, R. (2005) Sulfur assimilation and glutathione metabolism under cadmium stress in yeasts, protists, and plants. *FEMS Microbiology Reviews* 29:653-671
- Merchant SS, Prochnik SE, Vallon O, Harris EH, Karpowicz SJ, Witman GB, Terry A, Salamov A, Fritz-Laylin LK, Marechal-Drouard L, Marshall WF, Qu LH, Nelson DR, Sanderfoot AA, Spalding MH, Kapitonov VV, Ren QH, Ferris P, Lindquist E, Shapiro H, Lucas SM, Grimwood J, Schmutz J, Cardol P, Cerutti H, Chanfreau G, Chen CL, Cognat V, Croft MT, Dent R, Dutcher S, Fernandez E, Fukuzawa H, Gonzalez-Balle D, Gonzalez-Halphen D, Hallmann A, Hanikenne M, Hippler M, Inwood W, Jabbari K, Kalanon M, Kuras R, Lefebvre PA, Lemaire SD, Lobanov AV, Lohr M, Manuell A, Meir I, Mets L, Mittag M, Mittelmeier T, Moroney JV, Moseley J, Napoli C, Nedelcu AM, Niyogi K, Novoselov SV, Paulsen IT, Pazour G, Purton S, Ral JP, Riano-Pachon DM, Riekhof W, Rymarquis L, Schroda M, Stern D, Umen J, Willows R, Wilson N, Zimmer SL, Allmer J, Balk J, Bisova K, Chen CJ, Elias M, Gendler K, Hauser C, Lamb MR, Ledford H, Long JC, Minagawa J, Page MD, Pan JM, Pootakham W, Roje S, Rose A, Stahlberg E, Terauchi AM, Yang PF, Ball S, Bowler C, Dieckmann CL, Gladyshev VN, Green P, Jorgensen R, Mayfield S, Mueller-Roeber B, Rajamani S, Sayre RT, Brokstein P, Dubchak I, Goodstein D, Hornick L, Huang YW, Jhaveri J, Luo YG, Martinez D, Ngau WCA, Otilar B, Poliakov A, Porter A, Szajkowski L, Werner G, Zhou KM, Grigoriev IV, Rokhsar DS, Grossman AR (2007) The *Chlamydomonas* genome reveals the evolution of key animal and plant functions. *Science* 318:245-251
- Morrison TB, Weis JJ, Wittwer CT (1998) Quantification of low-copy number transcripts by continuous SYBR Green I monitoring during amplification. *Biotechniques* 24:954-962
- Navarro JM, Munoz MG, Contreras AM (2006) Temperature as a factor regulating growth and toxin content in the dinoflagellate *Alexandrium catenella*. *Harmful Algae* 5:762-769

- Ramakers C, Ruijter JM, Deprez RHL, Moorman AFM (2003) Assumption-free analysis of quantitative real-time polymerase chain reaction (PCR) data. *Neuroscience Letters* 339:62-66
- Rhodes L, Selwood A, McNabb P, Briggs L, Adamson J, van Ginkel R, Laczka O (2006) Trace metal effects on the production of biotoxins by microalgae. *African Journal of Marine Science* 28:393-397
- Saito K, Sei Y, Miki S, Yamaguchi K (2008) Detection of microcystin-metal complexes by using cryospray ionization-Fourier transform ion cyclotron resonance mass spectrometry. *Toxicon* 51:1496-1498
- Schloss JA, Silflow CD, Rosenbaum JL (1984) mRNA abundance changes during flagellar regeneration in *Chlamydomonas reinhardtii*. *Mol. Cell. Biol.* 4:424-434
- Sehringer B, Zahradnik H, Deppert W, Simon M, Noethling C, Schaefer W (2005) Evaluation of different strategies for real-time RT-PCR expression analysis of corticotropin-releasing hormone and related proteins in human gestational tissues. *Analytical and Bioanalytical Chemistry* 383:768-775
- Siu GKY, Young MLC, Chan DKO (1997) Environmental and nutritional factors which regulate population dynamics and toxin production in the dinoflagellate *Alexandrium catenella*. *Hydrobiologia* 352:117-140
- TaroncherOldenburg G, Kulis DM, Anderson DM (1997) Toxin variability during the cell cycle of the dinoflagellate *Alexandrium fundyense*. *Limnology and Oceanography* 42:1178-1188
- Taylor AB, Stoj CS, Ziegler L, Kosman DJ, Hart PJ (2005) The copper-iron connection in biology: Structure of the metallo-oxidase Fet3p. *Proceedings of the National Academy of Sciences* 102:15459-15464
- Uribe P, Espejo RT (2003) Effect of associated bacteria on the growth and toxicity of *Alexandrium catenella*. *Applied and Environmental Microbiology* 69:659-662
- Vasquez M, Gruttner C, Gallacher S, Moore ERB (2001) Detection and characterization of toxigenic bacteria associated with *Alexandrium catenella* and *Aulacomya ater* contaminated with PSP. *Journal of Shellfish Research* 20:1245-1249
- Velzeboer RMA, Baker PD, Rositano J (2001) Saxitoxins associated with the growth of the cyanobacterium *Anabaena circinalis* (Nostocales, Cyanophyta) under varying sources and concentrations of nitrogen. *Phycologia* 40:305-312

- Wang G, Barton C, Rodgers FG (2002) Bacterial DNA decontamination for reverse transcription polymerase chain reaction (RT-PCR). *J. Microbiol. Meth.* 51:119-121
- Wiramanaden CIE, Cullen JT, Ross ARS, Orians KJ (2008) Cyanobacterial copper-binding ligands isolated from artificial seawater cultures. *Marine Chemistry* 110:28-41
- Wong ML, Medrano JF (2005) Real-time PCR for mRNA quantitation. *Biotechniques* 39:75-85
- Wood PM (1978) Interchangeable Copper and Iron Proteins in Algal Photosynthesis. *European Journal of Biochemistry* 87:9-19
- www.dorak.info/genetics/realtime.html Real-Time PCR. May 2008
- www.ncbi.nlm.gov (as of December 2008)
- Yin QQ, Carmichael WW, Evans WR (1997) Factors influencing growth and toxin production by cultures of the freshwater cyanobacterium *Lyngbya wollei* Farlow ex Gomont. *Journal of Applied Phycology* 9:55-63
- Zuker M (2003) Mfold web server for nucleic acid folding and hybridization prediction. *Nucleic Acids Research* 31:3406-3415

Part VI

Phylogenetic analysis of *Pyrodinium bahamense* var. *bahamense* from the Indian River Lagoon, FL based on small subunit ribosomal DNA sequences

Abstract

Pyrodinium bahamense is currently classified as a single species, with two varietal forms, *bahamense* and *compressum*, distinguished by key morphological and biochemical differences. One of the fundamental differences between the two is the lack of paralytic shellfish toxin production in var. *bahamense*. However, over the past few years, saxitoxin outbreaks have occurred in the Indian River Lagoon, on the east coast of Florida, and *P. bahamense* var. *bahamense* has been identified as the source. This marks the first occurrence of toxin production for this variety, and has raised concerns over whether the use of the varietal designations is warranted. To date, no genetic information exists for var. *bahamense*. This study sought to obtain small subunit rDNA sequences from environmental samples of var. *bahamense* for comparison with published var. *compressum* sequences. *Pyrodinium*-specific primers were designed to amplify 665-bp and 1.2-kb regions of the SSU rDNA from single cells isolated from various locations in the lagoon. Six individual samples were each retrieved from two separate locations. The 665-bp sequences obtained from one of the sites differed to a degree incompatible with the current classification of *P. bahamense* as a single species. This was reflected in the phylogenetic analysis, as samples clustered more closely with *Karlodinium* and *Gymnodinium* spp. than with var. *compressum*. Following the successful amplification of the 665-bp region with the *Pyrodinium*-specific primers, a second reverse primer was designed which amplified an approximately 1.2-kb region (encompassing the 665-bp region plus an additional 535 bp downstream). Samples yielding the 1.2-kb fragment were retrieved from a separate site within the lagoon; these sequences identified *P. bahamense* var. *bahamense* as genetically identical to var. *compressum*, with 99% sequence identity. These results necessitate additional sequence data from both sites and warrant further investigation into the current classification of *P. bahamense*.

Introduction

Pyrodinium bahamense is the sole species within its genus. However, since its original description by Plate in 1906, multiple generic, species, and varietal designations have been used in its nomenclature (Badylak et al. 2004). It has historically been found throughout the Indo-Pacific and tropical Atlantic. In 1980, *P. bahamense* was designated as a single species, with intraspecific distinctions defined by two varietal forms based on key morphological and biochemical differences (Steidinger et al. 1980). The Indo-Pacific variety was designated “*compressum*,” while the Atlantic variety, derived from specimens collected from Tampa Bay on the west coast of Florida, was designated “*bahamense*.” In general, var. *compressum* has been found predominantly in the Indo-Pacific waters and var. *bahamense* in the Atlantic, though reports exist in which the range of both varieties extends beyond these locations, with var. *compressum* reported further north in the Mexican Pacific, and var. *bahamense* also observed in the Pacific (Martinez-Lopez et al. 2007, Morquecho 2008).

Major morphological attributes previously used to differentiate “*bahamense*” from “*compressum*,” include: (I) a more prominent apical horn; (II) decreased anterior-posterior compression of cells; and (III) chains comprised of a maximum of two cells (in contrast, the variety designated *compressum* has been reported to form chains of up to 30 cells) (Steidinger et al. 1980). One of the primary differences between the two was the absence of toxin production in the varietal form *bahamense* (Steidinger et al. 1980), as numerous reports exist in the literature linking the varietal form *compressum* to saxitoxin production and subsequent paralytic shellfish poisonings (Harada et al. 1982a, Gacutan et al. 1985, Azanza & Miranda 2001, Azanza & Taylor 2001, Llewellyn et al. 2006, Montojo et al. 2006).

A recent description of *P. bahamense* from the Indian River Lagoon, on the east coast of Florida, confirmed the species as the varietal form “*bahamense*,” based on morphological features (Badylak et al. 2004). While *P. bahamense* var. *bahamense* had been observed in the Indian River Lagoon, FL (Badylak & Phlips 2004), there had been no reported incidents of saxitoxin occurrence. However, in

2002, people from multiple states became ill after eating pufferfish harvested from the Indian River Lagoon (Bodager 2002). Saxitoxin was found within the tissues of the fish (Quilliam et al. 2004), and it was recently determined that the source of the saxitoxin was *P. bahamense* var. *bahamense* (Landsberg et al. 2006). Thus, one of the predominant attributes used to distinguish between the two varieties - the ability to produce toxin – was found to also occur in var. *bahamense*. This supports the argument presented by Balech (Balech 1985), who was unable to find a distinct morphological feature that would allow designation of isolates to any of the “varieties,” and presented the argument that toxin production by the species is a result of environmental influences rather than genetic differences. However, others have presented the argument that the morphological differences observed over the past 20 years from isolates in the Atlantic and Indo-Pacific have remained consistent, thus warranting varietal designation (Badylak et al. 2004). In addition to the recent confirmation of toxin production, *P. bahamense* var. *bahamense* from the Indian River Lagoon was observed to form chains of 2-4 cells (Badylak et al. 2004), less than that typically seen with var. *compressum* yet greater than the 2-cell maximum defined previously (Steidinger et al. 1980). The morphological and biochemical differences used to distinguish the two varieties no longer appear applicable, and it is evident genetic analysis will provide a level of resolution that is currently lacking.

Ribosomal DNA sequences are commonly used as phylogenetic markers. In recent years, rDNA sequences have become common in species identification and phylogenetic classifications among dinoflagellates (Lenaers et al. 1991, John et al. 2003, Yamaguchi & Horiguchi 2005). Different degrees of sequence variability exist within the subunits that comprise the rRNA gene unit, thus these sequences may have varying suitability for distinction at the species level (Adachi et al. 1996). The small subunit rRNA gene (also referred to as SSU rDNA, or 18S rDNA) in particular serves as a useful phylogenetic marker for general species classification, as this sequence exhibits little variation at the lower eukaryotic level. This is in contrast to the large subunit rRNA gene (LSU rDNA), which contains hypervariable regions that differ substantially even among closely-related species (Srivastava & Schlessinger 1991).

The objective of the study was to obtain SSU rDNA sequences of adequate length from single cells of *P. bahamense* var. *bahamense* for phylogenetic analysis with published *P. bahamense* var. *compressum* sequences, with the hypothesis that the two varietal forms of *P. bahamense* are genetically identical based on SSU rDNA sequences.

Methods and Materials

Numerous attempts were made to amplify various portions of the SSU region using multiple cells per tube and single cells per tube, with variations in extraction methods, primer sets, PCR reagents, and thermocycling parameters. These different variations and combinations are described in detail below:

Sample Collection

Water samples were collected from different locations in the Indian River Lagoon surrounding Kennedy Space Center, FL. Sample locations are depicted in Figure VI-1. Samples were not collected from all locations every time; additionally, on several occasions, the areas sampled did not yield any *P. bahamense* cells. A total volume of 6 liters was pumped from 0.5 m below the surface, and concentrated by passing through two successful sieves of 2 mm and 125 μ m mesh onto a 35 μ m filter; the plankton collected onto the 35 μ m mesh were rinsed into a sterile 1 L bottle using the filtrate. The remaining space in the bottle was then filled with un-filtered water from the respective sample site. Samples were placed on ice for transport back to the lab and subsequent cell isolation.

Cell Isolation

Approximately 1 mL volumes of sample water were placed in a petri dish and viewed with light microscopy. *P. bahamense* cells were identified based on morphological features previously defined in the literature under 400x and 1000x magnification. Figure VI-2 is a light microscopy image representative of cells isolated from sites VR13 and ML02 in the Indian River Lagoon. Drops of sterile HPLC water of approximately 250 μ l volume were deposited into a petri dish. Individual *P. bahamense* cells were isolated from the 1 mL samples with a sterile glass



Figure VI-1. Sampling sites in the Indian River Lagoon. Sites from which SSU rDNA sequences were successfully amplified from single cells of *P. bahamense* using *Pyrodinium*-specific primers are indicated in yellow.



Figure VI-2. Light microscopy image representative of *P. bahamense* cells isolated from sites within the Indian River Lagoon.

micropipet, alternating between 100x and 400x magnification. Individual cells were transferred 2-3 times to the drops of sterile water to facilitate removal of contaminants. Single cells, suspended in 1–5 μ l of water, were then placed in thin-walled 200 μ l sterile PCR tubes and stored at -20°C until DNA extraction. Alternatively, 20–30 cells were placed in sterile 1.5 mL centrifuge tubes and stored at -80°C until DNA extraction.

DNA Extraction from Multiple Cells

Freeze-thaw

Samples were centrifuged at 5,000g for 30 minutes at room temperature and most of the water removed using a micropipette tip. Cells were then re-suspended in 10 μ l HPLC- purified water. In some cases, samples were centrifuged and washed a second time. In general, samples were centrifuged and re-suspended in HPLC- purified water to remove any contaminants that might have carried over in initial isolation and wash steps. Cells were then subjected to five consecutive freeze-thaw cycles alternating between baths of dry ice and heating to 100°C in a heating block filled with sand. The 1.5 mL tube was then centrifuged for 15 min at 7000g at a temperature of 4°C. Aliquots of the supernatant were distributed into 200 μ L thin-walled PCR tubes for individual PCRs under a laminar flow hood. In order to minimize the loss of cells due to the possibility of adherence to the inside of the pipet tip, the same tip was used to aliquot the entire volume.

DNA Extraction from Single Cells

Freeze-thaw

Prior to lysis, the final volume of water in tubes to which single cells had been placed was brought to 10 μ L with HPLC-purified water. Samples were then subjected to five cycles of freeze-thaw as described above and centrifuged briefly at room temperature to collect all liquid to the bottom of the tubes. PCR reagents were added directly to the tubes used in the freeze-thaw lysis.

Primer Sets

Two sets of dinoflagellate-specific primers were utilized in attempts to amplify two segments of the SSU rRNA gene (Table VI-1). The primer set comprised

of Dino18F1/18ScomF1 (Lin et al. 2006) amplified an approximately 1.6-kb fragment. The primer set 18ScomF1/Dino18SR1 (Lin et al. 2006) amplified an approximately 650-bp fragment.

Pyrodictum-specific primers were designed based on published *P. bahamense* var. *compressum* DNA sequences. All *P. bahamense* sequences listed in the NCBI database were aligned using ClustalX, and two forward and three reverse primers designed based on regions of sequence identity (Table VI-1).

PCR Reagents

Several PCR kits were used with various primer sets and extraction methods (Table VI-2). The HotStar HiFidelity PCR kit (Qiagen, Valencia, CA) was used in combination with multiple primer sets. Reactions consisted of 10 μ l 5x buffer (containing dNTPs), primer concentrations ranging from 1–1.2 μ M, 0.5–1 μ l HotStar HiFidelity DNA polymerase (for final concentrations ranging between 1.25–2.5 U), and brought to a final volume of 50 μ l with nuclease-free water. Q-solution was included in some reactions at the concentration recommended by the manufacturer.

As the HotStar HiFidelity DNA polymerase contains proof-reading activity, it was hypothesized that reactions were not yielding successful amplifications because the SSU rRNA gene of *P. bahamense* may differ from the published forms, thus annealing of the primers and subsequent extension may be hindered due to nucleotide differences. Therefore, Platinum *Taq* (Invitrogen, Carlsbad, CA) was also utilized, as this DNA polymerase does not contain proof-reading activity. Reactions utilizing Platinum *Taq* DNA polymerase typically consisted of 5 μ l 10x buffer, 1 μ l dNTPs (for a final concentration of 0.2mM each dNTP), 1.5 μ l 50 mM MgCl₂ (final concentration 1.5 mM), 1 μ l each forward and reverse primer (final concentration 0.2 μ M), 0.2 μ l Platinum taq (final concentration of 1 U), template, and brought to a final volume with 50 μ l nuclease-free water.

The FailSafeTM PCR 2x PreMixes (EpiCentre Biotechnologies, Madison, WI) were also utilized in several attempts. This is a set of 12 premixes consisting of dNTPs, enzyme buffer, and varying concentrations of MgCl₂ and PCR Enhancer with Betaine. Reactions were conducted with all 12 FailSafeTM PreMixes and consisted of

Table VI-1. List of primers used in attempts to amplify various regions of the SSU rRNA gene from *Pyrodinium bahamense* obtained from several locations within the Indian River Lagoon, FL.

Primer	Sequence (5'-3')	T_M	Source or Reference
Dino18F1	AAGGGTTGTGTTYATTAGNTACARAAC	60.8	(Lin et al. 2006)
18ScomR1	CACCTACGGAAACCTTGTTACGAC	64.6	(Lin et al. 2006)
18ScomF1	GCTTGTCTCAAAGATTAAGCCATGC	62.9	(Lin et al. 2006)
Dino18SR1	GAGCCAGATRCDCACCCA	61.8	(Lin et al. 2006)
Pcomp700F	TCGAGAACTTTTACTTTGAG	54.2	This study
Pcomp400F	AAA TTA CCC AAT CCT GAC ACT	56.7	This study
PcompR	CAA AGA CTT CGA TTT CTC ATA	54.8	This study
PcompR2	AAGCTGATGACTCAGGCTTA	58.4	This study
PcompR2b	CTGATGACTCAGGCTTACT	58	This study

Table VI-2. List of primer combinations used in attempting to amplify 18S rDNA regions from environmental samples of *P. bahamense*. The column "PCR kits" refers to the various reagents and DNA polymerases employed. HS=HotStar HiFidelity PCR kit (Qiagen), FS=FailSafe PCR kit (EpiCentre), P=Platinum Taq PCR kit (Invitrogen).

Primer Combination	Expected Product Size	PCR kits
18ScomF1/Dino18SR1	650 bp	HS, FS
18ScomF1/18ScomR1	1.7 kb	HS
Dino18F1/18ScomR1	1.6 kb	HS
Pcomp700/PcompR	350 bp	P
Pcomp400/PcompR	665 bp	P
Pcomp400/PcompR2	1.2 kb	HS, P
18SDinoF1/PcompR2b	1.7 kb	HS
Pcomp400/PcompR2b	1.2 kb	HS, P

25 μ l 2x Buffer, 0.2 μ l Platinum *Taq*, 5 μ l each 18S comF1/18S DinoR1 (1 μ M final concentration), template (typically 2.5 μ l) and brought to a final volume of 50 μ l with nuclease-free water.

Thermocycling Programs

Multiple thermocycling conditions were employed when attempting to amplify the various fragments of the SSU rDNA gene. In PCRs employing the HotStar HiFidelity DNA polymerase, the initial denaturation step was 95°C for 5 min, followed by a denaturation step at 94°C for 15 s, annealing for 1 min, and extension at a rate of 1 kb min⁻¹. The initial denaturation step in PCR with Platinum *Taq* DNA polymerase was 95°C for 3 min and 94°C for 2 min, followed by cycles of denaturation at 94°C for 15 s, annealing for 30 sec, and extension at a rate of 1 kb min⁻¹. Amplification attempts used both standard and touchdown PCR conditions. Programs consisted of a total of 40-45 cycles. Initial attempts using standard PCRs used an annealing (T_A) temperature 5°C below the lowest T_M of the primer pair; this temperature was adjusted based on the results of the reactions. Touchdown PCR thermocycling conditions employed an initial three cycles in which the T_A was 8-10°C higher than the final T_A , with the T_A decreased 2°C every three cycles; the final 30-35 cycles were performed with the standard T_A .

Cloning and Phylogenetic Analysis of *P. bahamense* SSU rDNA

Concomitant with gel electrophoresis an aliquot of the PCR product was cloned into the pCR2.1 vector using a TOPO TA cloning kit (Invitrogen, Carlsbad, CA). Twenty-five microliters of each PCR were added to a PCR Ready-to-Go Bead and incubated at 72°C for 20 min for the addition of the dATP overhangs. Cloning reactions consisted of 14 μ l PCR product with dATP overhangs, 3 μ l salt, and 1 μ l pCR2.1 vector. Reactions were incubated for 30 min at room temperature and 8 μ l transformed into chemically competent *E. coli* TOP10 cells following the instructions of the manufacturer. Cells were spread onto selective plates of LB containing 50 μ g ml⁻¹ kanamycin and incubated at 37°C overnight.

Colony PCR was used to screen for clones with the proper-sized inserts. These reactions were performed with PCR Ready-to-Go Beads and the primer

combination used in the initial PCR. Sterile micropipette tips were used to transfer a small portion of the colony from the agar plate into the PCR tube. Thermocycling conditions consisted of a modified version of the touchdown programs used in the initial PCR. PCR products were visualized by gel electrophoresis to confirm product amplification of the proper size. Clones producing a band at the expected size were then grown overnight in LB_{kan50} broth and plasmid DNA purified using the Wizard Plus Minipreps kit (Promega, Madison, WI). Clones were sequenced using the M13 forward and reverse primers on an ABI 3100 genetic analyzer (Applied Biosystems, Foster City, CA) at the Molecular Biology Resource Facility, University of Tennessee (Knoxville, TN). Alignments and phylogenetic trees were constructed using MEGA (Molecular Evolutionary Genetics Analysis) software version 3.1 (<http://www.megasoftware.net>).

Verification of DNA Extraction and Dinoflagellate-Specific Primer Sets using *Alexandrium fundyense*

Due to multiple repeated failures in the initial attempts to amplify regions of the SSU rDNA gene from environmental samples of *P. bahamense*, the dinoflagellate *Alexandrium fundyense* (GTCA28/CCMP1719) was used to troubleshoot various parameters of the PCR. *A. fundyense* DNA extractions were used to determine if the freeze-thaw lysis method provided sufficient quantities of DNA and if the PCR was inhibited from cellular debris resulting from the lysis method. *A. fundyense* DNA also served as template in the verification and optimization of the dinoflagellate-specific degenerate primer sets.

Genomic DNA Extraction from Pure Culture and Isolated Cells (A. fundyense)

Axenic cultures of *A. fundyense* were maintained in 50 mL volumes in 125 mL flasks at 20°C on a 12:12 photoperiod under 100 µE illumination. Cells were harvested and the genomic DNA extracted using the DNeasy Tissue Kit (Qiagen, Valencia, CA) following the manufacturer's instructions without bead-beating and a Proteinase K incubation time of 3.5 hours at 55°C with mild agitation. Additionally, individual cells were isolated and washed using the protocol described for *P. bahamense* environmental samples and approximately 30 cells placed in a sterile 1.5

mL microcentrifuge tube. Multiple tubes were prepared and stored immediately at -80°C. Prior to lysis, samples were centrifuged at room temperature and re-suspended in 10 µl sterile HPLC water, which served as the template volume in subsequent PCRs. Cells were lysed following the freeze-thaw protocol as described for *P. bahamense*.

18S Community Primers to Examine DNA Extraction Efficiency from Freeze-Thaw Lysis

To determine if 30 cells provided adequate yields of DNA for PCR amplification following the freeze-thaw lysis, and also to examine possible inhibition of the reaction by cellular debris, an SSU community primer set (18ScomF1/18ScomR1 (Lin et al. 2006)) was used. The HotStar HiFidelity kit (Qiagen, Valencia, CA) was used for all reactions. PCR reactions consisted of: 5 µl 5x HiFidelity PCR buffer, 1 µM of both forward and reverse primers, 1.25U DNA polymerase, 10 µl template, and brought to a final volume of 50 µl with nuclease-free water. Reactions were conducted on a DNA Engine thermocycler using the following protocol: 95°C for 5 minutes; 50 cycles of denaturation at 94°C for 30 seconds, annealing at 58.5°C for 30 seconds, and extension at 72°C for 1 minute and 45 seconds; and a final cycle in which the denaturation time was increased to 1 minute. The PCR product was visualized on a 1% agarose gel; successful amplification was indicated by a band at the expected product size of 1.7 kb (Figure VI-3, Appendix D).

Optimization of Dinoflagellate-Specific Primers

The dinoflagellate-specific primer sets (Lin et al. 2006) were tested with *A. fundyense* DNA extracted using both the kit and the freeze-thaw lysis methods. The HotStar HiFidelity PCR kit was used in all reactions. For PCR reactions using kit-extracted DNA, 18 ng total DNA was added as template. Samples subject to freeze-thaw lysis were re-suspended in 10 µl nuclease-free water, which served as the template in the PCR reactions. A touchdown PCR program was created that consisted of an initial denaturation step of 95°C for 5 minutes, followed by 3 cycles of denaturation at 94°C for 30 seconds, annealing at 64°C for 30 seconds, and elongation at 72°C at a rate of 1 kb min⁻¹. The annealing temperature was decreased

by two degrees every third cycle, with the final thirty cycles performed at an annealing temperature of 54°C.

PCRs utilizing the primer set 18ScomF1/Dino18SR1 in which the kit-extracted DNA served as template produced a band of the expected size (Figure VI-4, Appendix I). However, initial PCRs using cells that were subject to freeze-thaw lysis were not successful (data not shown). All reactions conducted with primer set Dino18F1/18ScomR1 failed, including those utilizing the kit-extracted DNA as template (Figure VI-4, Appendix I). Therefore, this primer set was omitted from future PCR attempts with *P. bahamense*.

Following initial primer testing, reactions were then conducted to optimize the reagent concentrations of the HotStar HiFidelity kit for use with 18ScomF1/Dino18SR1, including primer titrations, polymerase amounts, and the inclusion of Q solution. Most combinations produced a band of the expected size (Figure VI-5, Appendix I). A control reaction was also conducted in which yeast genomic DNA served as the template. This reaction did not yield a visible product, indicating that the primers were specific for the dinoflagellate SSU rDNA (Figure VI-6, Appendix I).

Results

DNA Extraction of *P. bahamense* environmental samples

The single-cell freeze-thaw DNA extraction procedure resulted in successful amplification of various SSU rRNA gene regions targeted by two of the *Pyrodinium*-specific primer combinations. On multiple occasions, the freeze-thaw DNA extraction procedure appeared to be successful, yet the PCR reaction was not, as evidenced by the bands located slightly below the wells into which samples were loaded in the agarose gels (as an example, see Figure VI-7). The bands are indicative of genomic DNA, which is large and thus would not have migrated well in the 1% agarose gel.

None of the DNA extractions in which multiple cells were washed and placed in a single tube yielded successful PCR results. This may be due to the centrifuge speed used to collect the cells prior to re-suspension in the HPLC-purified water:

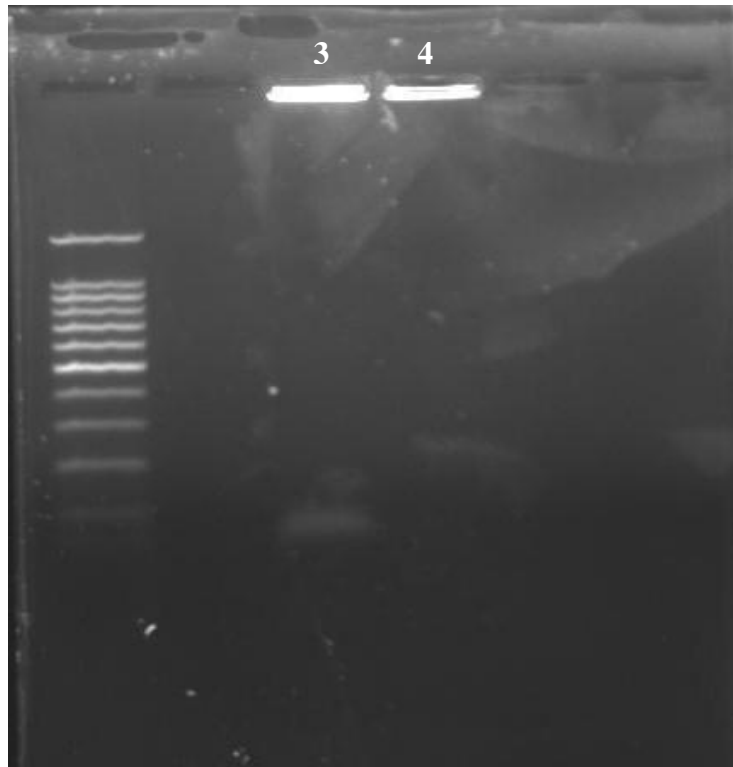


Figure VI-7. Gel image of genomic DNA from *P. bahamense* environmental samples. The bands located just below the wells of lanes 3 and 4 are indicative of a successful genomic DNA extraction following freeze-thaw lysis in an unsuccessful attempt to amplify a portion of the SSU rRNA gene.

while 5,000g-7,000g is the speed commonly cited in the literature for collection of dinoflagellate cells, this may have not been adequate with the type of tube used. The primary objective in the multiple-cell lysis method was to extract DNA in an environment that minimized contamination; thus, sterile 1.5 mL Eppendorf tubes were used without regard for cell adherence to the side of the tube. Centrifuge speeds of 5,000g-7,000g have also been cited in collection of *Chlamydomonas reinhardtii* cells; however, this centrifuge speed has proven to be inadequate using the same type of Eppendorf tube (pers. obs.).

Primer Sets and PCR Conditions

Single-cell PCRs utilizing the *Pyrodinium*-specific primer sets Pcomp400F/PcompR and Pcomp400F/PcompR2b resulted in successful amplification of the targeted regions within the SSU rRNA gene. PCRs performed with the other primer combinations (Table VI-2) either failed to produce a product or resulted in amplification of products whose DNA sequences most closely matched that of diatoms or uncultured marine picoplankton. This is not unexpected, as DNA was amplified from environmental samples in which all of these organisms are present. Of the three kits utilized in the PCR attempts, the Platinum *Taq* PCR kit was the only one that produced successful amplifications of the SSU rRNA gene.

Successful Amplification with Primer Set Pcomp400F/PcompR

The primer set Pcomp400F/PcompR, in combination with the Platinum *Taq* kit reagents, successfully amplified the targeted 665-bp region of the SSU rRNA gene from single-cell *P. bahamense* samples. Reactions consisted of 10x buffer, 200 μ M each dNTP, 1.5 mM MgCl₂, 200 nm each forward and reverse primer, 1 U Platinum *taq* polymerase, template, and adjusted to a final volume of 50 μ l with nuclease-free water. Samples were subjected to a touchdown PCR program consisting of an initial denaturation at 95°C for 3 min/94°C for 2 min; 3 cycles each of 94°C for 30s, 54°C/52°C/50°C for 30 sec, 72°C for 40 s; 33 cycles with a T_A of 48°C; and a final extension of 72°C for 10min.

Six individual samples were successfully cloned and sequenced; all were from location VR13, which is in the Mosquito Lagoon southeast of the Haulover Canal. A

neighbor-joining tree was constructed using the Kimura 2-parameter distance model which included both the 665-bp rDNA sequences obtained from samples collected at site VR13 and 1.2-kb rDNA sequences from site ML02 (Figure VI-8). Surprisingly, the two sets of sequences did not cluster together. Clones from site VR13 showed 92% sequence similarity to published *P. bahamense* SSU rDNA sequences and 99% sequence similarity to strains of *Karlodinium micrum*, *Gymnodinium galatheanum*, and *G. aureolum*.

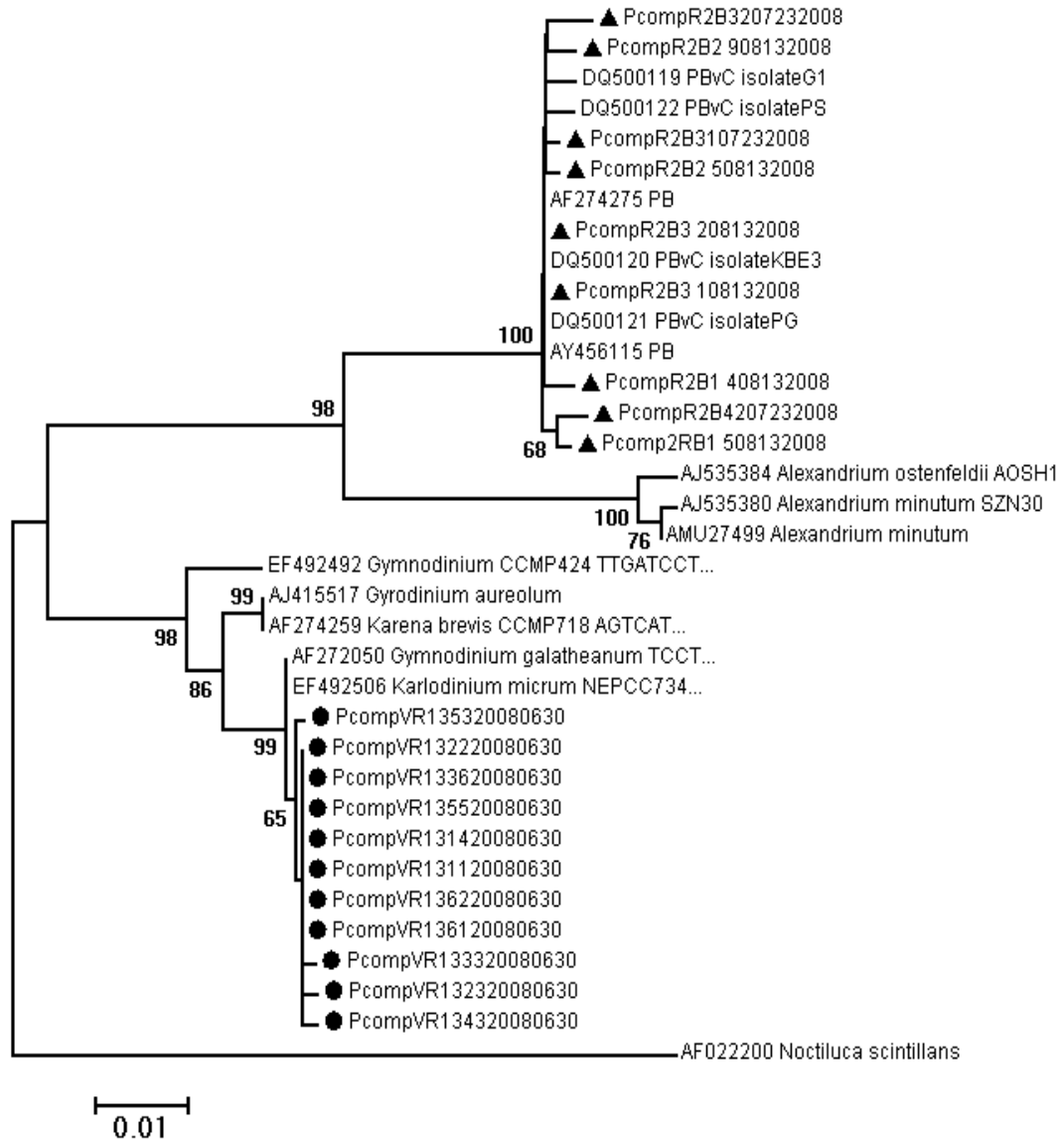
Successful Amplification with Primer Set Pcomp400F/PcompR2b

Following successful amplification of the 665-bp fragment, a reverse primer was designed to use in combination with the Pcomp400F to amplify a 1.2-kb segment of the SSU rRNA gene. Successful reactions utilized the Platinum *Taq* kit reagents at the same concentrations as described for the 665-bp amplifications. A modified touchdown PCR program similar to that used for the 665-bp amplification was used, with elongation at 72°C extended to 1 min 15 s per cycle, and the final 33 cycles conducted at a T_A of 50.5°C. Six individual samples were successfully cloned and sequenced; all samples were collected from site ML02 in the Mosquito Lagoon. A neighbor-joining tree using the Kimura 2-parameter distance model shows the phylogenetic relationship of these sequences (Figure VI-9). All sequences obtained here fall into the same cluster as existing *P. bahamense* sequences, as all clones from this site showed high sequence similarity (99%) to other published *P. bahamense* SSU rDNA sequences.

Discussion

The phylogenetic analysis of the 1.2-kb SSU rDNA sequences obtained from site ML02 indicate that the cell inhabiting this region of the Indian River Lagoon is genetically the same as that designated *P. bahamense* var. *compressum*. *P. bahamense* was previously classified as two varieties based on cell morphology and toxin production (Steidinger et al. 1980). It has recently been determined (Landsberg et al. 2006) that *P. bahamense* var. *bahamense* was the source of saxitoxin production in the IRL, marking the first recorded occurrence of toxin production by this variety.

Figure VI-8. Neighbor-joining tree of SSU rDNA sequences from Indian River Lagoon, FL (site VR13) retrieved using *Pyrodinium*-specific primers. Included are published SSU rDNA sequences from other *Pyrodinium bahamense* and 1.2-kb SSU rDNA sequences obtained from site ML02. *Noctiluca scintillans* was used as an outgroup. Two clones from each sample were included in tree construction to account for mismatches that may have occurred during the PCR or sequencing reactions. Bootstrap values (for 1000 iterations) over 50% are indicated on branches. (●) indicate sequences obtained from single-cell PCRs from site VR13, (▲) indicate sequences obtained from site ML02.



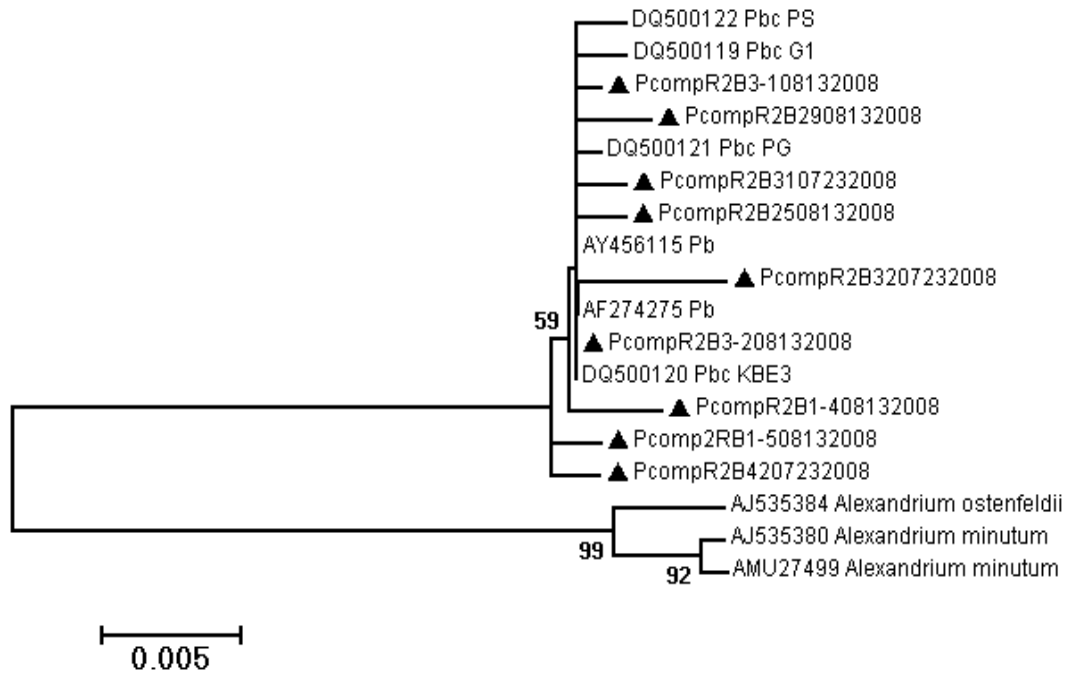


Figure VI-9. Neighbor-joining tree of SSU rDNA sequences from the Indian River Lagoon, FL (site ML02) retrieved using the *Pyrodinium*-specific primer set Pcomp400F/PcompR2b. Published *P. bahamense* SSU rDNA sequences and closely-related *Alexandrium* species are included in the analysis. Two clones from each sample were included in tree construction to account for mismatches that may have occurred during the PCR or sequencing reactions. Bootstrap values (for 1000 iterations) over 50% are indicated on branches. Sequences obtained in this study are indicated by (▲).

Based on this, it has been hypothesized that the varietal distinction is not warranted and is all one species (Landsberg et al. 2006). However, this hypothesis lends further confusion to the taxonomic designation of *P. bahamense*, as modern molecular phylogenetics recognizes the existence of strains and varieties within a single species. Based on the SSU rDNA sequences obtained from site ML02 in the Indian River Lagoon, *P. bahamense* is a single species. With a sequence identity 99% identical to that of *P. bahamense* var. *compressum*, and the recent confirmation of toxin production, the use of varietal designation does not seem applicable. However, in terms of molecular phylogeny, the LSU rDNA is phylogenetically more informative at the species level due to the presence of three hypervariable regions (Brodie & Lewis 2007). As the LSU rDNA evolve more quickly than the SSU rDNA, it is possible that greater sequence substitutions are evident within the LSU rDNA between the two *P. bahamense* varieties. In discriminating among strains within the *Alexandrium* species complex, a genus to which *Pyrodinium* is closely related, the D1/D2 region of the LSU rDNA was needed for resolution at the strain level (John et al. 2003). The LSU rDNA data ultimately revealed that isolates of the *Alexandrium* species complex do not separate out based on morphology, but instead form distinct clades based on geographic locations (Usup et al. 2002, John et al. 2003). Additionally, the internal transcribed spacer (ITS) region has been used to differentiate between strains of *A. tamarense* that were morphologically identical (Adachi et al. 1996). Thus, genetic differences may exist between the two varieties of *P. bahamense* that are only distinguishable in the more hypervariable regions of the rRNA unit, such as the D1 and D2 domains of the LSU rDNA or the ITS region.

While additional rDNA sequence data may reveal genetic differences between *P. bahamense* at the variety level, the primary aim of this study was to establish the relationship at the species level. In general, the SSU rRNA gene has been shown to sufficiently discriminate between major dinoflagellate species sequences (John et al. 2003). The SSU rDNA sequences retrieved from single cells at site VR13 displayed substantial variation from those of site ML02 and published *P. bahamense* sequences and differ to a degree incompatible with their assignment to a single species, as the

sequences diverge by approximately 8% over regions of precise alignment. These sequences are more similar to published *Karlodinium* and *Gymnodinium* strains, as reflected by their positions following phylogenetic analysis (Figure VI-8).

P. bahamense is unique among dinoflagellates in that it is comprised of a single species further classified into two varieties. Key characteristics previously used to define the two included toxin production and geographic location; however, with toxin production shown to occur in var. *bahamense*, and the range of both varieties spreading, these features are no longer adequate for distinguishing between the two. Additional genetic data is needed from the varietal form *bahamense*, including both SSU and LSU rDNA sequences from isolates across a range of locations in Florida waters (i.e Tampa Bay on the west coast and Indian River Lagoon on the east coast).

Acknowledgements

Many thanks to members of the Aquatic Group at Kennedy Space Center for water sample collection: Doug Scheidt, Karen Holloway-Adkins, Eric “Junior” Reier, and Russ Lowers. Dr. Mike Twiner (NOAA Charleston) provided the *A. fundyense* cultures. Jack McPherson suggested the construction of *Pyrodinium*-specific primers after countless PCRs using the published degenerate dinoflagellate primer sets were met with failure. Jennifer DeBruyn constructed the *Pyrodinium* phylogenetic trees presented here.

Appendix I

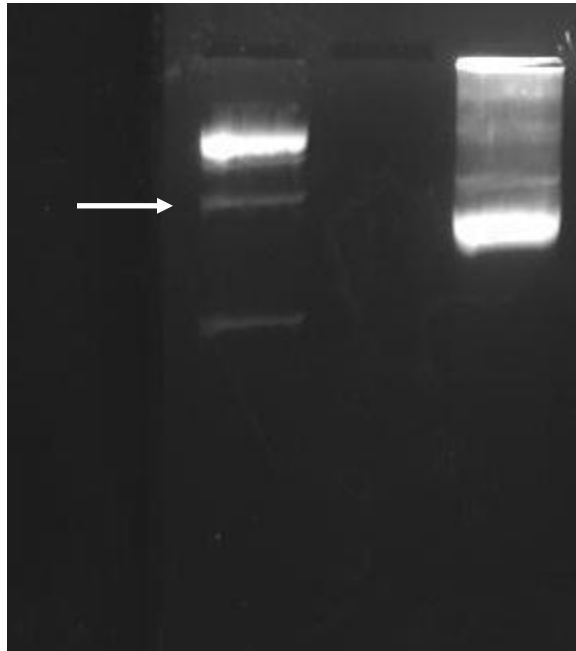


Figure VI-3. Gel image of PCR-amplified SSU rDNA from *A. fundeyense* using the universal primer set 18ScomF1/18ScomR1. This PCR was performed to confirm that the freeze-thaw lysis provided adequate DNA for PCR. Arrow indicates 2-kb size fragment in ladder.

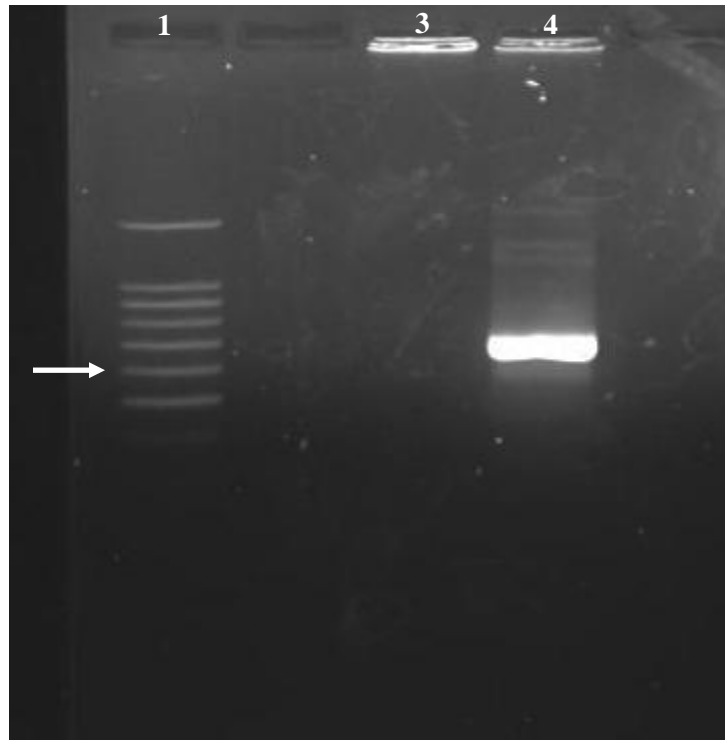


Figure VI-4. Dinoflagellate-specific primer sets were tested on *A. fundyense* genomic DNA extracted from both a commercially-available kit and the freeze-thaw lysis protocol utilized in this study. The 650-bp region of the SSU rDNA targeted by primer set 18ScomF1/Dino18SR1 was successfully amplified from the kit-extracted DNA, as indicated by the intense band in lane 4. All PCRs performed with primer set Dino18F1/18ScomF1 were unsuccessful, including those which utilized kit-extracted DNA as template, as evidenced by the absence of a band in lane 3. Arrow on gel indicates 600-bp size fragment in DNA ladder (lane 1).

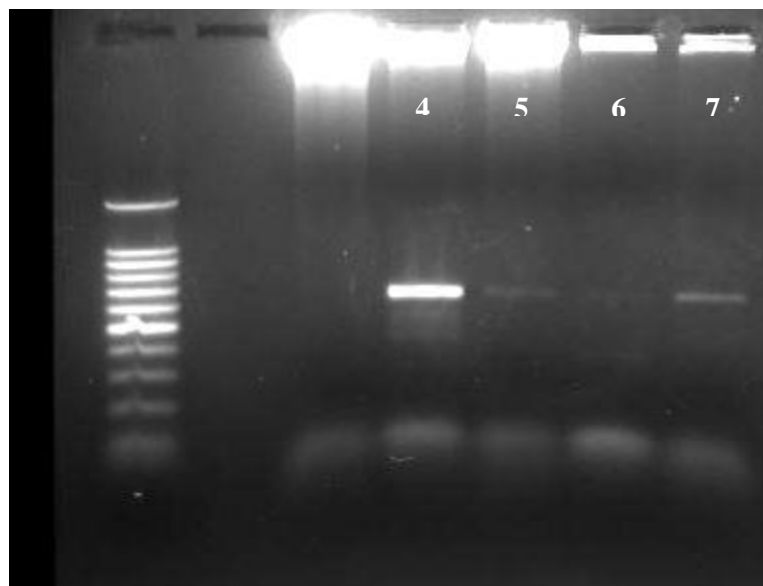


Figure VI-5. Optimization of primer set 18ScomF1/Dino18SR1. *A. fundyense* genomic DNA was extracted via freeze-thaw lysis of approximately 30 cells and served as template for optimization of PCR conditions. All reactions utilized the primer set 18ScomF1/Dino18SR1 and the reagents of the HotStar HiFidelity kit. Most reactions yielded a product of the expected size, as indicated by the 650-bp band in lanes 4, 5, 6, and 7.

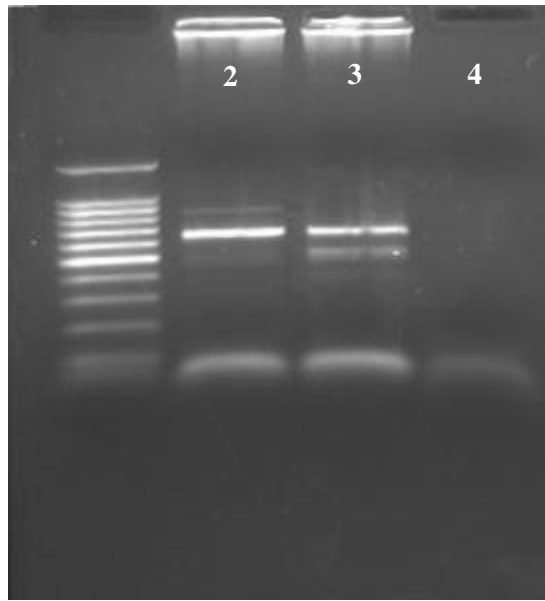


Figure VI-6. Specificity of primer set 18ScomF1/Dino18SR1 for dinoflagellate SSU rDNA. Reactions were conducted with primer set 18ScomF1/Dino18SR1 with either *A. fundyense* or yeast genomic DNA as template. Reactions utilizing *A. fundyense* DNA as template produced bands at the expected size of 650bp (lanes 2 and 3), while attempts to amplify the yeast genomic DNA were unsuccessful (lane 4), indicating the specificity of the primers for dinoflagellate SSU rDNA.

References

- Adachi M, Sako Y, Ishida Y (1996) Analysis of *Alexandrium* (dinophyceae) species using sequences of the 5.8S ribosomal DNA and internal transcribed spacer regions. *Journal of Phycology* 32:424-432
- Azanza RV, Miranda LN (2001) Phytoplankton composition and *Pyrodinium bahamense* toxic blooms in Manila Bay, Philippines. *Journal of Shellfish Research* 20:1251-1255
- Azanza RV, Taylor FJR (2001) Are *Pyrodinium* blooms in the Southeast Asian region recurring and spreading? A view at the end of the millennium. *Ambio* 30:356-364
- Badylak S, Kelley K, Philips EJ (2004) A description of *Pyrodinium bahamense* (Dinophyceae) from the Indian River Lagoon, Florida, USA. *Phycologia* 43:000-000
- Badylak S, Philips EJ (2004) Spatial and temporal patterns of phytoplankton composition in a subtropical coastal lagoon, the Indian River Lagoon, Florida, USA. *J. Plankton Res.* 26:1229-1247
- Balech E (1985) A revision of *Pyrodinium bahamense* Plate (Dinoflagellata). *Review of Palaeobotany and Palynology* 45:17-43
- Bodager D (2002) Outbreak of saxitoxin illness following consumption of Florida pufferfish. *Fl J Environ Health* 179:9-13
- Brodie J, Lewis J (eds) (2007) *Unravelling the algae: the past, present, and future of algal systematics*, Vol. CRC, Boca Raton, FL
- Gacutan RQ, Tabbu MY, Aujero EJ, Icatlo F (1985) Paralytic Shellfish Poisoning Due to *Pyrodinium bahamense* var. *compressa* in Mati, Davao-Oriental, Philippines. *Marine Biology* 87:223-227
- Harada T, Oshima Y, Kamiya H, Yasumoto T (1982) Confirmation of paralytic shellfish toxins in the dinoflagellate *Pyrodinium bahamense* var. *compressa* and bivalves in Palau. *Bulletin of the Japanese Society of Scientific Fisheries* 48:821-825
- John U, Fensome RA, Medlin LK (2003) The application of a molecular clock based on molecular sequences and the fossil record to explain biogeographic distributions within the *Alexandrium tamarense* "species complex" (Dinophyceae). *Mol Biol Evol* 20:1015-1027

- Landsberg JH, Hall S, Johannessen JN, White KD, Conrad SM, Abbott JP, Flewelling LJ, Richardson RW, Dickey RW, Jester ELE, Etheridge SM, Deeds JR, Van Dolah FM, Leighfield TA, Zou YL, Beaudry CG, Benner RA, Rogers PL, Scott PS, Kawabata K, Wolny JL, Steidinger KA (2006) Saxitoxin puffer fish poisoning in the United States, with the first report of *Pyrodinium bahamense* as the putative toxin source. *Environmental Health Perspectives* 114:1502-1507
- Lenaers G, Scholin C, Bhaud Y, Saint-Hilaire D, Herzog M (1991) A molecular phylogeny of dinoflagellate protists (Pyrrhophyta) inferred from the sequence of 24S rRNA divergent domains D1 and D8. *Journal of Molecular Evolution* 32:53-63
- Lin S, Zhang H, Hou Y, Miranda L, Bhattacharya D (2006) Development of a dinoflagellate-oriented PCR primer set leads to detection of picoplanktonic dinoflagellates from Long Island Sound. *Appl. Environ. Microbiol.* 72:5626-5630
- Llewellyn L, Negri A, Robertson A (2006) Paralytic shellfish toxins in tropical oceans. *Toxin Reviews* 25:159-196
- Martinez-Lopez A, Ulloa-Perez AE, Escobedo-Urias DC (2007) First record of vegetative cells of *Pyrodinium bahamense* (Gonyaulacales: GoniDOMATAceae) in the Gulf of California (1). *Pacific Science* 61:289(285)
- Montojo UM, Sakamoto S, Cayme MF, Gatdula NC, Furio EF, Relox JJR, Shigeru S, Fukuyo Y, Kodama M (2006) Remarkable difference in accumulation of paralytic shellfish poisoning toxins among bivalve species exposed to *Pyrodinium bahamense* var. *compressum* bloom in Masinloc bay, Philippines. *Toxicon* 48:85-92
- Morquecho L (2008) Morphology of *Pyrodinium bahamense* Plate (Dinoflagellata) near Isla San José, Gulf of California, Mexico. *Harmful Algae* 7:664-670
- Quilliam M, Wechsler D, Marcus S, Ruck B, Wekell M, Hawryluk T (2004) Detection and identification of paralytic shellfish poisoning toxins in Florida pufferfish responsible for incidents of neurologic illness. In: Steidinger KA LJ, Tomas CR, Vargo GA (ed) *Harmful Algae 2002*. Florida Fish and Wildlife Conservation Commission, Florida Institute of Oceanography, and Inter-governmental Oceanographic Commission of United Nations Educational, Scientific and Cultural Organization, St. Petersburg, FL, p 116-118
- Srivastava AK, Schlessinger D (1991) Structure and organization of ribosomal DNA. *Biochimie* 73:631-638

- Steidinger KA, Tester LS, Taylor FJR (1980) A redescription of *Pyrodinium bahamense* var. *compressa* (Bohm) stat. nov. from Pacific red tides. *Phycologia* 19:329-337
- Usup G, Pin LC, Ahmad A, Teen LP (2002) Phylogenetic relationship of *Alexandrium tamiyavanichii* (Dinophyceae) to other *Alexandrium* species based on ribosomal RNA gene sequences. *Harmful Algae* 1:59-68
- Yamaguchi A, Horiguchi T (2005) Molecular phylogenetic study of the heterotrophic dinoflagellate genus *Protoperidinium* (Dinophyceae) inferred from small subunit rRNA gene sequences. *Phycological Research* 53:30-42

Part VII
Conclusions

Expression Profiling to Elucidate the Mechanism of Action of Saxitoxin on Lower Eukaryotes

Saxitoxin is a secondary metabolite produced by several species of dinoflagellates and cyanobacteria, though due to its detrimental effects on human health, it is often referred to as a potent neurotoxin. While the sodium channel has been identified as the target of saxitoxin in mammalian cells, its molecular effects on planktonic community members (i.e. phyto- and zooplankton) found within the same aquatic habitats as the toxic cells are not known.

A significant portion of the experiments performed throughout this dissertation sought to identify the molecular effects and possible targets of saxitoxin on other lower eukaryotes as a means of beginning to elucidate the role of the toxin within the context of the algae that produce it. To accomplish this, initial transcriptomic data were collected with the yeast *Saccharomyces cerevisiae*. Expression profiles generated with *S. cerevisiae* were then extrapolated to the unicellular green alga *Chlamydomonas reinhardtii* as part of a comparative transcriptomics study. Collectively, the following conclusions have been drawn from these experiments:

I. Global expression profiling with *S. cerevisiae* identified copper and iron homeostasis and sulfur amino acid biosynthesis genes as differentially expressed upon exposure to saxitoxin. The first part of this dissertation utilized global expression profiling with the yeast *Saccharomyces cerevisiae* as a means of eliciting the mechanism of action of saxitoxin on lower eukaryotes. Genes typically associated with copper and iron homeostasis and sulfur amino acid biosynthesis were identified as significantly differentially expressed following short-term exposure to saxitoxin. The overall transcriptional response appeared to be similar to that of excess copper, as the metallothionein genes *CUP1* and *CRS5* were upregulated, while the *CTR1* and *FRE1* genes, which are involved in copper reduction and transport across the plasma membrane, were repressed.

II. Comparing the patterns of regulation in a set of copper homeostasis genes in *S. cerevisiae* following exposure to saxitoxin, excess copper, and excess iron indicated that saxitoxin was affecting internal copper levels. Quantitative reverse-transcriptase PCR assays were used to examine expression profiles of copper homeostasis genes following exposure to saxitoxin, copper, and iron in order to compare patterns of regulation under similar culture conditions. While the concentration of saxitoxin and length of exposure were the same in this study as for the microarray experiments, this study utilized a minimal media rather than the rich media employed for the microarray exposures in order to reduce the ambient levels of copper to which yeast were exposed. A resulting key difference between saxitoxin and copper expression patterns with yeast grown in minimal media was the regulation of the *FET3* gene: while it remained unchanged following copper treatments, it was repressed greater than 3.5-fold following exposure to saxitoxin. Fet3p requires the posttranslational insertion of four copper ions for proper enzyme functioning (Taylor et al. 2005); thus, repression of this gene in the presence of saxitoxin suggested inadequate intracellular copper levels. The plasma membrane protein Ctr1p, responsible for high-affinity copper transport and the source from which Fet3p receives the necessary copper ions (Askwith et al. 1994, Dancis et al. 1994a, Dancis et al. 1994b), was significantly repressed upon exposure to saxitoxin at levels comparable to those recorded for excess copper. Taken collectively, the transcriptional profiles obtained with yeast suggested that saxitoxin was altering internal copper levels.

III. Comparative transcriptomics with *C. reinhardtii* indicated a consistent trend of altered copper homeostasis among lower eukaryotes following exposure to saxitoxin. A comparative transcriptomics analysis was performed in which the expression data collected with *S. cerevisiae* were extrapolated to the unicellular green alga *Chlamydomonas reinhardtii*. The patterns of regulation in set of genes commonly associated with copper homeostasis and heavy metal chelation were examined following 24 hr exposure to either saxitoxin or excess copper. Of greatest

significance was the difference in regulation of the gene encoding cytochrome c6 (*CYC6*). *CYC6* was induced approximately three-fold following exposure to saxitoxin and repressed under conditions of excess copper. This protein is used interchangeably with plastocyanin, a copper protein, in the transfer of electrons from cytochrome *b6-f* to photosystem I. Selection is based solely on copper levels, as plastocyanin is utilized in copper-replete cells, while cytochrome c6 is used under conditions of copper deficiency (Hill et al. 1991, Li & Merchant 1992). At the level of transcription, an inverse relationship has been shown to exist between the level of *CYC6* transcripts and the availability of copper ions to the cell. Thus, induction of *CYC6* following *C. reinhardtii* exposure to saxitoxin indicated inadequate intracellular copper levels.

IV. Two possible mechanistic models can be proposed for saxitoxin based on the combined expression data of *S. cerevisiae* and *C. reinhardtii*. Based on the expression data generated with *S. cerevisiae* (Part III) and *C. reinhardtii* (Part V), the following models can be proposed as to the mechanism of action of the saxitoxin molecule: (I) saxitoxin complexes with extracellular copper ions, either preventing them from entering the cell or being taken into the cell as complex, thus rendering the copper ions unavailable as cofactors for enzymes; or (II) saxitoxin binds to a copper transporter, blocking the passage of copper ions into the cell in a mechanism similar to that determined for the sodium channel. The recent transcriptional profile obtained with *S. cerevisiae* coupled with the minimal expression profiling performed with *C. reinhardtii* appears to suggest a link between copper transport and algal toxins. The relationship between copper levels and toxin production in aquatic environments warrants further investigation, as copper sulfate is commonly used as an algicide in water reservoirs.

Phylogenetic Analysis of P. bahamense

The last part of this dissertation examined the phylogenetic relationship of *P. bahamense* var. *bahamense* with that of var. *compressum* using SSU rDNA sequences. One of the key features previously used to define varietal distinction was the inability of var. *bahamense* (found in the Atlantic) to produce toxins, in contrast to var. *compressum*, typically found throughout the Indo-Pacific and a documented toxin-producer. However, saxitoxin outbreaks in the Indian River Lagoon on the east coast of Florida extending back to 2002 have recently determined *P. bahamense* var. *bahamense* as the source. Thus, *Pyrodinium*-specific primers were designed to amplify 665-bp and 1.2-kb regions of the SSU rRNA gene from single cells isolated from various locations in the lagoon. The following results were obtained with respect to the phylogenetic classification of *P. bahamense*:

I. The cell currently classified as *P. bahamense* var. *bahamense* is genetically identical to that of var. *compressum* in certain regions of the Indian River Lagoon based on SSU rDNA sequences. Six individual samples were retrieved from two separate locations in the Indian River Lagoon. Samples from one of the sites, which yielded a 1.2-kb sequence of the SSU rRNA gene, identified *P. bahamense* var. *bahamense* as genetically identical to var. *compressum*, with 99% sequence identity.

II. Genetic variation exists within *P. bahamense* based on location with the Indian River Lagoon. Six individual samples obtained from a second site within the lagoon yielded a 665-bp sequence of the SSU rRNA gene. These sequences differed to a degree incompatible with the current classification of *P. bahamense* as a single species, and suggest that, similar to the *Alexandrium* species complex, different isolates or strains may exist which can be distinguished by location.

References

- Askwith C, Eide D, Van Ho A, Bernard PS, Li L, Davis-Kaplan S, Sipe DM, Kaplan J (1994) The FET3 gene of *S. cerevisiae* encodes a multicopper oxidase required for ferrous iron uptake. *Cell* 76:403-410
- Dancis A, Haile D, Yuan DS, Klausner RD (1994a) The *Saccharomyces cerevisiae* copper transport protein (Ctr1p). Biochemical characterization, regulation by copper, and physiologic role in copper uptake. *J. Biol. Chem.* 269:25660-25667
- Dancis A, Yuan DS, Haile D, Askwith C, Eide D, Moehle C, Kaplan J, Klausner RD (1994b) Molecular characterization of a copper transport protein in *S. cerevisiae*: An unexpected role for copper in iron transport. *Cell* 76:393-402
- Hill KL, Li HH, Singer J, Merchant S (1991) Isolation and structural characterization of the *Chlamydomonas reinhardtii* gene for cytochrome c6. Analysis of the kinetics and metal specificity of its copper-responsive expression. *J. Biol. Chem.* 266:15060-15067
- Li HH, Merchant S (1992) Two metal-dependent steps in the biosynthesis of *Scenedesmus obliquus* plastocyanin. Differential mRNA accumulation and holoprotein formation. *J. Biol. Chem.* 267:9368-9375
- Taylor AB, Stoj CS, Ziegler L, Kosman DJ, Hart PJ (2005) The copper-iron connection in biology: Structure of the metallo-oxidase Fet3p. *Proceedings of the National Academy of Sciences* 102:15459-15464

Vita

Kathleen Daumer Cusick was born in Allentown, PA on March 29, 1975 to parents Edward and Helen Daumer. She graduated from Notre Dame of Green Pond High School in 1993. She received her Bachelor of Science degree in Biology from Dickinson College in 1997. She obtained a Master's degree in Marine Biology from Florida Institute of Technology in 2000, conducting her thesis research at Harbor Branch Oceanographic Institute (Ft. Pierce, FL). Kathleen then worked as a microbiologist for three years in the Life Sciences Support Group at Kennedy Space Center, FL. In August 2004, she began the pursuit of her doctoral degree at the University of Tennessee (Knoxville). Her dissertation research was conducted in the Center for Environmental Biotechnology under the guidance of Dr. Gary Saylor. She received her PhD in Microbiology in 2009.